3D Numerical Techniques for Determining the Foot of a Continental Slope

Nicolette A. Pantland

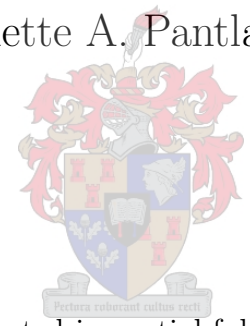

Thesis presented in partial fulfilment of
the requirements for the degree
Master of Science
at the Department of Applied Mathematics
of the University of Stellenbosch, South Africa

Supervisor: Prof. J.H. van Vuuren
December 2004

Declaration

I, the undersigned, hereby declare that the work contained in this thesis is my own original work and that I have not previously in its entirety or in part submitted it at any university for a degree.

Signature: _____ Date: _____

Abstract

The United Nations Convention on the Law of the Sea (UNCLOS) provides an opportunity for qualifying coastal signatory states to claim extended maritime estate. The opportunity to claim rests on the precept that in certain cases a continental shelf extends beyond the traditionally demarcated two hundred nautical mile (200M) Exclusive Economic Zone (EEZ) mark. In these cases a successful claim results in states having sovereign rights to the living and non–living resources of the seabed and subsoil, as well as the sedentary species, of the area claimed. Where the continental shelf extends beyond the 200M mark, the Foot of the Continental Slope (FoS) has to be determined as one of the qualifying criteria. Article 76 of UNCLOS defines the FoS as "... the point of maximum change in the gradient at its base." Currently Caris Lots is the most widely used software which incorporates public domain data to determine the FoS as a step towards defining the offshore extent of an extended continental shelf. In this software, existing methods to compute the FoS are often subjective, typically involving an operator choosing the best perceived foot point during consideration of a two dimensional profile of the continental slope. These foot points are then joined by straight lines to form the foot line to be used in the desk top study (feasibility study). The purpose of this thesis is to establish a semi–automated and mathematically based three dimensional method for determination of the FoS using South African data as a case study.

Firstly, a general background of UNCLOS is given (with emphasis on Article 76), including a brief discussion of the geological factors that influence the characteristics of a continental shelf and thus factors that could influence the determination of the FoS.

Secondly, a mathematical method for determination of the surfaces of extremal curvature (on three dimensional data), originally proposed by Vaníček and Ou in 1994, is detailed and applied to two smooth, hypothetical sample surfaces. A discussion of the bathymetric data to be used for application introduces the factors to be taken into account when using extensive survey data as well as methods to process the raw data for use. The method is then applied to two sets of gridded bathymetric data of differing resolution for four separate regions around the South African coast. The ridges formed on the resulting surfaces of maximum curvature are then traced in order to obtain a foot line definition for each region and each resolution.

The results obtained from application of the method are compared with example foot points provided by the subjective two dimensional method of computation within the Caris Lots software suite. A comparison of the results for the different resolutions of data is included to provide insight as to the effectiveness of the method with differing spatial coarseness of data.

Finally, an indication of further work is provided in the conclusion to this thesis, in the form of a number of recommendations for possible adaptations of the mathematical and tracing methods, and improvements thereof.

Opsomming

Die Verenigde Nasies se Konvensie oor die Wet van die See (UNCLOS) bied 'n geleentheid aan kwalifiserende state wat ondertekenaars van die Konvensie is om aanspraak te maak op uitgebreide maritieme gebied. Die geleentheid om op uitgebreide gebied aanspraak te maak berus op die veronderstelling dat 'n kontinentale tafel in sekere gevalle tot buite die tradisioneel afgebakende 200 seemyl eksklusiewe ekonomiese zone (EEZ) strek. In sulke gevalle het 'n suksesvolle aanspraak die gevolg dat die staat soewereine reg oor die lewende en nie-lewende bronne van die seevloer en ondergrond verkry, sowel as die inwonende spesies van die gebied buite die EEZ waarop aanspraak gemaak word.

Die voet van die kontinentale tafel (FoS) moet vasgestel word as een van die bepalende kriteria vir afbakening van die aanspraak waar die kontinentale tafel tot buite die EEZ strek. Artikel 76 van UNCLOS defineer die FoS as "... die punt van maksimale verandering in die helling by sy basis." Die mees algemeen gebruikte rekenaar sagteware wat openbare domein data aanwend om die voet van die helling te bepaal, is tans "*Caris Lots*." Die metodes wat in die program gebruik word om die voet van die helling te bepaal, is dikwels subjektief en berus tipies op 'n operateur se keuse van die beste afgeskatte punt van die voet van die helling uit 'n oorweging van 'n twee dimensionele profiel van die kontinentale tafel. Die berekende voet-punte word dan deur middel van reguit lyne verbind om 'n hellingsvoetlyn te vorm. Hierdie voetlyn kan dan in die Suid-Afrikaanse lessenaarstudie (doenlikheidstudie) oor die bepaling van die voet van die kontinentale tafel gebruik word. Die doel van hierdie verhandeling is om 'n semi-outomatiese en wiskundig gebaseerde drie–dimensionele metode te beskryf vir die vasstelling van die FoS, deur as 'n gevallestudie van Suid-Afrikaanse data gebruik te maak.

'n Algemene agtergrond van UNCLOS, met beklemtoning van Artikel 76, word eerstens gegee. 'n Kort bespreking van die geologiese faktore wat die kontinentale tafel beïnvloed en wat gevolglik 'n invloed kan hê op die vasstelling van die voet van die helling, is ingesluit.

Tweedens word 'n wiskundige metode, wat oorspronklik in 1994 deur Vaniĉek en Ou voorgestel is, vir bepaling van die oppervlaktes van maksimale kromming (gebaseer op drie–dimensionele data) in detail bespreek en 'n voorbeeld van 'n toepassing op twee gladde, denkbeeldige oppervaktes word beskryf. Die faktore wat in ag geneem moet word wanneer omvattende dieptemeting data gebruik word, en die metodes wat gebruik word om die rou data te verwerk, word ingelei deur 'n bespreking van die aard van die dieptemeting data wat gebruik is. Die metode word dan toegepas op twee stelle geruite dieptemeting data van verskillende resolusies vir vier afsonderlike streke om die Suid-Afrikaanse kus. Die riwwe wat op die resulterende oppervlaktes van maksimale kromming gevorm word, word dan nagetrek ten einde 'n lyndefinisie van die voet van die kontinentale tafel vir elke streek teen elke resolusie te bepaal.

Die resultate verkry uit toepassings van die metode word vergelyk met hellingsvoetpunte soos bepaal deur die subjektiewe twee dimensionele berekeningsmetode in die "*Caris Lots*" rekenaar–program. 'n Vergelyking van die resultate vir die verskillende data resolusies word ingesluit om die doeltreffendheid van die metode met betrekking tot die hantering van verskillende ruimtelike data resolusies te ondersoek.

'n Aanduiding van verdere werk, bestaande uit 'n aantal aanbevelings vir moontlike aanpassings en verbeterings van die wiskundige en natrek metodes, word ten slotte in die gevolgtrekking van die verhandeling verskaf.

Terms of Reference

In order to address the growing list of contentious issues relating to the uses and rights of a state with reference to its seas, the United Nations Convention on the Law of the Sea (UNCLOS), was drawn up and opened for signature on the 10th December 1982. South Africa signed and ratified the United Nations Convention on the Law of the Sea in 1998. As a ratified State, South Africa has 10 years to lay a once–off claim for extended maritime estate beyond its two hundred nautical mile (200M) Exclusive Economic Zone (EEZ) mark. This deadline was later extended to May 2009. Article 76, paragraph 4a, of UNCLOS outlines a method of determining the Foot of the Continental Slope (FoS) upon which this claim rests, namely: "In the absence of evidence to the contrary, the foot of the continental slope shall be determined as the point of maximum change in the gradient at its base."

Since 1997 the South African Navy (SAN) Hydrographic Office and the Institute for Maritime Technology have progressed towards understanding the legal and scientific requirements of UNCLOS. Through small projects, the issue was kept current while lobbying at a higher political level. In 2001 Mr Carl Wainman (Institute for Maritime Technology), Professor Deborah Hamman (Department of Mercantile Law, University of the Western Cape) and Captain Derick Law (SAN) presented a paper at the *Navy for Africa* conference, held at the Institute for Maritime Technology in Simons Town. This paper was entitled *South Africa's Outstanding Maritime Zones Claims and Boundaries: Time is Running Out!* and highlighted the urgent need for South Africa to instigate a scientifically sound plan for the completion of the claim process. It was foreseen that, should immediate action not be taken, South Africa would either not be able to submit its claim in time for the 2009 deadline or would submit a poorly researched and prepared claim. A poorly researched claim would lead to expensive revisions and not submitting a claim would result in South Africa missing out on an opportunity to add to its resource base in the future, where foreseen technological advances would make deep water exploration and exploitation possible. As a result of potential benefits being difficult to quantify, funding was difficult to justify and ownership at a higher political level was not forthcoming. The 2001 paper initiated a debate and in November 2002 a Cabinet memorandum approving funding of R23 million, from the Central Energy Fund, was filed. The Central Energy Fund is administered by the Department of Minerals and Energy. Petroleum Agency South Africa was appointed as project coordinator and a Steering Committee and Working Group were established. The Working Group consists of scientists and technicians from Petroleum Agency South Africa, the Council for Geoscience, the Institute for Maritime Technology and the South African Navy Hydrographic Office. The Working Group reports to the Steering Committee, which is made up of a member from each of the organizations comprising the Working Group, in addition to members from the Department of Foreign Affairs and the Department of Minerals and Energy amongst others.

A desktop study with respect to submitting a claim has been underway since April 2003. At the time of writing, the pertinence study section of the desktop study had established that South Africa stands to gain an estimated 400 000 km^2 in seaward estate during its claim process. This figure is considerably less than was first estimated. The estimate is conservative and does not include areas of low and medium probability of claim acceptance — including the Agulhas Plateau and certain Marion / Prince Edward Islands areas. Further, the initial computation of the FoS had begun, the process to generate public awareness was underway and a clear understanding of the legal and technical requirements contained in UNCLOS had been established. Once the desktop study is complete, detailed hydrographic and geological surveying of areas highlighted by the study will likely be undertaken to support the claim.

This thesis serves as an independent feasibility study of a mathematically justified method of FoS determination that might contribute to a more defendable and beneficial claim. Although the research involved in this thesis ran concurrently with the desktop study, the work contained in the thesis is not included in the official portfolio of the Working Group. The topic was suggested in January 2003 by Mr Carl Wainman who saw the opportunity for research to be conducted that could be beneficial to the claim process. Should the method (and its application) put forth in this thesis be feasible and practical, it will be considered for inclusion in the Working Group's portfolio of tools for use in the claim process. Should further work be required before the results can be of use to the claim process, this thesis will form the basis of motivation for such work. This thesis was funded independently by the Institute for Maritime Technology and therefore has no responsibility to the South African claim and is not defined as a deliverable for the project. Work on this thesis commenced in April 2003 and was completed in December 2004. Professor Jan van Vuuren was the supervisor for this thesis.

During the finalisation of work on this thesis some interesting developments occurred in both the international and South African arenas. The results of this thesis were presented to the South African Working Group on the 20th October 2004. All parties present were impressed by and interested in the work, the application of the methods and how the methods proposed could be included in the South African claim process. Members of the South African Working Group, who had recently returned from a claim-related trip to France and the United Kingdom, raised the point that the general international consensus was that the "Peucker Pick" in *Caris Lots* would not be considered as a basis for a claim as a direct result of the filter attracting the line too far offshore. Generally, it was found that the "Peucker Pick" line is located over deep ocean floor, which is unacceptable to the United Nations Commission on the Law of the Sea. This finding, although very recent, has prompted the Commission to consider issuing a formal statement with regards to the unacceptability of a claim based on this FoS choice. Indeed, the results of this thesis seem to support the general mistrust in the FoS determination via the "Peucker Pick," in the sense that the mathematically determined FoS was observed to be significantly more inshore than the "Peucker Pick" FoS in most cases, when using the South African bathymetric data.

As a direct result of the Working Group's interest in this thesis, another presentation of results was made to the South African Steering Committee on the 29th November 2004. This presentation was to create awareness of the work at a higher political level. During the meeting a proposal was put forward prompting the Steering Committee to set aside a portion of the budget for the South African claim for the continuation of this work. A time frame of two years was stated and the proposal was accepted by the attendees.

Acknowledgements

Nearly two years ago, a choice was made culminating in this thesis. The author hereby wishes to personally express her gratitude towards

- The Institute for Maritime Technology, Simon's Town, for providing the finance and support needed for this degree.
- Prof. Jan van Vuuren, for his patience, advice and unending belief that I could do this. It was wonderful to work under someone so understanding and yet determined to coax the very best from you.
- Carl Wainman, for his unending support and insight into the various other fields of study involved in this project and for putting up with the occasional emotional outbursts that invariably go with doing research such as this.
- Carl Sheffler, for his patience, humour, advice and assistance with programming and for his unique brand of subtle motivation.
- Dr Milton Maritz, for his valued assistance in the early stages of implementation of the mathematical method in Matlab and Mathematica. Much insight was gained regarding Matlab functions and their uses.
- Sven Coles for his assistance in fact checking the geological aspects of this thesis, and his impromptu spell checks.
- Friends and family, for their support, comfort and enthusiasm when late nights became early mornings (if at all).

Glossary

Abyssal Plain: A flat region of ocean floor usually at the base of the continental rise, whose slope is less than 1:1000. It is formed by the deposition of turbidity current and pelagic sediments.

Amagmatic: Said of a structure, region or process that does not involve magmatic activity.

Azimuth: A horizontal angle reckoned clockwise from a meridian; the horizontal direction of a point expressed as the angular separation from a reference direction.

Azimuthal Projection: A map projection on which the directions or azimuths of all points are shown correctly with respect to the centre. Generally this type of map projection is included in any of equal–area, equidistant or conformal projection and is also referred to as a *zenithal* projection.

Backarc Basin: A basin floored by oceanic crust on the opposite side of a volcanic arc from an oceanic trench.

Bank: A submarine elevation located on a continental margin over which the depth of water is relatively shallow.

Baseline: The line from which the outer limits of a state's territorial sea and certain other outer limits of coastal state jurisdiction are measured. The type of the territorial sea baseline (normal, straight) may vary, depending on the geographical configuration of locality.

Basement: The undifferentiated rocks, commonly igneous and metamorphic, that underlie the rocks of interest in a given area.

Basepoint: Any point on a baseline.

Bathymetry: The determination of ocean depths; the general configuration of the sea floor, as determined by analysis of depth data.

Beamwidth: The angular measure of the transverse section of an acoustic beam.

Cape Datum: The South African local datum in use until January 1999. The Cape Datum is referenced to the Modified Clarke 1880 ellipsoid and has its origin at Buffelsfontein, near Port Elizabeth.

Chart: A special–purpose map generally designed to meet the needs of marine navigation; also called *nautical chart* or *navigational chart*.

Chronometer: A portable timekeeper with a compensated balance, capable of showing time with extreme precision and accuracy — crucial to navigation at sea.

Clastic: Pertaining to a rock or sediment composed principally of fragments derived from pre–existing rocks or minerals and transported some distance from their places of origin; also said of the texture of such a rock — the most common clastics are sandstone and shale.

Collision Complex: The assemblage of geological features (terrains, structures, rocks) created as a result of continental collision with another continent or island arc.

Conformal Projection: A map projection that preserves the shape of all features, and in doing so, also preserves the angles within the features. Also referred to as an *orthomorphic* projection. Conformal projections are the most widely used map projections as a result of their significance in land surveying.

Conic Projection: A map projection which uses the cone as developable surface.

Contiguous Zone: A zone adjacent to a coastal state's territorial sea.

Continental Crust: The crustal rocks that underlie the continents.

Continental Margin: The submerged prolongation of the landmass of a coastal state, consisting of the seabed and subsoil of the shelf, slope and rise.

Continental Rise: A submarine feature which is that part of the continental margin lying between the continental slope and the deep ocean floor.

Continental Shelf: A zone adjacent to a continent, extending from the low–water line to the depth at which there is usually a marked increase of slope to greater depth.

Continental Slope: That part of the continental margin that lies between the shelf and the rise.

Convergent Plate Margin: A margin created by two plates that are moving toward each other; essentially synonymous with *subduction zone*.

Curvature: The rate of change, at a point, of the angle between a curve and a tangent to the curve.

Cylindrical Projection: A map projection which uses the cylinder as developable surface.

Datum: A set of parameters specifying the reference surface or the reference coordinate system used in the calculation of coordinates of points on the Earth's surface.

Deep Ocean Floor: The surface lying at the bottom of the deep ocean with its oceanic ridges, beyond the continental margin.

Developable Surface: A surface that can be created by transforming the plane without the introduction of distortion or stretching. The most common examples are the cylinder and the cone.

Divergent Plate Margin: A margin created by two plates which are moving apart, with mantle material and new oceanic crust moving in to fill the gap.

Earth Model: The set of coefficients of a spherical harmonic expression used to determine the geoid globally.

Eccentricity: A characteristic of elongation of an ellipsoid, defined in terms of the semi–major and semi–minor axes of the ellipsoid and denoted e.

Ellipsoidal Height: The linear distance of a point above (or below) a reference ellipsoid, measured along the normal to the ellipsoid.

Equal–Area Projection: A map projection where the area of features is preserved, but not the shape, angles and size. Also referred to as *equivalent*, *homolographic* or *homalographic*, *authalic* or equiareal.

Equidistance Line: See *Median Line*.

Equidistant Projection: A map projection in which the distances along all the meridians remain undistorted. This means that the shape and area of the features to be mapped are distorted, but the scale factor along the meridian is equal to one, or $k_m = 1$.

Equipotential Surface: A surface where a potential field (gravitational, magnetic or electric) is the same across the entire surface.

Exclusive Economic Zone: An area, not exceeding 200 nautical miles from the territorial sea baselines, which is subject to a specific legal regime under which a coastal state has certain rights and jurisdiction.

Feeder: The conduit through which magma passes from the magma chamber to a localized intrusion.

Flexural Loading: The process by which time–varying loads are regionally compensated as a consequence of the finite nonzero flexural rigidity of the lithosphere.

Foot of the Continental Slope: The point of maximum change of gradient at the base of the continental slope.

Forearc: The region between a subduction–related trench and a volcanic arc.

Forearc Basin: A sedimentary basin, usually elongated, lying between the volcanic arc and the shelf break in a convergent plate boundary zone. It is parallel to the arc and closer to it than to the trench–slope basin and the trench.

Fracture Zone Ridge: On the deep–sea floor, an elongated zone of unusually irregular topography where there are regions of ridges and depressions.

Frontal Arc: See *Forearc*.

Gauss Conformal Projection: The name sometimes used to refer to the transverse Mercator projection. Also sometimes referred to as the *Gauss–Krüger* projection.

Gaussian Distribution: Also called *normal distribution*; characterizing the distribution of measurement errors resulting in a symmetric, bell–shaped curve — $z(x, y) = e^{-(x^2+y^2)}$.

Gaussian Function: The function describing a Gaussian / Normal distribution.

Geocentric: Generally referring to a datum that has its origin at the centre of the Earth.

Geodesic: The curve representing the shortest distance between two points along the surface of an ellipsoid.

Geodetic Data: Information concerning points established by a geodetic survey, such as coordinate values, height and orientation.

Geodetic Datum: A set of parameters specifying the reference surface or the reference coordinate system used for geodetic control in the calculation of coordinates of points on the Earth.

Geodetic Latitude: The angle made by the normal to the surface of the (reference) ellipsoid, and the ellipsoidal equatorial plane.

Geodetic Longitude: The angle between the geodetic meridional plane and the defined zero meridian.

Geodetic Meridian: The plane through the normal to the surface of a reference ellipsoid, which also contains the minor axis of the ellipsoid.

Geodetic Reference System: Specification of a reference ellipsoid and the coordinates and orientation of an initial point.

Geographical Coordinates: A system of spherical or ellipsoidal coordinates for defining the positions of points on the Earth's surface.

Geoid: The equipotential surface of the Earth's gravity field which most closely approximates the global mean sea–level surface.

Geoid–Spheroid Separation: The height of the geoid above (or below) the ellipsoid being used to model it. Commonly referred to as, simply, the *separation*.

Geophysics: Study of the Earth by quantative physical methods. There are numerous specialties in the field, e.g. seismology and tectonophysics.

Global Positioning System (GPS): A United States Department of Defense system of satellites used to provide a global navigation and positioning service. GPS provides position information in the WGS84 global coordinate reference system.

Graticule: The set of parallels and meridians seen on a map.

Hartebeesthoek 94 Datum: The South African local datum in use since January 1999. The datum is based on the WGS84 reference ellipsoid, with the International Terrestrial Reference System 91 coordinates of Hartebeesthoek Radio Astronomy Tower near Pretoria as the initiation point for the datum.

Hydrographic Survey: The science of measuring and depicting those parameters necessary to describe the precise nature and configuration of the seabed and coastal strip, its geographical relationship to the landmass and the characteristics and dynamics of the sea.

Hydrothermal Vent: Submarine conduit for the extrusion of high–temperature fluids; typically found at sites where the extension of the Earth's crust is occurring and/or where new crust is being created.

Isobath: A curve representing the horizontal contour of the seabed at a given depth.

Lagrangian: The unconstrained optimization problem formulation obtained by means of Lagrange Multipliers.

Lagrange Multiplier: A method of dealing with constraints in mathematical optimization problems. The method introduces a new unknown scalar variable for each constraint and forms a linear combination of the optimization problem and the constraint involving the multipliers as coefficients. This transforms a constrained problem to an unconstrained problem.

Land Territory: Both insular and continental land masses that are above water at high tide.

Laplace's Equation: An equation extensively used in potential theory. Laplace's equation states that $\nabla^2 a = 0$, or the sum of the pure second order partial derivatives of a, with respect to x, y and z, is zero. The solution a has no local maxima or minima, since a has the property that the average value of a over a spherical surface is equal to the value of a at the centre of the sphere.

Latitude: One of the coordinates that describes a geographical position; angular distance of a position from the equator.

Local / Regional Datum: A datum defined by selecting an origin for a national or regional survey, chosen such that the geoid–spheroid separation and the vertical separation are zero. These datums typically approximate the geoid more accurately in the region of interest than does the global datum.

Longitude: One of the coordinates that describes a geographical position; angular distance of a position from an initial meridian — commonly the Greenwich Meridian.

Loxodrome: A path, also known as a *rhumb line*, which intersects a meridian on a given surface at any constant angle but a right angle. If the surface is a sphere, the loxodrome is a spherical spiral. The loxodrome is the path taken when a compass is kept pointing in a constant direction. It is a straight line on a Mercator projection. The loxodrome is *not* the shortest distance between two points on a sphere.

Mantle: The zone of the Earth below the crust and above the core. It is divided into the upper mantle and the lower mantle with a transition zone between.

Map Projection: An ordered system of meridians and parallels on a flat or plane surface. Usually refers to the mathematical formulae used to transform geodetic coordinates on an ellipsoid or sphere to grid coordinates on the plane surface.

Maritime Delimitation: The determination of a maritime boundary between states brought into effect by agreement.

Maximum Curvature Surface: The surface showing where the curvature of a reference surface is maximal.

Median Line: A line, every point of which is equidistant from the nearest points on the baselines of two states.

Mercator Projection: A conformal projection of the cylindrical type. Widely used in land survey and navigation.

Meridian of Longitude: Lines or curves of equal longitude. See *Longitude*.

Mile: See *Nautical Mile*.

Minimum Curvature Surface: The surface showing where the curvature of a reference surface is minimal.

Multi–Beam Echo Sounder: Wide–swath echo sounder using multiple acoustic beams directed below and transverse to a ship's track, to determine water depths.

Natural Prolongation: The submarine area of a coastal state that is the most natural extension of its land territory to the outer limit of its continental margin.

Nautical Chart: See *Chart*.

Nautical Mile (M): A unit of distance used primarily in navigation. Most of the maritime nations have accepted the international nautical mile of 1852 metres, adopted by the International Hydrographic Organization.

Oblate Spheroid: The resulting spheroid (ellipsoid) formed by compressing a sphere at its poles. The poles can be described as the outermost points on a diameter of the sphere.

Oblique Projection: Generally referring to a projection where the developable surface is rotated in any direction through an angle of θ, where θ is greater than 0 and less than $\frac{\pi}{2}$, in order for the point of contact between the developable surface and the sphere/ellipsoid to lie along neither a parallel of latitude nor a meridian of longitude. Used for the mapping of land that is oriented in a narrow strip angled across parallels of latitude and meridians of longitude.

Oceanic Crust: Rocks that underlie the ocean basins, typically having a density of 3.0 g/cm^3.

Oceanic Ridge: A long elevation of the deep ocean floor with either irregular or smooth topography and steep sides.

Orthometric Height: The linear distance of a point above (or below) a reference equipotential surface of the Earth's gravity field (usually the geoid), measured along the gravity vector.

Parallels of Latitude: Curves of equal latitude. See *Latitude*.

Passive Margin: A continental boundary or margin formed by rifting and continental rupture associated with divergent tectonism.

Pelagic Sediment: A very fine–grained marine sediment deposited from a dilute mineral suspension distributed throughout deep ocean water, often highly organic rich due to biological activity.

Physiography: Originally a description of the physical nature of objects, especially of natural features. Later synonymous with physical geography.

Plane Surface: A surface on which straight lines can be drawn through any point in any direction.

Plate Carrée: The flat, square appearance of the graticule.

Plate Tectonics: A theory of global tectonics in which the lithosphere is divided into a number of plates whose patterns of horizontal movement is that of torsionally rigid bodies that interact with one another at their boundaries, causing seismic and tectonic activity along these boundaries.

Potential Field: A field satisfying Laplace's equation, such as a gravity, magnetic or electric field.

Prime Meridian: The meridian of longitude 0, used as the origin for the measurement of longitude and generally equated with the Greenwich Meridian.

Principal Normal: The unit vector orthogonal to the unit vector tangential to a curve $\mathcal{C}$ at a point P on the seafloor and further in the plane of $\mathcal{C}$ at P; denoted by n.

Projection: See *Map Projection*.

Projection Scale: The amount of distortion introduced in the direction of the parallel and/or meridian as a result of application of a map projection to represent spherical data on a plane surface. This does not refer to the scale of the map itself.

Projection Scale Factor: The distance on the projection divided by the distance on a sphere or ellipsoid, giving a direct indication of the distortion that has occurred. The scale factor is denoted by k, but can be separated into the scale factor in the direction of the parallel (k_p) and the scale factor in the direction of the meridian (k_m).

Prolate Spheroid: The spheroid (ellipsoid) formed as a result of compressing a sphere at its equator (the outermost central locus of the sphere, perpendicular a diameter of the sphere).

Pure Shear Stretching: A particular example of irrotational strain in which the body is stretched in one direction and shortened at right angles to this. Compare with *simple shear*.

Realisation of a Datum: The process where the physical moments of the known coordinates are provided. This is performed as in addition to the simple translation between datums; there may exist rotations and changes to scale.

Reef: A mass of rock or coral which either reaches close to the sea surface or is exposed at low tide.

Regular Projection: Generally referring to a projection where the developable surface remains unrotated, in order for the point of contact between the developable surface and the sphere/ellipsoid to lie along a parallel of latitude.

Rift: 1. A long, narrow trough bounded by normal faults; often associated with volcanism. 2. A narrow cleft, fissure or other opening in rock, as a result of cracking or splitting.

Rise: See *Continental Rise*.

Rhumb Line: See *Loxodrome*.

Sag: 1. A saddle–like pass or gap in a ridge or mountain range. 2. A shallow depression in an otherwise flat or gently sloping land surface; a small valley between ranges of low hills or between swells and ridges in an undulating terrain.

Scale: The ratio of a distance between two points on a chart or map and the distance between the corresponding two points measured along a physical surface.

Sea–Based Platform: Also referred to as an *offshore installation*. Refers to a synthetic structure usually built for the exploration or exploitation of marine resources, marine scientific research, tide observations, etc. Common examples are ships and oil rigs.

Seabed: The top of the surface layer of sand, rock, mud or other material lying at the bottom of the sea and immediately above the subsoil.

Seamount: An elevation of the seafloor, 1000 m or higher than the surrounding seafloor, either flat–topped or peaked. Seamounts may occur singly, arranged in a linear or random grouping, or connected at their bases and aligned along a ridge or rise.

Sedimentary Rock: A layered rock resulting from a consolidation of sediment.

Separation: See *Geoid–Spheroid Separation*.

Shear: A deformation resulting from stresses that cause contiguous parts of a rock body to slide relative to each other in a direction parallel to their plane of contact. It is the mode of failure in which the portion of a mass on one side or a plane or surface slides past the portion on the opposite side. In geological literature the term refers almost invariably to strain rather than to stress. It is also used to refer to surfaces and zones of failure by shear, and to surfaces along which differential movement has taken place.

Shelf: See *Continental Shelf*.

Single–Beam Sounder: A device using a single acoustic beam to determine water depths directly below the ship's track.

Slope: See *Continental Slope*.

Slump: The downward slipping of a mass of rock or unconsolidated material, moving as a unit.

Spheroid (Ellipsoid) Normal: A line from the point in question that is perpendicular to the surface of an ellipsoid.

Spreading Ridge: Midoceanic ridge.

Stereographic: A perspective projection, from a sphere to a plane, having the point of projection at the opposite end of the diameter of the sphere from the point of tangency of the plane of the projection.

Straight Line: Mathematically, the line of shortest distance between two points in a specified space or on a specified surface.

Strain: Change in the shape or volume of a body as a result of stress; a change in relative configuration of the particles of a substance.

Subdetachment: That part of the lithosphere lying below a detachment fault.

Subduction Zone: A long, narrow belt in which subduction takes place, e.g. along the Peru–Chile trench, where the Pacific plate descends beneath the South American plate.

Submarine Ridge: An elongated elevation of the seafloor, with either irregular or relatively smooth topography and steep sides.

Subsidence: A gradual sinking or downwarping of a large part of the Earth's crust relative to its surrounding parts, such as the formation of a rift valley or the lowering of a coast due to tectonic movement.

Subsoil: All naturally occurring matter lying beneath the seabed or deep ocean floor.

Swath: The strip or lane on the seafloor scanned by a multi–beam echo sounder when a vessel proceeds along its course. Also sometimes spelt *swathe*.

Synrift: A geological process that occurs at the same time as the rifting process. Commonly refers to the sediments deposited during rifting or active movement on a fault.

Tangent: A straight line is tangent to a curve $f(x)$ at a point x_0 on the curve if the line passes through the point $(x_0, f(x_0))$ and has slope $f'(x_0)$, where $f'(x)$ is the derivative of $f(x)$.

Territorial Sea: A belt of water of a defined breadth measured seaward from the territorial sea baseline, usually to 12 nautical miles offshore.

Transverse Projection: Generally referring to a projection where the developable surface has been rotated by an angle of $\frac{\pi}{2}$ to facilitate the point of contact between the developable surface and the sphere/ellipsoid being along a meridian of longitude as opposed to a parallel of latitude.

Trench: A narrow, elongated depression of the deep ocean floor, with steep sides, oriented parallel to the trend of the continent and lying between the continental margin and the abyssal hills. It is typically 2 km deeper than the surrounding ocean floor and may be thousands of kilometres long.

Underplating: Addition of magmatic material to the base of the crust, which commonly occurs during rifting and extension of relatively "hot" lithosphere, e.g. volcanic margins.

Undevelopable Surface: A surface that cannot be reached by means of a transformation from a plane without introducing distortion or stretching. The most common example is the sphere.

Unit Bi–Normal: A unit vector orthogonal to the unit–normal of a curve $\mathcal{C}$ at a point P on the seafloor, but also orthogonal to the plane of $\mathcal{C}$ at P; denoted by $\underline{b}$.

Uplift: A structurally high area in the crust of the Earth, produced by movements that raise the rocks, as in a broad dome or arch.

Vent: The opening at the Earth's surface through which volcanic and hydrothermal materials are extruded; also the channel or conduit through which they pass.

Vertical Separation: The angle at which the geoid intersects with an ellipsoid.

Volcanic Arc: A generally curved, linear belt of volcanoes above a subduction zone.

World Geodetic System 1984 (WGS84): The United States Department of Defence World Geodetic System 1984 is the most recent realization of the WGS series. WGS84 consists of a global reference frame and the collection of associated models providing a single, common, accessible three–dimensional global coordinate system. WGS84 is the internationally accepted global reference datum (especially for GPS work).

Reserved Symbols

Maximum Curvature Computation

(l^*, m^*)	A point satisfying the necessary first–order conditions for being an extremal point of $\kappa(l, m)$ subject to $g(l, m) = 0$.
$\underline{b}$	The *unit bi–normal* to a curve $\mathcal{C}$ at a point P. This is a unit vector orthogonal to $\underline{t}$ and to the plane of $\mathcal{C}$ at P.
$\mathcal{C}$	The shortest curve between points P and P' along the seafloor, parameterised by s.
$d\underline{r}$	The distance between the point P and another point P' on the seafloor.
ds	The arcdistance between P and P' along $\mathcal{C}$ the seafloor.
$f'(x)$	The first–order derivative of the function $f(x)$ evaluated at the point x.
$f''(x)$	The second–order derivative of the function $f(x)$ evaluated at the point x.
$g(l, m)$	The constraint for the optimisation problem of finding the surfaces of extremal curvature corresponding to a given surface.
h	The step size, or distance between points, used in derivative approximation formulae.
$\underline{i}$	A unit vector in the x direction.
$\underline{j}$	A unit vector in the y direction.
$\underline{k}$	A unit vector in the z direction.
$\kappa(s)$	The curvature of a curve $\mathcal{C}$ along the seafloor at a point P, expressed as a function of the arclength of $\mathcal{C}$ from some reference point on $\mathcal{C}$.
$\kappa(l, m)$	The curvature of the seafloor surface, expressed as a function of the directional coefficients l and m.
l	The directional coefficient $\frac{dx}{ds}$.
$\mathcal{L}(\kappa, \lambda)$	The Lagrangian for the optimisation problem of finding the surfaces of extremal curvature, corresponding to a given surface.
λ	The Lagrangian multiplier used in the optimisation problem of finding the surfaces of extremal curvature, corresponding to a given surface.
m	The directional coefficient $\frac{dy}{ds}$.
$\underline{n}$	The *principal normal* to $\mathcal{C}$ at P. This is a unit vector orthogonal to $\underline{t}$ and in the plane of $\mathcal{C}$ at P.
P	A general point on the seafloor corresponding to surface position (x, y) and position vector $\underline{r}(x, y)$.
P'	A point on the seafloor with position vector $\underline{r} + d\underline{r}$.
$\underline{r}(x, y)$	The position vector, $\underline{r}(x, y) = x\underline{i} + y\underline{j} + z(x, y)\underline{k}$, of a point P on the seafloor.
s	The seafloor arclength parameter along a curve $\mathcal{C}$, parameterised by s.
$\underline{t}$	Unit vector tangential to a curve $\mathcal{C}$ at a point P in the limit as $\|d\underline{r}\| \to 0$.
τ	The torsion of a curve $\mathcal{C}$ at a point P.

Datums and Map Projections

a	The semi–major axis length of an ellipsoid.
α_1	The datum realisation rotation component in the x direction (an Euler angle).
α_2	The datum realisation rotation component in the y direction (an Euler angle).
α_3	The datum realisation rotation component in the z direction (an Euler angle).
b	The semi–minor axis length of an ellipsoid.

C_{eq}	The circumference of the Earth at the equator.
C_ϕ	The circumference of the Earth at a parallel of latitude ϕ.
e	The eccentricity of an ellipsoid.
f	The flattening, or degree of oblateness of an ellipsoid.
h	The height of a point P, in metres, and indicating the distance of the point above (or below) the surface of a sphere or an ellipsoid.
k_m	The projection scale factor in the direction of a meridian in a map projection.
k_p	The projection scale factor in the direction of a parallel in a map projection.
k_0	The scale factor along the central meridian λ_0 in the transverse Mercator map projection.
λ	The longitude of a point P on the Earth's surface. Longitude is measured as positive in the Easterly direction.
λ_0	The longitude point of origin for a map projection.
μ	The datum realisation scale factor for a map projection.
N	The height of the geoid above the ellipsoid, referred to as the geoid–ellipsoid separation.
ϕ	The latitude of a point P on the Earth's surface. Latitude is measured as positive in the Northerly direction.
ϕ_0	The latitude point of origin for a map projection.
R	The radius of the spherical Earth.
$\mathbf{R}$	The datum realisation rotation matrix for a map projection.
θ	The angle of rotation experienced by the developable surface for a specific map projection.

List of Acronyms

COB:	Continent Ocean Boundary
COT:	Continent Ocean Transition Zone
EEZ:	Exclusive Economic Zone
ETOPO:	Earth Topography
FoS:	Foot of the (Continental) Slope
GEBCO:	General Bathymetric Chart of the Oceans
GPS:	Global Positioning System
IRTF:	International Terrestrial Reference System
LoS:	Law of the Sea
SA:	South Africa
SAN:	South African Navy
SMC:	Surface of Maximum Curvature
SmC:	Surface of Minimum Curvature
SSDRs:	Seaward Dipping Reflector Sequences
UNCLOS:	United Nations Convention on the Law of the Sea
WGS84:	World Geodetic System 1984

Table of Contents

List of Figures

List of Tables

List of Algorithms

Chapter 1

Introduction

All over the world certain qualifying coastal nations have a once–off opportunity to claim extended maritime seafloor estate. As signatories to the Law of the Sea (LoS) Convention these claims, and the requisite procedures, are received and assessed by the United Nations Commission on the Law of the Sea. The opportunity to claim rests on the precept that in certain cases a continental shelf extends beyond the traditionally demarcated maritime zone, namely the 200 nautical mile (hereafter referred to as 200M) Exclusive Economic Zone (EEZ). A legally acceptable definition of the continental shelf is given later in this chapter, which serves to introduce the myriad factors and restrictions that go with researching such a claim, as well as imparting a general understanding of how and why this thesis, and the corresponding restrictions, came into being.

1.1 United Nations Convention on the Law of the Sea

The United Nations Commission on the Law of the Sea governs the procedure for making a claim, including a specification that a multidisciplinary approach should be taken. This section aims to serve as an introduction to the United Nations Convention on the Law of the Sea (UNCLOS) in general, and the LoS in particular. A history of the Commission and how it came into being is discussed briefly, followed by a discussion of the particular article of the LoS pertaining to making a claim (Article 76).

1.1.1 History of UNCLOS

In the 18th century an accurate chronometer was developed by Harrison [29] which was critical in developing an accurate means to establish longitude and thus effectively chart the oceans for the first time. The ability to chart the oceans led to coastal nations laying claim to newly explored ocean areas where they exerted authority to monitor trade routes, document hazards and exploit ocean resources.

In the 19th century, the collection of data as a result of this informal claim process, led to the establishment of most of the world's territorial baselines. Some of the 19th century data collected is the only information of its type available for certain areas to this day. The General Bathymetric Charts of the Oceans (GEBCO), first compiled in the 1930s, form the starting point for most LoS claims. From the 1950s onwards there have been major advances in knowledge and technology, including the use of seismic profiling techniques. The 1970s saw the first move to deep ocean resource exploitation in the form of deep ocean drilling. Current knowledge of sediment transport, the form and age of ocean basins, how the seafloor is defined by plate movement and general ocean processes in combination with major advances in technology have made researchers come up with new uses for the ocean floor and its resources. This has caused states to accept responsibility for sustainment and management of the resources of their seas for the common good of mankind [37].

To address the growing list of contentious issues relating to the uses and rights of a state with reference to its seas, UNCLOS was formed and opened for signature on the 10th December 1982. The convention

came into force in 1994 for those states acceding to the LoS. The LoS deals with delimitation, environmental impact and management, scientific research, economic and commercial aspects and technological advancements. It provides for peaceful settlement of disputes, which is particularly important as there are 151 coastal states, all with sovereign rights to their adjacent seas and continental shelves [6].

UNCLOS provides, at a minimum, a framework for all uses of the sea. The major features of this framework are:

1. The creation of baselines and the definition of four maritime zones described by the four Geneva conventions of 1958, namely: Territorial seas (12M from baseline), a Contiguous Zone (24 M from baseline), High Seas (seaward of the EEZ) and a Continental Shelf (in which modest payment is received for exploitation). The reader is referred to Figure 1.1 for a graphic representation of these zones.

2. The formulation of definitions of notions such as Innocent Passage, Transit Passage, Archipelagic Waters, the EEZ (exclusive right to the exploration and exploitation of resources only), Islands, Enclosed Seas, the Rights of Landlocked States, the International Seabed Area as well as Preservation of the Marine Environment, Marine Scientific Research, Development and Transfer of Marine Technology and the Settlement of Disputes. Of the above list, only the EEZ is of relevance to this thesis.

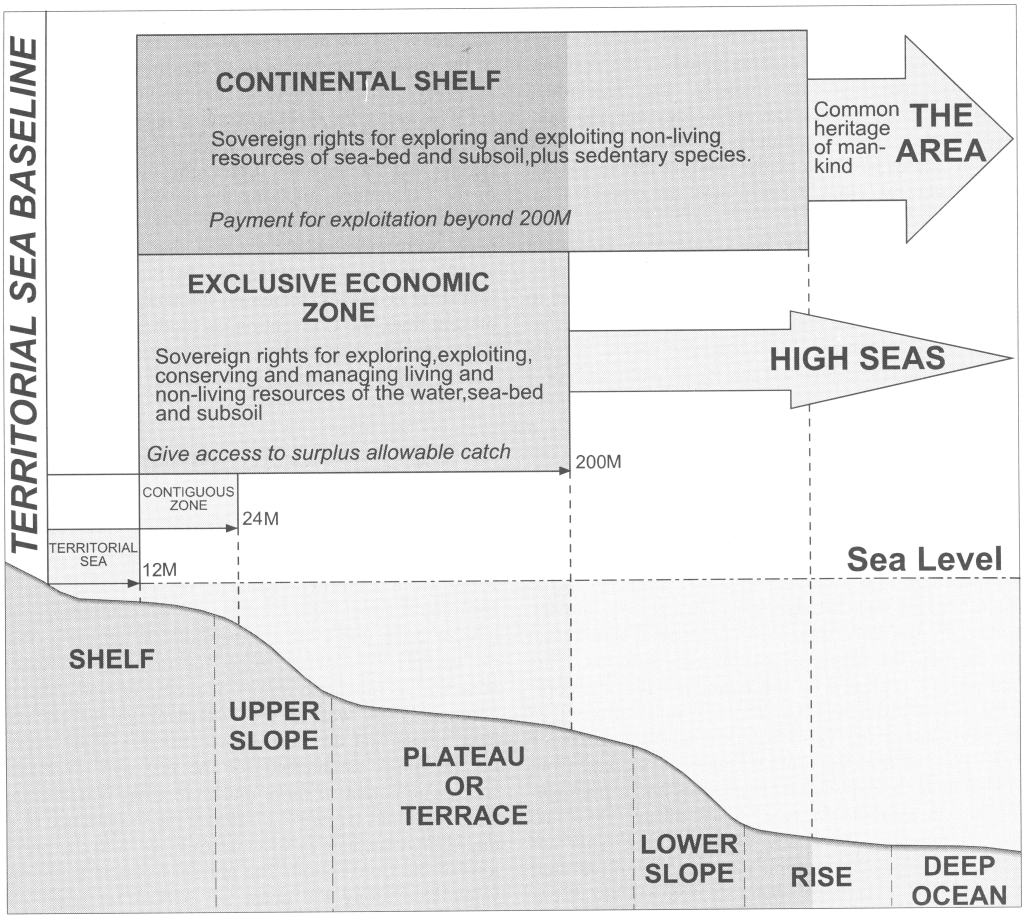

Figure 1.1*: Maritime Zones and their relationship to sub sea topography (Source: Australian Geological Survey Organisation) [7].*

It was noted by the Commission that UNCLOS should apply to all states equally and thus that there had to be technology and information transfer to the developing states in order to allow them to gain

full benefit from the opportunity to claim. For this purpose the Inter–governmental Oceanographic Commission and the International Hydrographic Organisation were approached to take the responsibility of producing information on the scientific aspects of Article 76 of UNCLOS that would be helpful to the international community and that would promote technology and knowledge transfer to developing states.

States that have acceded to the LoS have ten years to lay their claim for extended seaward estate and, although there may be no apparent economic gain in claiming now, with technological advances (such as deeper drilling techniques) the potential offered by a claim could grow exponentially with time.

1.1.2 Article 76 of UNCLOS

UNCLOS consists of 17 parts, 320 articles and 9 annexes, and provides the legal framework for exercising the rights and duties of states with respect to their uses of the ocean and its resources. Of all the articles of the Convention the one applicable to claiming additional seaward estate, is Article 76. The provisions of Article 76 most applicable to this thesis are discussed briefly in this section. For a complete summary of the application of Article 76 the reader is referred to the flowchart in Figure 1.2.

Article 76 defines the continental shelf in a manner that is scientifically based, legally defendable and politically acceptable. It further attempts to maximise the area that a state can claim, where the continental shelf extends beyond the 200M EEZ limit, subject to certain restrictions. From a geological perspective the continental shelf is made up of several geomorphologic sections of the prolongated land territory offshore, starting at the territorial baseline and moving out to sea, which are progressively labelled the continental shelf, the continental slope and the continental rise. The combination of these three sections is known as the continental margin, but to avoid confusion due to the earlier use of the words "continental shelf" with regards to the whole, the term "continental shelf" is used within Article 76 to refer to the whole.

Paragraph 1 of Article 76 defines the continental shelf as follows:

> "The continental shelf of a coastal state comprises the seabed and subsoil of the submarine areas that extend beyond its territorial sea throughout the natural prolongation of its land territory to the outer edge of the continental margin, or to a distance of 200 nautical miles from the baselines from which the breadth of the territorial sea is measured where the outer edge of the continental margin does not extend up to that distance [37]."

Paragraph 3 states:

> "The continental margin comprises the submerged prolongation of the land mass of the coastal state, and consists of the seabed and subsoil of the shelf, slope and rise. It does not include the deep ocean floor with its oceanic ridges or subsoil thereof [37]."

Paragraphs 2 and 4 provide restrictions on the extension of the continental shelf from the determined Foot of the Slope (FoS) and baselines. In particular, paragraph 4a of the convention outlines a method of determining the FoS upon which this claim rests, namely:

> "In the absence of evidence to the contrary, the foot of the continental slope shall be determined as the point of maximum change in the gradient at its base [37]."

1.1.3 Potential Gains in terms of Resources

The continental margin is essentially composed of the same material as the continents and is rich in silica and alumina. It has a density less than $2.7 g/cm^3$ and is between $35 km$ and $60 km$ thick (with respect to depth). Individuals have harvested living resources from the continental margin (like lobster and seaweed) for thousands of years and offshore resource mines have extended under the sea since the

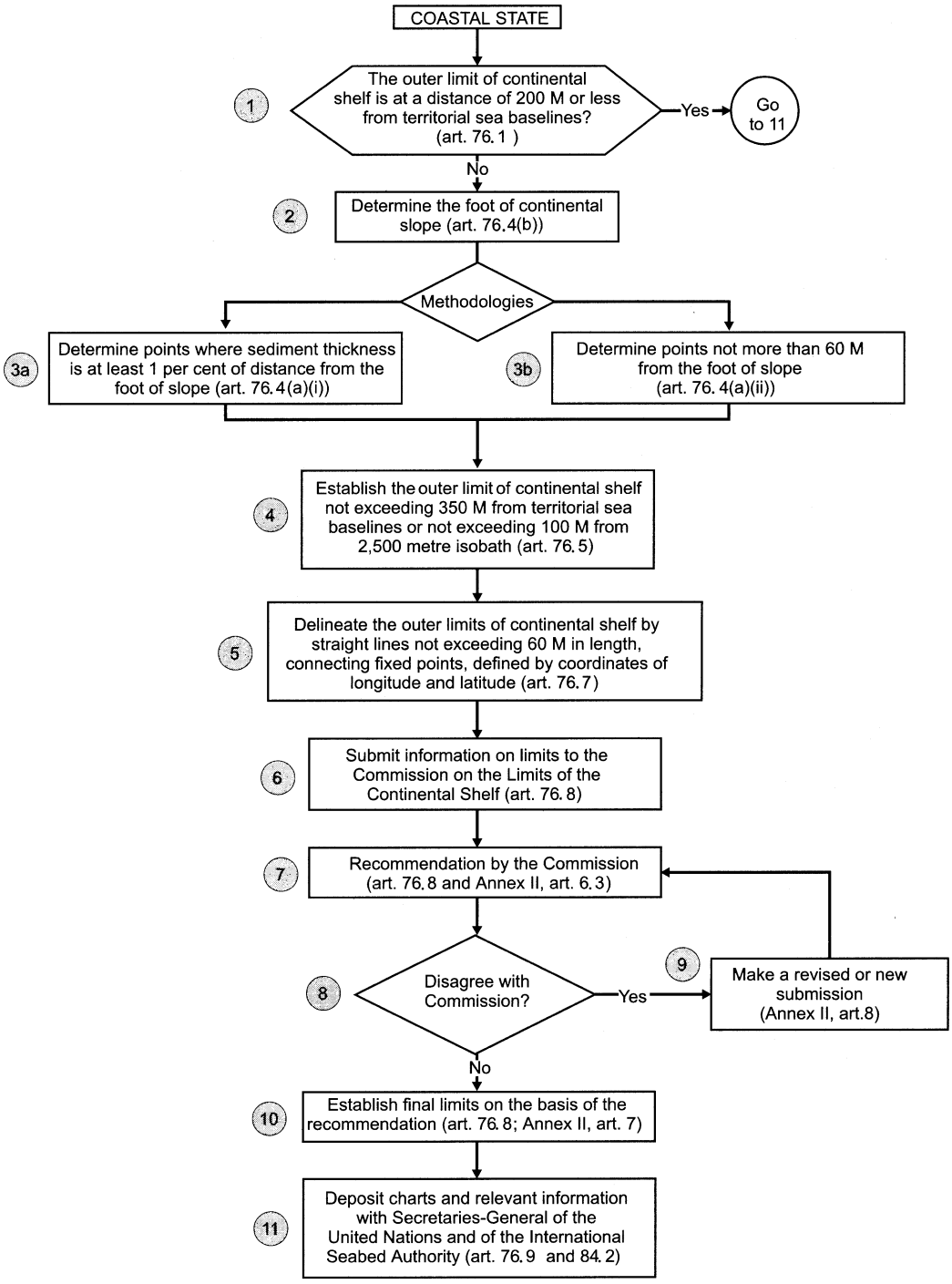

Figure 1.2: *Schematic flowchart illustrating the entire procedure for a coastal state to establish the outer limits of its continental shelf under Article 76 of UNCLOS [7].*

1600s. If a state is successful in claiming parts of the margin beyond 200M it may then develop non–living resources and sedentary species within that area, incurring a payment for usage of up to 7% of the value of the resource developed to the International Seabed Authority. The state then has rights and responsibilities for the seafloor, non–living resources and sedentary species in that area, but not the water column nor the air above it. There are four main classes of non–living resources on the continental margin: hydrocarbons (such as oil), construction aggregates (such as gravel and sand), minerals in placer deposits (such as diamonds, gold and ilmenite), and industrial chemicals (such as sulphur and phosphate). A description of these four main classes of non–living resources, as well as sedentary species found in the continental margin, follows.

1. *Hydrocarbons*

   Although a large number of the world's oil and gas fields are located on continental shelves, the potential for other deep water hydrocarbon resources exists. Until technological advances expose or negate the existence of resources in these deep waters, it should be assumed that future resources may occur there [3, 14].

   Gas hydrates are recently discovered (but undeveloped) hydrocarbon fuels that are known to occur on some continental slopes and rises. With the world depending heavily on fuel, a move could soon be made to develop and use this source of energy as an oil or petroleum surrogate. It has been reported that methane hydrates contain twice as much combustible carbon as all other fossil fuels, meaning that as little as 1% of the most conservative estimates of available methane from gas hydrates would equal half the known conventional gas reserves. This unexploited energy potential is currently limited by a lack of feasible methods for extraction and use of these gas hydrates [20].

2. *Construction Aggregates and Sand*

   Gravel and sand on the continental margin exceed in volume and potential value any other non-living resource, except oil and gas. Offshore gravel and sand are used mainly in the construction industry and for beach replenishment purposes. As this is a low-cost bulk operation it is preferable that the materials be mined close to the site of use and thus close to the state using them. It is unlikely that deep sea reserves of gravel and sand can be cost effectively mined, when compared with land based reserves for many states.

3. *Placer deposits*

   Placer deposits are formed in much the same way as alluvial deposits on land and may consist of tin, ilmenite, gold or diamonds. The spatial density of the deposits decreases with increased offshore distance, so there is little chance that a state would claim extended continental shelf for reasons of mining this resource.

4. *Industrial minerals*

   The main drive behind claiming for possibilities of this type of resource are the potentials offered by the marine phosphorites as they are relatively high grade and extend far offshore, beyond the 200M limit. At this stage it is not known what environmental impact mining of this type of resource will have as there are currently no effective methods in place for such operations [8].

5. *Sedentary Species*

   These species include "living organisms belonging to sedentary species, that is to say organisms which, at the harvestable stage, are either immobile on or under the seabed, or are unable to move, except in constant physical contact with the seabed or the subsoil" [7]. Included in this definition are: molluscs (like abalone, pearl oysters and scallops), crustaceans (such as rock lobsters, bugs and mud crabs) and echinoderms (such as sea urchins, sponges, coral and bait worms). Further exploitable vegetable species are seaweed and sea grasses. Of special interest here is the bacterial extremophiles, which have the potential to be extremely valuable in medicine [45].

1.2 South Africa's Claim

South Africa is a signatory to the LoS and as such has until May 2009 to submit a claim for extended seaward estate beyond its 200M EEZ. South Africa may stand to gain a substantial area of approximately 400 000 km^2 of seafloor. This figure may change for the positive or the negative pending the outcome of a desktop study currently in progress. The reader is referred to Figure 1.3 for an indication of the areas tentatively identified by the desktop study as potential claim areas[1]. South Africa's Claim is funded by the Central Energy Fund, which is administered by the Department of Minerals and Energy. Funding of R23 million was approved by Cabinet in November 2003 and Petroleum Agency South Africa was appointed project coordinator for the claim process. A Working Group has been established to do the research and applicable preparation work for the claim. The group consists of scientists and technicians from the following institutions: The Institute for Maritime Technology, a division of Armscor Business; Petroleum Agency South Africa; The Council for Geoscience and The South African Navy (SAN) Hydrographic Office. The Working Group is answerable to a Steering Committee which oversees the progress of the group on a largely political level. The Steering Committee is made up of a member from each of the following organisations: Petroleum Agency SA (Chair), the Council for Geoscience, the Department of Foreign Affairs, The Department of Minerals and Energy and the SAN Hydrographic Office.

A desktop study has been underway since April 2003, consisting of the following activities:

1. Pertinence Study. In this study tests are performed to determine whether it is worthwhile for South Africa to submit a claim. A submission is only pertinent if a substantial area is identified as possible extension in such a claim. The approximations are intentionally conservative so as to ensure acceptance, should a claim be made.
2. Establishment of a combination of straight and normal baselines.
3. Determination of the FoS.
4. Calculation of the Extension of the Shelf as per Article 76 Regulations. This consists of seven steps:
   (a) Calculation of the line 60M offshore from and parallel to the FoS. Call this line A.
   (b) Calculation of the line offshore where the sediment thickness is 1% of the distance from the FoS. Call this line B.
   (c) Taking the seaward combination of lines A and B. Call this line 1.
   (d) Calculation of the line 100M offshore from and parallel to the 2500m bathymetric isobath. Call this line C.
   (e) Calculation of the line 350M offshore from and parallel to the baselines. Call this line D.
   (f) Taking the seaward combination of lines C and D. Call this line 2.
   (g) Taking the landward combination of lines 1 and 2. This is the claim line.
5. Gathering of existing national and international data sets.

Once the desktop study is completed, additional detailed surveying of bathymetric, seismic, magnetic and gravimetric variables will be undertaken in the areas highlighted by the study. Many other geological factors come into play, some of which are part of the desktop study and some part of the actual claim process. With the conservative FoS calculated, surveys may provide geological evidence of a more reliable and specific FoS using a combination of geodesy, geology and geomorphology. There are currently many unknowns with respect to the areas that may be claimed as the desktop study is not yet complete. These areas include: certain areas around the Marion/Prince Edward Islands and the Agulhas Plateau.

Other tasks faced by the South African team during the claim process, are the finalisation of maritime boundaries with Namibia, Mozambique and France, the processing of data from the desktop study, hydrographic and geographic surveys, and the final compilation and submission of the claim itself.

[1] This graphic was provided courtesy of Petroleum Agency South Africa and is used with their consent.

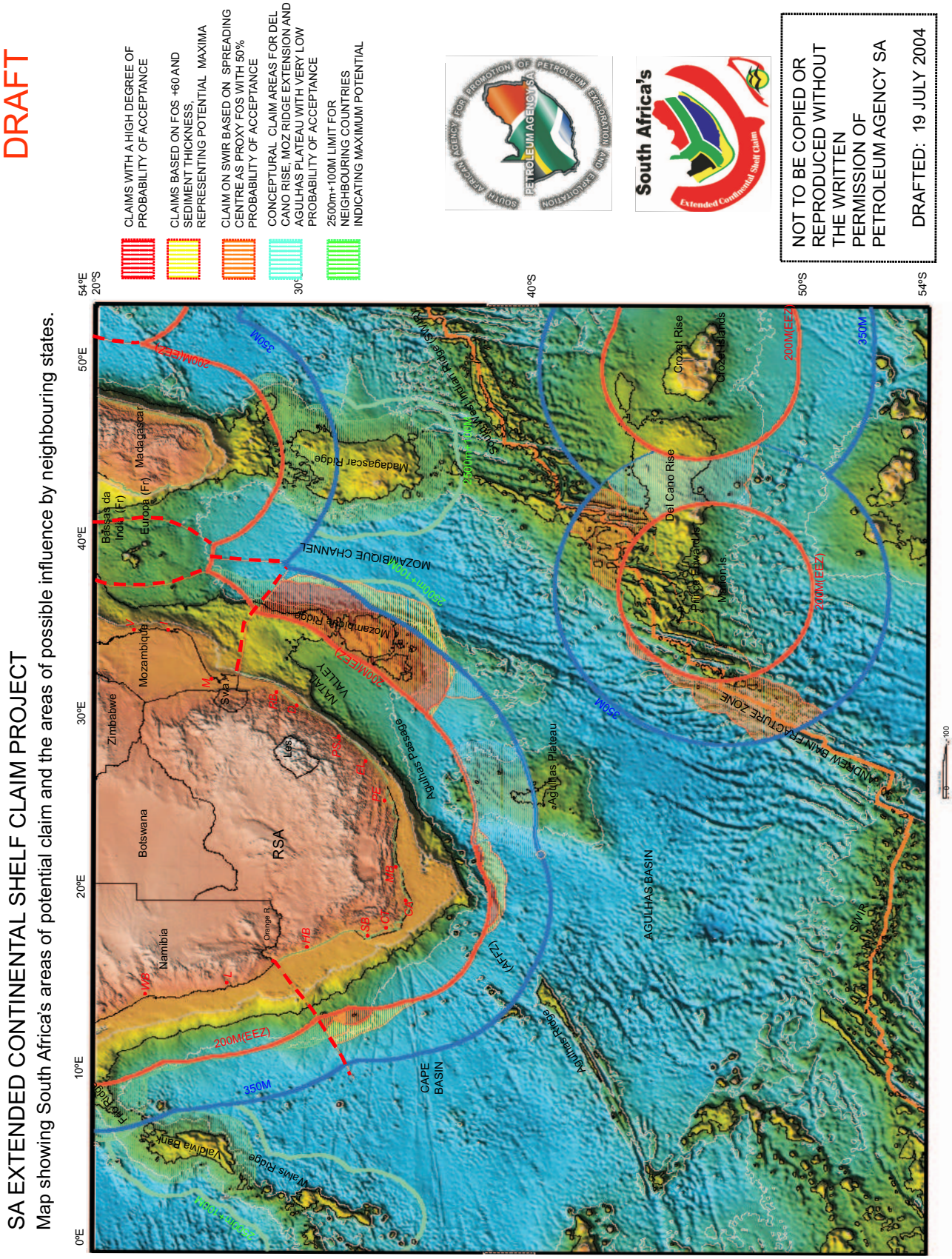

Figure 1.3: *Potential areas for the South African claim (graphic courtesy of Petroleum Agency South Africa and used with their consent).*

1.3 The Scope and Objectives of this Thesis

Extended Continental Shelf territories exist, beyond 200 nautical miles, in many offshore areas throughout the world (see Figure 1.4 for a graphical display of these areas). For a coastal state as a signatory to

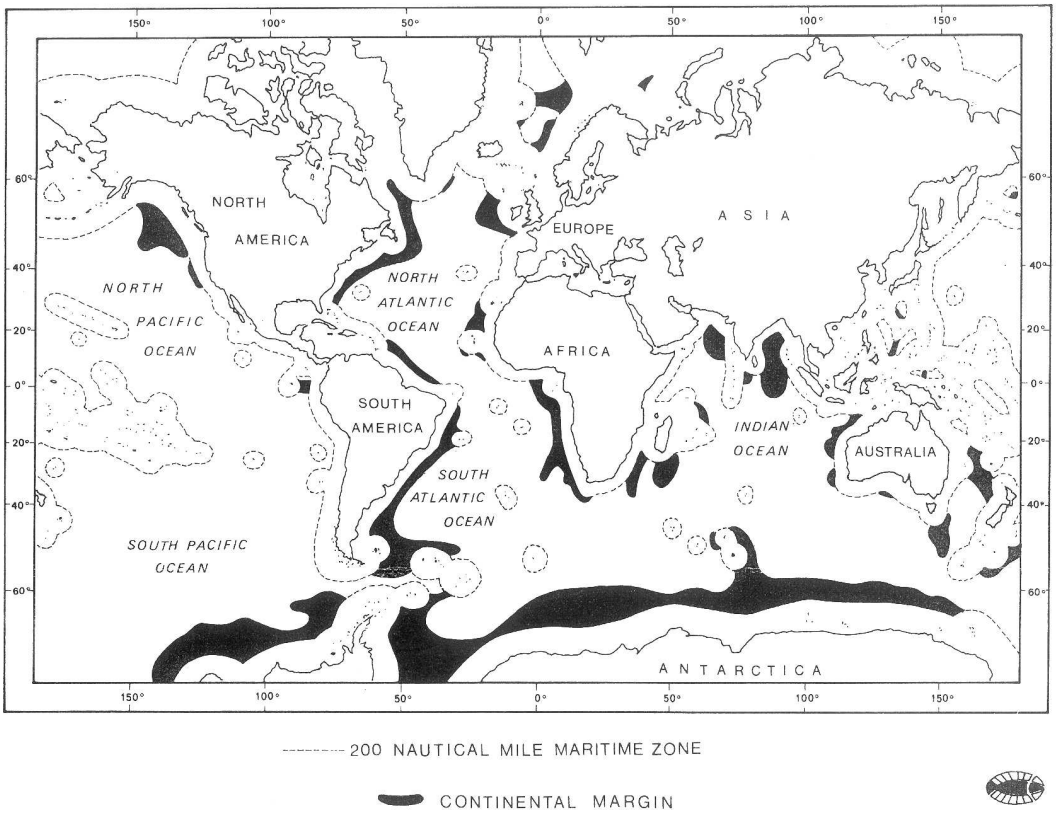

Figure 1.4: *Areas where the continental shelf extends beyond the 200M limit.*

UNCLOS, the onus exists to measure and prove continental shelf extension, according to strict criteria. One important criterion is the accurate numerical determination of the FoS as defined in the regulations, which is critical in defining the offshore claim extent. The scope of this thesis, therefore, is the determination of the FoS as defined by "... the point of maximum change in the gradient at its base."

Consideration of a mathematical method to determine the FoS excludes any geological considerations that may be included in the restrictions specified by the Convention. The focus of this thesis is on the curvature (a measure of the directional gradient) of the seafloor and how this may be used in the determination of the FoS. Further, a method for tracing of the foot line so obtained is put forth so as to make tracing feasible for computation purposes (from bathymetric data) and is not specifically designed to comply with all of the restrictions pertaining to the FoS as specified by the Convention.

Foot line determination within the South African desktop study is performed with use of the Caris Lots software suite of Caris (Pty. Ltd.) [5]. Within Caris Lots a set of lines are taken perpendicular to the coastal baseline of the relevant state. The two dimensional, cross–sectional profiles of the continental shelf corresponding to these lines are then examined by an operator, who chooses what is perceived as the best foot point. The foot points thus obtained for each profile are then joined by straight lines and the result is a subjectively chosen foot line. It is plausible to expect that a foot point chosen by one operator may differ greatly from that chosen by another. Furthermore, the set of lines chosen for specification of profiles to be considered is not necessarily optimum, and changing even one line (and thus profile) in the set could potentially change the foot line chosen and, as a result, the area of potential claim. The subjectivity of this method, and the lack of definite scientific backing for the foot line chosen, could potentially cause a loss of benefit for South Africa with regards to its claim. The generalised aim of any state's claim process is to maximize the area that it can claim by means of adequate scientific backing.

At this stage, scientific backing of a chosen foot line is restricted to hydrographic survey data (geographic variables in particular). Hydrographic surveys are costly and time consuming and the results from such surveys are not guaranteed to support the foot line chosen in Caris Lots.

The main drive behind the proposition of this thesis was to ascertain whether a more objective and mathematically based method of computation of the FoS was possible and, if so, whether it would be beneficial to the claim process. Benefit, in this sense, is seen as a mathematically defendable maximization of the area proposed for claiming purposes. Taking advantage of the high resolution grids of recent bathymetric data and applying a spatial analysis method, a FoS can indeed be determined in a mathematical sense. With this in mind, the specific objectives of this thesis are:

I Formalising a mathematical method to determine the maximum gradient at the base of the continental slope.

II Application of the method established in I to South African one and two minute gridded bathymetric data.

III Establishing a method to trace the line of foot points obtained in I.

IV Application of the method in III to the results obtained in II.

V Comparison of the resulting foot lines for the one and two minute bathymetric data to give an indication of how data resolution impacts on the method established in I.

VI Comparison of the results in IV to example foot lines, chosen in Caris Lots (similar to what could be chosen during the current South African desktop study), to give an indication of the feasibility of mathematical methods as an alternative with respect to optimization of the extent of the area claimed.

This thesis serves as an independent investigation into methods that might contribute to a more defendable and beneficial claim. Although the research involved in this thesis is running concurrently with the desktop study, the work is not included in the official portfolio of the Working Group. Should the results of this thesis be feasible, suitable and defendable they will be considered for inclusion in the Working Group's portfolio of tools for use in the claim process. Should further work be required before the results can be of use to the claim process, this thesis will form the basis of motivation for such work. This thesis was funded independently by the Institute for Maritime Technology and therefore has no responsibility to the South African claim process and is not defined as a deliverable for the project.

To the best of the author's knowledge, this is the first time bathymetric data of South Africa has been represented three dimensionally for the process of a mathematically based determination of the FoS.

1.4 The Structure of this Thesis

The geomorphologic aspects of the seafloor are discussed in Chapter 2. A description of different margin types, and the impact of these types on the morphology of a margin, are provided in addition to a brief summary of the application of margin types to Article 76. The information offered in Chapter 2 is to provide background to the reader, and is not used in the mathematical approach of the rest of the thesis.

Two mathematical methods to determine the FoS were identified during research for this thesis. The first method was that of Vaníček and Ou [38], published in 1994. The second method was by Bennet [4], published in 1998, and detailing a generalisation and alternative approach to the method proposed by Vaníček and Ou. The generalisation was as a result of the perceived drawbacks of the work of Vaníček and Ou, which in this thesis are hypothesised to be as a result of the poor resolution of data available at the time of publication. As a result of this hypothesis only the method of Vaníček and Ou is considered in this thesis and, in Chapter 3, the Survey of Literature is combined with the mathematical background necessary for the discussion of this method. The chapter details the computation of the surfaces of extremal curvature and the method is then applied to two hypothetical seafloor surfaces, as an example of the working of the method, by means of both analytical and numerical techniques.

The data to be used in this thesis is the topic of Chapter 4. The chapter opens with a discussion of the background and details of factors influencing data generated by a land (or sea) survey. The necessary processing of the raw data required to achieve a format suitable for computational methods is then explored, inclusive of a discussion of the source of the data and the intermediate processing stages. Finally, the data themselves are introduced and graphical representation of the data is provided.

In Chapter 5 the method for determining the surface of maximum curvature, established in Chapter 3, is applied to the bathymetric data sets introduced in Chapter 4. A method to trace the ridge formed on the surface of maximum curvature is then discussed and applied to the two hypothetical seafloor surfaces used as examples in Chapter 3, in addition to the surfaces of maximum curvature obtained for the bathymetric data sets. The traced ridge lines define the FoS for their respective data sets (areas). A comparison between the foot lines obtained for the one and two minute data sets is then discussed and the implications of the comparison results with respect to the effects of data resolution on the effectiveness of the methods noted. The chapter closes with a comparison of the computed foot lines for the one minute data and the example foot lines chosen in Caris Lots for the specific data sets (areas). The result of this comparison is then used as a reference for the debate as to the benefit offered by each method of foot line determination.

Conclusions and final remarks, in addition to a discussion of unresolved problems and potential future extensions of and improvements to this work are offered in Chapter 6.

Chapter 2

Geographical Background

The continents and the oceans are the two major features of the Earth, with the oceans consisting of approximately 70% of the Earth's area. The appearance of the oceans is a combination of geomorphic and geological characteristics which, in turn, are a function of tectonic, magmatic and sedimentary history. This chapter serves to provide the reader with a general background of some of the more important issues relating to Article 76 of UNCLOS with respect to geomorphic, geological and geodetic concepts. Although the information to follow is of great importance in the claim process as a whole, only a small portion of the geomorphic concepts have a direct impact on the results of and methodology in this thesis. Most of the definitions provided in Article 76 are a combination of legal, geomorphological, geological and geodetic concepts. For example, the legal definition of the continental shelf is not the same as the morphologically defined continental shelf of a geographer.

Methods to locate the FoS, other than that contained in the Article 76 definition of the point of maximum change in gradient, include the use of various features and characteristics of continental margins to argue for a particular FoS. Therefore, for purposes of thoroughness in introducing the project as a whole, this chapter aims to introduce and give a brief summary of some of the features and characteristics of continental margins and how they may be used to compliment or change the mathematically derived FoS location.

2.1 Article 76 and the FoS

Article 76 of UNCLOS refers to the "natural prolongation of the land" and defines the position of the FoS to lie on the outer limit of the prolongation. There are two ways to perceive natural prolongation of the land — through the eyes of either a geologist or a geomorphologist. The geomorphologist sees the natural prolongation of land to consist of the three sections as discussed in Chapter 1, namely the shelf, slope and rise (depicted in Figure 1.1); whereas the geological viewpoint consists of a combination of geomorphic concepts, including seabed and subsoil. In other words, the geologist considers the material of which the seafloor and subsoil consists, in addition to the general appearance of the margin. It is important, however, to note that although the geomorphic outer limit for prolongation is the edge of the rise, this is not the FoS according to Article 76. Geologically the rise normally forms over the primary tectonic boundary or transition zone, meaning the boundary between continental and oceanic crust, which is considered the geological outer limit of natural prolongation of the land. Article 76 defines the FoS as the outer limit of geological prolongation and not in geomorphic terms. This complexity is due to the fact that the geological view of natural prolongation is embraced in Article 76, although the Article largely adopts a geomorphic approach to define it. The reader is referred to Figure 2.1 for a schematic representation of the two views of a continental margin.

As may be seen in Figure 2.1, the geomorphic view of a margin constitutes purely the appearance of the sections of the margin and the form they take as a whole. The geological viewpoint, on the other hand, not only includes the appearance of the margin, but also embraces the specific sediment and

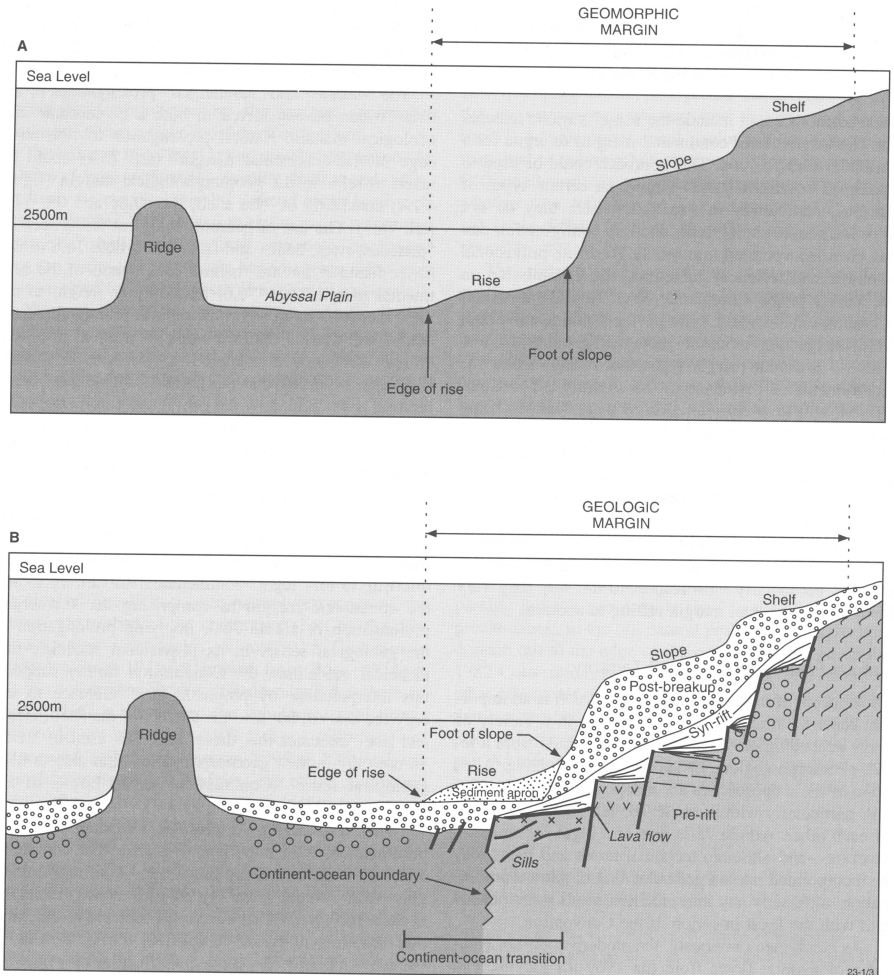

Figure 2.1: *Schematic profiles across a continental margin showing (A) the geomorphological and (B) the geological view of what constitutes a margin [7].*

lithotype associated with each section of the margin in combination with the underlying tectonic form and structure.

2.2 Continental Margins

Continental margins underlie about 28% of the total area of the oceans and consist of three sections labelled according to increasing offshore depth (or distance), namely the *shelf, slope* and *rise*. The classification of margins into a shelf, a slope and a rise refers largely to the type of margins found in the Atlantic Ocean. Continental margins along the Pacific coast generally consist of a shelf and a slope that ends in a deep trench. The reader is referred to Figure 2.2 for a graphic representation of such margins. The environment, however, is not uniform and does not prescribe to one standard or idealized form of margin classification and thus continental margins can be complex, incorporating saddles, plateaus and terraces, as shown in Figure 2.3. This is largely due to varying rates of continental derived (and pelagic) sedimentation, erosion, flooding, slumping and many other seafloor metamorphic processes that occur over millions of years. In general a continental margin has both simple and complex sections, invariably with transition zones. This makes it imperative, in calculations of the position of the FoS, to be able to identify the different areas of a margin, in order to prevent mistaking a saddle or terrace as part of a possible FoS (perhaps due to not sampling to adequate depths). The continental rise, bordering the foot

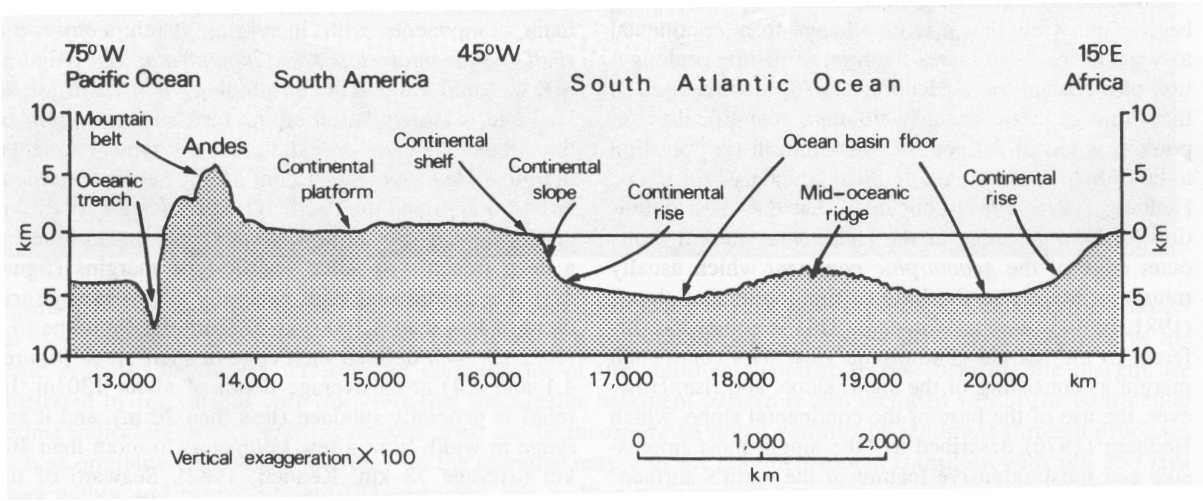

Figure 2.2: *Schematic profile from the Pacific Ocean off western South America across the Atlantic Ocean to the west coast of Africa at the Tropic of Cancer. Note that the curvature of the earth is not shown [7].*

of the slope, is a depositional feature caused by the accumulation of sediment from the continent that was transported down and along the slope and thus should be identified not only by its gradient and surface texture, but by aspects such as sediment thickness and underlying seabed characteristics (see Figure 2.1 (B)). Another generalized method of determining the approximate location of the continental rise is by examining vertical profiles of the seafloor, such as those shown in Figure 2.1.

Three main classifications of margins are known to exist, namely the *active* or *Pacific–type margins*, the *passive* or *Atlantic–type margins* and *Transform margins*. Active margins are associated with intense earthquake and volcanic activity and are known as sites of oceanic crust destruction (plates coming together). Passive margins are associated with little seismic and volcanic activity and are known as sites of oceanic crust creation and the formation of new ocean basins (plates moving apart). Active, Passive and Transform margins are referred to by many names, depending on the characteristics focussed on in the discussion. To summarise the different names, the three main classifications of margins are:

1 Divergent, Rifted, Passive, Aseismic or Atlantic.

2 Convergent, Active, Seismic or Pacific.

3 Transform, Translational, Sheared.

Transform margins are a lesser classification and may occur in both convergent and divergent settings, hence transform margins will be discussed mainly in the divergent setting later in this chapter. The reader is referred to Figure 2.4 for an indication of the different margin types found around the world. Mainly transform–sheared and divergent–rifted margin types occur in South Africa's offshore region.

2.2.1 Divergent Margins

Divergent margins are formed by deformation and modification (rifting) of continental lithosphere and mark the first event in the formation of a major ocean basin. The margin is the site of active divergent plate tectonic processes and is thus the area from which the basin grows. There are essentially three types of divergent margins, namely: Non–volcanic, Volcanic and Transform divergent margins.

Divergent margins differ in width and symmetry, with rifts in older, stable lithosphere being narrower and simpler and those found in areas of change broader with more complex geometries. Plate kinematics, initial rift and plate geometry during the transition from rifting to seafloor spreading significantly influence margin evolution, style and geometry [9]. Plate motion more or less perpendicular to the rift axis

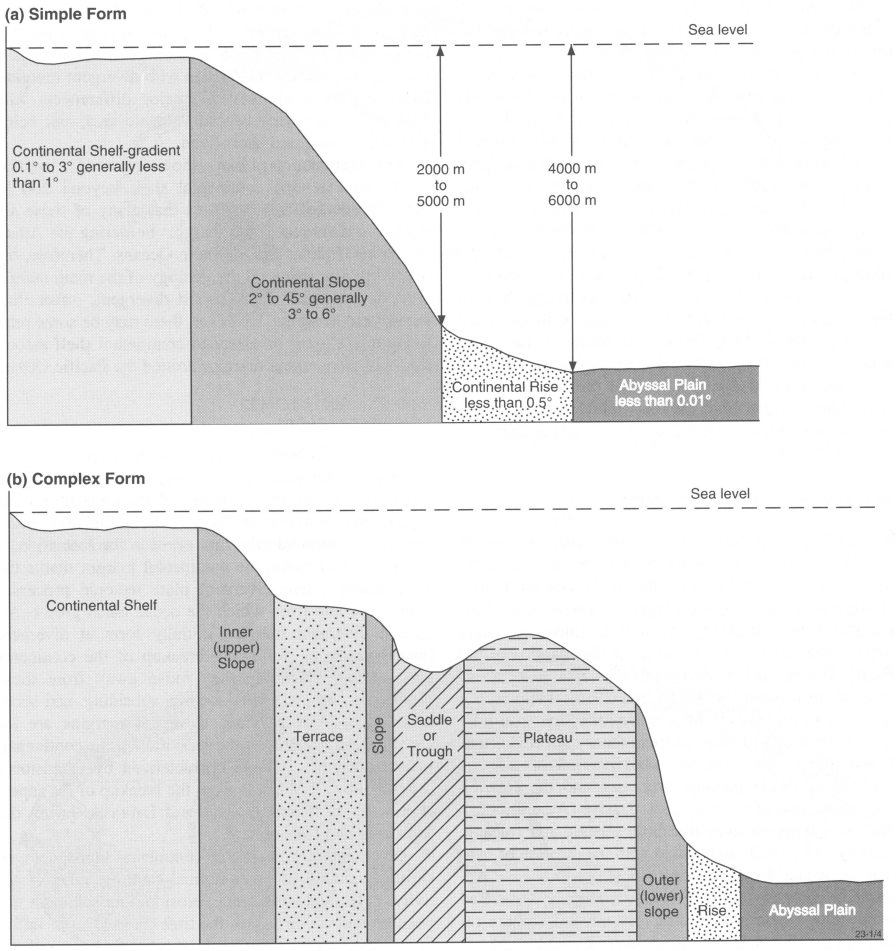

Figure 2.3: *Generalised cross sections showing the seafloor morphology and gradients associated with (a) simple and (b) complex continental margins [7].*

will typically produce opposing, divergent margins on each side of a midoceanic ridge, representing about 70 – 75% of the divergent margins around the world. Non–volcanic rifted margins, in particular, are of extreme economic importance as a result of their significant hydrocarbon potential, already explored and exploited in many areas of the world. With this in mind, about 70% of the Atlantic Ocean's rift margins are volcanic according to a presentation at the 1997 Volcanic Margin Workshop in Potsdam [7], and so far exploration of volcanic margins has had variable success.

Non–volcanic Rifted Margins

A continental margin is formed when, in an intracontinental rift system, two diverging pieces of lithosphere are separated by a seafloor spreading centre, creating new oceanic crust and thus a new plate boundary. The development of a non–volcanic rifted margin may be summarised in three phases:

Rifting. This includes simple shear in the upper crust (and possibly upper mantle) with associated syndrift deposition and stretching/thinning of the lower crust and upper mantle by pure shear.

Breakup (or the onset of drifting). This includes the processes associated with the initial emplacement of oceanic crust and the formation of a new ocean basin by means of the start of "normal" seafloor spreading.

Postbreakup (or postdrift). This involves lithosphere cooling and thermal subsidence as the spreading ridge moves away from the margin.

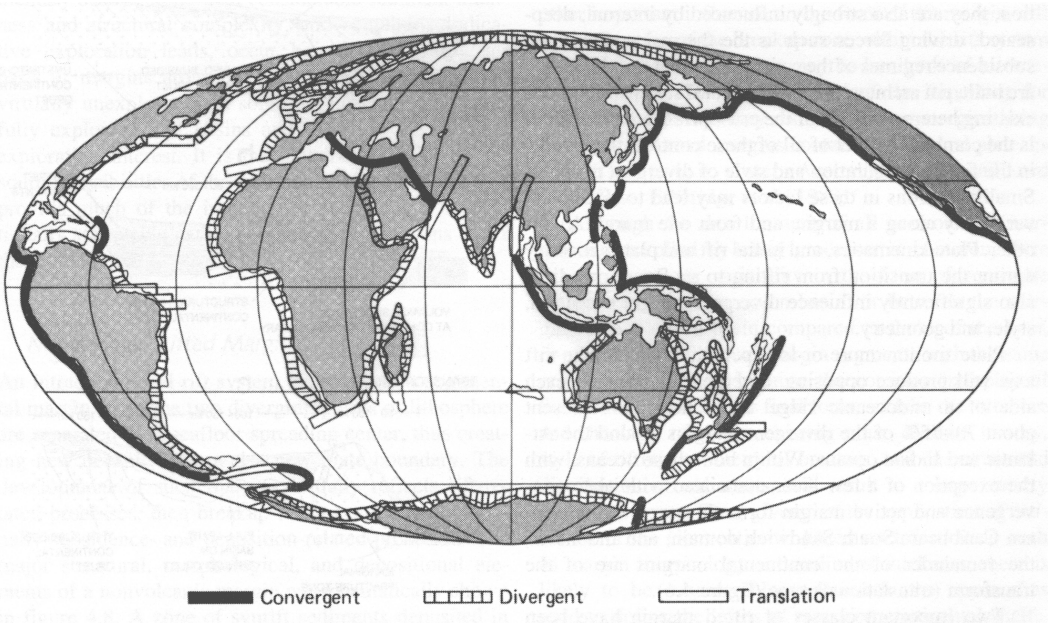

Figure 2.4: *Generalised distribution of divergent, convergent and translation margins around the world [7].*

The development of non–volcanic and volcanic margins may be very similar until the time of breakup, from when the differences are vastly evident. The final morphology of the margin is largely influenced by the amount of postdrift sedimentation — however, if the margin was originally sediment poor, then the original morphology of the rift will remain the main influence. The structure and interplay of the pre–existing crust influences how the margin forms, thus neighbouring margins may display marked differences despite the fact that they are in the same area.

Sediment rich non–volcanic margins occur off the eastern United States, northwest Africa, both sides of the South Atlantic and off northwest Australia. These margins generally have well developed continental rises and are therefore good candidates for the extension of the "legal" continental shelf past the 200M boundary.

Volcanic Rifted Margins

A large proportion of the world's divergent rifted continental margins shows signs of large–scale magmatic activity attributed to the breakup of continents and the formation of oceanic basins. The activity is manifested in extensive volcanism, both above sea level and in shallow waters, centred along the line of continental breakup. The magmatic activity takes place during the final stages of continental thinning and beginning phases of seafloor spreading. As the excess volcanism abates, the main feeder system subsides to become a midoceanic ridge that produces new crust, and the young ocean grows wider and deepens. Therefore indicators of breakup volcanism may be found on the outer margin through subsurface geological records [13].

The distinction between volcanic and non–volcanic margins is relatively new and as a result did not play a role in the consideration of continental margins during the development of UNCLOS. The episodic, massive melting associated with volcanic rifted margins is commonly related to so–called *hot spot activity*; that is, thermal plumes arising from deep within the Earth. When a plume head impacts on the lithosphere, during continental thinning and rifting, enhanced short lived melting takes place during continental breakup, initiating a volcanic margin [7].

Early seismic profiles on some rifted margins have revealed that the rough oceanic basement surface had changed, in a landward direction, into a smooth opaque horizon that covers the transition zone between oceanic and continental crust. Many margins may be considered intermediate cases relative to

the volcanic and non–volcanic end members, typified by the north eastern Atlantic and Bay of Biscay margins respectively [7]. The reader is referred to Figure 2.5 for a graphical representation of the global distribution of volcanic rifted margins.

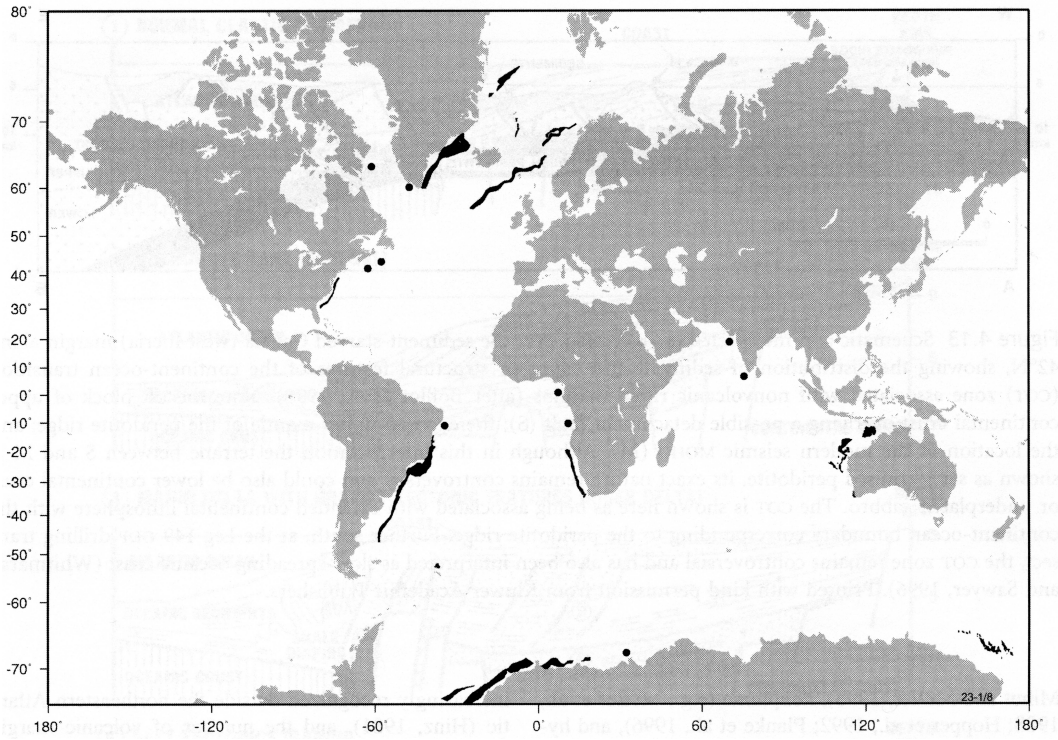

Figure 2.5*: Global distribution of volcanic rifted margin segments based on reported observations of seaward dipping reflector sequences in seismic data [7].*

Transform Margins

Plate tectonic motion is more or less orthogonal to the rift system and the point of origin of breakup creates divergent rifted margins, as commonly seen in the Atlantic and Indian Oceans. In some places these rifted margin segments are linked by margins where the point of origin of breakup is more or less parallel to the initial plate motions between continents that are moving apart. Margins formed in this manner are called *transform* or *rift–transform margins*. Transform margins attribute many of their morphological, crustal and sedimentary characteristics to the pronounced contrast between the continental domain and the nearby younger oceanic crust. Large segments of transform margins may now be found around the Atlantic, Indian and Southern Oceans and are thought to constitute about 20% of divergent margins [33].

Transform margins possess distinctive morphological characteristics such as strong linearity and large scale margin-parallel ridges (called *marginal ridges*) [7]. The resultant steep continental slopes typically preclude substantial sedimentary deposition and therefore represent geological scars resulting from the transcurrent movement between the separating continents. An important distinction between the divergent margin types is that where rifted margin basins form a subsiding feature, basins adjacent to transform margin ridges are high–standing and partly eroded. The transition from continental to oceanic crust at transform margins typically appears to be quite abrupt (and therefore narrow). Transform margins are margins where the limits of natural prolongation of the continent should be well defined and the application of Article 76 of UNCLOS will likely become complicated. In the South African case, the southern shelf exhibits transform margin properties, with complex portions such as the Agulhas Plateau, Agulhas Passage and Mozambique Ridge.

2.2.2 Convergent Margins

When two converging tectonic plates intersect, the common result is that one of the plates will be subducted down into the Earth's interior. This deformation and destruction of crust mark the boundaries between the two converging plates and, further, the convergent margin. Where a divergent margin and the adjacent ocean floor belong to the same tectonic plate, the convergent margin and the adjacent ocean floor belong to different tectonic plates. There are a variety of crustal interactions that can take place at a convergent margin. These interactions include oceanic crust underthrusting continental crust (or modified ocean crust) — both of which have at times been referred to as *B (Benioff)–subduction* — and the so–called *A–subduction*, where one piece of continental crust is underthrust by another piece of continental crust (commonly as a result of continental collision). Convergent margins may thus be associated with oceanic trenches, volcanic arcs (and backarc basins) or orogenic mountain ranges, depending on the nature of the crustal interaction experienced. As a result of these crustal interactions, the various convergent plate boundaries are characterised by shallow to deep earthquakes as well as volcanism, crustal deformation, metamorphism and, in places, extension [13]. Convergent margins are referred to as *active* or *seismic margins* as a direct result of these characteristics, and form a large portion of the margins around the Pacific Ocean, as well as parts of the Southern Atlantic Ocean, the northeast Indian Ocean and the Southwest Pacific region.

The transition between continental crust and oceanic crust at a convergent margin is, to a greater extent, decisively more complex and variable than the transition found on divergent margins. As mentioned previously, the morphology of a typical Pacific active margin consists of a continental shelf and slope, that drops off abruptly on the seaward side in a trough or trench. The morphology of the continental margin, in particular the deep trench, hinders the transport of sediment from the landmass to the deep oceans and, as a direct result, sediment accumulation on the slope of the margin has been recorded as being less than that for a divergent margin. There is also a general absence of a continental rise as a result of the blocking of sediment transport across the trench, further offshore. The complex interrelationships of structural, sedimentary and volcanic processes to which convergent margins are subject ensure a great range in the margin types, features and characteristics found.

The nature of the interaction between the two converging plates — subduction or collision — may be used to classify two main types of convergent margins. *Subduction type margins* are the most prolific and may be found around much of the Pacific Ocean, in south east Asia and the Caribbean. *Collision type margins* occur, for example, between Australia-Indonesia and Australia-New Guinea and vary along the point of contact of the collision zone from continent-continent to continent-arc and continent-ocean interactions.

Subduction-Type Margins

Subduction is the consumption of one piece of lithosphere beneath another adjacent segment, sometimes referred to as underthrusting. Convergent subduction margins are characterised by deep sea-trenches at their seaward (forearc) margins. A large portion of convergent margins have active volcanic arcs and many have rifted (backarc) basins behind the volcanic arc. Subduction type margins have high variability, in both morphology and sediment thickness. The foot of the continental slope (FoS) in the forearc lies within the trench, whereas the FoS in the backarc is the major change in slope from the arc region to the backarc basin floor and as such is more difficult to define [7].

1 *Forearcs*

  At the seaward edge of the frontal thrust of the plate subduction, there is a major change in slope — corresponding to the transition from the overthrusting to the underthrusting plate — to which the FoS should correspond. The overall width (between the volcanic arc and the trench) of the forearc may be greater than 300km. This entire forearc region should be considered part of the continental shelf/slope/rise as a result of sediment thickness, basement type and morphology [13].

2 *Backarc Basins*

  Rifting near the active volcanic arc of convergent margins results in the formation of backarc basins. The FoS definition of a typical divergent margin, with the added complexity of active volcanoes on

the one side and a remnant arc on the other, should give a good approximation to the definition of the FoS for a backarc basin. Seafloor spreading processes are largely responsible for the generation of backarc basins and as a direct result the crust of a backarc basin is very similar to that of oceanic crust [34].

Collision-Type Margins

Collision of topographic/structural features on the subducting plate (such as continental margins, arc systems, ridges and seamounts) significantly alter the position of the FoS and the sediment thickness on convergent margins. Prior to collision a convergent margin would have one of the forms described previously, with the only variation being significant differences in sediment thickness and type. When topographic irregularities, or large amounts of sediment, enter the trench it results in the modification of the forearc. For example, the foot of the Chinese continental slope is deflected around Taiwan, with Taiwan being a collision complex that is now an extension of the geomorphic continental shelf [7].

2.3 Continental Margins and the Application of Article 76

There are several indirect approaches that may be used to determine the end of natural land prolongation, as defined by Article 76 of UNCLOS:

- The general relationship of parts of the continental margin to various isobaths may be identified and used to compliment the mathematical computation of the FoS. If one has a general idea of the isobath that corresponds to the slope or the rise, then the effort to find the FoS could be concentrated on those isobaths — possibly resulting in a reduction of computation and analysis required.
- The physiography of the margin, which is related to crustal type, subsidence history, structural style and sediment supply may be researched, giving an indication as to areas where an extension of the continental shelf would most likely be.
- The gravitational field, from which a general estimate of crustal thickness, and possibly crustal type, may be obtained, as well as the seismic velocity structure of the crust as determined by seismic refraction (and wide angle reflection studies), the change in seismic reflection character of continental and oceanic crust and the termination of linear seafloor spreading magnetic anomalies, which are related to the formation of oceanic crust, commonly in the general vicinity of the Continent–Ocean Boundary (COB). These data would assist in the approximation of ocean–continent boundaries and thus give a more educated estimate as to the location of the FoS relative to the transition zone.
- Purely legal definitions based on the distances from baselines, water depth, morphology, sediment thickness, or combinations of these factors, may be employed to confirm an estimated FoS, to motivate the need for further sampling or motivate a change to the computed FoS in a seaward direction.

In terms of the determination of the FoS, the following is likely to occur: on sediment starved non–volcanic or volcanic rifted margins, morphology is largely controlled by rift architecture and volcanism respectively. The FoS is likely to overlie either extended continental crust or the Continent Ocean Transition Zone (COT) on non–volcanic margins and transitional volcanic margin crust on volcanic margins. The underlying control will generally mean that the FoS location is relatively easy to determine. However, on sediment-rich rifted margins, morphology is controlled by the interplay of sedimentation and flexural loading. As the sediment apron (continental rise) builds out and up, and margin declivity reduces, the FoS location tends to shallow and lie further landward of the edge of the rise. In these situations the determination of the position of the FoS may be difficult and open to subjectivity. On rift transform margins, FoS determination is a relatively simple matter, due to the steep slopes and narrow COT [7].

As mentioned in Chapter 1, the "evidence to the contrary" approach may be used to argue for a particular FoS position other than that defined by the "maximum change in gradient at its base." This would imply that the FoS lies in a zone of possible positions, but is not the conventional choice. The Commission's provisional guidelines imply that subsurface information can be used in the identification of the FoS where "the rule of maximum change in gradient would not, for example, equate to the limit of the geological margin." However, in legal terms this places a heavy burden of supplying evidence and will have to be researched well and be entirely convincing, from a technical point of view.

The divergent non–volcanic and volcanic rifted margins of the Atlantic, Arctic and Indian Oceans provide by far the greatest potential contribution to the global area of extended continental shelf, with only minor contributions from the convergent margins of the Pacific. A good understanding of the evolution and characteristics of the various margin types is vital to optimize the outer limit of the continental shelf. This is particularly true in places where unconventional interpretations are employed under the "evidence to the contrary" provision and where there are specific issues related to the determination of the FoS and the use of the 2500m isobath cutoff [7].

Chapter 3

Maximum Curvature Computation

In the previous chapter the different classifications of continental margins (and their associated characteristics) were discussed. The chapter was included to highlight the complex nature of determination of the FoS and that a determination relying on geological support carries with it the heavy burden of well researched and convincing evidence. The processes required to collect and interpret this evidence are costly and time–consuming and as a result it is hoped that a mathematical method to determine the FoS would provide adequate scientific support to the choice of a foot line, consequently reducing the amount of geological evidence required to ensure claim success.

Methods for the objective computation of the FoS are not abundant. In fact, to the best knowledge of the author, there have only been two mathematical papers published on the topic. The method proposed by Vaniček and Ou [38] in 1994, was the first exploration of the topic and the second method, published by Bennett [4] in 1998, was a closer look at the problem as a direct result of the perceived drawbacks and shortcomings of the work of Vaniček and Ou. Bennett's work is essentially a generalisation and re–formulation of the method proposed by Vaniček and Ou. The author's hypothesis is that the perceived shortcomings of Vaniček and Ou's method were, to a greater extent, a result of the poor data resolution available at the time of the method's development. It is only recently that the higher resolution one and two minute bathymetric data sets have become available, extensively reducing the coarseness of the five minute data that was explored by Vaniček and Ou and by Bennett. For this reason, the author undertook to examine only the original work proposed by Vaniček and Ou.

3.1 The Gaussian Fundamental Forms of the Seafloor

Since the change of the gradient of a surface is measured by its the curvature, Vaniček and Ou simplified the definition of the foot line of a continental shelf by assuming that it corresponds to the ridge line formed by the maximum curvature of the seafloor. The seafloor may be expressed as a continuous function of horizontal position (x, y) by writing $z = z(x, y)$, where z denotes the depth of the sea at position (x, y). Hence the surface of the sea is given by the plane $z(x, y) = 0$. Let the position of a point P on the seafloor be given by the position vector

$$\underline{r}(x, y) = x\underline{i} + y\underline{j} + z(x, y)\underline{k},$$

where $\underline{i}, \underline{j}$ and $\underline{k}$ are unit vectors in the x-, y- and z-directions respectively. Also consider another point P' on the seafloor with position vector $\underline{r} + d\underline{r}$ and let $\mathcal{C}$ be the shortest curve between P and P' along the seafloor, parameterised by the seafloor arclength parameter s. Then

$$\underline{t} = \frac{d\underline{r}}{ds}$$

is a unit vector tangential to $\mathcal{C}$ at P in the limit as $\|d\underline{r}\| \to 0$ and the *curvature* of $\mathcal{C}$ at P is defined as

$$\kappa = \left\| \frac{d\underline{t}}{ds} \right\|. \tag{3.1}$$

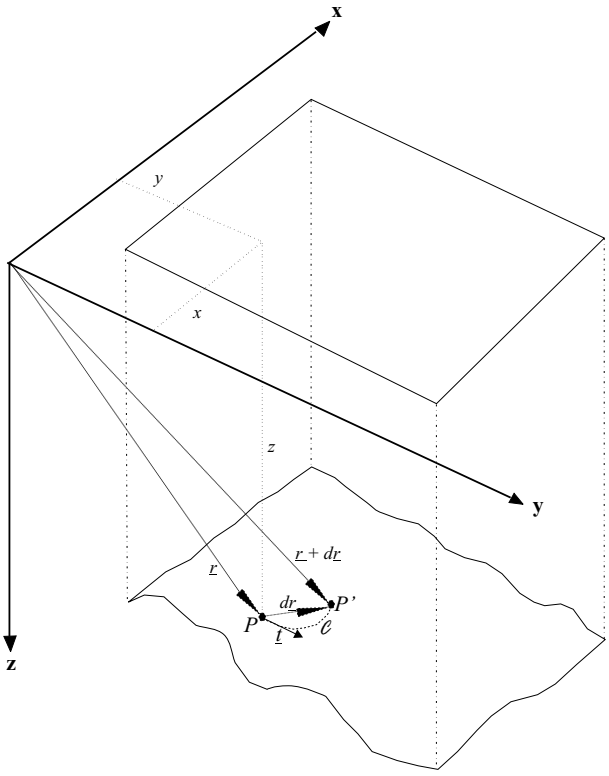

Figure 3.1: *A point P on the seafloor and the corresponding vectors.*

Since $\underline{t}$ has constant length it follows that $\frac{d\underline{t}}{ds}$ is orthogonal to $\underline{t}$ and may hence be written as

$$\frac{d\underline{t}}{ds} = \kappa \underline{n} \tag{3.2}$$

by (3.1), where $\underline{n}$ is a unit vector orthogonal to $\underline{t}$ and in the plane of $\mathcal{C}$ at P, called the *principal normal* to $\mathcal{C}$ at P. Another unit vector orthogonal to $\underline{t}$, but also orthogonal to the plane of $\mathcal{C}$ at P, may be found by taking the vector product

$$\underline{b} = \underline{t} \times \underline{n}.$$

The vector $\underline{b}$ is known as the *unit bi-normal* to $\mathcal{C}$ at P. Since $\underline{b}$ has constant length, $\frac{d\underline{b}}{ds}$ must be orthogonal to $\underline{b}$. But, since $\underline{t} \cdot \underline{b} = 0$, it also follows that

$$\underline{t} \cdot \frac{d\underline{b}}{ds} + \frac{d\underline{t}}{ds} \cdot \underline{b} = \underline{t} \cdot \frac{d\underline{b}}{ds} + \kappa \underbrace{(\underline{n} \cdot \underline{b})}_{=0} = 0$$

and hence $\frac{d\underline{b}}{ds}$ is also orthogonal to $\underline{t}$. Consequently $\frac{d\underline{b}}{ds}$ must be in the direction of $\underline{n}$ and may thus be written as

$$\frac{d\underline{b}}{ds} = \alpha \underline{n}, \tag{3.3}$$

for some $\alpha \in \mathbb{R}$. The torsion of $\mathcal{C}$ at the point P is defined as

$$\tau = -\underbrace{\left\| \frac{d\underline{b}}{ds} \right\|}_{=\alpha}$$

and hence (3.3) may be rewritten as

$$\frac{d\underline{b}}{ds} = -\tau \underline{n}. \tag{3.4}$$

Finally,

$$\begin{aligned}\frac{d\underline{n}}{ds} &= \frac{d}{ds}\left(\underline{b}\times\underline{t}\right)\\ &= \underline{b}\times\frac{d\underline{t}}{ds}+\frac{d\underline{b}}{ds}\times\underline{t}\\ &= \underline{b}\times(\kappa\underline{n})+(-\tau\underline{n})\times\underline{t}\\ &= \kappa\left(\underline{b}\times\underline{n}\right)-\tau\left(\underline{n}\times\underline{t}\right)\\ &= \tau\underline{b}-\kappa\underline{t}\end{aligned} \tag{3.5}$$

by utilization of (3.1), (3.2) and (3.4). Equations (3.1), (3.4) and (3.5) are known as the *Frenet-Serret equations* of $\mathcal{C}$, and may be summarised in matrix form as

$$\frac{d}{ds}\begin{bmatrix}\underline{t}\\ \underline{b}\\ \underline{n}\end{bmatrix}=\begin{bmatrix}0 & 0 & \kappa\\ 0 & 0 & -\tau\\ -\kappa & \tau & 0\end{bmatrix}\begin{bmatrix}\underline{t}\\ \underline{b}\\ \underline{n}\end{bmatrix}.$$

In the limit as $\|d\underline{r}\|\to 0$ the square of the magnitude of the rate of change of the difference vector $d\underline{r}$ between the two points, P and P', along the sea floor is given by

$$\begin{aligned}\left(\frac{ds}{ds}\right)^2 &= \left\|\frac{d\underline{r}}{ds}\right\|^2\\ &= \frac{d\underline{r}}{ds}\cdot\frac{d\underline{r}}{ds}\\ &= \left(\frac{dx}{ds}\underline{i}+\frac{dy}{ds}\underline{j}+\frac{dz(x,y)}{ds}\underline{k}\right)\cdot\left(\frac{dx}{ds}\underline{i}+\frac{dy}{ds}\underline{j}+\frac{dz(x,y)}{ds}\underline{k}\right)\\ &= \left(\frac{dx}{ds}\right)^2+\left(\frac{dy}{ds}\right)^2+\left(\frac{dz(x,y)}{ds}\right)^2\\ &= \left(\frac{dx}{ds}\right)^2+\left(\frac{dy}{ds}\right)^2+\left(\frac{\partial z}{\partial x}\frac{dx}{ds}+\frac{\partial z}{\partial y}\frac{dy}{ds}\right)^2\\ &= \left(\frac{dx}{ds}\right)^2+\left(\frac{dy}{ds}\right)^2+\left(\frac{\partial z}{\partial x}\frac{dx}{ds}\right)^2+2\frac{\partial z}{\partial x}\frac{\partial z}{\partial y}\frac{dx}{ds}\frac{dy}{ds}+\left(\frac{\partial z}{\partial y}\frac{dy}{ds}\right)^2\\ &= \left[1+\left(\frac{\partial z}{\partial x}\right)^2\right]\left(\frac{dx}{ds}\right)^2+2\left[\left(\frac{\partial z}{\partial x}\right)\left(\frac{\partial z}{\partial y}\right)\right]\frac{dx}{ds}\frac{dy}{ds}+\left[1+\left(\frac{\partial z}{\partial y}\right)^2\right]\left(\frac{dy}{ds}\right)^2\\ &= E\left(\frac{dx}{ds}\right)^2+2F\frac{dx}{ds}\frac{dy}{ds}+G\left(\frac{dy}{ds}\right)^2,\end{aligned} \tag{3.6}$$

after repeated application of the chain rule, where ds is the arc distance between the points P and P' measured along the seafloor as before, and where

$$E=1+\left(\frac{\partial z}{\partial x}\right)^2,\quad F=\left(\frac{\partial z}{\partial x}\right)\left(\frac{\partial z}{\partial y}\right),\quad G=1+\left(\frac{\partial z}{\partial y}\right)^2. \tag{3.7}$$

The identity (3.6) may be rewritten as

$$E\left(\frac{dx}{ds}\right)^2+2F\frac{dx}{ds}\frac{dy}{ds}+G\left(\frac{dy}{ds}\right)^2=1, \tag{3.8}$$

which is known as the *first Gaussian fundamental form* of the seafloor. Furthermore, the pair $\left[\frac{dx}{ds},\frac{dy}{ds}\right]$ are the components of a unit vector in the tangent plane to the sea floor at the point P. It follows that

$$\begin{aligned}\kappa\underline{n} &= \frac{d\underline{t}}{ds}\\ &= \frac{d^2\underline{r}}{ds^2}\end{aligned}$$

$$
\begin{aligned}
&= \frac{d}{ds}\left(\frac{\partial \underline{r}}{\partial x}\frac{dx}{ds}+\frac{\partial \underline{r}}{\partial y}\frac{dy}{ds}\right)\\
&= \frac{\partial \underline{r}}{\partial x}\frac{d^2x}{ds^2}+\frac{d}{ds}\left(\frac{\partial \underline{r}}{\partial x}\right)\frac{dx}{ds}+\frac{\partial \underline{r}}{\partial y}\frac{d^2y}{ds^2}+\frac{d}{ds}\left(\frac{\partial \underline{r}}{\partial y}\right)\frac{dy}{ds}\\
&= \left[\frac{\partial}{\partial x}\left(\frac{\partial \underline{r}}{\partial x}\right)\frac{dx}{ds}+\frac{\partial}{\partial y}\left(\frac{\partial \underline{r}}{\partial x}\right)\frac{dy}{ds}\right]\frac{dx}{ds}+\frac{\partial \underline{r}}{\partial x}\frac{d^2x}{ds^2}+\left[\frac{\partial}{\partial x}\left(\frac{\partial \underline{r}}{\partial y}\right)\frac{dx}{ds}+\frac{\partial}{\partial y}\left(\frac{\partial \underline{r}}{\partial y}\right)\frac{dy}{ds}\right]\frac{dy}{ds}+\frac{\partial \underline{r}}{\partial y}\frac{d^2y}{ds^2}\\
&= \frac{\partial^2 \underline{r}}{\partial x^2}\left(\frac{dx}{ds}\right)^2+2\frac{\partial^2 \underline{r}}{\partial x\partial y}\left(\frac{dx}{ds}\right)\left(\frac{dy}{ds}\right)+\frac{\partial^2 \underline{r}}{\partial y^2}\left(\frac{dy}{ds}\right)^2+\frac{\partial \underline{r}}{\partial x}\frac{d^2x}{ds^2}+\frac{\partial \underline{r}}{\partial y}\frac{d^2y}{ds^2}
\end{aligned}
$$

again by repeated application of the chain rule. But $1=\|\underline{n}\|^2=\underline{n}\cdot\underline{n}$, so that

$$
\begin{aligned}
\kappa &= \kappa(\underline{n}\cdot\underline{n})\\
&= \underline{n}\cdot(\kappa\underline{n})\\
&= \left(\underline{n}\cdot\frac{\partial^2 \underline{r}}{\partial x^2}\right)\left(\frac{dx}{ds}\right)^2+2\left(\underline{n}\cdot\frac{\partial^2 \underline{r}}{\partial x\partial y}\right)\left(\frac{dx}{ds}\right)\left(\frac{dy}{ds}\right)+\left(\underline{n}\cdot\frac{\partial^2 \underline{r}}{\partial y^2}\right)\left(\frac{dy}{ds}\right)\\
&\quad+\left(\underline{n}\cdot\frac{\partial \underline{r}}{\partial x}\right)\left(\frac{d^2x}{ds^2}\right)+\left(\underline{n}\cdot\frac{\partial \underline{r}}{\partial y}\right)\left(\frac{d^2y}{ds^2}\right).
\end{aligned}
\tag{3.9}
$$

Since $\underline{n}$ is orthogonal to both $\frac{\partial \underline{r}}{\partial x}$ and $\frac{\partial \underline{r}}{\partial y}$ it follows that

$$
\left(\underline{n}\cdot\frac{\partial \underline{r}}{\partial x}\right)=0 \quad\text{and}\quad \left(\underline{n}\cdot\frac{\partial \underline{r}}{\partial y}\right)=0. \tag{3.10}
$$

Furthermore

$$
\frac{\partial^2 \underline{r}}{\partial x^2}=\left[0,0,\frac{\partial^2 z}{\partial x^2}\right],\quad \frac{\partial^2 \underline{r}}{\partial x\partial y}=\left[0,0,\frac{\partial^2 z}{\partial x\partial y}\right]\quad\text{and}\quad \frac{\partial^2 \underline{r}}{\partial y^2}=\left[0,0,\frac{\partial^2 z}{\partial y^2}\right], \tag{3.11}
$$

whilst

$$
\begin{aligned}
\underline{n} &= \left(\frac{\partial \underline{r}}{\partial x}\times\frac{\partial \underline{r}}{\partial y}\right)\Big/\left\|\frac{\partial \underline{r}}{\partial x}\times\frac{\partial \underline{r}}{\partial y}\right\|\\
&= \left(\left[1,0,\frac{\partial z}{\partial x}\right]\times\left[0,1,\frac{\partial z}{\partial y}\right]\right)\Big/\left\|\left[1,0,\frac{\partial z}{\partial x}\right]\times\left[0,1,\frac{\partial z}{\partial y}\right]\right\|\\
&= \left|\begin{array}{ccc}\underline{i} & \underline{j} & \underline{k}\\ 1 & 0 & \frac{\partial z}{\partial x}\\ 0 & 1 & \frac{\partial z}{\partial y}\end{array}\right|\Big/\left\|\begin{array}{ccc}\underline{i} & \underline{j} & \underline{k}\\ 1 & 0 & \frac{\partial z}{\partial x}\\ 0 & 1 & \frac{\partial z}{\partial y}\end{array}\right\|\\
&= \left[-\frac{\partial z}{\partial x},-\frac{\partial z}{\partial y},1\right]\Big/\left\|\left[-\frac{\partial z}{\partial x},-\frac{\partial z}{\partial y},1\right]\right\|\\
&= \frac{1}{H}\left[-\frac{\partial z}{\partial x},-\frac{\partial z}{\partial y},1\right],
\end{aligned}
\tag{3.12}
$$

where $H=\sqrt{1+\left(\frac{\partial z}{\partial x}\right)^2+\left(\frac{\partial z}{\partial y}\right)^2}$. Substitution of (3.10)–(3.12) into (3.9) yields

$$
\begin{aligned}
\kappa &= \frac{1}{H}\frac{\partial^2 z}{\partial x^2}\left(\frac{dx}{ds}\right)^2+\frac{2}{H}\frac{\partial^2 z}{\partial x\partial y}\left(\frac{dx}{ds}\right)\left(\frac{dy}{ds}\right)+\frac{1}{H}\frac{\partial^2 z}{\partial y^2}\left(\frac{dy}{ds}\right)^2\\
&= L\left(\frac{dx}{ds}\right)^2+2M\left(\frac{dx}{ds}\right)\left(\frac{dy}{ds}\right)+N\left(\frac{dy}{ds}\right)^2,
\end{aligned}
\tag{3.13}
$$

where

$$
L=\frac{1}{H}\frac{\partial^2 z}{\partial x^2},\quad M=\frac{1}{H}\frac{\partial^2 z}{\partial x\partial y},\quad N=\frac{1}{H}\frac{\partial^2 z}{\partial y^2}. \tag{3.14}
$$

The expression for the curvature in (3.13) is known as the *second Gaussian fundamental form* of the seafloor.

3.2 The Surfaces of Extremal Curvature of the Seafloor

Since we seek the ridge of maximum curvature of the seafloor in terms of its directional coefficients $[l, m] = \left[\frac{dx}{ds}, \frac{dy}{ds}\right]$, the objective is to maximise the curvature

$$\kappa(l, m) = Ll^2 + 2Mlm + Nm^2 \tag{3.15}$$

derived in (3.13), subject to the constraint (3.8), which may be written as $g(l, m) = 0$, where

$$g(l, m) = El^2 + 2Flm + Gm^2 - 1. \tag{3.16}$$

The Lagrangian for the optimisation problem (3.15)–(3.16) is

$$\mathcal{L}(\kappa, \lambda) = \kappa(l, m) + \lambda g(l, m),$$

where λ is a Lagrangian multiplier. The first order necessary condition for a point $(l^*, m^*) \in \mathbb{R}^2$ to be an extremal point of (3.15)–(3.16) is that

$$\left.\frac{\partial \mathcal{L}}{\partial l}\right|_{(l^*,m^*)} = 0, \quad \left.\frac{\partial \mathcal{L}}{\partial m}\right|_{(l^*,m^*)} = 0 \text{ and } \left.\frac{\partial \mathcal{L}}{\partial \lambda}\right|_{(l^*,m^*)} = 0,$$

which results in the system of equations

$$\begin{aligned} Ll^* + Mm^* - \lambda El^* - \lambda Fm^* &= 0, & (3.17)\\ Ml^* + Nm^* - \lambda Fl^* - \lambda Gm^* &= 0, & (3.18)\\ E(l^*)^2 + 2Fl^*m^* + G(m^*)^2 &= 1. & (3.19) \end{aligned}$$

Multiplying (3.17) by l^* and (3.18) by m^*, and adding together the resulting equations, we obtain the relationship

$$(l^*)^2(L - \lambda E) + 2l^*m^*(M - \lambda F) + (m^*)^2(N - \lambda G) = 0. \tag{3.20}$$

It follows by the constraint $g(l^*, m^*) = 0$ in (3.19) that

$$\lambda = \lambda E(l^*)^2 + 2\lambda Fl^*m^* + \lambda G(m^*)^2.$$

Hence

$$\kappa(l^*, m^*) - \lambda = (l^*)^2(L - \lambda E) + 2l^*m^*(M - \lambda F) + (m^*)^2(N - \lambda G) = 0$$

by (3.15) and (3.20), so that $\lambda = \kappa(l^*, m^*)$. Substituting this relationship into (3.18) yields the relationship

$$l^* = \frac{(\lambda F - M)}{(L - \kappa E)} m^*,$$

which, if substituted into (3.17), yields the quadratic equation for κ, in terms of the coordinates (x, y),

$$\begin{aligned} 0 &= (L - \kappa E)(\kappa G - N) + (M - \kappa F)(M - \kappa F)\\ &= (EG - F^2)\kappa^2 - (EN + GL - 2FM)\kappa + (LN - M^2). \end{aligned} \tag{3.21}$$

The roots of (3.21) are called the *surfaces of maximum and minimum normal (principal) curvatures*, abbreviated by SMC and SmC respectively, and are given by

$$\kappa^*_{\pm}(x, y) = \frac{(EN + GL - 2FM) \pm \sqrt{(EN + GL - 2FM)^2 - 4(EG - F^2)(LN - M^2)}}{2(EG - F^2)}. \tag{3.22}$$

The computation of derivatives for a surface is, of course, directional. At a point (x, y), the derivative in a northerly direction is not the same as that computed for, say, a westerly direction. Therefore, for the point (x, y), there are infinitely many potentially distinct values of the curvature – each of which is dependent on the direction in which the derivatives are computed. It is a direct result of the directionality of the derivatives of a surface that it is possible to have both a maximum and a minimum curvature value at a single point on the surface. In this case κ_- describes the minimum value of the curvature at the point (x, y) and κ_+ describes the maximum value of the curvature.

3.3 Analytical Computation Examples

In this section the process of computation of the surfaces of extremal normal (principal) curvature of a seafloor is illustrated by means of a series of examples for two hypothetical seafloor surfaces, namely the Gaussian function and a slightly more realistic (periodic) surface. An analytical approach towards the computation of the extremal surfaces is considered for both examples. The analytical computation of the surfaces of extremal curvature were performed by means of the Wolfram Research symbolic mathematics package, *Mathematica* [23].

Example 3.1 : A Simple Analytical Example

Consider the Gaussian function

$$z(x,y) = 1 - e^{-(x^2+y^2)} \tag{3.23}$$

shown in Figure 3.2 as a hypothetical seafloor surface. The derivatives of $z(x,y)$ are given by

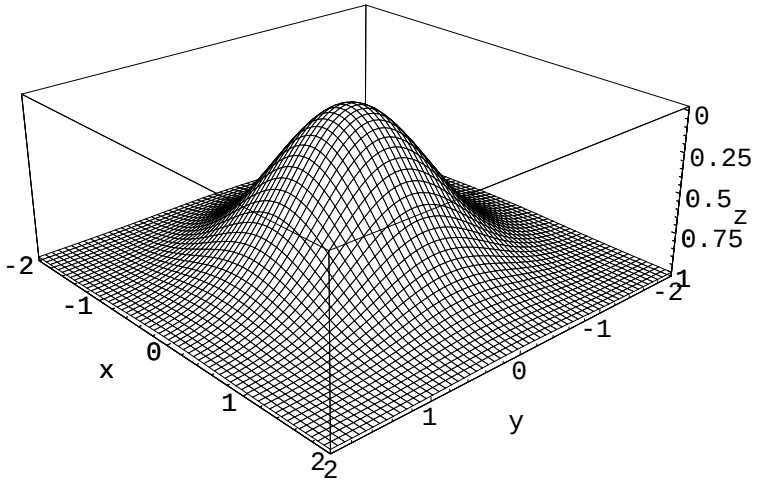

Figure 3.2: *The Gaussian surface $z(x,y)$ in (3.23).*

$$\begin{aligned}
\frac{\partial z}{\partial x} &= 2x\, e^{-(x^2+y^2)}, \\
\frac{\partial z}{\partial y} &= 2y\, e^{-(x^2+y^2)}, \\
\frac{\partial^2 z}{\partial x^2} &= (2-4x^2)\, e^{-(x^2+y^2)}, \\
\frac{\partial^2 z}{\partial y^2} &= (2-4y^2)\, e^{-(x^2+y^2)} \quad \textit{and} \\
\frac{\partial^2 z}{\partial x \partial y} &= -4xy\, e^{-(x^2+y^2)} = \frac{\partial^2 z}{\partial y \partial x}.
\end{aligned}$$

Further, for this surface the functions of E, F, G, L, M, N and H as defined in (3.7) and (3.14), are given by

$$E = 1 + 4x^2\, e^{-2(x^2+y^2)}, \tag{3.24}$$

$$F = 4xy\, e^{-2(x^2+y^2)}, \tag{3.25}$$

$$G = 1 + 4y^2\, e^{-2(x^2+y^2)}, \tag{3.26}$$

$$L = (2-4x^2)e^{-2(x^2+y^2)}/H, \tag{3.27}$$

$$M = 4xy\, e^{-2(x^2+y^2)}/H \quad \textit{and} \tag{3.28}$$

$$N = (2-4y^2)e^{-2(x^2+y^2)}/H, \quad \textit{where} \tag{3.29}$$

$$H = \sqrt{e^{-2(x^2+y^2)}(e^{2(x^2+y^2)}+4(x^2+y^2))}. \tag{3.30}$$

Substitution of (3.24)–(3.30) into (3.22) and simplification yields the surfaces of minimum and maximum curvature,

$$\begin{aligned}\kappa^*_-(x,y) = &\Big(2e^{-(x^2+y^2)}\Big(-e^{4(x^2+y^2)} - 6x^2\, e^{2(x^2+y^2)} + x^2\, e^{4(x^2+y^2)} - 8x^4 + 4x^4\, e^{2(x^2+y^2)}\\ &-6y^2\, e^{2(x^2+y^2)} + y^2\, e^{4(x^2+y^2)} - 16x^2y^2 + 8x^2y^2e^{2(x^2+y^2)} - 8y^4 + 4y^4\, e^{2(x^2+y^2)}\\ &+\sqrt{(2+e^{2(x^2+y^2)})^2(x^2+y^2)^2(e^{2(x^2+y^2)}+4(x^2+y^2))^2}\Big)\Big)\\ &\Big/\Big((e^{2(x^2+y^2)}+4(x^2+y^2))^2\sqrt{e^{-2(x^2+y^2)}(e^{2(x^2+y^2)}+4(x^2+y^2))}\Big) \quad \textit{and}\end{aligned}$$

$$\begin{aligned}\kappa^*_+(x,y) = &-\Big(2e^{-(x^2+y^2)}\Big(e^{4(x^2+y^2)} + 6x^2\, e^{2(x^2+y^2)} - x^2\, e^{4(x^2+y^2)} + 8x^4 - 4x^4\, e^{2(x^2+y^2)}\\ &+6y^2\, e^{2(x^2+y^2)} - y^2\, e^{4(x^2+y^2)} + 16x^2y^2 - 8x^2y^2e^{2(x^2+y^2)} + 8y^4 - 4y^4\, e^{2(x^2+y^2)}\\ &+\sqrt{(2+e^{2(x^2+y^2)})^2(x^2+y^2)^2(e^{2(x^2+y^2)}+4(x^2+y^2))^2}\Big)\Big)\\ &\Big/\Big((e^{2(x^2+y^2)}+4(x^2+y^2))^2\sqrt{e^{-2(x^2+y^2)}(e^{2(x^2+y^2)}+4(x^2+y^2))}\Big)\end{aligned}$$

repectively. The minimum and maximum curvature surfaces are shown graphically in Figure 3.3. It can be seen that the expected positions of the ridges of maximum and minimum curvature, namely the base and tip of the bell–shaped Gaussian surface in Figure 3.2 respectively, are indeed what is achieved by application of the method. ■

The Gaussian function offers uniform and easily calculable curvature, as may be seen from the above example. The seafloor is, however, neither smooth nor uniform. For this reason the surface in the following example was chosen: it offers a more complex curvature surface, and further a main ridge line that is not closed. Example 3.2 is also a better approximation to smoothed data of some areas of seafloor where the margin topology is not complex and a standard shelf morphology is found.

Example 3.2 : A more complicated Analytical Example

Consider the function

$$z(x,y) = 1 - 2\left(2 + \frac{e^{-2\left(-2+x+\sin\left[\frac{\pi y}{2}\right]\right)} - e^{2\left(-2+x+\sin\left[\frac{\pi y}{2}\right]\right)}}{e^{-2\left(-2+x+\sin\left[\frac{\pi y}{2}\right]\right)} + e^{2\left(-2+x+\sin\left[\frac{\pi y}{2}\right]\right)}}\right) \tag{3.31}$$

as an alternate hypothetical seafloor surface, shown graphially in Figure 3.4. Due to the complexity of the derivatives of $z(x,y)$ in (3.31) they are not given here explicitly. The surfaces of minimum and maximum curvature are shown in Figure 3.5 and the contour plots of these surfaces are provided in Figure 3.6.

On the SMC, one can see the ridge line formed at the base of the surface as well as the ridge line indicating the vertical inward curve of the surface, between the protruding sections of the surface. Furthermore, inspection of the contour plots in Figure 3.6 confirms that the surfaces of extremal curvature adequately represent the symmetry of the surface described by (3.31). The surfaces of extremal curvature are shifted mirror images of each other, as expected. Note that the bottom left corner of the contour plots corresponds to the right–most corner of the extremal curvature plots in Figure 3.5. ■

3.4 Numerical Approach

For real seafloor surfaces the analytical approach is not possible. This is due to the fact that bathymetric data is raw data and therefore cannot be expressed as an analytical function and as a result its derivatives

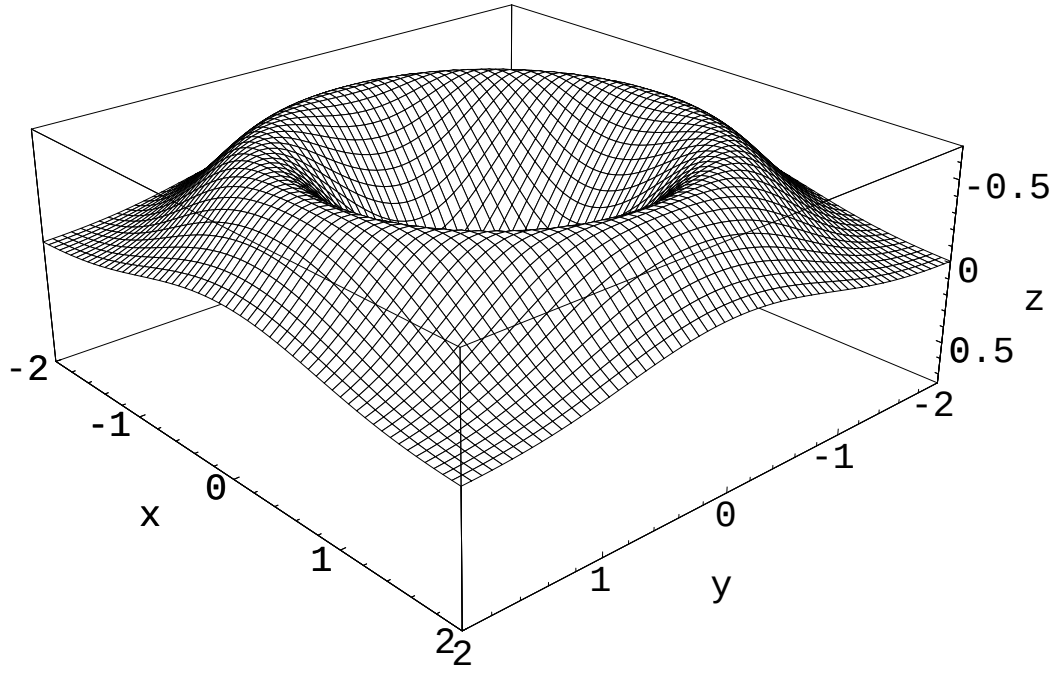

(a) The SMC, $\kappa_+^*(x, y)$

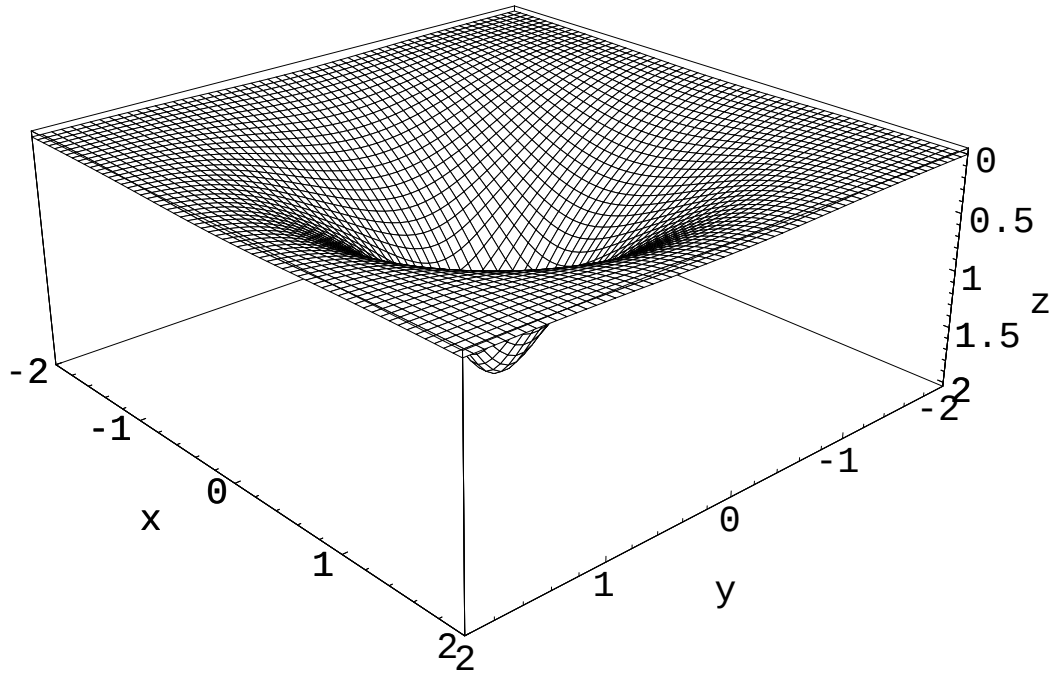

(b) The SmC, $\kappa_-^*(x, y)$

Figure 3.3*: Surfaces of maximum and minimum curvature for Example 3.1 — Surface Plots.*

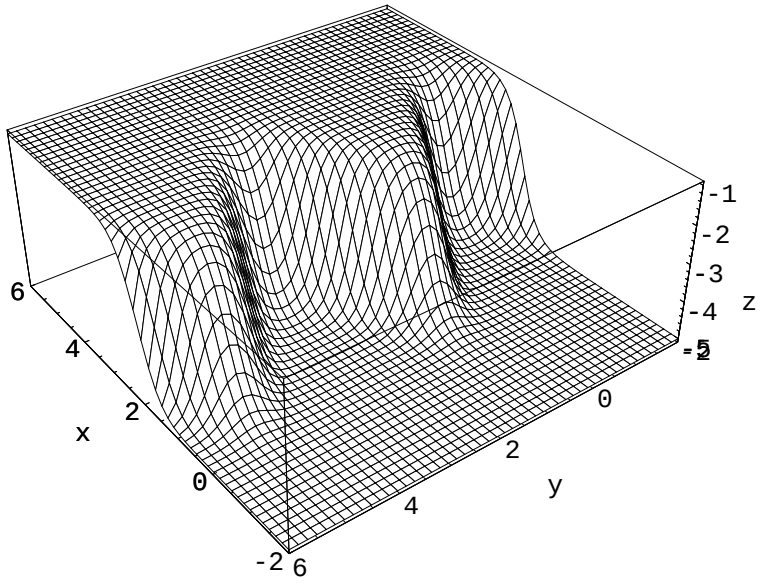

Figure 3.4: *The surface $z(x, y)$ in (3.31).*

cannot be calculated analytically. In order to apply the method for determining the surfaces of extremal curvature, it is thus necessary to consider numerical techniques for determining the derivatives required for the computation. The following section serves to introduce the notion of approximation of numerical derivatives before proceeding to the application of these methods to the two hypothetical seafloor surfaces used for the analytical examples.

3.4.1 Numerical Derivatives

The derivative of a function $f(x)$ is given by

$$f'(x) = \lim_{h \to 0} \frac{f(x+h) - f(x)}{h}$$

if the limit exists. For small values of $h = x_{k+1} - x_k = x_k - x_{k-1}$ in Figure 3.7 the expressions

$$\frac{f(x_{k+1}) - f(x_k)}{h}, \tag{3.32}$$

$$\frac{f(x_k) - f(x_{k-1})}{h} \quad \text{and} \tag{3.33}$$

$$\frac{f(x_{k+1}) - f(x_{k-1})}{2h} \tag{3.34}$$

are approximations to $f'(x_k)$. The expression (3.32) is referred to as the *forward difference* formula for derivative computation and the expressions (3.33) and (3.34) are referred to as the *backward difference* and *central difference* formulae respectively. However, from a computational perspective, one should not choose h too small in (3.32)–(3.34), as then the fractional error in the numerator becomes large as a result of the cancellation and roundoff errors in the values of $f(x_{k+1})$ and $f(x_k)$ being greatly magnified when these nearly equal numbers are subtracted. On the other hand, if h is too large, then the approximation error becomes large. The construction of formulae for numerical derivatives is largely based on the use of the Taylor expansion of a function. The use of a Taylor series facilitates an indication of the order of accuracy of the particular approximation. In order to find an upper bound on the approximation error incurred, we use Taylor's thoerem,

$$f(x_{k+1}) = f(x_k) + hf'(x_k) + \frac{1}{2}h^2 f''(x_k) + \cdots + \frac{1}{n!}h^n f^{(n)}(x_k) + \frac{1}{(n+1)!}h^{n+1} f^{(n+1)}(c),$$

where c is some unknown number between x_k and x_{k+1}. The Taylor formula with $n = 1$ is

$$f(x_{k+1}) = f(x_k) + hf'(x_k) + \frac{1}{2}h^2 f''(c).$$

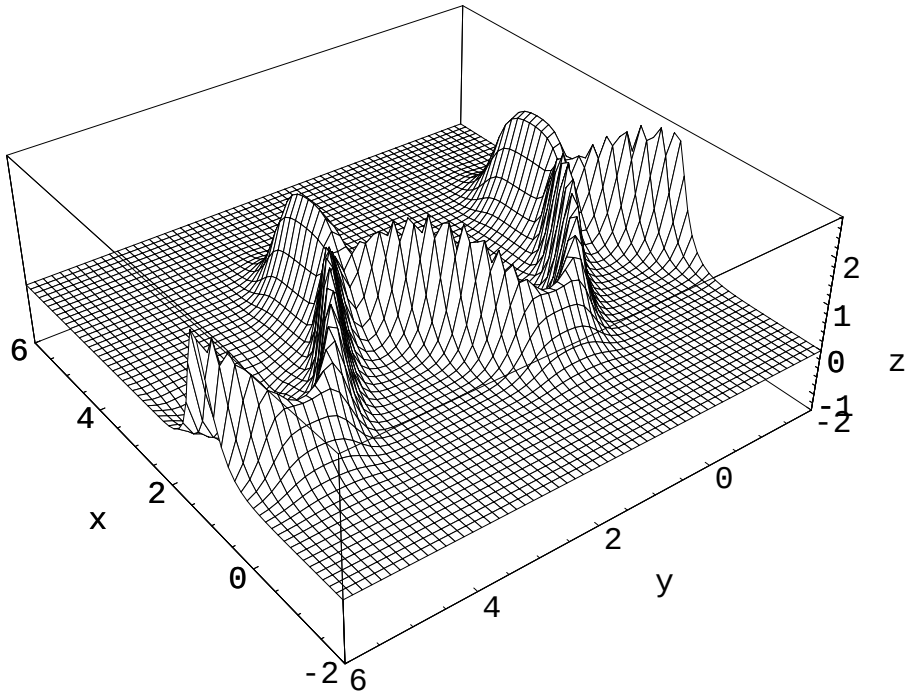

(a) The SMC, $\kappa_+^*(x, y)$

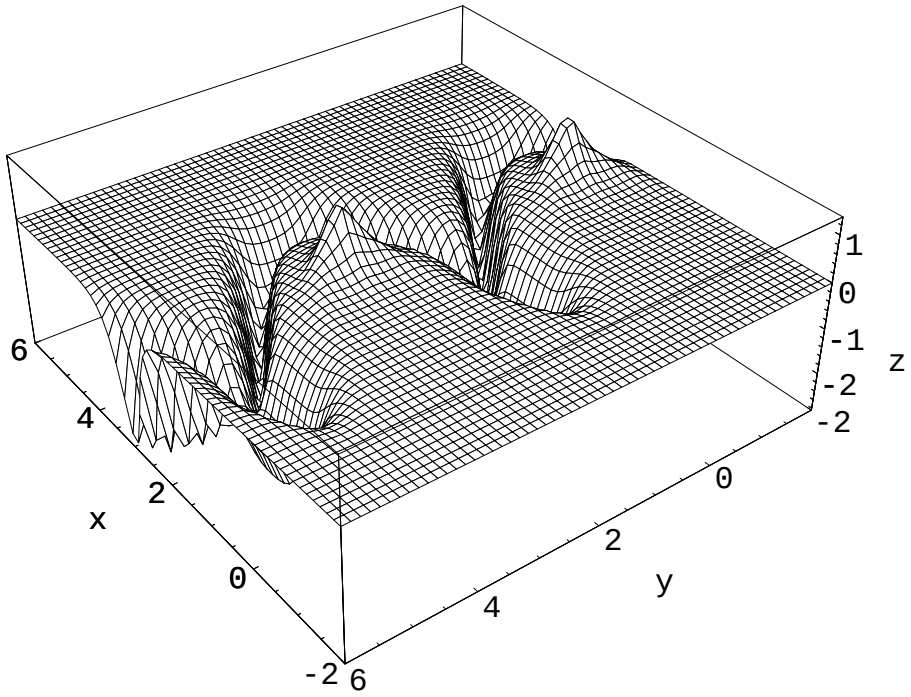

(b) The SmC, $\kappa_-^*(x, y)$

Figure 3.5*: Surfaces of maximum and minimum curvature for Example 3.2 — Surface Plots.*

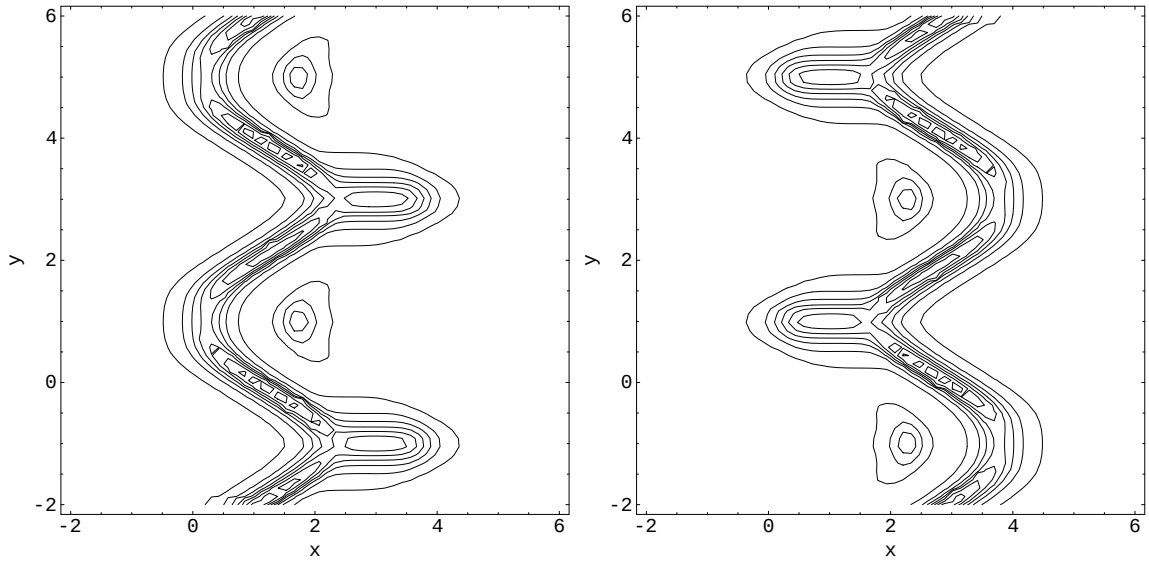

(a) Contours of the SMC, $\kappa_+^*(x,y)$ (b) Contours of the SmC, $\kappa_-^*(x,y)$

Figure 3.6: *Surfaces of maximum and minimum curvature for Example 3.2 — Contour Plots.*

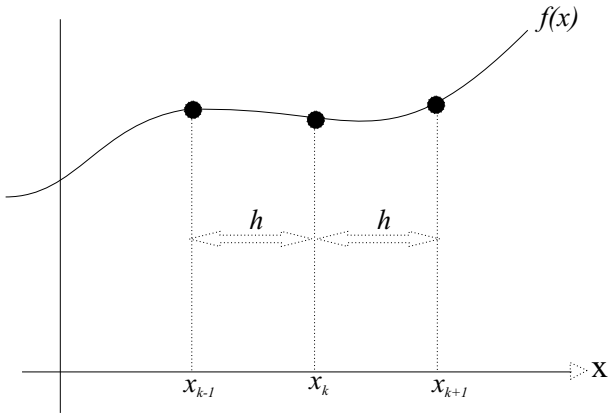

Figure 3.7: *The spacing of points used in the numerical approximation of the derivative $f'(x)$.*

Thus

$$hf'(x_k) \quad = \quad f(x_{k+1}) - f(x_k) - \frac{1}{2}h^2 f''(c)$$

and dividing by h, we obtain

$$f'(x_k) \quad = \quad \frac{f(x_{k+1}) - f(x_k)}{h} - \frac{1}{2}hf''(c).$$

The first term gives precisely the approximation in (3.32), which means that the second term gives the error incurred in the approximation. The error in the forward difference formula (as derived above), and that for the backward difference formula, are $O(h)$. For the central difference formula, if we observe that

$$f(x_{k+1}) \quad = \quad f(x_k) + hf'(x_k) + \frac{1}{2}h^2 f''(x_k) + \frac{1}{3!}h^3 f^{(3)}(c_1) \quad \text{and} \tag{3.35}$$

$$f(x_{k-1}) \quad = \quad f(x_k) + (-h)f'(x_k) + \frac{1}{2}h^2 f''(x_k) + \frac{1}{3!}(-h)^3 f^{(3)}(c_2), \tag{3.36}$$

where $x_k \leq c_1 \leq x_{k+1}$ and $x_{k-1} \leq c_2 \leq x_k$. Subtracting Equation (3.36) from (3.35) gives

$$f(x_{k+1}) - f(x_{k-1}) \quad = \quad 2hf'(x_k) + \frac{1}{6}h^3(f^{(3)}(c) + f^{(3)}(c_1)).$$

Solving for $f'(x_k)$ yields

$$f'(x_k) = \frac{f(x_{k+1}) - f(x_{k-1})}{2h} - \frac{1}{12}h^2(f^{(3)}(c) + f^{(3)}(c_1)).$$

From the intermediate value theorem it follows that there is some number ξ where $c_2 \leq \xi \leq c_1$ such that

$$f^{(3)}(\xi) = \frac{1}{2}(f^{(3)}(c_1) + f^{(3)}(c_2)),$$

and therefore the central difference formula becomes

$$f'(x_k) = \frac{f(x_{k+1}) - f(x_{k-1})}{2h} - \frac{1}{6}h^2 f^{(3)}(\xi).$$

It can now be seen that the order of error of the approximation obtained by means of the central difference formula is $O(h^2)$.

To obtain a more accurate approximation for the derivative, the notion of an interpolating polynomial may be employed. Recall that the Lagrange interpolating polynomial of order n is given by

$$f(x) = \sum_{k=0}^{n} f_k L_k(x) + \frac{1}{(n+1)!}\prod_{k=0}^{n}(x - x_k)f^{(n+1)}(c), \tag{3.37}$$

where

$$L_k(x) = \prod_{j=0, j\neq k}^{n} \frac{x - x_j}{x_k - x_j}$$

for some number $c \in (x_0, x_n)$ that depends on x, where f has continuous derivatives of the $(n+1)^{th}$ order over the interval $[x_0, x_n]$ and $f_i = f(x_i)$ [12, 30, 47]. The first term in (3.37) is the interpolating polynomial and the second term gives the remainder, which is used to approximate the error incurred. Differentiating (3.37) with respect to x and simplifying the result yields the $(n+1)$–point approximation formula

$$f'(x_i) = \sum_{k=0}^{n} f_k L'_k(x_i), \tag{3.38}$$

where the error is given by the remainder formula

$$\frac{1}{(n+1)!}f^{(n+1)}(c(x_i)) \prod_{k=0, k\neq i}^{n}(x_i - x_k). \tag{3.39}$$

To obtain the two point formulae given by (3.32)–(3.34), one would set $n = 1$ in (3.38) and (3.39). For greater accuracy, one could consider three (set $n = 2$) or five (set $n = 4$) point formulae, noting that the use of such formulae requires either a combination of forward, central and backward formulae or the loss of one to two data points on either side of the data. In this thesis only the two point formulae are used — in order to achieve faster computation times. This is preferred as the data sets used in this thesis are very large matrices and application of higher point number derivative formulae increases the computation time required to determine the surfaces of extremal curvature considerably with a marginal benefit in the accuracy of results.

For second order derivatives, the formulae for the first order derivatives may be re–applied to the result obtained for the first derivative. The resulting formulae for the second derivative, when re–applying the two point forward, backward and central difference formulae, are

$$f''(x_k) \quad = \quad \frac{1}{h^2}\left[f(x_{k+2}) - 2f(x_{k+1}) + f(x_k)\right], \quad \textit{(forward difference)} \tag{3.40}$$

$$f''(x_k) \quad = \quad \frac{1}{h^2}\left[f(x_k) - 2f(x_{k-1}) + f(x_{k-2})\right] \quad \textit{(backward difference)} \text{ or} \tag{3.41}$$

$$f''(x_k) \quad = \quad \frac{1}{h^2}\left[f(x_{k+1}) - 2f(x_k) + f(x_{k-1})\right] \quad \textit{(central difference)}. \tag{3.42}$$

For all the second order derivative formulae shown above, a similar process as executed for the first order derivative formulae can be followed to ascertain that all three of the second order formulae are of order $O(h^2)$ accuracy.

Of course first order partial derivatives of a function $z(x, y)$ of two independent variables x and y may be approximated by applying any of the formulae (3.32)–(3.34) in the x–direction (keeping y constant) or in the y–direction (keeping x constant), to obtain

$$\frac{\partial}{\partial x}z(x_k, y_l) \approx \frac{1}{h_x}[z(x_{k+1}, y_l) - z(x_k, y_l)] \quad (\textit{forward difference}), \text{ or} \tag{3.43}$$

$$\approx \frac{1}{h_x}[z(x_k, y_l) - z(x_{k-1}, y_l)] \quad (\textit{backward difference}), \text{ or} \tag{3.44}$$

$$\approx \frac{1}{2h_x}[z(x_{k+1}, y_l) - z(x_{k-1}, y_l)] \quad (\textit{central difference}) \tag{3.45}$$

and

$$\frac{\partial}{\partial y}z(x_k, y_l) \approx \frac{1}{h_y}[z(x_k, y_{l+1}) - z(x_k, y_l)] \quad (\textit{forward difference}), \text{ or} \tag{3.46}$$

$$\approx \frac{1}{h_y}[z(x_k, y_l) - z(x_k, y_{l-1})] \quad (\textit{backward difference}), \text{ or} \tag{3.47}$$

$$\approx \frac{1}{2h_y}[z(x_k, y_{l+1}) - z(x_k, y_{l-1})] \quad (\textit{central difference}), \tag{3.48}$$

where h_x and h_y are given by $h_x = x_{k+1} - x_k = x_k - x_{k-1}$ and $h_y = y_{l+1} - y_l = y_l - y_{l-1}$ respectively, as shown in Figure 3.8.

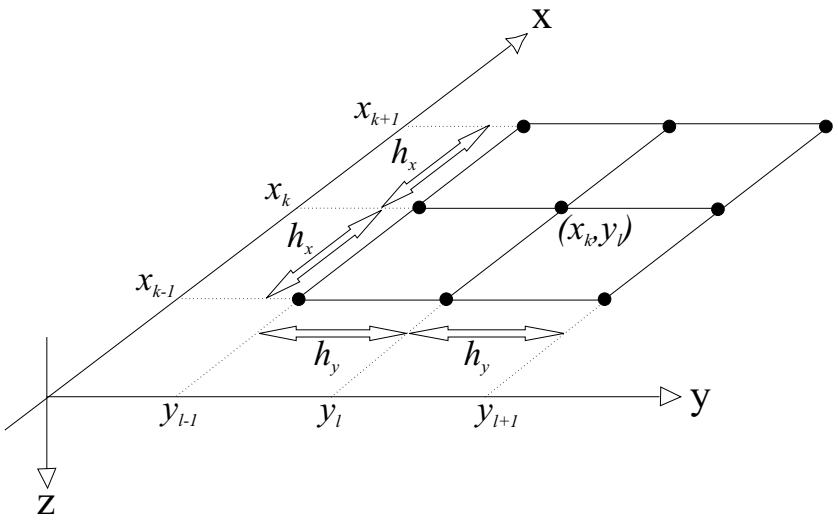

Figure 3.8: *The spacing of points used in numerical approximation of partial derivatives.*

Second order partial derivatives of $z(x, y)$ may be obtained by re–applying the first order derivative approximations to any of the results of (3.43)–(3.48). By re–applying the same difference formula as used to obtain the first derivative, the pure second order derivatives with respect to x are

$$\frac{\partial^2}{\partial x^2}z(x_k, y_l) \approx \frac{1}{h_x^2}[z(x_{k+2}, y_l) - 2z(x_{k+1}, y_l) + z(x_k, y_l)] \quad (\textit{forward difference}), \text{ or} \tag{3.49}$$

$$\approx \frac{1}{h_x^2}[z(x_k, y_l) - 2z(x_{k-1}, y_l) + z(x_{k-2}, y_l)] \quad (\textit{backward difference}), \text{ or} \tag{3.50}$$

$$\approx \frac{1}{4h_x^2}[z(x_{k+2}, y_l) - 2z(x_k, y_l) + z(x_{k-2}, y_l)] \quad (\textit{central difference}) \tag{3.51}$$

and similarly the pure second order derivatives with respect to y are

$$\frac{\partial^2}{\partial y^2}z(x_k,y_l) \approx \frac{1}{h_y^2}[z(x_k,y_{l+2})-2z(x_k,y_{l+1})+z(x_k,y_l)] \quad (\textit{forward difference}), \text{ or} \tag{3.52}$$

$$\approx \frac{1}{h_y^2}[z(x_k,y_l)-2z(x_k,y_{l-1})+z(x_k,y_{l-2})] \quad (\textit{backward difference}), \text{ or} \tag{3.53}$$

$$\approx \frac{1}{4h_y^2}[z(x_k,y_{l+2})-2z(x_k,y_l)+z(x_k,y_{l-2})] \quad (\textit{central difference}). \tag{3.54}$$

Approximations for the mixed second order derivatives may be obtained by applying one of (3.43)–(3.45) to any one of (3.46)–(3.48) or vice versa. There are therefore nine possible combinations of formulae that may be considered, however, the order of application (application of a difference formula with respect to x to a partial derivative with respect to y or reversed) changes the result obtained for the mixed second derivative. There are, however, three special cases where the order of application does not change the result, namely those cases where the same classification of difference formula as that used to obtain the partial derivative is applied to obtain the mixed derivative. This means that, in total, there are fifteen possible formulae for the computation of a mixed derivative. The formulae for the special cases are presented first, and then the eight possible formulae for each order of application are supplied. The first special case, where only the forward difference formula is considered, is obtained by applying (3.46) to (3.43), or (3.43) to (3.46), and yields the mixed derivative

$$\frac{\partial^2}{\partial x\partial y}z(x_k,y_l)=\frac{\partial^2}{\partial y\partial x}z(x_k,y_l)\approx\frac{1}{h_xh_y}[z(x_{k+1},y_{l+1})-z(x_k,y_{l+1})-z(x_{k+1},y_l)+z(x_k,y_l)]. \tag{3.55}$$

The second special case, where only the backward difference formula is considered, is obtained by applying (3.47) to (3.44), or (3.44) to (3.47), and yields the mixed derivative

$$\frac{\partial^2}{\partial x\partial y}z(x_k,y_l)=\frac{\partial^2}{\partial y\partial x}z(x_k,y_l)\approx\frac{1}{h_xh_y}[z(x_k,y_l)-z(x_{k-1},y_l)-z(x_k,y_{l-1})+z(x_{k-1},y_{l-1})]. \tag{3.56}$$

The third (and final) special case, where only the central difference formula is considered, is obtained by applying (3.48) to (3.45), or (3.45) to (3.48), and yields the mixed derivative

$$\frac{\partial^2 z}{\partial x\partial y}=\frac{\partial^2}{\partial y\partial x}z(x_k,y_l)\approx\frac{1}{4h_xh_y}[z(x_{k+1},y_{l+1})-z(x_{k+1},y_{l-1})-z(x_{k-1},y_{l+1})+z(x_{k-1},y_{l-1})]. \tag{3.57}$$

The approximations

$$\frac{\partial^2}{\partial x\partial y}z(x_k,y_l) \approx \frac{1}{h_xh_y}[z(x_{k+1},y_l)-z(x_{k+1},y_{l-1})-z(x_k,y_l)+z(x_k,y_{l-1})], \quad \text{and} \tag{3.58}$$

$$\approx \frac{1}{2h_xh_y}[z(x_{k+1},y_{l+1})-z(x_{k+1},y_{l-1})-z(x_k,y_{l+1})+z(x_k,y_{l-1})] \tag{3.59}$$

are obtained by application of (3.47) and (3.48) to (3.43) respectively. Using the partial derivative with respect to x obtained by application of the central difference formula, (3.45), as input to (3.46) and (3.47) yields the mixed derivatives

$$\frac{\partial^2}{\partial x\partial y}z(x_k,y_l) \approx \frac{1}{2h_xh_y}[z(x_{k+1},y_{l+1})-z(x_{k+1},y_l)-z(x_{k-1},y_{l+1})+z(x_{k-1},y_l)], \quad \text{and} \tag{3.60}$$

$$\approx \frac{1}{2h_xh_y}[z(x_{k+1},y_l)-z(x_{k+1},y_{l-1})-z(x_{k-1},y_l)+z(x_{k-1},y_{l-1})] \tag{3.61}$$

respectively. Similarly, using (3.44) as input to (3.46) and (3.48) yields the mixed derivatives

$$\frac{\partial^2}{\partial x\partial y}z(x_k,y_l) \approx \frac{1}{h_xh_y}[z(x_k,y_{l+1})-z(x_k,y_l)-z(x_{k-1},y_{l+1})+z(x_{k-1},y_l)], \quad \text{and} \tag{3.62}$$

$$\approx \frac{1}{2h_xh_y}[z(x_k,y_{l+1})-z(x_k,y_{l-1})-z(x_{k-1},y_{l+1})+z(x_{k-1},y_{l-1})] \tag{3.63}$$

respectively.

Changing the order of application, so that a partial derivative with respect to y corresponding to one of (3.46)–(3.48) is used as input into (3.43)–(3.45), the final six formulae for computation of a mixed derivative may be determined. Application of (3.44) and (3.45) to (3.46) yield the approximations

$$\frac{\partial^2}{\partial y \partial x} z(x_k, y_l) \approx \frac{1}{h_x h_y}[z(x_k, y_{l+1}) - z(x_{k-1}, y_{l+1}) - z(x_k, y_l) + z(x_{k-1}, y_l)], \quad \text{and} \tag{3.64}$$

$$\approx \frac{1}{2h_x h_y}[z(x_{k+1}, y_{l+1}) - z(x_{k-1}, y_{l+1}) - z(x_{k+1}, y_l) + z(x_{k-1}, y_l)] \tag{3.65}$$

respectively. Using (3.48) as input to (3.43) and (3.44) respectively, the approximations

$$\frac{\partial^2}{\partial y \partial x} z(x_k, y_l) \approx \frac{1}{2h_x h_y}[z(x_{k+1}, y_{l+1}) - z(x_k, y_{l+1}) - z(x_{k+1}, y_{l-1}) + z(x_k, y_{l-1})], \quad \text{and} \tag{3.66}$$

$$\approx \frac{1}{2h_x h_y}[z(x_k, y_{l+1}) - z(x_{k-1}, y_{l+1}) - z(x_k, y_{l-1}) + z(x_{k-1}, y_{l-1})] \tag{3.67}$$

may be obtained. Finally, application of (3.43) and (3.45) to (3.47) yield the approximations

$$\frac{\partial^2}{\partial y \partial x} z(x_k, y_l) \approx \frac{1}{h_x h_y}[z(x_{k+1}, y_l) - z(x_k, y_l) - z(x_{k+1}, y_{l-1}) + z(x_k, y_{l-1})], \quad \text{and} \tag{3.68}$$

$$\approx \frac{1}{2h_x h_y}[z(x_{k+1}, y_l) - z(x_{k-1}, y_l) - z(x_{k+1}, y_{l-1}) + z(x_{k-1}, y_{l-1})]. \tag{3.69}$$

With the host of partial derivative approximation formulae derived for a function of two independent variables, it is now possible to compute the surfaces of extremal curvature using a numerical instead of an analytical approach.

3.4.2 Numerical Examples

The numerical computations for this section were accomplished by means of the Mathworks numerical mathematical package, *MATLAB* [24]. *MATLAB* has a built–in function, called `gradient`, which calculates derivatives numerically. The function applied to a one–dimensional array uses the two point forward difference formula (3.32) at the start of the data series, the central difference formula (3.34) in the body of the data series and the backward difference formula (3.33) at the end of the data series. This prevents data point loss. The function may also be applied to a matrix, as opposed to merely a one–dimensional array, of data. When applied to a matrix the function returns two resultant matrices, one where the derivative was taken along each of the rows (with respect to x) and one where it was taken along each of the columns (with respect to y). Within the function the default value for the step size (h) is 1, but the user may specify the step size by means of variables passed to the function. This function assumes regularly spaced data and thus the step sizes specified for the x and y directions, namely h_x and h_y respectively, remain constant throughout use in the row or column. Examples of calls to the function are

```
[Ux,Uy]=gradient(data,hx,hy);
[Uxx,Uxy]=gradient(Ux,hx,hy);
[Uyx,Uyy]=gradient(Uy,hx,hy);
```

where `data` is the matrix containing the surface data. The first partial derivative with respect to x, $\mathtt{U_x}$, is computed by means of equations (3.43)–(3.45) in a similar manner to the derivative computation for a one dimensional array. Each row of `data` is taken as a one dimensional array. The first partial derivative with respect to y, $\mathtt{U_y}$, is computed by means of (3.46)–(3.48) along each column of `data`. The second partial derivative with respect to x, $\mathtt{U_{xx}}$, is computed by means of (3.49)–(3.51) along each row of $\mathtt{U_x}$ and the second partial derivative, $\mathtt{U_{yy}}$, by means of (3.52)–(3.54) along each column of $\mathtt{U_y}$. The second order mixed derivative, $\mathtt{U_{xy}}$, is computed by means of (3.55)–(3.63) applied to each column of

$\mathtt{U_x}$. Similarly the mixed derivative, $\mathtt{U_{yx}}$, is computed by application of (3.55)–(3.57) and (3.64)–(3.69) to each row of $\mathtt{U_y}$. The above illustration of the use of the MATLAB gradient function was used in the numerical recomputation of the surfaces of extremal curvature found analytically in Examples 3.1 and 3.2. The MATLAB script for computing the surfaces of extremal curvature is given in Algorithm 1.

Algorithm 1 `Computation of Maximum Curvature`

Input: The data matrix, `data`, of the seafloor surface for which the surfaces of extremal curvature are required, in addition to the step sizes for the x and y directions respectively — passed to the procedure in the variables `hx` and `hy`.

Output: The surfaces of maximum (`Kmax`) and minimum (`Kmin`) curvature. The surface of maximum curvature is returned as the result of the function, but both surfaces are available as global variables.

1: $[\mathtt{Ux,Uy}] \leftarrow \mathbf{gradient}(\mathtt{data,hx,hy})$
2: $[\mathtt{Uxx,Uxy}] \leftarrow \mathbf{gradient}(\mathtt{Ux,hx,hy})$
3: $[\mathtt{Uyx,Uyy}] \leftarrow \mathbf{gradient}(\mathtt{Uy,hx,hy})$
4: $\mathtt{Uxy} \leftarrow (\mathtt{Uxy} + \mathtt{Uyx})/2$
5: $\mathtt{E} \leftarrow 1 + \mathtt{Ux}^2$
6: $\mathtt{F} \leftarrow \mathtt{Ux*Uy}$
7: $\mathtt{G} \leftarrow 1 + \mathtt{Uy}^2$
8: $\mathtt{H} \leftarrow \mathbf{sqrt}(1 + \mathtt{Ux}^2 + \mathtt{Uy}^2)$
9: $\mathtt{L} \leftarrow \mathtt{Uxx}/\mathtt{H}$
10: $\mathtt{M} \leftarrow \mathtt{Uxy}/\mathtt{H}$
11: $\mathtt{N} \leftarrow \mathtt{Uyy}/\mathtt{H}$
12: $\mathtt{A} \leftarrow \mathtt{EN} + \mathtt{GL} - 2\mathtt{FM}$
13: $\mathtt{B} \leftarrow \mathbf{sqrt}((\mathtt{EN} + \mathtt{GL} - 2\mathtt{FM})^2 - 4(\mathtt{EG} - \mathtt{F}^2)(\mathtt{LN} - \mathtt{M}^2))$
14: $\mathtt{C} \leftarrow 2(\mathtt{EG} - \mathtt{F}^2)$
15: $\mathtt{Kmax} = (\mathtt{A} + \mathtt{B})/\mathtt{C}$
16: $\mathtt{Kmin} = (\mathtt{A} - \mathtt{B})/\mathtt{C}$
17: return $\mathbf{max}(\mathtt{Kmax}, 0)$

Lines 5–11 are a substitution of the partial derivatives obtained in lines 1–4 into equations (3.7) and (3.14). The result from lines 5–11 is then substituted into lines 12–14, which are designed to speed up computation by decomposing the expression for the surfaces of extremal curvature, (3.22), into smaller components that have faster computation times. The result is then reconciled in lines 15 and 16, where `Kmax` represents the SMC and `Kmin` the SmC. Line 17 is included for use with the application of the algorithm to bathymetry data later in this thesis. Taking the maximum of the `Kmax` and 0 removes the negative values found on the SMC. When tracing the ridge formed on the SMC, negative values interfere with the optimality of the results obtained by the tracing algorithm, and these values are further irrelevant to the process of determination of the FoS, as they do not indicate a maximum curvature value.

Example 3.3 : Simple Analytical Example Revisited Numerically

In this example, the Gaussian surface described in (3.23) and shown in Figure 3.2 will be computed using the numerical methods described above. Running Algorithm 1 in MATLAB to compute the surfaces of extremal curvature yields the results shown in Figure 3.9. ■

A comparison of Figures 3.3 and 3.9 leads to the conclusion that the numerical methods are capable of correctly computing the surfaces of extremal curvature for the Gaussian surface in (3.23).

Example 3.4 : More Complicated Analytical Example Revisited Numerically

In this example, the surfaces of extremal curvature for the surface described in (3.31) and shown in Figure 3.4 are computed using the numerical methods described above. Running Algorithm 1 in MATLAB to compute the surfaces of extremal curvature yields the results shown in Figure 3.10, with the corresponding contour plots of these surfaces given in Figure 3.11. Once again, the bottom left corner of the contour plots corresponds to the right–most corner of the extremal curvature plots in Figure 3.10. ■

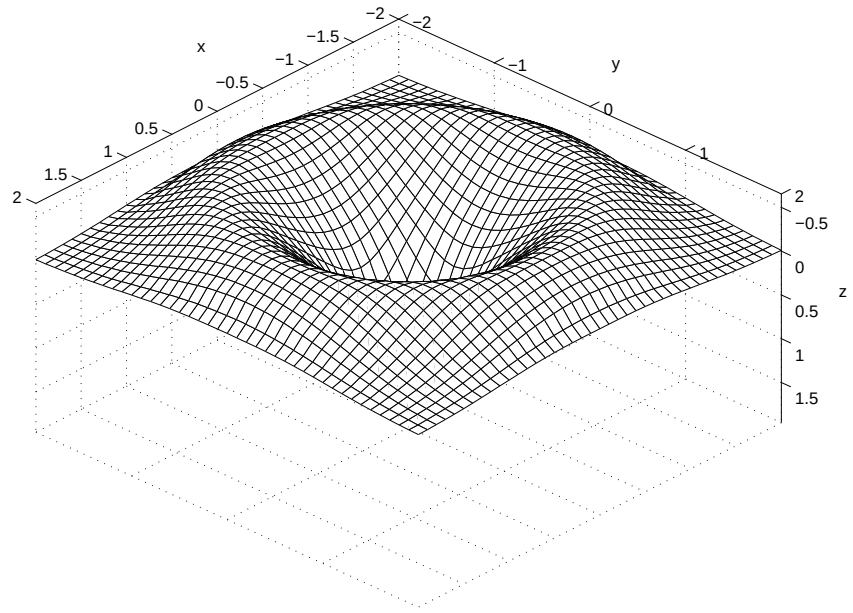

(a) The SMC, $\kappa_+^*(x, y)$

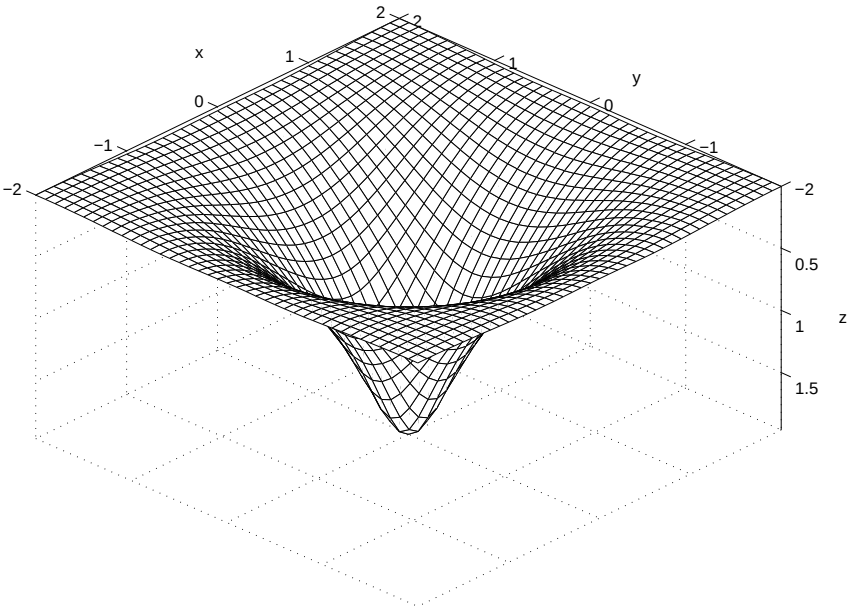

(b) The SmC, $\kappa_-^*(x, y)$

Figure 3.9*: Surfaces of maximum and minimum curvature for Example 3.3 — Surface Plots.*

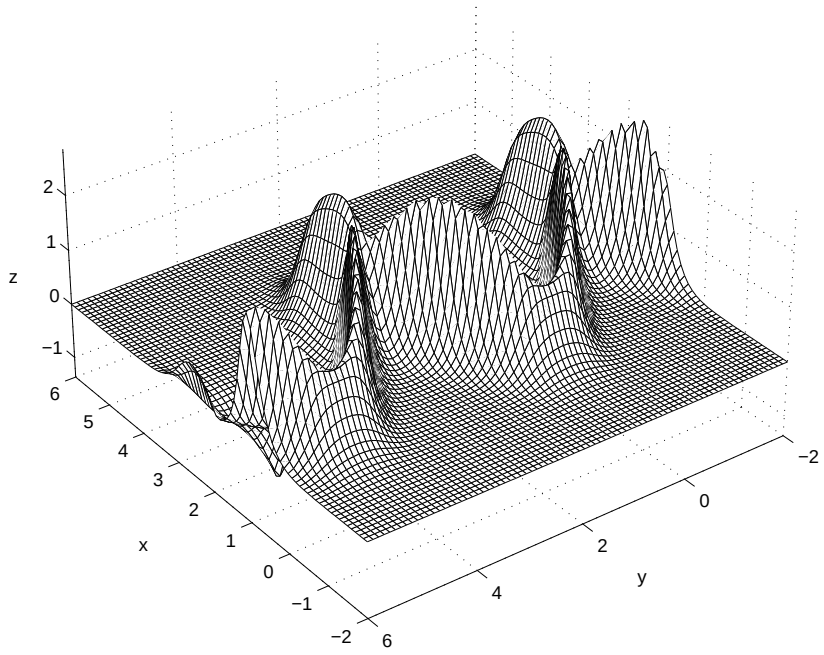

(a) The SMC, $\kappa_+^*(x, y)$

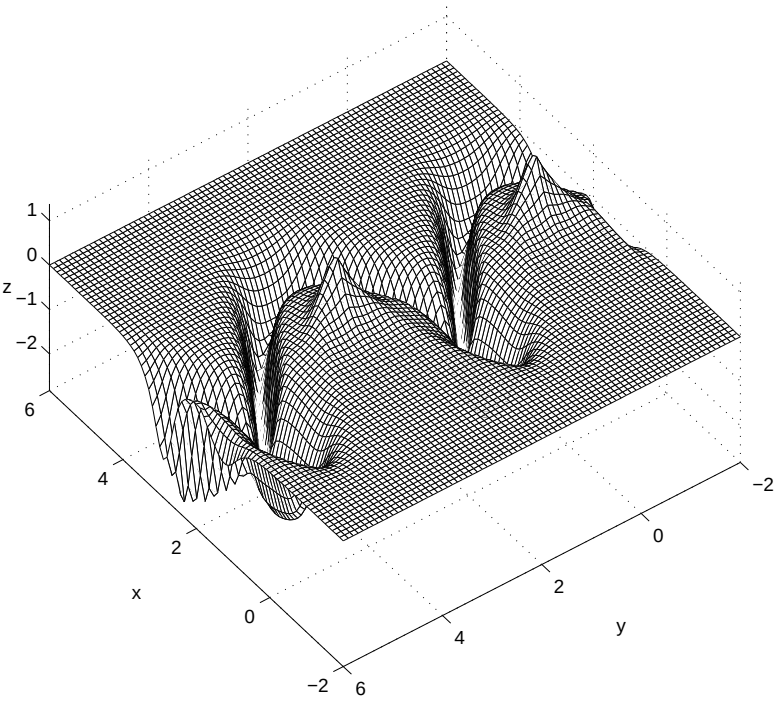

(b) The SmC, $\kappa_-^*(x, y)$

Figure 3.10: *Surfaces of maximum and minimum curvature for Example 3.4 — Surface Plots.*

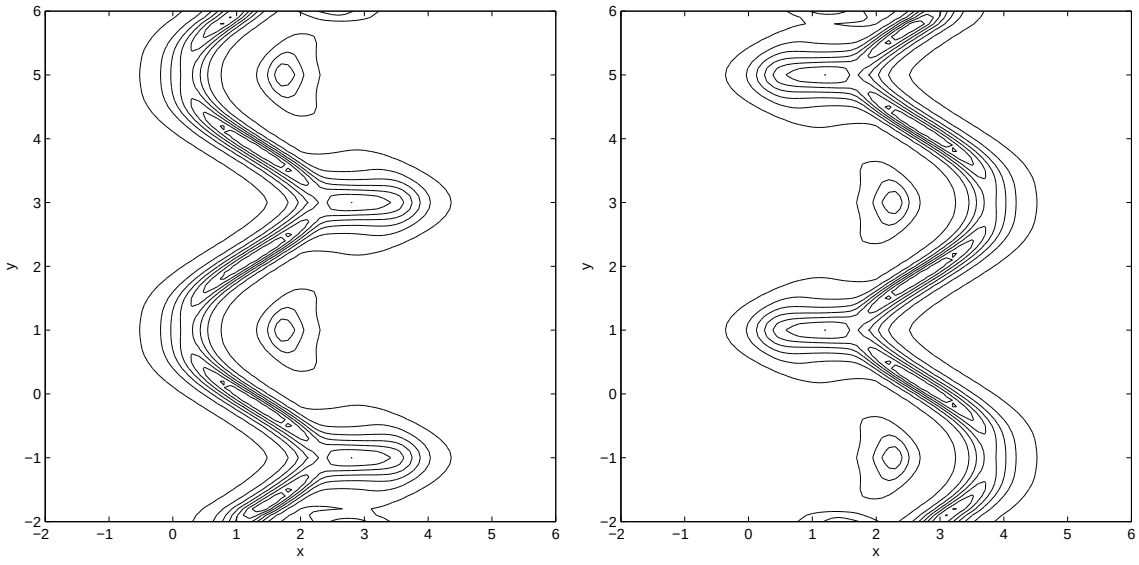

(a) Contours of the SMC, $\kappa_+^*(x, y)$

(b) Contours of the SmC, $\kappa_-^*(x, y)$

Figure 3.11: *Surfaces of maximum and minimum curvature for Example 3.4 – Contour Plots.*

A comparison of Figures 3.5 and 3.10 leads to the conclusion that the numerical methods are even capable of computing the surfaces of extremal curvature for the more complicated surface in (3.31). This conclusion is further supported by comparisons of Figures 3.6 and 3.11 which display the same contour patterns.

3.5 Chapter Summary

In this chapter a method to compute the surfaces of maximum and minimum curvature of a seafloor surface was discussed. The surface of maximum curvature will be used in Chapter 5 during the determination of the FoS for various seafloor regions around the South African coast, and the method to determine the surface of maximum curvature (offered in the previous sections) forms the mathematical basis for this determination. The surfaces of extremal curvature were computed for two hypothetical, smooth sample surfaces using both analytical and numerical approaches. The mathematical background of numerical determination of derivatives was discussed in detail, and an algorithm for the numerical application of the method to determine the extremal surfaces of curvature presented.

Chapter 4

Bathymetric Data

In the previous chapter a mathematical method to determine a foot line (detailing the FoS) was established. The method computes the surface of maximum curvature of the seafloor surface. With successful testing on example surfaces, these methods may now be applied to the bathymetric data to be used as case study for this thesis. Before these methods may be applied, however, it is necessary to examine the factors that influence and shape the form of bathymetric data, as well as the processing that needs to be performed on the data before it is in a format that can be used. This chapter serves to introduce these factors and necessary processing related to any land survey generated data — but to bathymetric data in particular — as well as to introduce and discuss the processed data to be used in the next chapter.

Bathymetric data is a set of numerical values indicating the depth of the sea as measured by a sea based platform using some form of echo sounder to take depth readings. As a result the raw data is related to a specific datum ellipsoid and measured relative to the datum reference height. Section 4.1 serves to introduce the definition of the reference system for geodetic coordinates. Sections 4.2 and 4.3 introduce the fundamental concepts relating to a method of transferring data from a spherical surface to a computation and reference friendly flat or plane surface — in addition to discussing the projection methods applicable to this thesis. The Chapter concludes with an introduction, in Section 4.4, to the data to be used in this thesis.

4.1 Datums

Cartography is the study of maps and of methods for the making of geographical maps. The study of datums and map projections is a subfield of cartography and an important one for this thesis. Data detailing a section of the seafloor may be obtained in two ways: via satellite or via the use of a sea based platform taking bathymetric readings. The earth may be approximated by a sphere or ellipsoid and thus the data collected from the seafloor describes a portion of the surface of the Earth with respect to that sphere / ellipsoid. All measurements require a starting or reference point with regards to height or depth. Geographically, such a reference point, in terms of which the coordinates of spatial data may be described, is called a *datum*. A datum, in the context of bathymetric data, is a reference height.

The angle North or South of a point on the Earth's surface, measured from the equatorial plane is called the *latitude* of the point in question and is denoted by the symbol ϕ in Figure 4.1. The equatorial plane is taken as having zero latitude and latitude is taken as positive in the northerly direction and negative in the southerly direction. The angle East or West of a point on the Earth's surface, measured from the Greenwich Meridian is called the *longitude* of the point in question and is denoted by the symbol λ in Figure 4.1. The Greenwich Meridian is taken as having zero longitude and longitude is taken as positive to the east of Greenwich and negative to the west of Greenwich. The *height* of a point P in space above the Earth's surface is the distance, in metres, of the point above a sphere or ellipsoid used to approximate the shape of the Earth and is denoted by the measurement h in Figure 4.1. This measurement could also pertain to the distance below the sphere or ellipsoid, in which case the measurement would be negative.

The surface of a sphere or ellipsoid may be covered with curves of equal latitude and these are called the *Parallels of Latitude*. Similarly the surface contains lines of equal longitude and these are called the *Meridians of Longitude*. For applications not requiring high accuracy it is adequate to consider the Earth

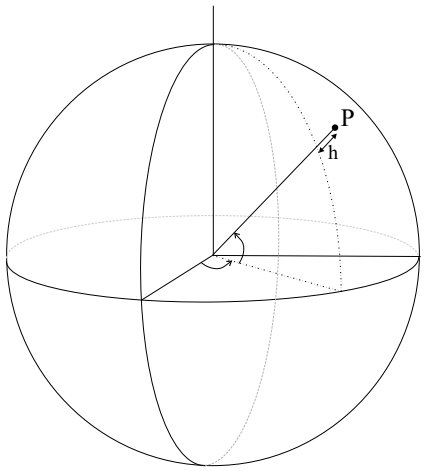

Figure 4.1*: The angle configuration for geographic referencing.*

as a sphere with radius $r = 6371$ km. Should a better approximation of the Earth's shape be required, an ellipsiod of revolution (spheroid) is used. This ellipsoid is formed by compressing the spherical Earth at the poles. This type of deformation of a sphere is called an *oblate* spheroid (ellipsoid) — should the spherical Earth be extended at the poles (or compressed at the equator) the resulting object would be referred to as a *prolate* spheroid (ellipsoid). The ellipsoid is defined by a semi–major axis of length a and a semi–minor axis of length b as shown in Figure 4.2. Certain well–known characteristics of the

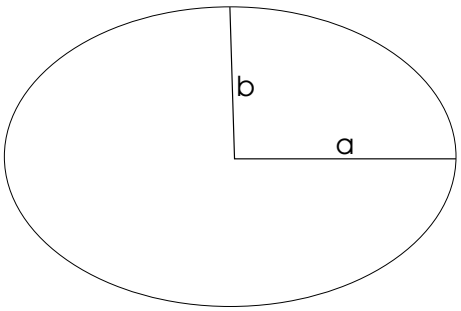

Figure 4.2*: Spheroid semi–major and semi–minor axes.*

spheroid may be defined in terms of the values of the semi–minor and semi–major axes. For example, the *flattening*, f, of an ellipsoid, defined as the degree of oblateness, is measured as

$$f = \frac{a - b}{a}, \tag{4.1}$$

whilst the *eccentricity*, e, of the ellipsoid is expressed as

$$e^2 = \frac{a^2 - b^2}{a^2}. \tag{4.2}$$

The eccentricity and flattening are related in the following ways: $e^2 = 2f - f^2$ or alternatively $\sqrt{1 - e^2} = (1 - f) = \frac{b}{a}$. In most cases an ellipsoid is referred to and specified by a combination of its semi–major axis length, a, and either the eccentricity or the flattening. Typically for the Earth the values $a = 6\ 378\ 137$m and $f = \frac{1}{298}$ are used.

Coordinates defined for points on the spheroid are called the geodetic coordinates and consist of latitude (ϕ in Figure 4.1) and longitude (λ in Figure 4.1) values defined with respect to the direction of the spheroid

(ellipsoid) normal. The spheroid normal is a line from the point in question that is perpendicular to the surface of the ellipsoid. Geodetic coordinates traditionally formed the basis for all mapping systems, but have recently been superceded by the use of Cartesian coordinates. In the Cartesian coordinate system, the origin is at the centre of the ellipsoid, the z axis is aligned with the semi–minor axis (the polar axis) and the x axis is aligned with the Greenwich Meridian in the equatorial plane. To transform from geodetic coordinates to Cartesian coordinates, the transformations

$$\begin{aligned} X &= (\nu + h)\cos\phi\cos\lambda, \\ Y &= (\nu + h)\cos\phi\sin\lambda, \quad \text{and} \\ Z &= \left\{(1 - e^2)\nu\right\}\sin\phi \end{aligned}$$

are used, where

$$\nu = \frac{a}{\sqrt{1 - e^2\sin^2\phi}}, \tag{4.3}$$

where ϕ denotes the latitude with North being positive, where λ denotes the longitude with East being positive, where h denotes the height of the point above the ellipsoid (as depicted in Figure 4.1) and where e denotes the eccentricity of the ellipsoid. The inverse transformation, to return to geodetic coordinates from Cartesian coordinates, is given by

$$\begin{aligned} \tan\lambda &= \frac{Y}{X}, \\ \tan\phi &= \frac{Z + \epsilon b\sin^3 u}{p - e^2 a\cos^3 u} \quad \text{and} \\ h &= \sec\phi\sqrt{X^2 + Y^2} - \nu, \end{aligned}$$

where

$$\begin{aligned} p &= \sqrt{X^2 + Y^2}, \\ \tan u &= \frac{2a}{pb} \quad \text{and} \\ \epsilon &= \frac{e^2}{1 - e^2}, \end{aligned}$$

with ν as defined previously. However, the true shape of the Earth is not ellipsoidal — it is irregular. This kind of shape is called a geoid. Generally the equipotential surface that most closely corresponds to mean sea level is taken to be the geoid of the Earth. The height of the geoid above the ellipsoid being used to model it is called the *geoid–spheroid separation* or more commonly just the *separation* and is usually denoted by N. The value of N may be either positive, negative or zero — and N is oriented normal to the ellipsoid. The geoid–spheroid separation is shown in Figure 4.3. The *vertical separation* is defined as the angle at which the geoid intersects with the ellipsoid. Globally the geoid used is found

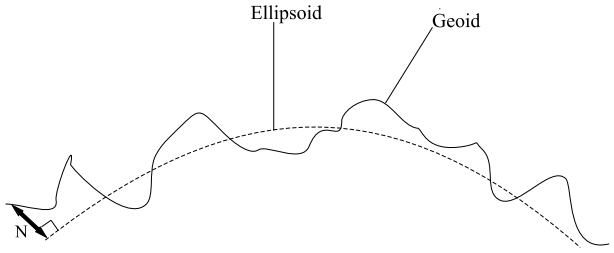

Figure 4.3*: Geoid – spheroid relationship and separation.*

from a set of coefficients of a spherical harmonic expansion referred to as the Earth Model. The Earth Model expresses the geoid as a series of functions over a sphere that are of decreasing wavelength. The smallest wavelength expressed is a function of the highest degree of accuracy obtainable [17].

Globally the most appropriate datum is an ellipsoid which has its origin at the Earth's centre of mass (centre of the Earth) and has a shape and size best approximating the geoid. This global datum generally

forms the basis for all satellite reference systems or other datums. A datum with its origin at the centre of the Earth is referred to as being geocentric. The most recent and most widely used global datum is currently the WGS84 datum (World Geodetic System). The WGS84 datum is a geocentric datum with $a = 6\,378\,137$ and $f = \frac{1}{298.257\,223\,563}$ (as well as measurements relating to the Earth's gravitational field and rotation rate) [2].

4.1.1 Local or Regional Datums

A local or regional datum is a datum defined by selecting an origin for a national or regional survey chosen such that N and the vertical separation are zero. In other words an ellipsoid is fixed to the geoid at the point of origin of the survey, and this point becomes the reference for the local or regional datum. The orientation of the minor axis is taken parallel to the spin axis of the Earth by means of Laplace azimuth observations (made with respect to the stars and the pole of the Earth's rotation). This astronomical based azimuth is converted to a geodetic azimuth (which is defined on the ellipsoid) by a formula forcing the poles to be the same. It is important to note here that the ellipsoid need not be geocentric. The local / regional datum is then defined by a combination of the shape and size of the ellipsoid and its position (given by fixing an origin). An ellipsoid on its own is *not* a datum.

All national datums are defined independently of each other. Therefore, if one were to consider two national datums which are both used to specify an overlapping area, for a specific point, the coordinates are generally different in the two reference systems. Local datums approximate the geoid in the region more closely than a global datum would, as illustrated in Figure 4.4. Should the WGS84 ellipsoid be used, then the origin for a local datum is expressed as $(\Delta X, \Delta Y, \Delta Z)$ in a relationship of the form

$$\begin{pmatrix} X \\ Y \\ Z \end{pmatrix}_{\text{WGS84}} = \begin{pmatrix} \Delta X \\ \Delta Y \\ \Delta Z \end{pmatrix} + \begin{pmatrix} X \\ Y \\ Z \end{pmatrix}_{\text{local}}.$$

Transformation from geodetic coordinates in one datum to geodetic coordinates in another are performed

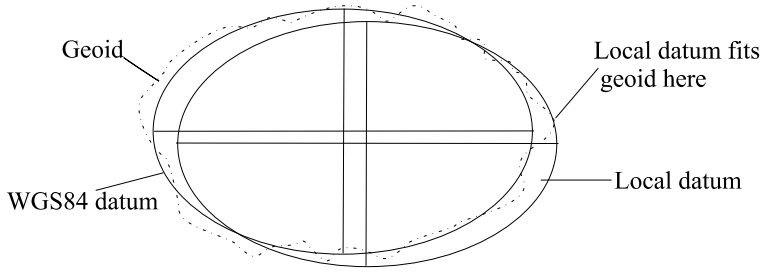

Figure 4.4: *Local datum using the WGS84 spheroid.*

by use of the Molodensky formulae [10],

$$\begin{aligned}
\Delta\phi &= \frac{-\Delta X \sin\phi\cos\lambda - \Delta Y \sin\phi\sin\lambda + \Delta Z\cos\phi + \Delta a\left[\frac{\nu e^2 \sin\phi\cos\phi}{a}\right] + \Delta f\left[\rho\left(\frac{a}{b}\right) + \nu\left(\frac{b}{a}\right)\sin\phi\cos\phi\right]}{(\rho+h)\sin\lambda}, \\
\Delta\lambda &= \frac{-\Delta X\sin\lambda + \Delta Y\cos\lambda}{(\nu+h)\cos\phi\sin\lambda} \quad \text{and} \\
\Delta h &= \Delta X\cos\phi\cos\lambda + \Delta Y\cos\phi\sin\lambda + \Delta Z\sin\phi - \Delta a\frac{a}{\nu} + \Delta f\frac{b}{a}\nu\sin^2\phi,
\end{aligned}$$

where ϕ, λ, e and f are as defined previously and refer to the geodetic coordinates of the datum to be transformed. Further, ν is as defined in (4.3) and

$$\rho = \frac{a(1-e^2)}{(1-e^2\sin\phi)^{\frac{3}{2}}}.$$

The values of $\Delta\phi$, $\Delta\lambda$ and Δh are the geodetic coordinates for the origin of the transformed datum. Before one can make use of a defined datum, the datum needs to be *realised*. Realisation of a datum is the process whereby the physical moments of the known coordinates are provided. This is done as, in addition to the simple transformation between two datums, there may exist rotations and changes to scale. The full transformation thus becomes

$$\begin{pmatrix} X \\ Y \\ Z \end{pmatrix}_{WGS84} = \begin{pmatrix} \Delta X \\ \Delta Y \\ \Delta Z \end{pmatrix} + \begin{pmatrix} X \\ Y \\ Z \end{pmatrix}_{local} \mu R, \tag{4.4}$$

where μ represents the scale factor and R is the rotation matrix

$$R = \begin{bmatrix} 1 & \alpha_3 & -\alpha_2 \\ -\alpha_3 & 1 & \alpha_1 \\ \alpha_2 & -\alpha_1 & 1 \end{bmatrix}.$$

The alphas are small and therefore R approximates a transformation matrix well. The rotation components of R are the well–known Euler angles, *roll* (α_1), *pitch* (α_2) and *yaw* (α_3) depicted in Figure 4.5.

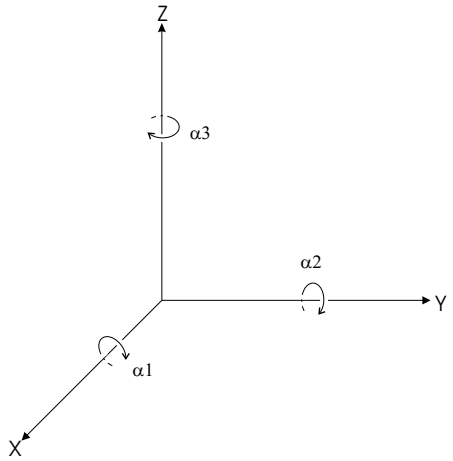

Figure 4.5*: Rotation components for datum realisation.*

4.1.2 The South African Local Datum

Previously South Africa used the *Cape Datum* as local coordinate system. The Cape Datum is referenced to the Modified Clarke 1880 ellipsoid and has its origin at Buffelsfontein, near Port Elizabeth. However, since January 1st, 1999 the official coordinate system for South Africa is based on the WGS84 ellipsoid, with the International Terrestrial Reference System (ITRF) 91 coordinates of Hartebeesthoek Radio Astronomy Tower near Pretoria as the initiation point for the new datum. This is called the *Hartebeesthoek 94 Datum*. Transformation of systems to the new Hartebeesthoek 94 Datum are still underway. All heights within the datum remain referenced to the mean sea level as determined in Cape Town and verified at tide guages in Port Elizabeth, East London and Durban [18]. The $(\Delta X, \Delta Y, \Delta Z)$ values in equation (4.4) for the Clarke 1880 ellipsoid with respect to the WGS84 ellipsoid are shown in Table 4.1 and the differences between the Modified Clarke 1880 ellipsoid and the WGS84 ellipsoid are shown in Table 4.2. It is important at this stage to note that a national geodetic coordinate system is related to a geodetic datum by two main factors: the geodetic reference ellipsoid and the orientation, position and scale of the datum in space. For the Cape Datum, the orientation and scale characteristics are defined by periodic astronomical azimuth and base line measurements, whereas for the Hartebeesthoek 94 Datum, the scale and orientation characteristics are defined within the Global Positioning System (GPS) operational environment and have been confirmed to be incident with the ITRF 91 determination (a land survey coordinate specification).

Ellipsoid	ΔX **(m)**	ΔY**(m)**	ΔZ**(m)**
Modified Clarke 1880	136	108	292

Table 4.1: *$(\Delta X, \Delta Y, \Delta Z)$ values in (4.4) for the Clarke 1880 ellipsoid.*

Ellipsoid	a	b	**Unit**	**Where Used**
Modified Clarke 1880	6 378 249.145	6 356 514.967	Int. m	RSA, Botswana, Zimbabwe
WGS84	6 378 137.000	6 356 752.314	Int. m	Global

Table 4.2: *Comparison of the Clarke 1880 and WGS84 ellipsoid parameters.*

4.2 Fundamentals of Map Projections

The majority of maps are printed on a two dimensional surface. Two dimensional surfaces are preferred due to the advantages they offer with respect to presentation and computational aspects typically associated with the use of maps. However, there is one disadvantage to this preference, and that is that the Earth is a three dimensional object and thus the information pertaining to its surface is similarly three dimensional. It is impossible to achieve a projection from a sphere onto a plane without some distortion[1]. Consider attempting to wrap a sheet of paper around a ball so that the paper has no folds and touches the ball everywhere and is not distorted. Unless the paper is wet and then stretched over the ball, this is an impossible task. In stretching the paper in order to cover the ball, distortion is introduced. A sphere is considered an undevelopable surface, in the sense that it cannot be produced from a plane by any transformation without introducing distortion or stretching.

The set of parallels and meridians on a map are known as the graticule. The graticule does not constitute the basis of a coordinate system that is suitable for computational purposes, or for placing of features on a projection. For this reason a rectangular coordinate system (grid) is super–imposed over the projection for placement and computation purposes.

The scale factor of a projection does not refer to the scale of the map, but rather to the projection used and the distortion it brings with it. The scale factor k is defined as the distance between two points on the projection divided by the distance between the corresponding points on the sphere or ellipsoid modelling the Earth, and is a direct indication of the amount and direction of distortion that has occurred. Therefore k is different at each point in the projection and may have different values in each direction[2]. The scale factor for a certain block of information on the sphere may thus be decomposed into two components: the scale factor in the direction of the meridian, k_m and the scale factor in the direction of the parallels, k_p.

The scale factor, in theory, applies to all lines of infinitesimally short length. In practice, the scale factor changes so slowly across a projection that a single scale factor is often considered applicable for all distances in localised surveys. The question is how slow and how significant the change is in distance. The answer depends on the projection used, but generally the area mapped is restricted to prevent having to perform scaling corrections. In cases where the point of tangency is in the middle of the region, the region with the most extreme rate of change of scale factor is the edge of the projection. The scale factor introduced should be the average computed over the entire length of the projection. Generally for a projection distance of 5km, this averaging introduces a potential error of approximately 8 cm, and for a distance of 3km, this error is approximately 3cm. For target accuracy of at least 1cm and distances over 1km it is advisable to calculate the scale factor for each line of the projection. A line, in this context, refers to a row or column of data in the region to be projected. For areas of less than one square kilometre a general scale factor may be used over the entire projection area. A good projection minimises the scale factor over the region. If it is not possible to do this, then one should consider splitting the region into

[1] A projection is an ordered system of meridians and parallels on a flat surface or plane surface. A plane surface is one on which straight lines can be drawn through any point in any direction upon the plane.

[2] No map projection shows scale correctly throughout the map, but there is usually one or more lines along the map where scale remains true, i.e. where $k = 1$.

zones in order to render the scale factor k as close as possible to 1 in each zone. However, splitting the region into zones increases the effort of computation of interrelations between the points in the different zones.

It is possible to derive mathematical formulae to transform geodetic coordinates to grid coordinates. Historically projections were derived by first projecting the data from the sphere onto an intermediate shape. The intermediate shape traditionally used was a developable surface: a surface that can be unravelled into a plane surface without distortion. The three main developable surfaces thus considered are: the *cone*, the *cylinder* and the *plane* itself. The advantage of these surfaces is that the curvature is in one direction only and is therefore easily unravelled without distortion. The general method of projection is that the developable surface is first brought into contact with the sphere and then a set of rules is formulated for the method of transfer of features from the sphere to the surface. It is immediately obvious that the region around the point of contact between the two surfaces has minimal distortion, in other words the scale factor seen in that region is $k \approx 1$.

Most projections are classified firstly according to the shape of the developable surface and the desired function of the map, and secondly by the features to be preserved. The choice of developable surface is generally dictated by the geographic extent of the region to be mapped. Traditionally the cylinder is used for mapping equatorial regions and the cone for the mapping of areas of mid latitude with large extent in longitude. The plane can be used anywhere. It is further possible to orientate the developable surface at different angles or to change the shape of the cone in order to facilitate mapping of other areas. Most large scale mapping is likely to be based on the Transverse Mercator Projection, the Lambert Conformal Conic Projection and to a lesser extent the Azimuthal Stereographic / Oblique Mercator Projections. When a projection is referred to as being transverse, it indicates that the developable surface has been rotated through ninety degrees. Using the cylinder as an example, this means that the point of contact between the cylinder and the sphere is no longer along the equator, but rather along one of the meridians. Oblique similarly refers to the developable surface being rotated through an angle greater than zero degrees and less than ninety degrees in any direction so that the point of contact between the cylinder and the sphere would lie at an angle to either a meridian or parallel, or both. The reader is referred to Figure 4.6 for a schematic example of the orientation of the developable surfaces for the different orientation reference classes of projections.

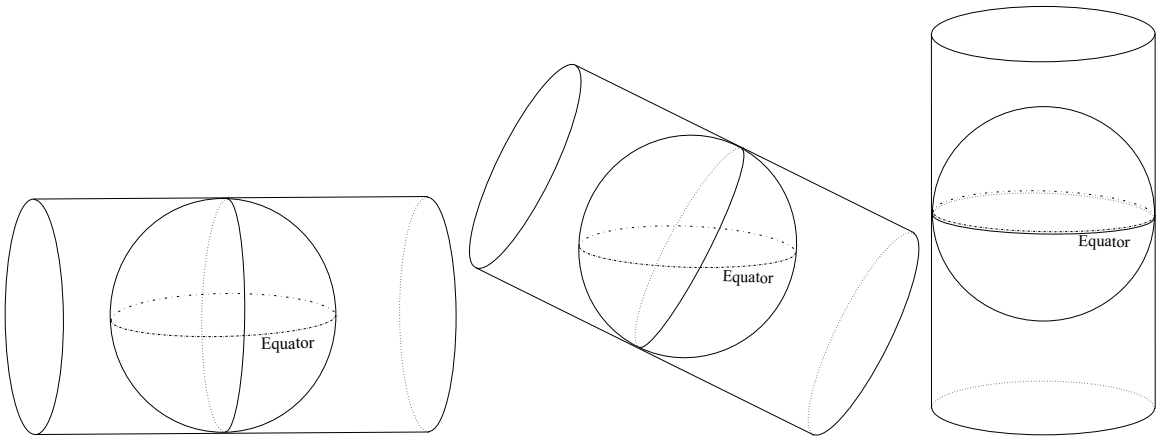

(a) Transverse (b) Oblique (c) Regular

Figure 4.6: *Possible cylinder orientations for map projections.*

The set of rules derived for the transfer of features depends on the purpose for which the projection was devised. The usual approach in the derivation of these rules is to preserve one of the characteristics of the features, namely the *shape*, *size*, or *area* of or *angles* within the region to be projected. For an *equidistant* projection the distances along all the meridians remain undistorted. This means that the shape and area of the features are distorted, but the scale factor along the meridian is given by $k_m = 1$.

An *equal area* projection preserves area but not shape, angles or size, meaning that $k_m k_p = 1$. Other terms used to describe an equal area projection are *equivalent, homolographic or homalographic, authalic* and *equiareal*. *Orthomorphic* or *conformal* projections preserve the shape of all features. However, on a conformal map of the entire Earth, there are some singular points at which shape is still distorted — this is due to the fact that a large landmass must still be shown as distorted in shape even though all of its small features are correctly shaped relative to each other. Preserving shape means that for a block on the sphere $k_m = k_p$. It is to be noted that in preserving the shape of features one is, in addition, preserving the angles within the features. In other words, relative angles at each point are correct and the local scale in every direction around one point is constant. Areas, however, are generally enlarged or reduced along the projected map. The Conformal projection is the most significant projection in land surveying, due to the computational accuracy requirements of land surveying and is therefore the most frequently used projection for any large scale mapping[3]. Another option for features to be preserved, although seldom used, is the *azimuthal* or *zenithal* projection on which the directions or azimuths of all points are shown correctly with respect to the centre. Generally this type of projection is included in one of the above three main classifications.

While the above features and characteristics should generally be considered when choosing a map projection, using them to identify which projection was used in the construction of a map is not obvious. If the region shown on the map is no larger than South Africa or the United States (say), then even the trained eye could not pick out the type of projection used. Measurements would have to be taken to determine small differences in spacing or location of meridians and parallels, and even then this information would not be sufficient to identify accurately the type of projection used. Some projections are none of the above mentioned types and do not preserve any of shape, area, angles or distance (size).

There are several hundred published map projections, some of which are rarely used novelties, and there is an infinite number of ways to define a map projection. Furthermore, a specific map projection may be varied in infinite ways by changing the point of contact of the developable surface on the Earth's surface and / or changing the orientation or size of the developable surface used. Several map projections provide special characteristics that no other projection provides. Of these projections, the most applicable to this thesis is the *Mercator* projection which shows all rhumb lines (loxodromes)[4] as straight lines. This is important as rhumb lines are essential in maritime navigation and in land surveys. It cannot be said that there is one "best" projection for use in mapping, as each map is produced with certain aims and requirements in mind and the projection is chosen to best facilitate these aims and requirements — there is even risk in claiming to have found the "best" projection from a certain class for a specific application.

4.3 Cylindrical Map Projections

The best known map projection is the Mercator Projection — one of the cylindrical projections. Regular cylindrical projections are perhaps the easiest to draw if secant reference tables are on hand. They consist of meridians which are equidistant parallel straight lines, intersected at right angles by straight parallel lines of latitude (generally not equidistant). *Regular* here means that the cylinder has not been orientated to another angle, as shown in Figure 4.6(c), and has its point of contact on the equator. Generally the class of cylindrical projections are the most widely used for land surveying and construction of land maps. Furthermore, the Mercator projection is one of the most significant and widely used conformal cylindrical projections throughout the world, and is the basis for most land survey work. Considering that the bathymetric data to be used in this thesis is of a land survey nature, and that the data available can only be extracted from the source using either the equidistant cylindrical or regular Mercator projections, these two projections are described in some detail in this section. Emphasis, however, will be on the regular Mercator projection which, being conformal, widely known and eminently suited to the type of

[3]Land surveying has two principal aspects: preservation of distances and angles. For this reason the set of conformal projections is preferred. Use of conformal projections indicates that the distance on the projection is the scale factor multiplied by the distance on the sphere. For a meridian, this means that the scale factor is the same in all directions.

[4]A path, also known as a *rhumb line*, which intersects a meridian on a given surface at any constant angle but a right angle. If the surface is a sphere, the loxodrome is a spherical spiral. The loxodrome is the path taken when a compass is kept pointing in a constant direction. It is a straight line on a Mercator projection. The loxodrome is *not* the shortest distance between two points on a sphere.

bathymetric data available, will be used as the extraction projection for the data in this thesis.

4.3.1 The Cylindrical Equidistant Map Projection

The equidistant cylindrical projection is one of the simplest projections to construct and one of the oldest. The projection probably originated with either Eratosthenes (300 B.C.), the scientist, philosopher and geographer best known for his fairly accurate measure of the Earth's circumference, or with Marinus (A.D. 100). The meridians and parallels are all equidistant straight parallel lines, intersecting at right angles in this projection. The projection is now used primarily for maps on which distortion is considered less important than the need for ease of displaying special information. If the equator is the standard parallel, true to scale and free of distortion, then the meridians are spaced at the same distances as the parallels and the graticule appears square. The projection is used largely for ease in computerized plotting, is used only in spherical form and is neither area preserving nor conformal.

The projection is formed by bringing a cylinder into contact with the sphere and "peeling" the meridians off the sphere and onto the cylinder with no distortion — the scale factor along the meridian is given by ($k_m = 1$). It is therefore necessary to stretch each parallel of latitude to be the same length as the equator. If the circumference of the equator is $C_{eq} = 2\pi R$, where R is the radius of the spherical Earth, then the circumference of a parallel of latitude ϕ would be $C_\phi = 2\pi R \cos\phi$. This means that

$$k_p \quad = \quad \frac{2\pi R}{2\pi R \cos\phi} = \frac{1}{\cos\phi} = \sec\phi.$$

Therefore all meridians are straight and parallel to each other, with the distances along them undistorted. The equator is true to scale, but the scale distortion of the parallels of latitude increases towards the poles causing the shape and area of features in the region to be more distorted. Further, the poles themselves cannot be used in the projection as $\sec\frac{\pi}{2}$ does not exist. The flat square appearance of the graticules is referred to as *plate carrée* [17].

The projection is performed as follows. A point of origin (a contact point) for the projection is chosen, and identified by assigning the symbols (ϕ_0, λ_0) to the point of reference within the projection formulae. The distance along the equator between the projection point and the origin is denoted by x, and the distance along the meridian from the origin to the projection point is denoted by y. Given R, λ_0, λ, ϕ_0, and ϕ, the values of the cartesian coordinates, x and y, are found by means of the transformation

$$x = R(\lambda - \lambda_0)\cos\phi_0 \quad \text{and} \quad y = R\phi. \tag{4.5}$$

where

$$k_p \quad = \quad \frac{\cos\phi}{\cos\phi_0}. \tag{4.6}$$

The x axis corresponds to the equator with x increasing easterly, while the y axis coincides with the central meridian λ_0 and y increasing northerly. It is necessary to adjust the quantity $(\lambda - \lambda_0)$ if it is beyond the range $[-\pi, \pi]$ by adding or subtracting 2π [15]. The standard parallel is ϕ_0, also $-\phi_0$ if working in the southern hemisphere. For the inverse transformation, given R, λ_0, ϕ_0, x, and y, the spherical coordinates λ and ϕ may be found by means of the transformation

$$\phi = \frac{y}{R} \quad \text{and} \quad \lambda = \lambda_0 + \frac{x}{R\cos\phi_0}.$$

The equations for the cylindrical equidistant projection can be used for any standard parallel. Use for a parallel of origin (contact) ϕ_1, where ϕ_1 does not refer to the equator, does not change (4.5) and (4.6). Table 4.3 gives some special cases of the cylindrical equidistant projection.

Example 4.1 : Cylindrical Equidistant Application
In this example the working of the cylindrical equidistant projection is demonstrated using a simple grid of points, shown in Figure 4.7. The cylindrical equidistant projection is only defined for use on a sphere. As mentioned previously the Earth can be approximated by a sphere with radius $R = 6\,371\,000m$. For

ϕ_1	**Projection Name**
$0°$	Equirectangular projection
$37°30'$	Miller equidistant projection
$43°$	Miller equidistant projection
$45°$	Gall orthographic projection
$50°28'$	Miller equidistant projection

Table 4.3: *The special cases of cylindrical equidistant projection.*

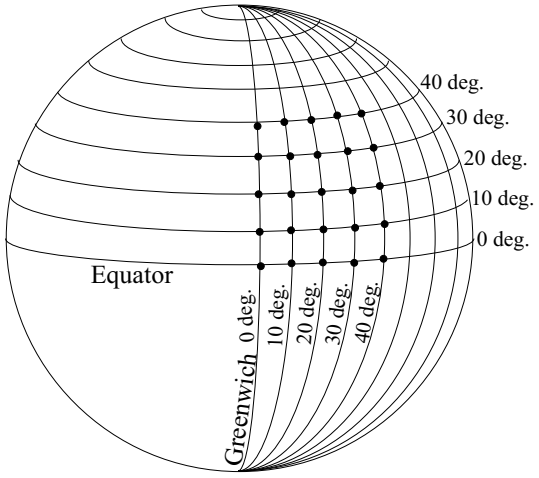

Figure 4.7: *The grid of points to be projected using the Cylindrical Equidistant projection in Example 4.1.*

this example the point of origin for the projection is $(\phi_0, \lambda_0) = (0, 0)$ *— making this an equirectangular projection. Application of (4.5) and (4.6) yields the results shown in Table 4.4 and given graphically in Figure 4.8. Note that all distances (R, x and y) are given in metres. As can be seen in Figure 4.8, the projection has a flat square appearance. The points on their own do not, however, give an indication as to the distortion of features that has taken place. For an indication of this, the reader is referred to Figure 4.9 which shows an equirectangular projection of the Earth.* ■

4.3.2 The Mercator Map Projection

The widely known Mercator projection was the first projection to be referred to regularly when atlases started to name the projections used, over a century ago. The projection was apparently used for the first time by Erhard Etzlaub of Nuremburg (1462–1532) on a small map covering sundials constructed in 1511 and 1513. Gerhardus Mercator (1512–1594) independently developed and presented the projection, which had remained obscure (in principle) since the early 1500s, in 1569 on a large world map of 21 sheets totalling about 1.3m by 2m [28]. Mercator was probably originally named Gerhard Cremer (or Kremer) but always used the latinized version of his name. He was born at Rupelmonde in Flanders, and is attributed the reputation of being the first person to use the name "atlas" to describe a collection of maps in a volume.

Mercator developed his projection specifically to aid navigation. He described, in Latin, the nature of the projection in a large panel covering much of his portrayal of North America on his 1569 map, entitled "*Nova et Aucta Orbis Terrae Descriptio ad Usum Navigantium Emendate Accomodata*" (A new and enlarged description of the Earth with corrections for use in navigation) as follows:

> "In this mapping of the world we have [desired] to spread out the surface of the globe into a plane that the places shall everywhere be properly located, not only with respect to their true direction and distance, one from another, but also in accordance with their due longitude

ϕ–degrees	λ–degrees	ϕ–radians	λ–radians	x	y	k_p
0	0	0	0	0	0	1
0	10	0	0.174 533	1 111 949.266	0	1
0	20	0	0.349 066	2 223 898.533	0	1
0	30	0	0.523 599	3 335 847.799	0	1
0	40	0	0.698 132	4 447 797.066	0	1
10	0	0.174,329	0	0	1 111 949.266	0.984 808
10	10	0.174 533	0.174 533	1 111 949.266	1 111 949.266	0.984 808
10	20	0.174 533	0.349 066	2 223 898.533	1 111 949.266	0.984 808
10	30	0.174 533	0.523 599	3 335 847.799	1 111 949.266	0.984 808
10	40	0.174 533	0.698 132	4 447 797.066	1 111 949.266	0.984 808
20	0	0.349 066	0	0	2 223 898.533	0.939 693
20	10	0.349 066	0.174 533	1 111 949.266	2 223 898.533	0.939 693
20	20	0.349 066	0.349 066	2 223 898.533	2 223 898.533	0.939 693
20	30	0.349 066	0.523 599	3 335 847.799	2 223 898.533	0.939 693
20	40	0.349 066	0.698 132	4 447 797.066	2 223 898.533	0.939 693
30	0	0.523 599	0	0	3 335 847.799	0.866 025
30	10	0.523 599	0.174 533	1 111 949.266	3 335 847.799	0.866 025
30	20	0.523 599	0.349 066	2 223 898.533	3 335 847.799	0.866 025
30	30	0.523 599	0.523 599	3 335 847.799	3 335 847.799	0.866 025
30	40	0.523 599	0.698 132	4 447 797.066	3 335 847.799	0.866 025
40	0	0.698 132	0	0	4 447 797.066	0.766 044
40	10	0.698 132	0.174 533	1 111 949.266	4 447 797.066	0.766 044
40	20	0.698 132	0.349 068	2 223 898.533	4 447 797.066	0.766 044
40	30	0.698 132	0.523 599	3 335 847.799	4 447 797.066	0.766 044
40	40	0.698 132	0.698 132	4 447 797.066	4 447 797.066	0.766 044

Table 4.4: *Numerical results of the Cylindrical Equidistant projection.*

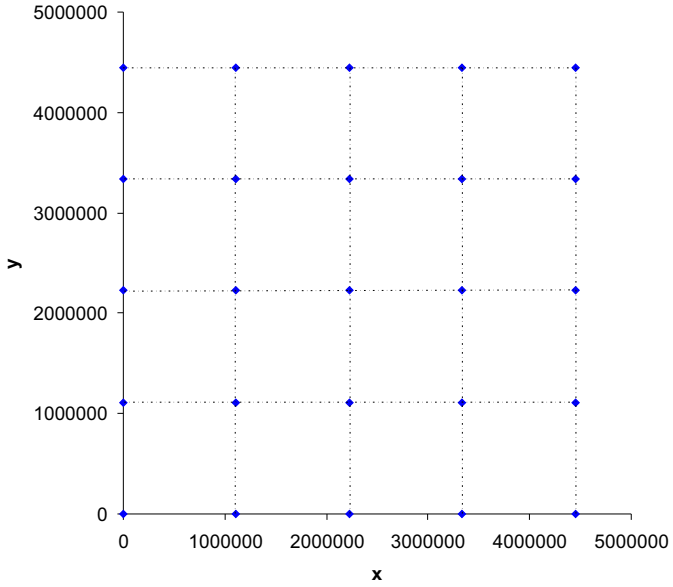

Figure 4.8: *The result of Cylindrical Equidistant projection of Example 4.1 for the points in Figure 4.7.*

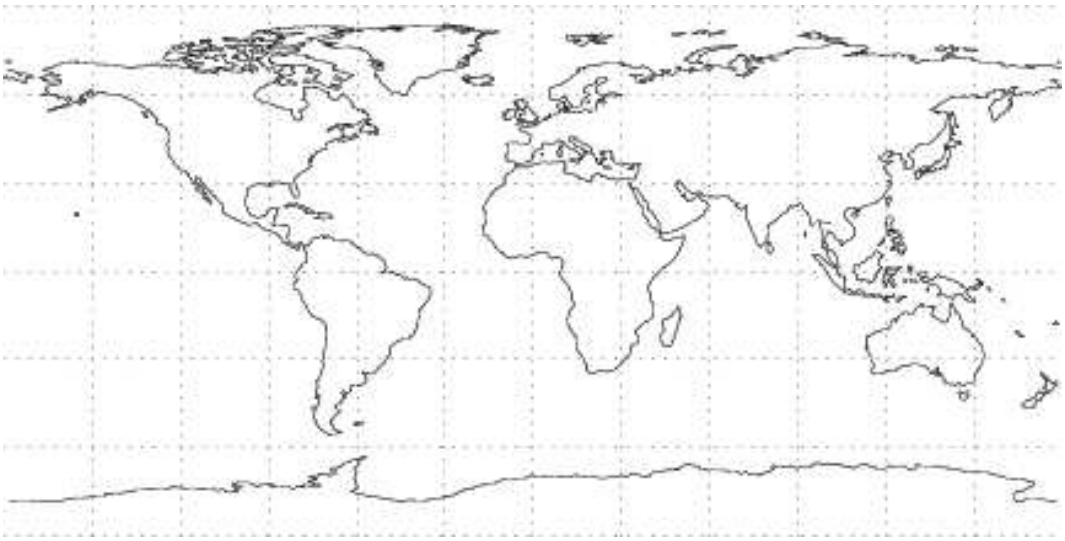

Figure 4.9: *An equirectangular projection of the Earth.*

> and latitude; and further that the shape of the lands, as they appear on the globe, shall be preserved as far as possible. For this there was needed a new arrangement and placing of meridians, so that they shall become parallels, for the maps hitherto produced by geographers are, on account of the curving and the bending of the meridians, unsuitable for navigation. Taking all this into consideration, we have somewhat increased the degrees of latitude toward each pole, in proportion to the increase of the parallels beyond the ratio they really have to the equator." [28]

When Mercator developed his projection, tables of secants had not yet been invented and therefore he most likely determined the spacing graphically. Edward Wright (1558 – 1615) of England later developed the mathematics of the projection and published tables of cumulative secants in 1599, indicating the true spacing from the equator. The meridians of longitude of the Mercator projection are vertical, parallel and equally spaced lines, cut at right angles by horizontal straight parallels which are increasingly spaced

towards the poles so that conformality exists. The spacing of the parallels at a given latitude on the sphere is proportional to the secant of the latitude. This means that as one moves closer to the poles on a large scale map, the distortion of the size and shape of features increases, and further that the poles themselves cannot be represented in a large scale Mercator projection as they are at infinite distance from other parallels on the projection. Scale is true along the equator or along the two alternately defined standard parallels equidistant from the equator. The major feature of the Mercator projection with regards to navigation is that rhumb lines are straight. The Mercator projection was fundamental in the development of conformal map projections. It further remains a standard navigation tool and is also especially suitable for conformal maps of equatorial regions and maps as a result of a land surveying.

There are three main types of Mercator projection: the regular Mercator projection, the transverse Mercator projection and the oblique Mercator projection. The regular projection is described in some detail in the following section. The transverse Mercator projection and the oblique Mercator projection are not used in this thesis and are therefore not discussed.

The Regular Mercator Projection

The Mercator transformation is defined for both a sphere and an ellipsoid. There is, however, no suitable geometrical construction of the Mercator projection, and therefore the forward transformation for rectangular coordinates on a sphere is given, using the same definition of symbols as used in the cylindrical equidistant discussion, by

$$x = R(\lambda - \lambda_0), \tag{4.7}$$

$$y = R \ln \tan\left(\frac{\pi}{4} + \frac{\phi}{2}\right) = R \operatorname{arctanh}(\sin\phi). \tag{4.8}$$

Recall that ϕ and λ are measured in radians. As before, the x axis lies along the equator with x increasing easterly and the y axis lies along the central meridian λ_0 with y increasing northerly. It is necessary to adjust the quantity $(\lambda - \lambda_0)$ if it is beyond the range $[-\pi, \pi]$ by adding or subtracting 2π. The second expression on the right hand side of (4.8) may be more convenient to use than the first if hyperbolic functions are standard to the computational device. The scale factor for the Mercator projection is

$$k_m = k_p = \sec\phi.$$

The areal scale factor for the Mercator projection in spherical form is thus $k^2 = \sec^2\phi$. The inverse transformation for the sphere, to regain ϕ and λ from the rectangular Cartesian coordinates, is given by

$$\phi = \frac{\pi}{2} - 2\arctan\left(\exp(-\frac{y}{R})\right) \quad \text{and} \tag{4.9}$$

$$\lambda = \lambda_0 + \frac{x}{R}. \tag{4.10}$$

The transformation for an ellipsoid is given by

$$x = a(\lambda - \lambda_0) \quad \text{and} \tag{4.11}$$

$$y = a \ln\left[\tan\left(\frac{\pi}{4} + \frac{\phi}{2}\right)\left(\frac{1 - e\sin\phi}{1 + e\sin\phi}\right)^{\frac{e}{2}}\right], \tag{4.12}$$

where a is the semi–major axis length (equatorial radius) of the ellipsoid and e is its eccentricity. Further, the scale factor is given by

$$k_m = k_p = \frac{\left(1 - e^2\sin^2\phi\right)^{\frac{1}{2}}}{\cos\phi} \tag{4.13}$$

and the areal scale factor is $k^2 = \frac{1-e^2\sin^2\phi}{\sec^2\phi}$. The inverse formulae for the ellipsoid require a rapidly converging iteration scheme. If the closed forms of the equations for finding ϕ are used, then

$$\phi_{n+1} = \frac{\pi}{2} - 2\arctan\left\{t\left[\frac{1 + e\sin\phi_n}{1 - e\sin\phi_n}\right]^{\frac{e}{2}}\right\}, \tag{4.14}$$

where

$$t = \exp(-\frac{y}{a})$$

and the first trial is given by

$$\phi_0 = \frac{\pi}{2} - 2\arctan t.$$

The iteration process is repeated until the change in ϕ is less than a chosen convergence tolerance, which is dependent on the accuracy required. For λ,

$$\lambda = \frac{x}{a} + \lambda_0. \tag{4.15}$$

The scale factor is calculated from equation (4.13) using the value calculated for ϕ.

Example 4.2 : Regular Mercator Application
In this example the working of the regular Mercator projection for an ellipsoid is demonstrated, using a simple grid of points, shown in Figure 4.10.

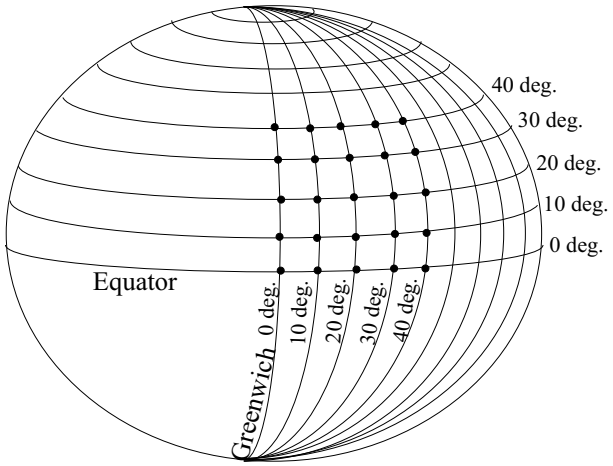

Figure 4.10: *The grid of points to be projected by means of the regular Mercator projection.*

For this example the point of origin for the projection is $(\phi_0, \lambda_0) = (0, 0)$. *Further, the values used for the semi–major axis length and the eccentricity are* $a = 6\,378\,137.00$ *and* $e = 0.081\,819\,19$ *respectively. Application of (4.11), (4.12) and (4.13) yields the results shown in Table 4.5 and given graphically in Figure 4.11. Note that all distances (a, x and y) are given in metres. As may be seen in Figure 4.11, the distance between the projected parallels increases with increasing latitude, ensuring the preservation of the shape of features in the area by rescaling the distance along the meridian so that it matches the stretching of the parallel to the length of the equator. The points on their own do not, however, give an indication as to the fact that the shape of features has been preserved. For a graphical indication of this, the reader is referred to Figure 4.12 which shows a regular Mercator projection of the Earth. Note that Figure 4.12 is a large scale map and therefore does show some distortion of large land masses near the singular points. Recall that even though there is visual distortion, all of the small features are correctly shaped relative to each other.* ■

The Regular Mercator Projection with another standard parallel

The regular Mercator projection assumes the equator as the standard parallel (point of contact) and thus the equator is true to scale. It is also possible to have another parallel as the standard parallel, and thus have the region around that parallel true to scale. For the Mercator projection, the map will look exactly the same, only the scale will be different. If the latitude ϕ_1 is taken as standard parallel then

ϕ–degrees	λ–degrees	ϕ–radians	λ–radians	x	y	k_p
0	0	0	0	0	$-7.081\,15E-10$	1
0	10	0	0.174 533	1 113 194.908	$-7.081\,15E-10$	1
0	20	0	0.349 066	2 226 389.816	$-7.081\,15E-10$	1
0	30	0	0.523 599	3 339 584.724	$-7.081\,15E-10$	1
0	40	0	0.698 132	4 452 779.632	$-7.081\,15E-10$	1
10	0	0.174 533	0	0	1 111 475.103	1.015 324
10	10	0.174 533	0.174 533	1 113 194.908	1 111 475.103	1.015 324
10	20	0.174 533	0.349 066	2 226 389.816	1 111 475.103	1.015 324
10	30	0.174 533	0.523 599	3 339 584.724	1 111 475.103	1.015 324
10	40	0.174 533	0.698 132	4 452 779.632	1 111 475.103	1.015 324
20	0	0.349 066	0	0	2 258 423.649	1.063 761
20	10	0.349 066	0.174 533	1 113 194.908	2 258 423.649	1.063 761
20	20	0.349 066	0.349 066	2 226 389.816	2 258 423.649	1.063 761
20	30	0.349 066	0.523 599	3 339 584.724	2 258 423.649	1.063 761
20	40	0.349 066	0.698 132	4 452 779.632	2 258 423.649	1.063 761
30	0	0.523 599	0	0	3 482 189.085	1.153 734
30	10	0.523 599	0.174 533	1 113 194.908	3 482 189.085	1.153 734
30	20	0.523 599	0.349 066	2 226 389.816	3 482 189.085	1.153 734
30	30	0.523 599	0.523 599	3 339 584.724	3 482 189.085	1.153 734
30	40	0.523 599	0.698 132	4 452 779.632	3 482 189.085	1.153 734
40	0	0.698 132	0	0	4 838 471.398	1.303 601
40	10	0.698 132	0.174 533	1 113 194.908	4 838 471.398	1.303 601
40	20	0.698 132	0.349 066	2 226 389.816	4 838 471.398	1.303 601
40	30	0.698 132	0.523 599	3 339 584.724	4 838 471.398	1.303 601
40	40	0.698 132	0.698 132	4 452 779.632	4 838 471.398	1.303 601

Table 4.5*: Numerical results of the regular Mercator projection in Example 4.2.*

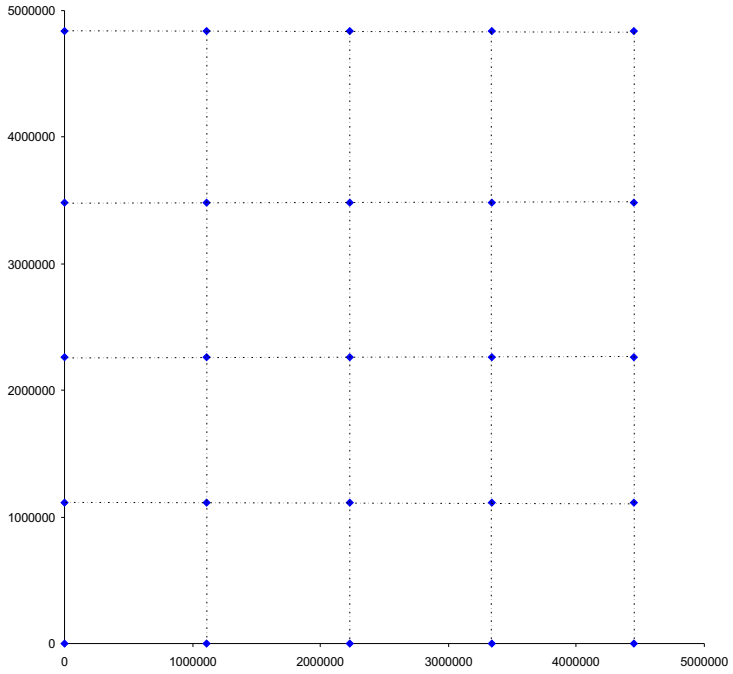

Figure 4.11: *The result of a regular Mercator projection in Example 4.2 for the points in Figure 4.10.*

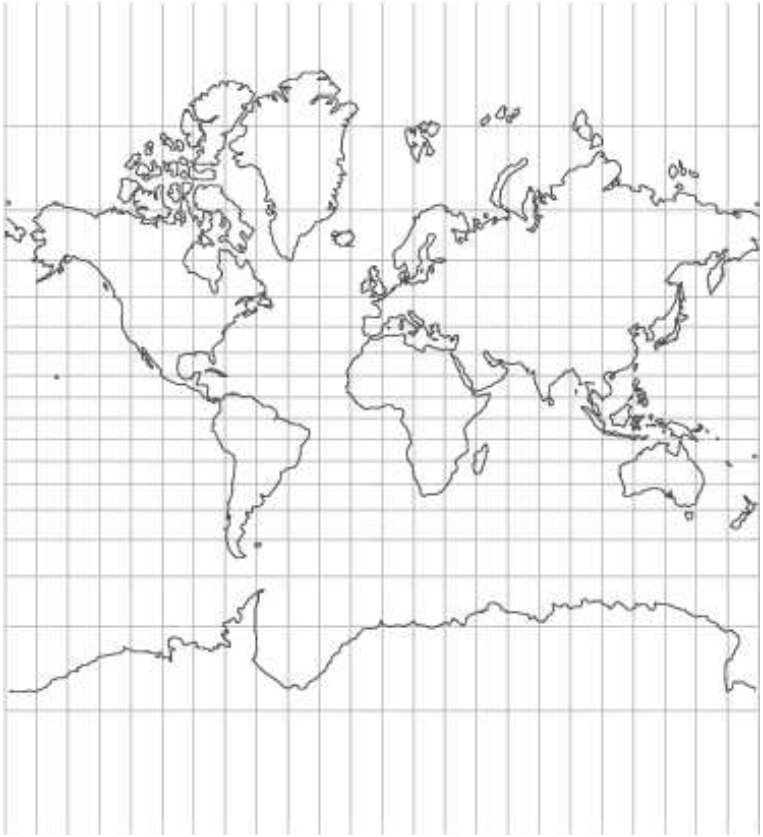

Figure 4.12: *A regular Mercator projection of the Earth.*

the opposite latitude, $-\phi_1$ will also be standard. To visualise this, picture a cylinder with circumference smaller than that of the sphere. Then the cylinder will intersect with the sphere in two places, at a distance above the equator along a parallel of latitude and at the same distance below the equator on the opposite or negative parallel of latitude. The smaller the cylinder circumference is made, relative to that of the sphere, the greater the distance between the equator and the parallels of latitude where the cylinder comes into contact with the sphere. The equations given above are specifically for the regular Mercator projection with the equator as standard parallel.

To adapt the above formulae to another standard parallel, the forward transform equations for the sphere are adapted by multiplying the right hand sides of equations (4.7)–(4.8) by $\cos\phi_1$. For the ellipsoid, the forward transformation equations are adapted by multiplying the right hand sides of equation (4.11)–(4.12) by

$$\frac{\cos\phi_1}{\left(1-e^2\sin^2\phi_1\right)^{\frac{1}{2}}}.$$

For the inverse equations, the values of x and y are divided by the same magnitudes before use in Equations (4.9) and (4.10) or Equations (4.14) and (4.15). This modification of the standard parallel is most commonly used for mapping parts of the ocean for navigational purposes, but has also been used to map areas along a parallel of latitude away from the equator, such as South Africa. The data extracted for use in this thesis was projected onto the plane by means of the regular Mercator projection using a standard parallel of 33° in order to achieve results that are approximately true to scale throughout South Africa's sea territory.

4.4 Data Sets

In order to safely navigate the oceans, sea–going vessels require information pertaining to the depth of water that the vessel is in or moving towards. A measurement of oceanic water depth is referred to as a bathymetric measurement and is achieved by means of an echo sounder in the vessel's hull. An echo sounder propagates a sound signal through the water column towards the ocean floor, typically angled directly below the vessel or slightly ahead of it, and then records the time taken for the echo of the signal off the ocean floor to return to the sensor. The depth of the ocean at that point may then be computed using the recorded return time, the frequency of the sound signal, the propagation angle and information relating to the specific characteristics of the water column itself.

Modern navigation charts incorporate general depth information (in the form of depth contours) with indications of oceanic features, navigational hazards and other navigation related information. Most maritime states have accurate charts of their seas that are regularly updated and improved upon. The construction of these charts depend on accurate bathymetry for the region to be mapped. Once in the deep ocean, however, the requirement for high accuracy bathymetry reduces as a direct result of the reduction in the probability of a vessel running aground or colliding with a submerged oceanic feature. As a result, the extremely accurate bathymetry used for construction of local navigational charts does not extend to the deeper waters where the FoS would typically be located (typically below or at a $2\,500m$ water depth).

In the initial exploration of the seas, bathymetry readings were taken by most vessels and these readings do extend into the deeper oceanic waters. The bathymetry readings recorded throughout history by vessels willing to submit their information for the general public good have been compiled into public–domain data sets and these data sets are readily available. Public–domain data sets are, however, not guaranteed to be easy to utilise and are not necessarily in a viable format for use. Most of the public–domain data sets have compiled the bathymetric data such that the data points themselves are in equally spaced grids. The spacing between the data points in the grid thus defines the data resolution of the data set.

The *Caris Lots* software suite [5] serves as a platform for the distribution and use of some of the public–domain bathymetry data sets. Specifically, *Caris Lots* offers three digital bathymetry libraries: the ETOPO five minute data set, the ETOPO two minute data set and the GEBCO one minute data set.

These three digital bathymetry libraries offer gridded bathymetry in three different resolutions. In the five minute data set there are five minutes of latitude or longitude between two consecutive data points in the set. One minute of latitude or longitude is equivalent to one international nautical mile which is exactly $1\,852\,m$. It can be seen that the five minute data set is thus a very coarse data set, with approximately $9\,260\,m$ between each data point. The two minute data set, similarly, has two minutes of latitude or longitude between each pair of consecutive data points ($3\,704\,m$) and the one minute data set has one minute or $1\,852\,m$ between each pair of consecutive data points. Although both the ETOPO and GEBCO bathymetry data sets offer gridded data, the cumulative source of the ETOPO data sets is not as reliable as that of the recent GEBCO data sets, and is of a lesser quality.

It was suggested, by Mr Carl Wainman [42], that the five minute bathymetry was too coarse for use in this thesis, and that the results obtained from use of this data set would not be of high enough resolution to be considered by the Working Group for possible use in the claim process[5]. The one and two minute data sets are, however, used in this thesis. Three regions of the South African coast were initially identified for consideration and were located on the west, south and east coasts. After determination of the surfaces of maximum curvature for each of the regions using one minute data, it was found that the west coast data would better serve as an example of a case where the mathematical method is not, on its own, sufficient for determination of the FoS. For this reason a fourth region (on the south west coast of South Africa) was identified for additional use. This was done in order to ensure a range of shelf profiles for consideration and comparison. The reader is referred to Figure 4.13 (a screen shot from the *Caris Lots* operational environment) for an indication of the geographical position of these regions. The blocks seen in the figure are the blocks defined in *Caris Lots* for extraction of data and the labelling of the blocks is a photo edit performed by means of the Jasc software package *Paintshop Pro* [19] to facilitate ease of identification. All data in the *Caris Lots* digital bathymetry libraries are defined with respect to

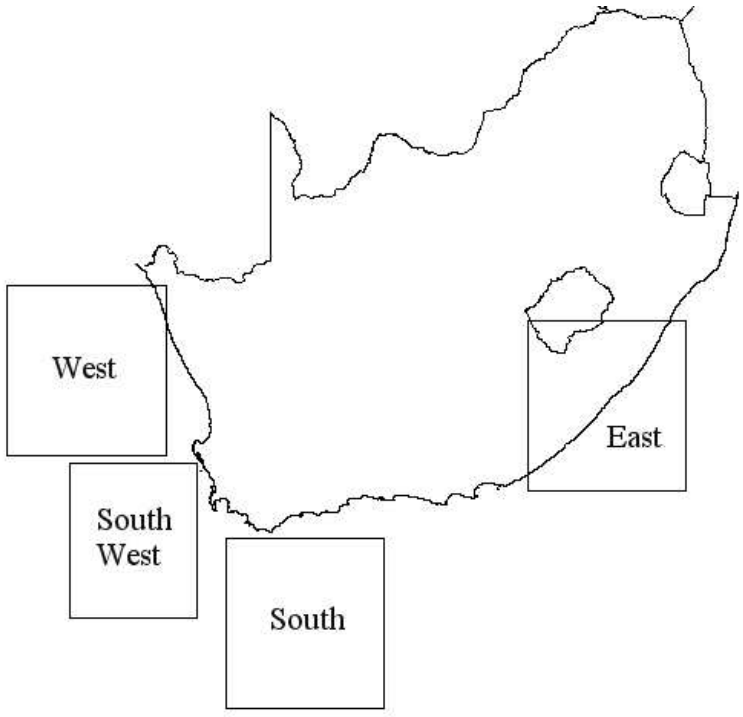

Figure 4.13*: The positioning of the blocks of bathymetric data used.*

the WGS84 global datum and is thus ellipsoidal data. An example of *Caris Lots's* datum information is given verbatim below. This datum information forms part of a file created after each data extraction (as shown below), specifying the datum used and the corner points of the block of data extracted.

[5]Mr Carl Wainman is an oceanographic expert and member of the Working Group and Steering Committee for South Africa's claim, and as such acted as advisor to all technical issues relating to the data to be used in this thesis.

```
!Datum Information:
Datum Name:  WG84
Major Axis:  6378137.000
Minor Axis:  6356752.314
Shifts (x,y,z):  0.000    0.000    0.000
Rotation (x,y,z):  0.000    0.000    0.000
Scale factor:  1.000000
```

During data extraction from the *Caris Lots* libraries, *Caris Lots* allows the user to choose either the cylindrical equidistant projection or the regular Mercator projection. For this thesis the regular Mercator projection was chosen. *Caris Lots* automatically optimizes the scale factor for the projection by using a standard parallel that minimizes distortion in the region to be extracted. The data for this thesis was therefore extracted using equations (4.11) and (4.12), where these equations were adapted for use with a standard parallel of 33° as discussed in the section pertaining to the regular Mercator projection with another standard parallel.

The next two subsections serve to introduce the data extracted for the one and two minute data sets. The processing required to achieve a format viable for computational purposes is discussed for each data resolution, and the seafloor surfaces and their corresponding contour plots are given for each region. The section concludes with a discussion of the foot points chosen in *Caris Lots* for each region, in addition to the foot point data as extracted from *Caris Lots*.

4.4.1 Two Minute Bathymetry

Extraction of a block of ETOPO two minute bathymetry data in *Caris Lots* yields an ASCII file containing data in the format shown in the sample below. The sample is the first few lines of the data file for the east coast data.

```
Last edited:  6-SEP-2004 14:03


 KEY ========   ===== CHARTED  POSITION =====   ======== DEPTH   SOURCE

                 29-54-00.003S  27-07-59.997E        -1603.      C00-00.XYZ
                 29-54-00.003S  27-10-00.000E        -1640.      C00-00.XYZ
                 29-54-00.003S  27-12-00.003E        -1606.      C00-00.XYZ
                 29-54-00.003S  27-13-59.998E        -1703.      C00-00.XYZ
                 29-54-00.003S  27-16-00.002E        -1782.      C00-00.XYZ
                 29-54-00.003S  27-17-59.997E        -1545.      C00-00.XYZ
```

As can be seen, the latitude and longitude values are not in decimal format and therefore need to be transformed to this format for further use. Transformation to decimal format is achieved by taking the value for the seconds of latitude or longitude and dividing it by 60. The result is then added to the minutes and this sum is then divided by 60 before being added to the value for latitude or longitude. Further, the height and depth values of the data have the correct signs and therefore do not need to be edited.

Processing of this data was performed by means of the Microsoft Office package *Excel* [25]. The ASCII data file was imported into *Excel*, the decimal values of longitude and latitude calculated and the sign of the depth values corrected. The resulting *Excel* document was then imported into *Matlab* [24] by means of *Matlab's* built in **xlsread** function. The extracted data is given in three columns, which need to be built into a matrix. In *Matlab* this is achieved by running down the latitude data column and stopping when the latitude value changes. This point of change gives the m value for the matrix dimension, where matrix dimension is taken as being $m \times n$. The longitude vector is then the elements of the longitude column from the start of the column to column number m (inclusive). The latitude vector is then constructed by taking the first element of the latitude data column as the first vector element,

the second vector element as the $(2+m)^{\text{th}}$ column element and so on. The size of the latitude vector gives the second matrix dimension, n. The depth matrix is finally constructed by creating a vector where each vector element is a block of length n from the depth column. Blocks are included in the vector consecutively. This results in a matrix (longitude $\times$ latitude) that is in a format applicable for computational purposes.

4.4.2 One Minute Bathymetry

Extraction of a block of GEBCO one minute bathymetry data in *Caris Lots* yields an ASCII file containing data in the format shown in the sample below. The sample is the first few lines of the data file for the east coast data.

```
Gridded data provided through the GEBCO Centenary Edition software interface
Data source GEBCO One Minute Grid version 1.00
Minimum longitude : 27.1 degrees (+ve East)
Maximum longitude : 31.4833333333333 degrees (+ve East)
Minimum latitude : -33.8833333333333 degrees (+ve North)
Maximum latitude : -29.9 degrees (+ve North)
Data spacing : 1 minute
Rows*Columns : 240x264
Units : Depths in Metres (terrestrial values are positive)
Points start at the North-West corner working eastwards across to the North-East before
restarting in the West
    Longitude       Latitude   Depth
  27.1000000000 -29.9000000000 1508
  27.1166666667 -29.9000000000 1541
  27.1333333333 -29.9000000000 1563
  27.1500000000 -29.9000000000 1589
  27.1666666667 -29.9000000000 1584
  27.1833333333 -29.9000000000 1591
  27.2000000000 -29.9000000000 1584
```

As can be seen, the latitude and longitude values are in decimal format and therefore do not need to be transformed before use. Further, the depth values for the landmass are given positive values, while the depth values for the ocean have a negative value. In this thesis, as depicted in Figure 3.1, the height of a point is taken to mean the distance *above* sea level and the depth of a point the distance *below* sea level. Therefore, to avoid confusion, the depth values offered in this data file need to be edited accordingly — ensuring that depth values are positive. The data header for the GEBCO data offers useful information to the user, inclusive of the maximum and minimum values of longitude and latitude, the block dimensions and the data points themselves.

Processing of this data was also performed by means of the Microsoft Office package *Excel*. The ASCII data file was imported into *Excel*, and the data header removed. The resulting *Excel* document was then imported into *Matlab* by means of *Matlab's* built in **xlsread** function. Once again, the extracted data is given in three columns, which were incorporated into a matrix. This was accomplished in the same manner as described in §4.4.1.

4.4.3 The Seafloor Surfaces

In this subsection the bathymetric seafloor surfaces obtained for the gridded one and two minute data sets are described and shown graphically. The data are sectioned according to spatial region, so that a comparison of the one and two minute surfaces for each region may be discussed. The discussion for each region opens with a short description of the characteristics of the seafloor surface and how this relates to the margin characteristics explained in Chapter 2. The general seafloor surface characteristics and features, common to both data sets, are then described. This is followed by a graphical comparison of the

differences between the seafloor surfaces for the one and two minute data sets and how these differences could influence the determination of the FoS.

The labelling of the axes for the plots to come is consistent with the principals of latitude and longitude. The longitude axis has positive values as South Africa lies east of the Greenwich Meridian and longitude is measured as positive east of the Greenwich Meridian. The latitude axis has negative values as South Africa lies south of the equator and latitude is measured as positive north of the equator.

East Coast Seafloor Surfaces

The South African east coast is characterized by both rifting and shearing. This passive margin is bounded by the Agulhas Marginal Fracture Zone, a transform feature which developed during the translational movement of the Falkland Plateau past South Africa, and resulted in the development of a narrow continental shelf and steep slope, seen in both the two and one minute seafloor surfaces (given in Figures 4.14 and 4.15 respectively). The continental rise is the section at the base of the slope that is demarcated by the two visible lines on the seafloor (these lines are most evident in the one minute seafloor surface). The east coast is the region of South Africa where the Agulhas current passes closest to the land mass. The extension of the continental shelf is bordered by the path taken by the current (the so–called eastern–boundary current), referred to as the Agulhas passage. On the seaward side of the Agulhas passage there is a region called the Agulhas plateau. It is uncertain as to whether this area may be considered for claim. To prevent inclusion of the Agulhas plateau, the east coast data were specifically restricted to extend only into the Agulhas passage area and as a result there is a large portion of landmass included in the data. The landmass is seen on the seafloor surfaces as the noisy portion of the surface typified by negative "depth" values. Proceeding from the landmass seaward, the region of zero depth indicates the coastline, not shown on the contour maps of the surfaces. The relatively flat region seaward of the coastline is the continental shelf, which dips into the continental slope and then to the continental rise. The relatively flat section after the continental rise is the deep ocean floor (abyssal plain).

The general discussion of the features common to both one and two minute surfaces, in the previous paragraph, allows a comparison to be made between the surfaces obtained for the two data resolutions. The two minute data displays a much coarser surface than that of the one minute data, as expected. On the two minute seafloor surface it is seen that, in the longitude region of 28.5–31.5 degrees, the relatively flat area indicating the deep ocean floor appears to be "pockmarked". These hills and valleys (assumed to be caused by spurious data), although appearing to be small on the seafloor surface, have significant curvature associated with them and are thus expected to add significant noise to the SMC computed for the two minute east coast data. Further, the demarcation of the continental rise is not evident on the two minute seafloor surface as a direct result in the decrease of data resolution. It is expected that this will affect the ridge line obtained from the two minute surface, pushing it further out to sea than it should be.

South Coast Seafloor Surfaces

The South African south coast is characterised by a non–volcanic transform–sheared margin type. This is evidenced in the two and one minute seafloor surfaces (given in Figures 4.16 and 4.17 respectively) by the presence of areas of peaked, linear seamounts connected at their bases and aligned along the continental rise. The presence of these seamounts is expected to offer interesting results with respect to the determination of the FoS. It is uncertain in areas, in both data sets, whether the perceived seamounts are, in fact, a portion of a complex margin topology or whether they are, indeed, seamounts. The true nature of these peaks on the surface is yet to be verified in the areas close to the continental slope. The line of seamounts seen at the southern most (greatest negative latitude) portion of the seafloor surfaces is definitely not included in the continental margin, whereas the peaks closer to the main body of elevated area may be interpreted as part of the continental shelf. The region under consideration is situated offshore of the continent and as a result does not include land mass data. It is to be noted that the surface does not include an indication of the coast line of the continent, as this is outside of the region under consideration.

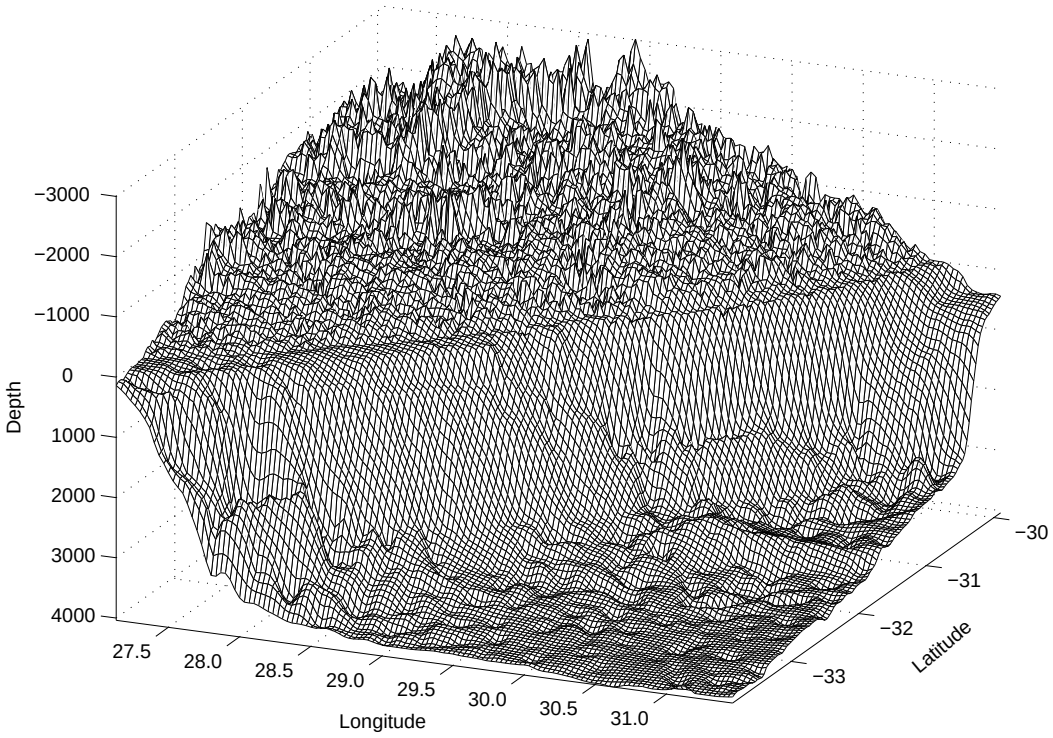

(a) Seafloor surface plot

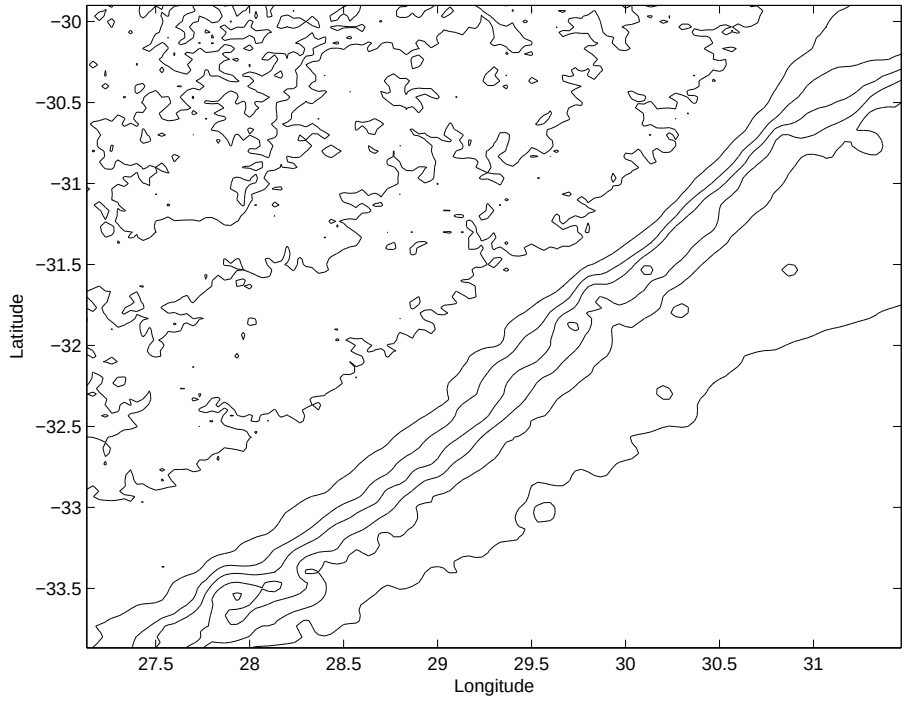

(b) Seafloor contour plot

Figure 4.14*: Two minute ETOPO bathymetry: South African east coast.*

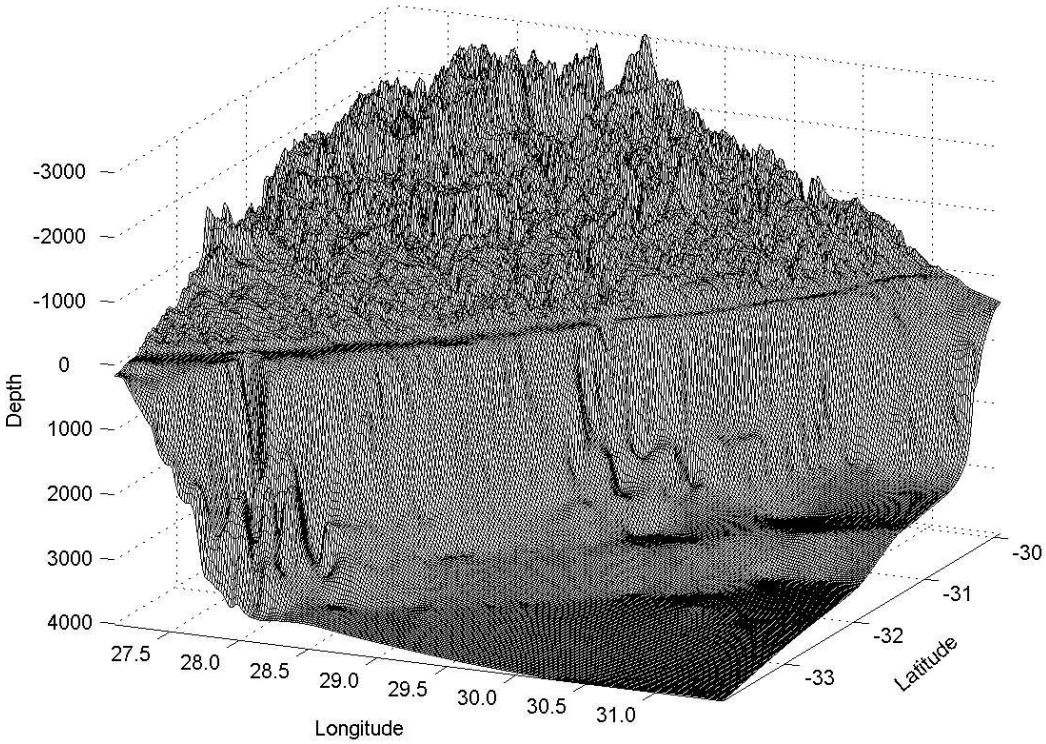

(a) Seafloor surface plot

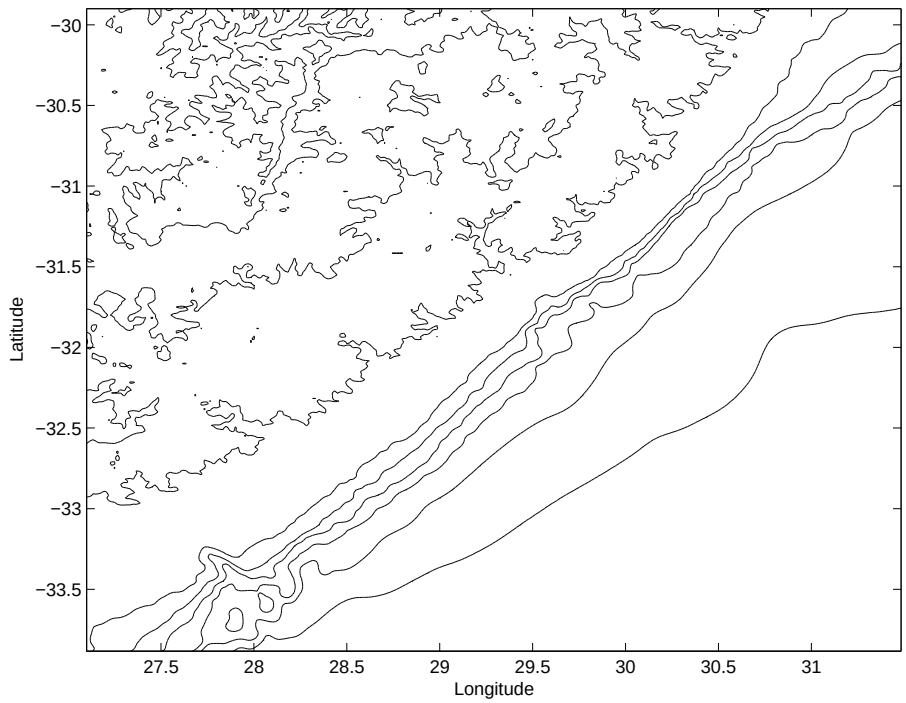

(b) Seafloor contour plot

Figure 4.15*: One minute GEBCO bathymetry: South African east coast.*

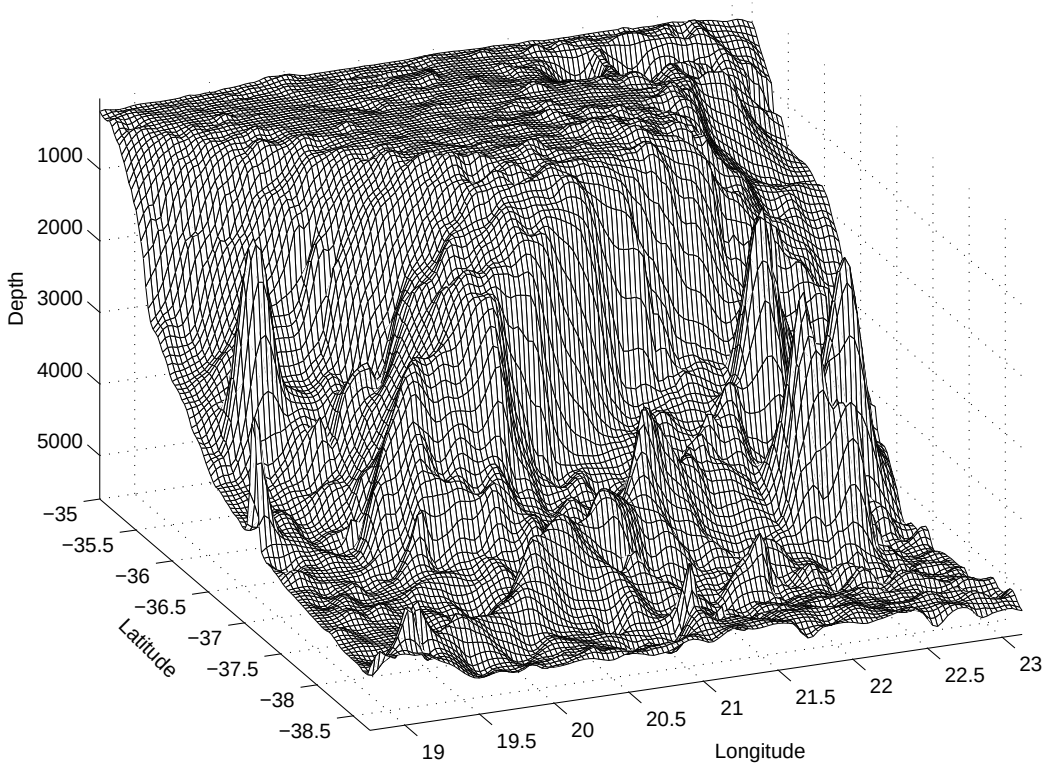

(a) Seafloor surface plot

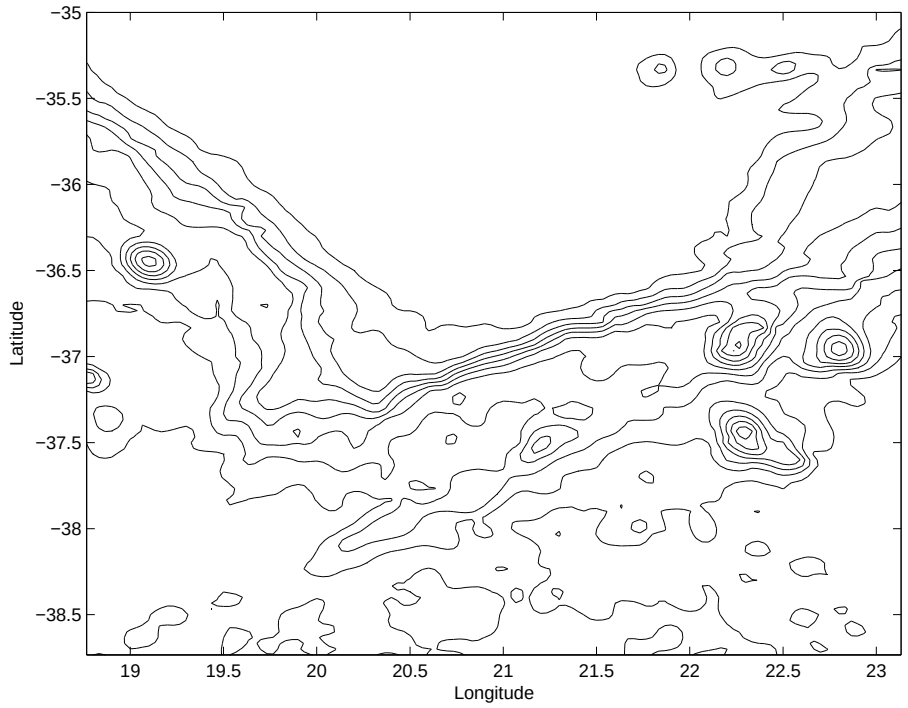

(b) Seafloor contour plot

Figure 4.16*: Two minute ETOPO bathymetry: South African south coast.*

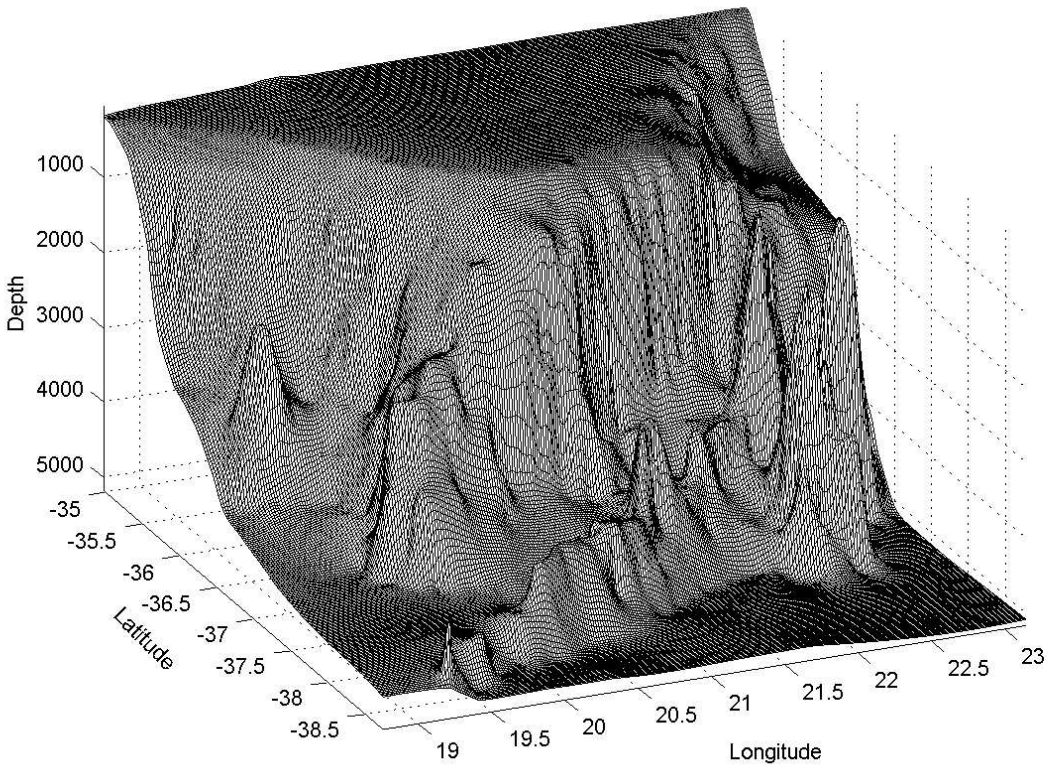

(a) Seafloor surface plot

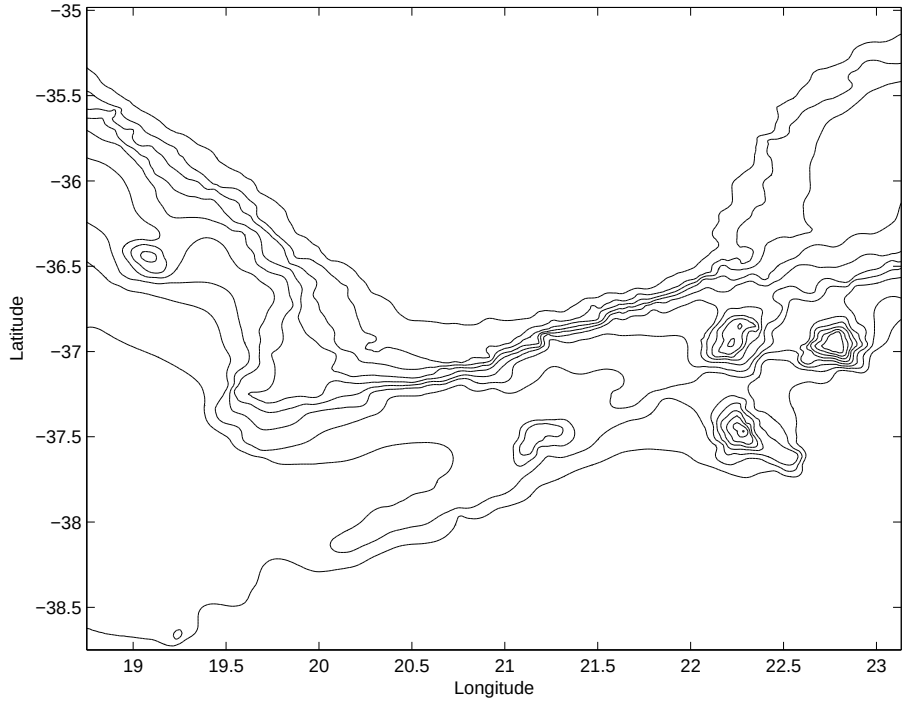

(b) Seafloor contour plot

Figure 4.17*: One minute GEBCO bathymetry: South African south coast.*

The general discussion of the features common to both one and two minute surfaces, in the previous paragraph, allows for a comparison between the surfaces obtained for the two data resolutions. The one minute seafloor surface shows a distinct area of reduced depth between the continental shelf and the southern most line of seamounts, whereas in the two minute data this reduction in depth is not immediately evident. Visually it may be interpreted that this area is part of the continental shelf. This is once again expected to bias the foot line chosen to be situated further to the south and inclusive of the line of seamounts. Once again, the ocean floor of the two minute data is characterised by extensive hills and valleys and the distinction of the start of the ocean floor is not as evident as that seen in the one minute data. As mentioned for the east coast data, although these hills and valleys are not visually imposing on the seafloor surface, they do have extensive curvature associated with them and therefore are expected to add significant noise to the SMC computed for the two minute south coast data. The reduction in definite distinction between the ocean floor and the foot of the continental rise is further expected to complicate the tracing of the foot line for this region, and possibly push it further seaward than it should be.

South West Coast Seafloor Surfaces

The South African south west coast is an interesting region. It is a region of transition from the transform–sheared margin type in the south to a sediment–rich, non–volcanic divergent–rifted margin type in the west. This region contains the feature commonly referred to as the *Cape Valley*. The transition between margin types is characterised by the "cut" in the continental slope seen in both the two and one minute seafloor surfaces (given in Figures 4.18 and 4.19 respectively). The continental shelf is well defined in this area, with a steep enough slope to allow a relatively accurate determination of the FoS. Once again, the region is situated sufficiently offshore that no landmass is included in the seafloor surface.

A visual inspection of the one minute seafloor surface indicates that the continental rise is once again well demarcated by the two visible lines on the surface. The two minute seafloor surface, however, does not give any indication as to the position of the continental rise, and the ocean floor is once again characterised by a large number of hills and valleys in addition to small ridges extending radially down from the continental shelf to the ocean floor. These radial ridges are expected to prevent tracing of a foot line for the two minute data, as the curvature associated with them will overshadow that of the actual FoS. The one minute seafloor, however, is expected to offer a good platform for determination of the FoS.

West Coast Seafloor Surface

The west coast data was only extracted for the one minute data set, as mentioned during the discussion of bathymetric data at the beginning of this section. The west coast is included only as an example where the mathematical method described in this thesis is insufficient, on its own, for use in the determination of the FoS. Inspection of the seafloor surface for the one minute west coast data, shown in Figure 4.20, reveals a very gradual change in the continental slope. This gradual change in slope is expected to result in an indefinite ridge line on the SMC computed for the region. The seafloor surface shows two independent, peaked seamounts and it is uncertain whether these seamounts are situated on the continental slope or on the ocean floor as a result of the very gradual change in the slope itself. It is not immediately evident where the continental rise is situated, and therefore where the ocean floor begins. Further, there is extensive slumping on the continental slope in the latitude region of 30.5–31 degrees. This area of slumping will have extreme curvature associated with it, as will the seamounts, and these associated curvatures are expected to form the main features on the computed SMC, further hindering an accurate determination of the FoS for this region. The very gradual change in the continental slope can be attributed to continental sedimentation, that is, sediment being carried from the continent out to sea. The *Orange River* may be considered one of the large rivers that would contribute to this, and is situated in the west coast region. Episodic and long term Orange River flooding, with the associated offshore bedload transport, is most likely directly responsible for the accumulation of sediments on the continental shelf in the west coast region.

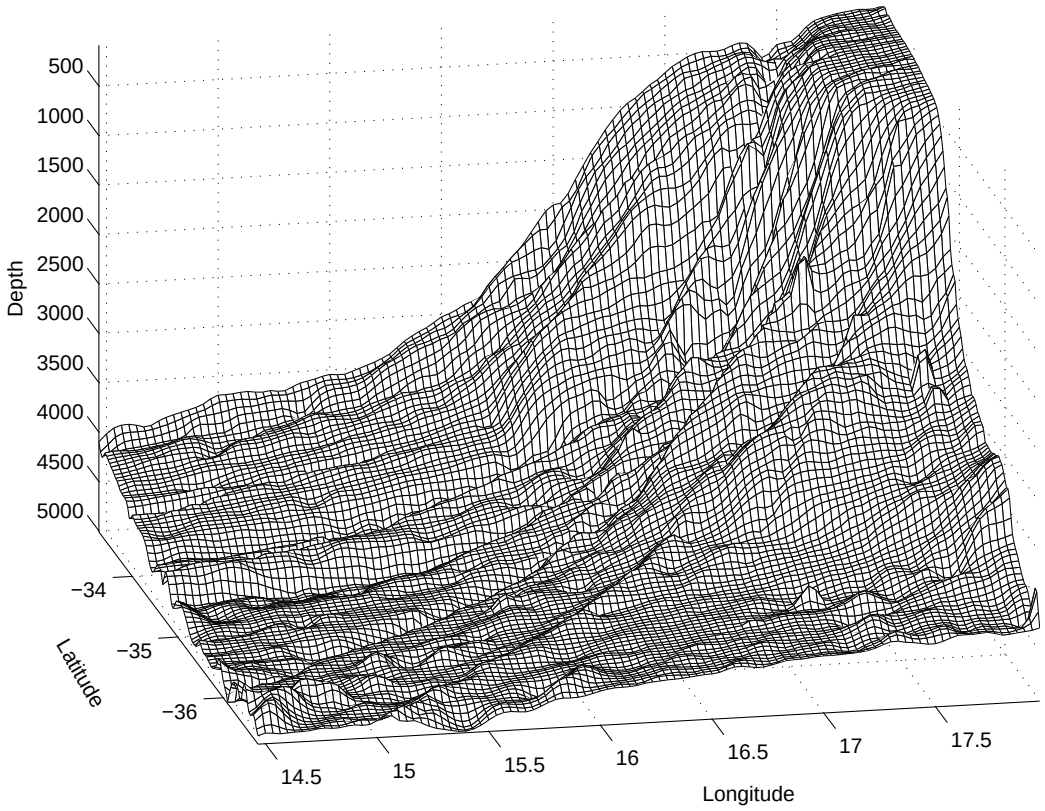

(a) Seafloor surface plot

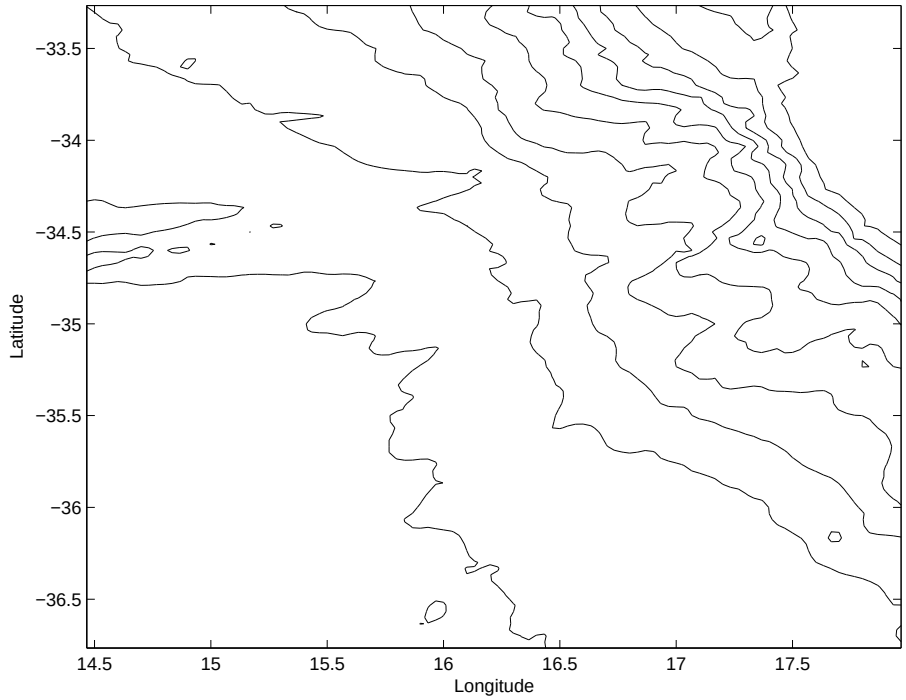

(b) Seafloor contour plot

Figure 4.18*: Two minute ETOPO bathymetry: South African south west coast.*

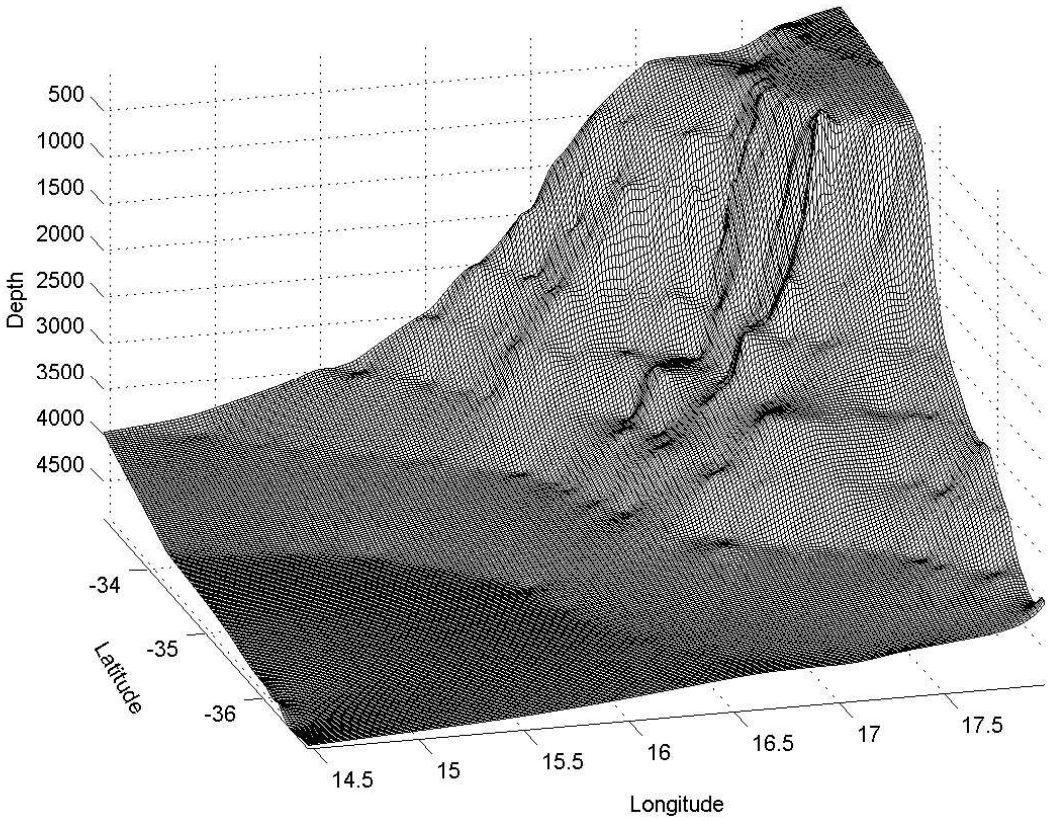

(a) Seafloor surface plot

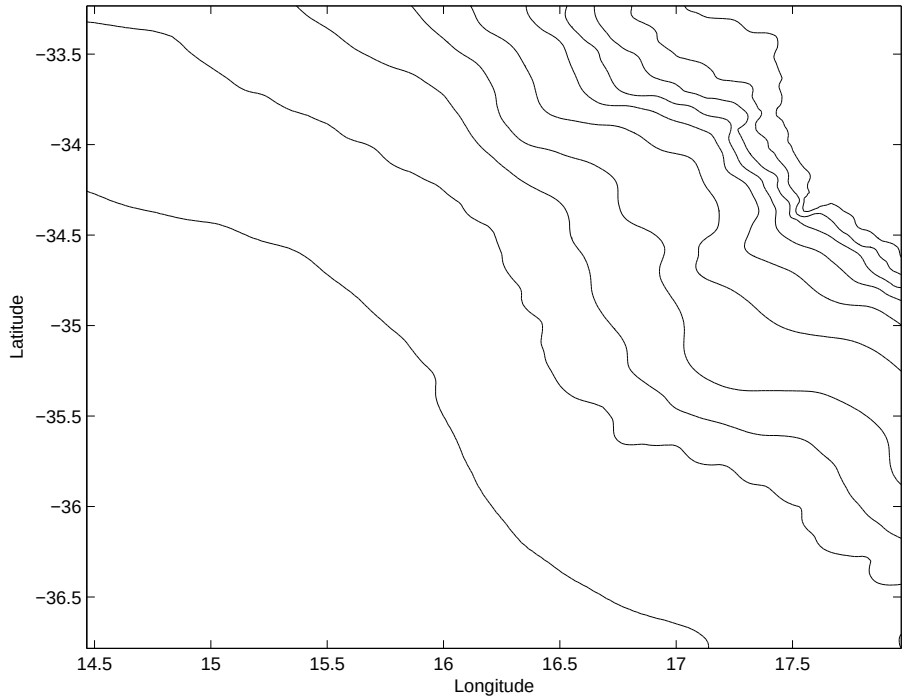

(b) Seafloor contour plot

Figure 4.19*: One minute GEBCO bathymetry: South African south west coast.*

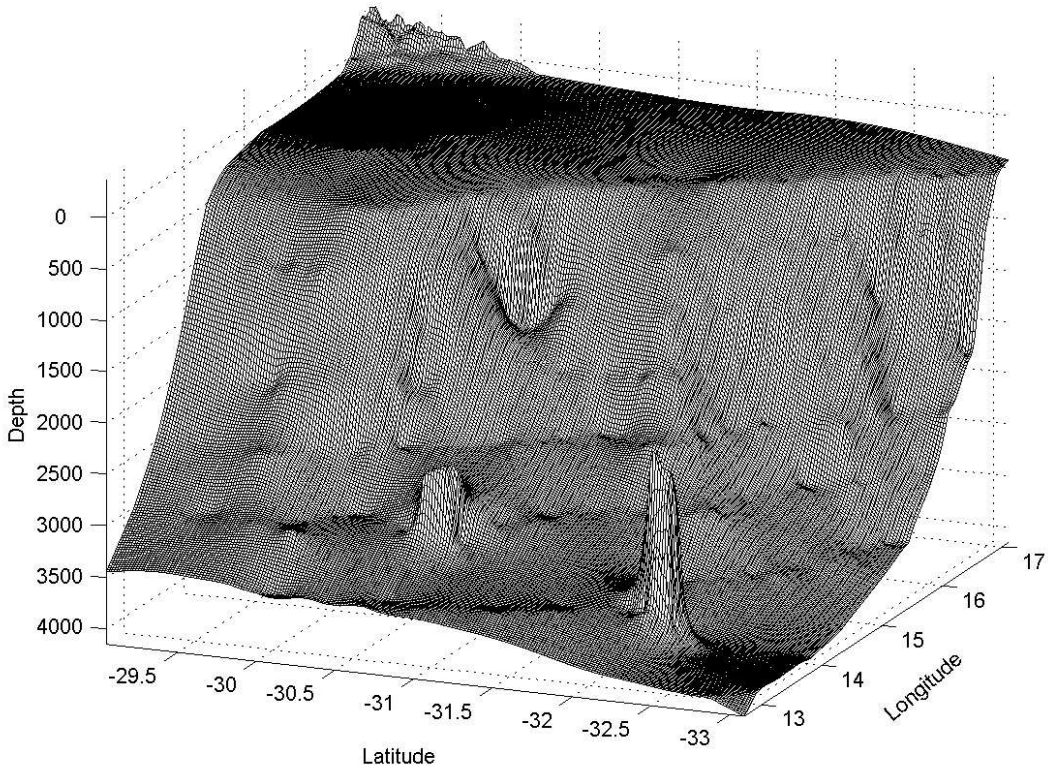

(a) Seafloor surface plot

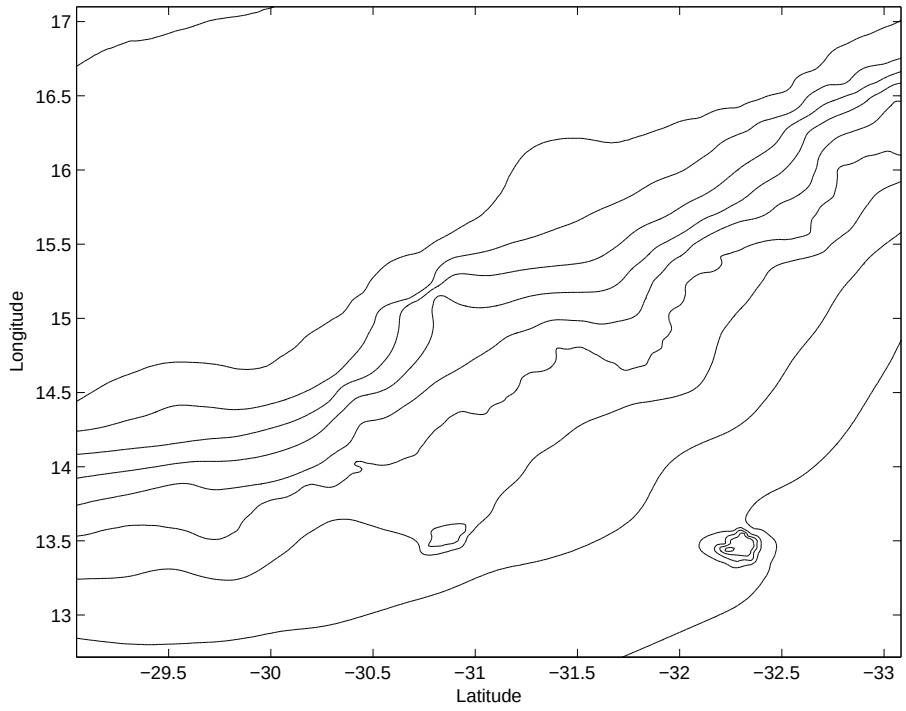

(b) Seafloor contour plot

Figure 4.20*: One minute GEBCO bathymetry: South African west coast.*

4.4.4 *Caris Lots* Foot Points

Foot line determination within the South African desktop study is performed by means of the software package *Caris Lots*, as mentioned before. *Caris Lots* is a software package which provides a user friendly method of determining the FoS and other criteria in applying Article 76 to user and public domain data sets. The software package provides for two methods of locating the FoS, namely by means of gridded data sources (such as the ETOPO and GEBCO data) or by means of a "three–dimensional" ship's track. *Caris Lots* displays the seafloor as a two dimensional image colour coded with respect to height. The colourmap to be used for this display may be specified by the user. The user then examines the seafloor image visually and identifies an area where there is a probable FoS. The general guideline for a user, with respect to making this choice, is that the top of the continental shelf is generally indicated by closely spaced contours (and abrupt colour changes) and the FoS is generally found where the contours widen and the colours change gradually. Once an area has been identified a profile is made for that area. A profile is a line that is perpendicular to the continental margin and the profile formed is thus a cross–section of the margin in the specified area. The starting point of the profile should be chosen on the continental shelf and the end point near the start of the abyssal plain. *Caris Lots* further offers the option for operators to filter the chosen profile line using either a Douglas Peucker filter or a Fourier Transform filter. The Douglas Peucker filter allows the operator to adjust the tolerance of a simplified line until a satisfactory approximation of the abyss, rise, slope and shelf are obtained. The filter uses the Douglas Peucker line simplification algorithm [11] (an algorithm that reduces the number of points needed to represent the line whilst maintaining the general shape). The Fourier Transform filter allows the user to filter excess noise or "spikes" in the data. The filter uses the Fourier Transform to transform the profile line data into the spatial frequency domain. A filter is then applied to this to remove the unwanted frequencies. The user has a choice of four filters to use, the low pass filter (preserves the long wavelengths equivalent to low spatial frequency), the high pass filter (preserves the short wavelengths equivalent to high spatial frequency), the band pass filter (isolates part of the spectrum in a band, removing all frequencies outside the band) or the band reject filter (inverse of the band pass — removes all filters within a specified band). The filtered profile line is then used in the foot point determination.

A FoS point is determined as one proceeds from seaward to landward along the chosen and possibly filtered profile. This point is determined by analyzing the profile slope using the *Caris Lots* foot of slope tool. This tool calculates the second derivative of the profile line and then marks the point where the maximum second derivative value is found. The profile under examination is then displayed with the marked foot point indicated by a tan coloured line. Further information displayed are lines indicating sediment thickness and a geodetic analysis of the profile. The operator then manually adjusts the marked foot point until satisfied with the result. A change to the marked foot point will be made if the operator feels that the changes in the profile line slope or geodetic factors contradict the placement of the marked point.

Once a number of foot points have been computed for a certain area (one foot point per profile line or ship's track), the points are manually evaluated by the operator and only those points offering the most advantageous claim area retained. The final foot points chosen may not exceed a distance of 60M apart. These points are then joined with straight lines to form the foot line. The subjectivity in *Caris Lots* is, therefore, introduced by the ability to choose a profile line (and the angle this line makes with the coastline), the ability to change the position of a marked foot point, and the choice of which computed foot points should be retained for use in calculation of the final line. The subjectivity is thus a result of the operator choice rather than software identification.

The chosen example foot points for the blocks of data used in the previous subsection were extracted from *Caris Lots* using the method described above. These foot points are typically those chosen by an experienced *Caris Lots* operator as an example but are not official points for the South African claim and should therefore not be used outside this thesis. The points were chosen using the Douglas Peucker filter and constitute what is commonly referred to as a "Peucker Pick." The resulting file is a list of latitude and longitude coordinates specifying each foot point for the specific block. The coordinates of the foot points for the east, south, south west and west coast blocks of data are given in Tables 4.6, 4.7, 4.8 and 4.9 respectively. The optimum foot line from these points is taken as being the line formed by joining the seaward most foot points (which are no more than 60M apart) with straight lines. The depth

Latitude	Longitude	Latitude	Longitude
−33.659 200	28.640 701	−30.850 599	30.990 999
−33.334 899	28.768 201	−30.597 951	31.329 240
−32.083 801	30.121 401		

Table 4.6: *The Caris Lots example foot points for the east coast.*

Latitude	Longitude	Latitude	Longitude
−37.329 001	20.730 999	−37.053 699	21.228 300
−37.367 299	20.690 000	−37.212 431	21.596 643
−37.537 000	20.445 000	−37.244 000	21.575 999
−37.626 000	19.600 999	−37.357 100	21.268 899
−37.279 001	19.359 000	−36.850 401	21.579 101
−37.797 888	19.890 890	−37.015 000	21.650 000
−36.748 400	22.048 699	−36.772 858	21.759 341
−36.632 600	22.308 901	−36.801 801	21.751 000
−35.881 490	18.899 900	−36.875 701	22.010 701
−36.824 000	19.019 699	−36.546 800	23.067 099
−36.906 401	21.324 100		

Table 4.7: *The Caris Lots example foot points for the south coast.*

of each point is not specified and as a result the extracted foot points and the resulting optimum foot line cannot be plotted on the seafloor surface for each area. However, the foot points and the resulting foot line for each block of data were plotted on the contour plots for the one minute bathymetry data for each area. The *Caris Lots* example foot points and optimum foot line for the east coast, south coast, south west coast and west coast are given in Figures 4.21, 4.22, 4.23 and 4.24 respectively. In the next chapter, the foot lines obtained from application of the mathematical method discussed in Chapter 3 are plotted on the same contour plots (one minute bathymetry contours) along with the foot lines shown in this section for comparison purposes.

4.5 Chapter Summary

In this chapter the notion of a reference system for geodetic coordinates was discussed. A description of the fundamental concepts of map projections was given in addition to the specific information for two cylindrical projections, namely: the cylindrical equidistant projection and the regular Mercator projection. The chapter further described the factors influencing bathymetric data in particular and detailed the processing required to obtain computational feasible formats of extracted seafloor data. The seafloor surfaces for three areas along the South African coast, from both the one and the two minute data sets, were shown graphically in three dimensions and the *Caris Lots* chosen example foot lines were shown on the contour plots of the one minute bathymetry data for each region.

Latitude	Longitude	Latitude	Longitude
−33.993 501	16.035 101	−34.724 700	16.144 601
−33.955 300	16.053 301	−34.609 699	16.248 300
−33.897 257	16.058 899	−35.004 132	16.020 070
−33.874 800	16.050 700	−34.856 000	16.188 001
−33.706 999	15.474 000	−35.026 857	16.118 718
−33.267 201	15.640 500	−34.218 331	17.051 668
−33.800 718	16.065 657	−34.591 601	17.068 599
−33.696 000	16.100 000	−35.473 299	16.676 900
−33.338 600	15.558 699	−35.659 689	16.742 870
−36.666 700	17.874 700	−34.665 830	17.481 582
−35.521 570	17.727 893	−35.609 742	17.024 750
−36.187 300	17.543 801	−35.458 630	16.442 581
−36.066 862	17.217 082	−34.109 580	16.111 289
−36.079 239	17.128 860	−34.116 701	16.200 800
−36.005 949	17.005 843	−34.005 410	16.770 801
−34.721 361	15.994 432		

Table 4.8: *The Caris Lots example foot points for the south west coast.*

Latitude	Longitude	Latitude	Longitude
−29.186 799	13.169 300	−32.025 032	15.017 040
−29.806 801	13.391 999	−32.097 201	14.736 400
−30.365 900	13.518 700	−32.097 201	14.736 400
−30.630 489	14.350 200	−32.334 869	14.062 800
−30.950 399	14.257 400	−32.624 301	15.307 499
−31.251 201	14.916 900	−32.707 200	15.312 301
−31.374 588	14.859 000	−32.816 440	15.300 099
−31.382 557	13.991 270	−32.896 601	15.129 100
−31.500 700	14.802 300	−32.950 801	15.886 499
−31.633 782	14.568 868	−33.053 981	15.764 919
−31.860 219	14.304 000		

Table 4.9: *The Caris Lots example foot points for the west coast.*

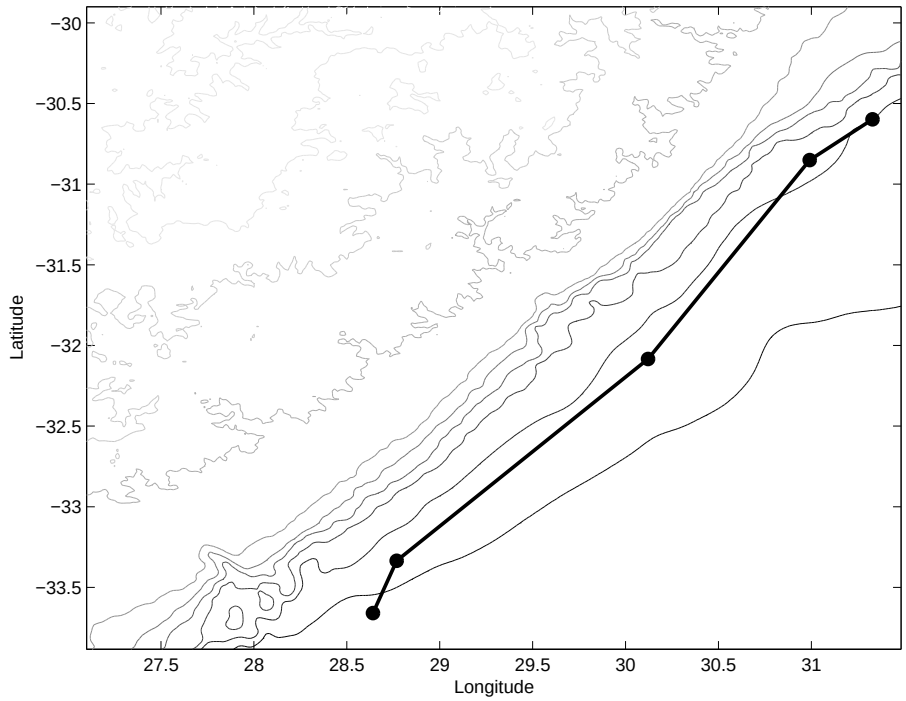

Figure 4.21: *Caris Lots example foot points and optimum foot line for the South African east coast.*

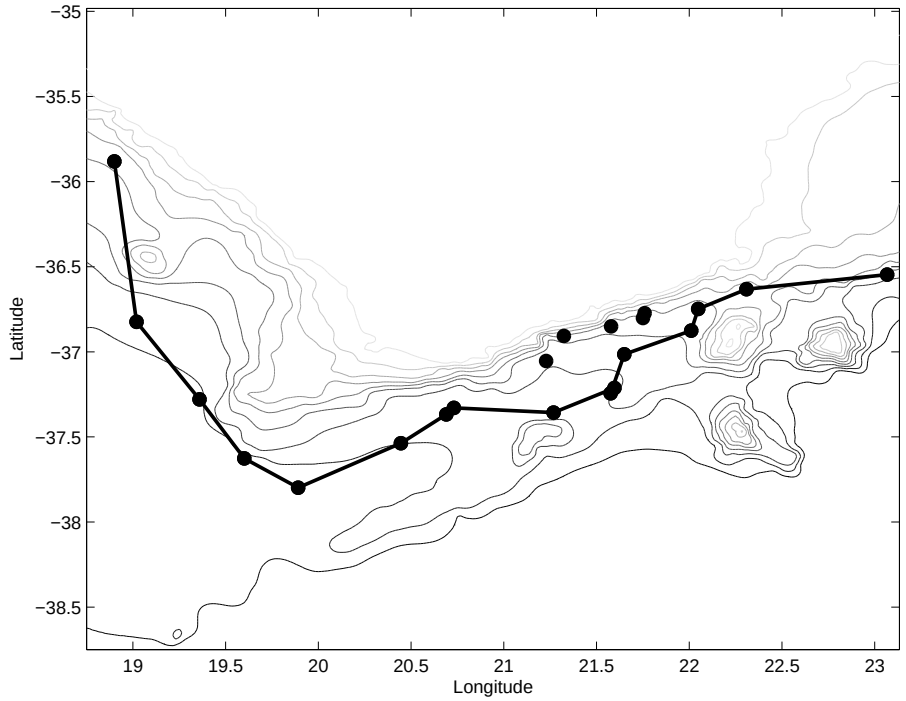

Figure 4.22: *Caris Lots example foot points and optimum foot line for the South African south coast.*

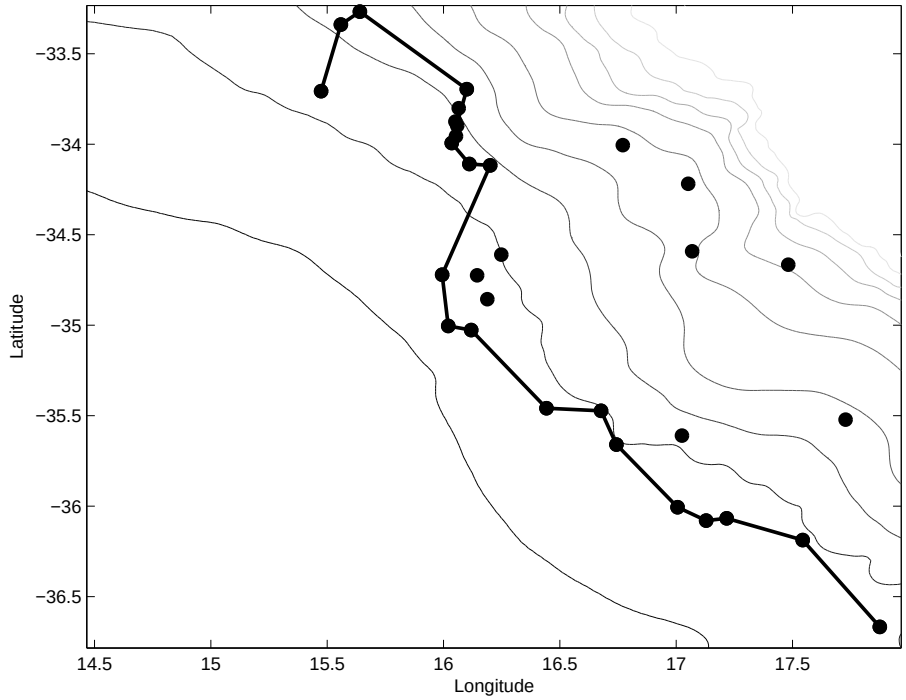

Figure 4.23: *Caris Lots example foot points and optimum foot line for the South African south west coast.*

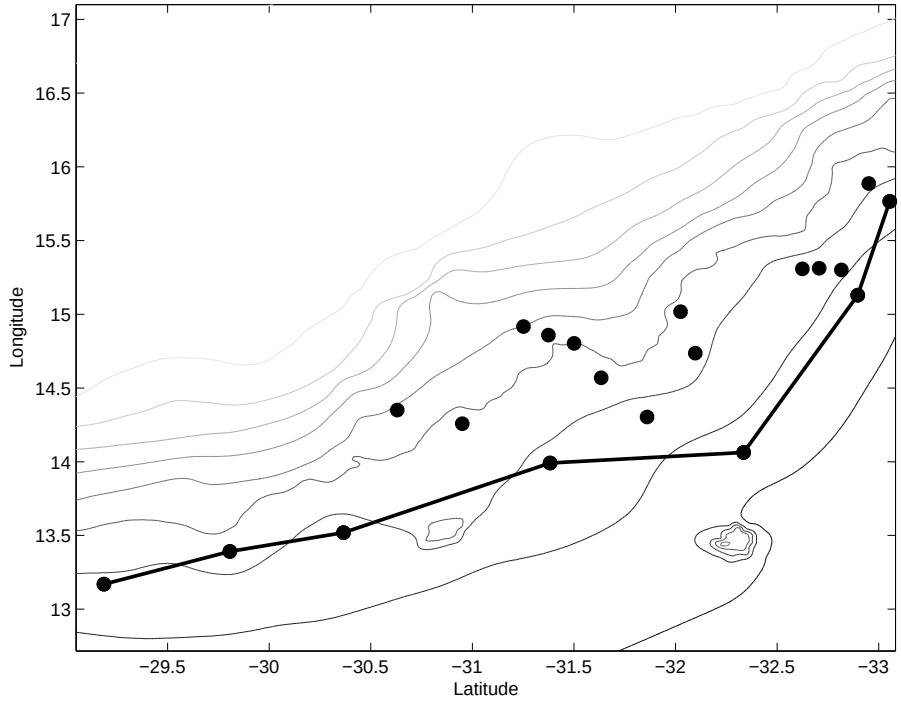

Figure 4.24: *Caris Lots example foot points and optimum foot line for the South African west coast.*

Chapter 5

Determination of the FoS

In the previous chapter the gridded bathymetric data sets to be used in this thesis were introduced and discussed. The seafloor surfaces of four regions around the South African coast were described and shown in three dimensional format. Three of these regions — the east, south and south west regions — will be used in this chapter to illustrate the advantages and disadvantages of applying the method for computation of the SMCs and the method to trace the ridge line formed on the SMC (discussed in Section 5.2). The fourth region, the west coast data, will be used to demonstrate a case where the methods of this thesis are not suitable and yield a result with a low confidence rating.

The application of the method to determine the SMC (described in Chapter 3) is applied to the data sets described above in Section 5.1. Once the SMC has been computed, the ridge formed on the surface has to be traced in order to determine the line corresponding to the FoS. In Section 5.2, a method to trace the ridge is proposed and discussed. The ridges for each data set are then traced and the resulting foot lines shown on both the seafloor surfaces and the seafloor contours for each data set.

The chapter closes with a comparison of the computed foot lines, from both the one minute data and the two minute data sets, with the foot lines chosen via the *Caris Lots* software package as examples.

5.1 Determination of the SMC

In Chapter 3 the method to compute the SMC was applied to two smooth hypothetical seafloor sample surfaces. In this section the method is applied to real gridded bathymetric data which have not been smoothed in any way and which, from inspection of the seafloor surfaces given in the previous chapter, include areas which could potentially clutter the results obtained with noise. The purpose of this section is two–fold: to find the SMCs for each data set and to investigate the robustness of the method with respect to different data resolutions. The purpose of line 17 in Algorithm 1 (in Chapter 3) is to ensure that only the maximum curvature is considered on the SMCs. This line ensures that only the positive values on the SMC are considered, removing the negative values introduced by the transition from maximum to minimum curvature

As mentioned in the previous chapter, the bathymetric data is gridded and the spacing between the points is dependent on the resolution of the data set. During utilization of Algorithm 1 the step size for computation of the numerical derivatives in the x and y directions is a required input. The distance between the data points in the bathymetric data grids is equal in the x and y directions, meaning that the input variables $\mathtt{h_x}$ and $\mathtt{h_y}$ for Algorithm 1 are similarly equal. Further, the numerical values of these variables are given by the distance, in metres, between the data points of the matrix given as input. Thus, for the region under consideration, the input for Algorithm 1 for the one minute data is the surface data matrix, `data1`, and a step size of $\mathtt{h_x} = \mathtt{h_y} = 1\,852\mathtt{m}$. Similarly, the input for the two minute data is the surface data matrix, `data2`, and a step size of $\mathtt{h_x} = \mathtt{h_y} = 3\,704\mathtt{m}$. The results of application of Algorithm 1 for the one and two minute data sets for each region are given below.

5.1.1 East Coast SMC

The computed SMCs, and their corresponding contour plots, for the two and one minute east coast bathymetric data are given in Figures 5.1 and 5.2 respectively. On visual inspection of the computed SMCs it is immediately evident that the SMC obtained for the two minute data set is much noisier than that obtained for the one minute data set, especially in the longitude region 28.5–31.5 degrees. The discussion of the seafloor surfaces for the east coast in the previous chapter highlighted the "pock" marks on the ocean floor of the two minute data in this longitude region and stated that these features would most likely influence the results seen on the SMC. This expectation was not unfounded as the hills on the ocean floor in the two minute surface have spawned a number of disjoint ridges on the SMC that have approximately the same curvature values as that of the ridge itself. It is expected that this noise on the SMC for the two minute data set will influence the tracing of the main ridge and therefore the foot line chosen.

The option to smooth the two minute data so as to remove the roughness of the surface was decided against. It was thought that smoothing the data would unnecessarily reduce the overall resolution of the data to an unacceptable extent, and in doing so, would move the position of the foot line by reducing the gradient of the slope itself.

5.1.2 South Coast SMC

The computed SMCs, and their corresponding contour plots, for the two and one minute south coast bathymetric data are given in Figures 5.3 and 5.4 respectively. On visual inspection of the computed SMCs it is immediately evident that the SMC obtained for the two minute data set has extensively more noise than that obtained for the one minute data set, both in the region of the ocean floor and on the continental shelf itself. The SMC computed for the one minute data has a distinct ridge that should be easily traceable, whereas the SMC for the two minute data does not have a definite ridge, but rather a broad region displaying similar curvature values. The southern most line of seamounts is well represented on the one minute SMC and is not even identifiable on the two minute SMC.

The discussion of the seafloor surfaces for the south coast in the previous chapter noted that the two minute data would provide extensive noise in the SMC. However, the amount of noise found was greater than expected. On the two minute seafloor surface it was noted that the depth between the continental slope and the southern most line of seamounts was reduced in comparison to that seen on the one minute seafloor surface. It is as a result of this depth reduction between the slope and the seamounts, in addition to the noise introduced by the hills and valleys on the ocean floor, that the computed SMC for the two minute data does not have a distinct ridge line. It is hoped that careful selection of tolerances and starting points for the tracing algorithm to be discussed later would allow the determination of a foot line for the two minute data. It is evident, from easily noticeable visual differences between the one and two minute computed SMCs, that any foot line obtained for the two minute data will be declared to have a low confidence rating as a direct result of the absence of a discernable ridge line on the two minute SMC [43].

The option to smooth the two minute data so as to remove the roughness of the surface was again decided against. It was thought that smoothing the data would unnecessarily reduce the overall resolution of the data to an unacceptable extent, and in doing so, would move the position of the foot line by reducing the gradient of the slope itself. It was further suspected that smoothing the south coast data would bring with it the possibility that a seamount, found in an area (where it was uncertain whether the seamount was a part of the continental margin or simply aligned with its base), would become a part of the continental slope.

5.1.3 South West Coast SMC

The computed SMCs, and their corresponding contour plots, for the two and one minute south west coast bathymetric data are given in Figures 5.5 and 5.6 respectively. It is immediately evident, on visual inspection of the SMCs for the one and two minute data, that the two minute SMC cannot be used

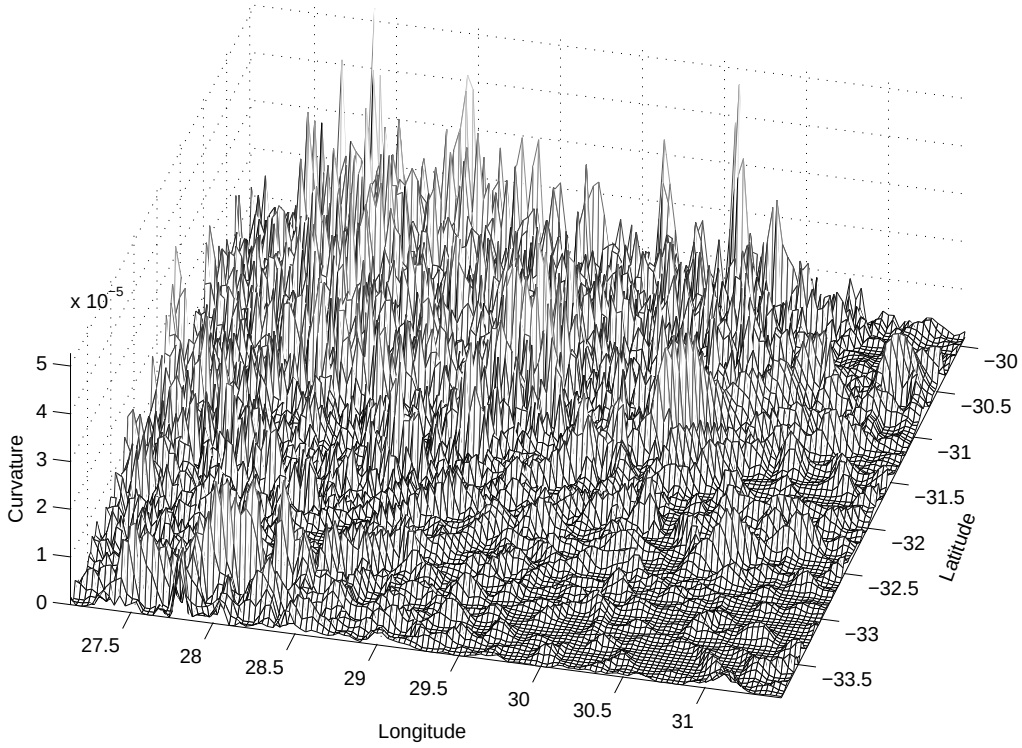

(a) Surface plot of the SMC

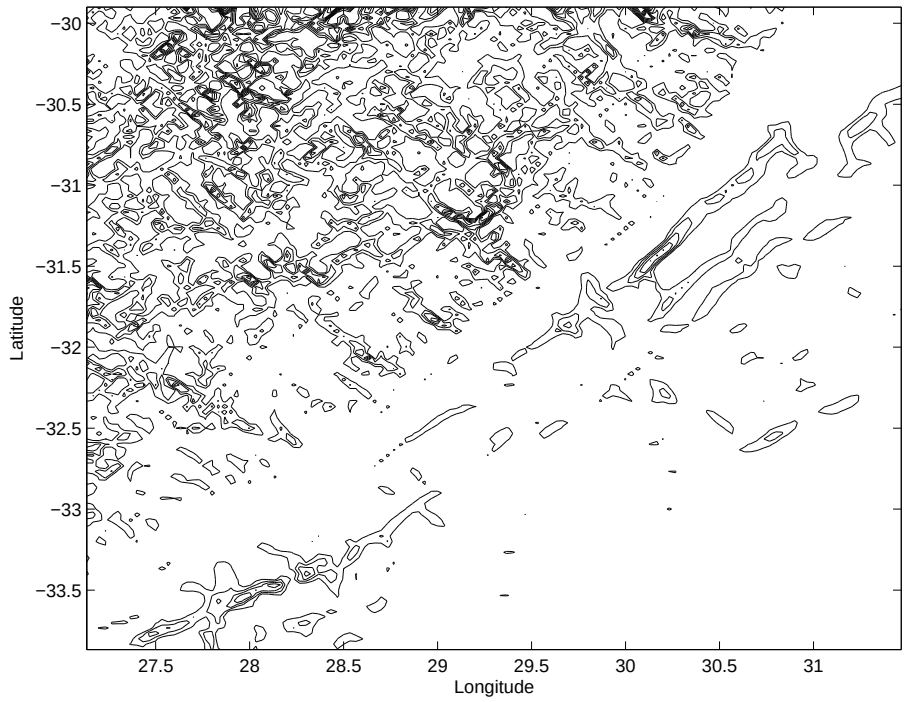

(b) Contour plot of the SMC

Figure 5.1: *The SMC for the east coast ETOPO two minute data set.*

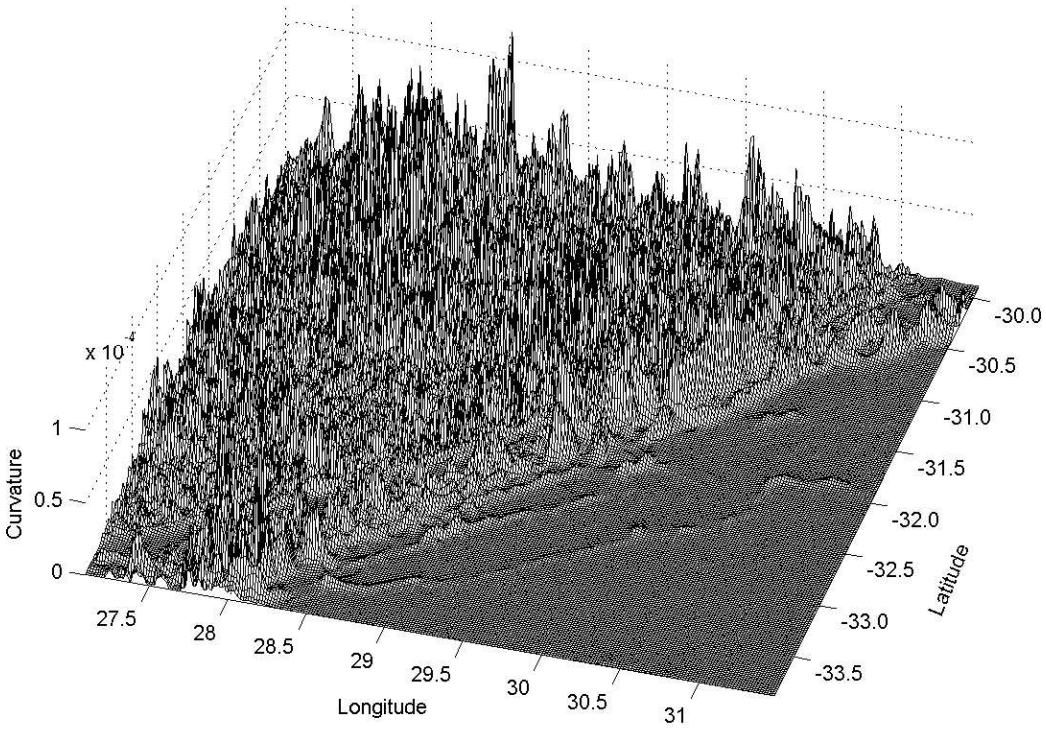

(a) Surface plot of the SMC

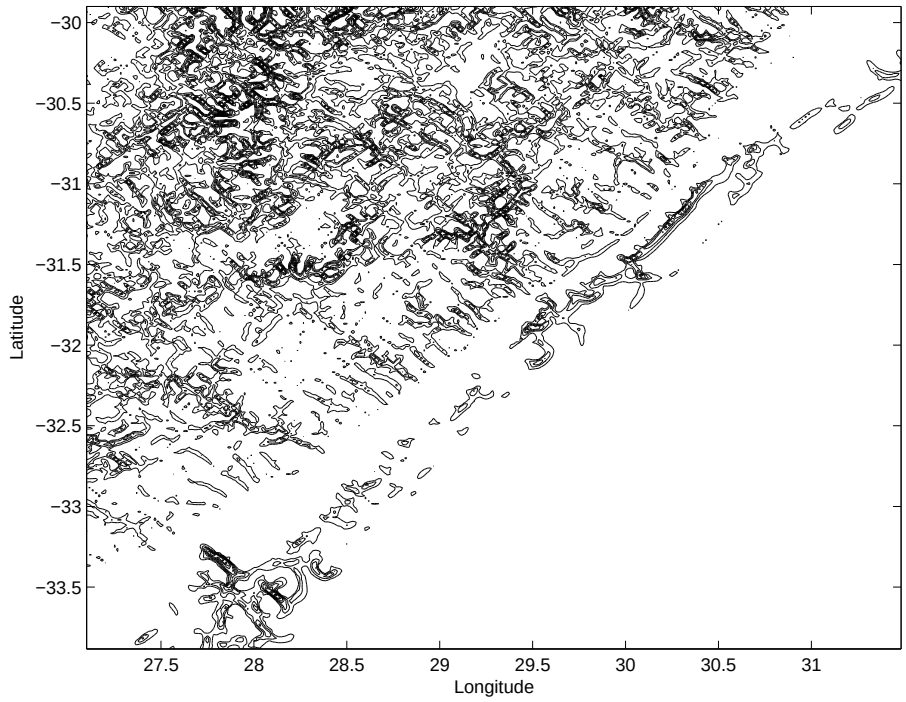

(b) Contour plot of the SMC

Figure 5.2*: The SMC for the east coast GEBCO one minute data set.*

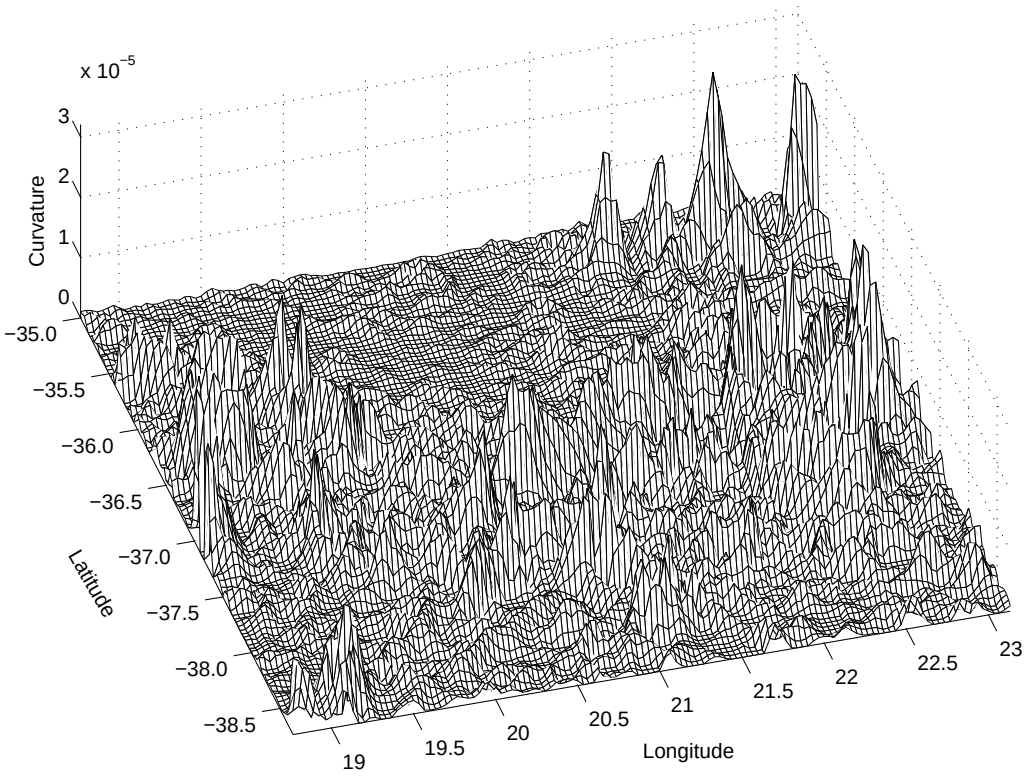

(a) Surface plot of the SMC

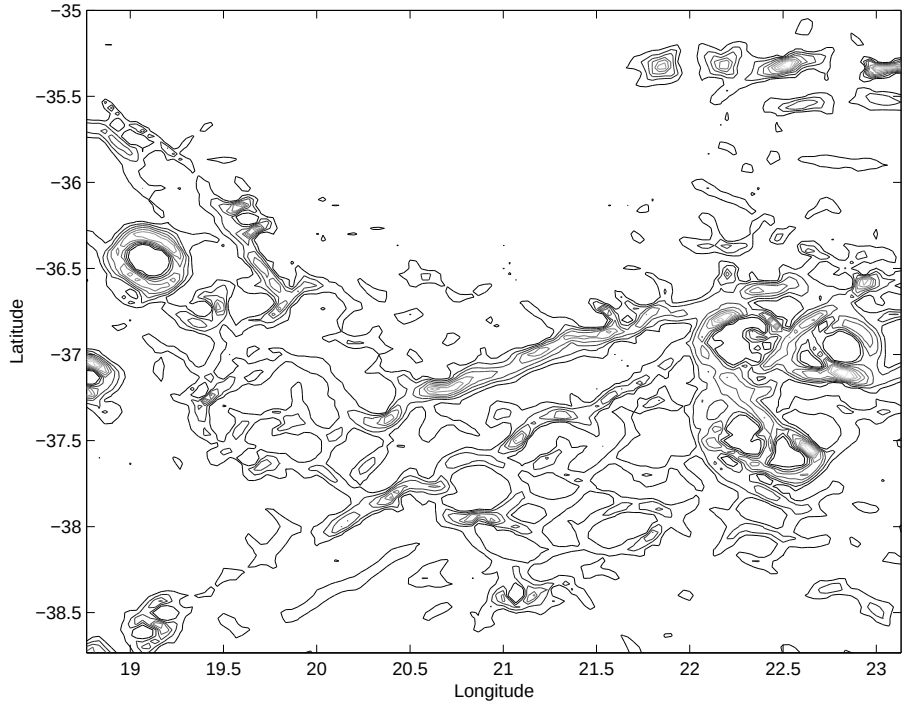

(b) Contour plot of the SMC

Figure 5.3: *The SMC for the south coast ETOPO two minute data set.*

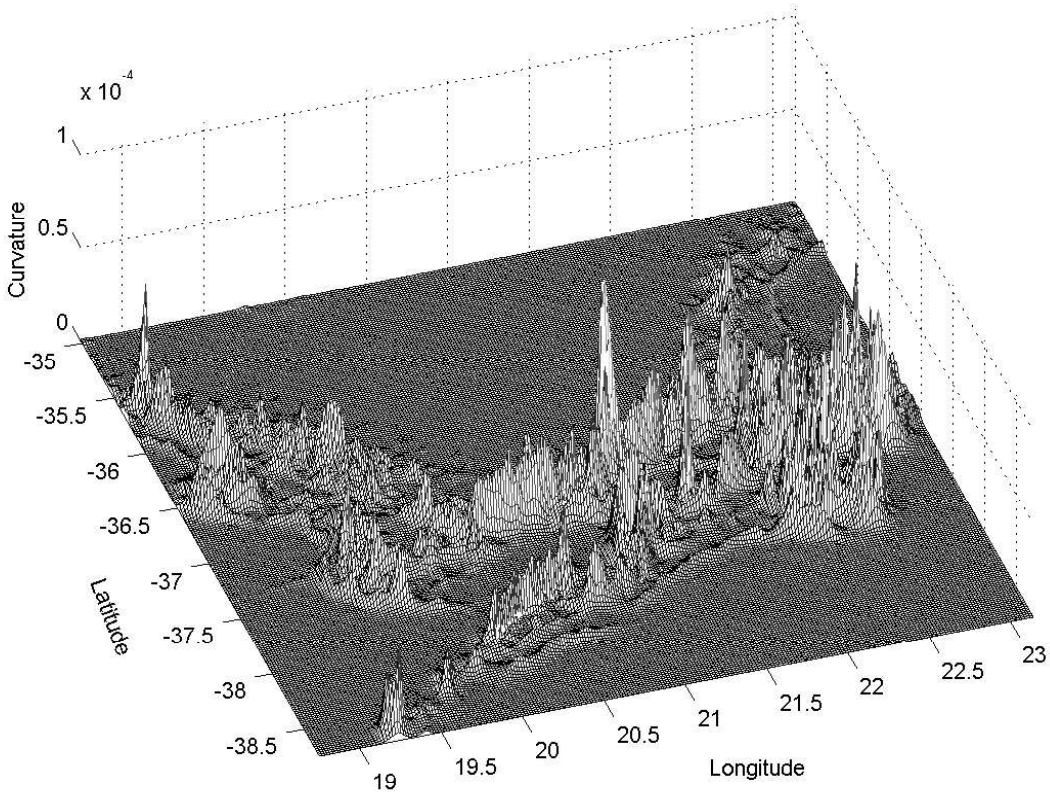

(a) Surface plot of the SMC

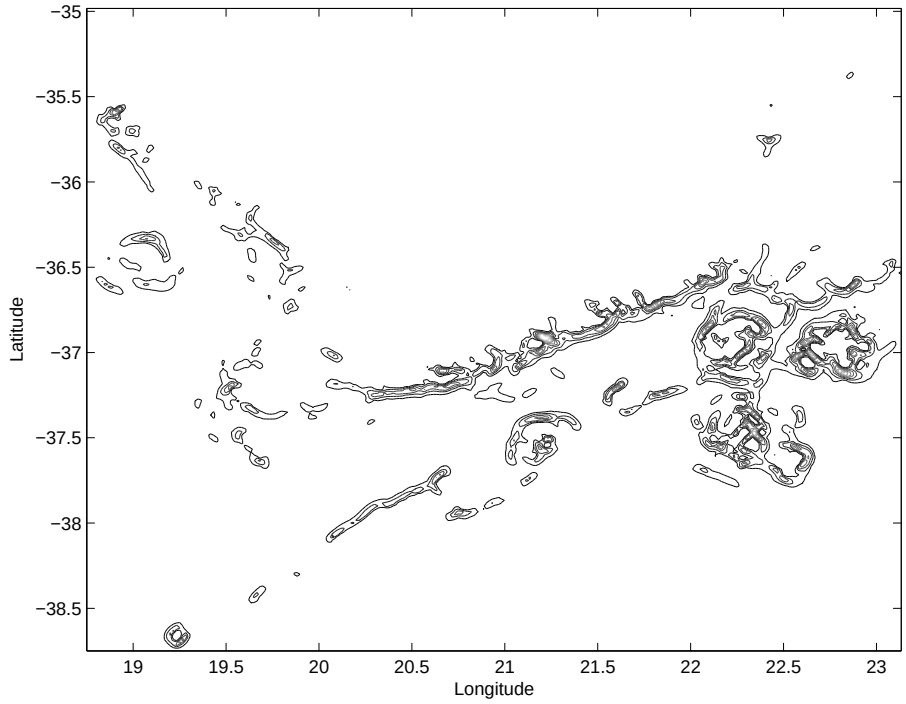

(b) Contour plot of the SMC

Figure 5.4: *The SMC for the south coast GEBCO one minute data set.*

for foot line determination. As was expected in the discussion of the two minute seafloor surface in the previous chapter, the ridges running radially from the continental shelf to the ocean floor dominate the SMC, the orientation of these ridges are highlighted on the contour plot of the SMC. The large curvatures associated with these ridges dominate the SMC, with the result that there is no visible ridge that could possibly correspond to the FoS. Furthermore, the two minute SMC is very noisy as a result of the hills and valleys seen on the two minute seafloor surface throughout the extent of the surface. However, on the one minute SMC there are two possible ridge lines that could be traced. The ridge with the greatest seaward position corresponds to the visual line on the one minute seafloor surface indicating the foot of the continental rise and the second corresponds to the visual line indicating a possible FoS position. The presence of these two distinct ridges is an advantage in the sense that the line corresponding to the foot of the continental rise can be traced by adjusting the point deviation tolerance in the tracing algorithm and this line can then be used to form a seaward bound on the position of the FoS chosen.

Even though the two minute SMC cannot be used to determine the FoS for the south west coast, the possible advantages offered by the SMC for the one minute data eclipse this loss of a comparison basis. The two minute data for the south west coast may, therefore, be used as a case study as to where the resolution of the data prevents a successful result with respect to the working of the mathematical method to compute the SMC (and from the SMC, the FoS). Where the noise introduced by resolution reduction in the east and south coast data made the determination of the FoS more difficult, the reduction of resolution in the south west coast data completely removes the option of using the SMC for FoS determination purposes. The two minute data SMC is the only regional SMC where this phenomenon was observed, and as such is a powerful example of how data resolution may, in certain cases, be a major drawback in the determination of the FoS. Smoothing of the two minute data does not resolve the problem introduced by the radial ridges and further compromises the confidence rating of any possible FoS choice and was therefore not considered as an option to overcome the problem.

5.1.4 West Coast SMC

The computed SMC, and its corresponding contour plot, for the one minute west coast bathymetric data is given in Figure 5.7. The first and most important feature noticable on the SMC for the one minute west coast data is the distinct absence of a continuous ridge line. There is a series of disjoint ridges that are overshadowed by the large curvatures characterising the slumping and seamounts observed on the west coast seafloor surface. The absence of a continuous ridge line is a direct result of the very gradual change in gradient of the continental slope for the region. This gradual slope is most likely due to the extensive sediment transport from the landmass to the sea and down the slope via the Orange River. Where careful selection of starting points and tolerances in the tracing method may yield a possible foot line, this line will definitely have a low confidence rating and will likely not be deemed reliable enough for consideration [43].

5.2 Tracing the FoS

In the previous section the SMCs for each data set were computed and shown graphically. Some expectations were given with regards to the tracing of the resulting ridges, but to this point there has not been a discussion as to what the tracing requirements and method might be. This section serves to introduce the tracing method developed for use in this thesis, the use of the devised algorithm in determination of the FoS and a discussion and comparison of results obtained from application of the tracing method for each region of data.

Inspection of the computed SMCs for all regions seems to indicate that a primitive tracing algorithm involving investigation of the neighbours of an already identified ridge point so as to continue following the ridge is insufficient for tracing of the ridge as a whole. Generally, the ridges formed on all the SMCs have regions along the ridge (if not along the entirety of the ridge) where the maximum value of the area is shared by many data point neighbours. Further, there are areas where the ridge height diminishes rapidly and the combination of the bands of maximum values and the dips in the ridge ensure that a primitive tracing method will not be able to trace the ridge in its entirety. For this reason, the SMCs

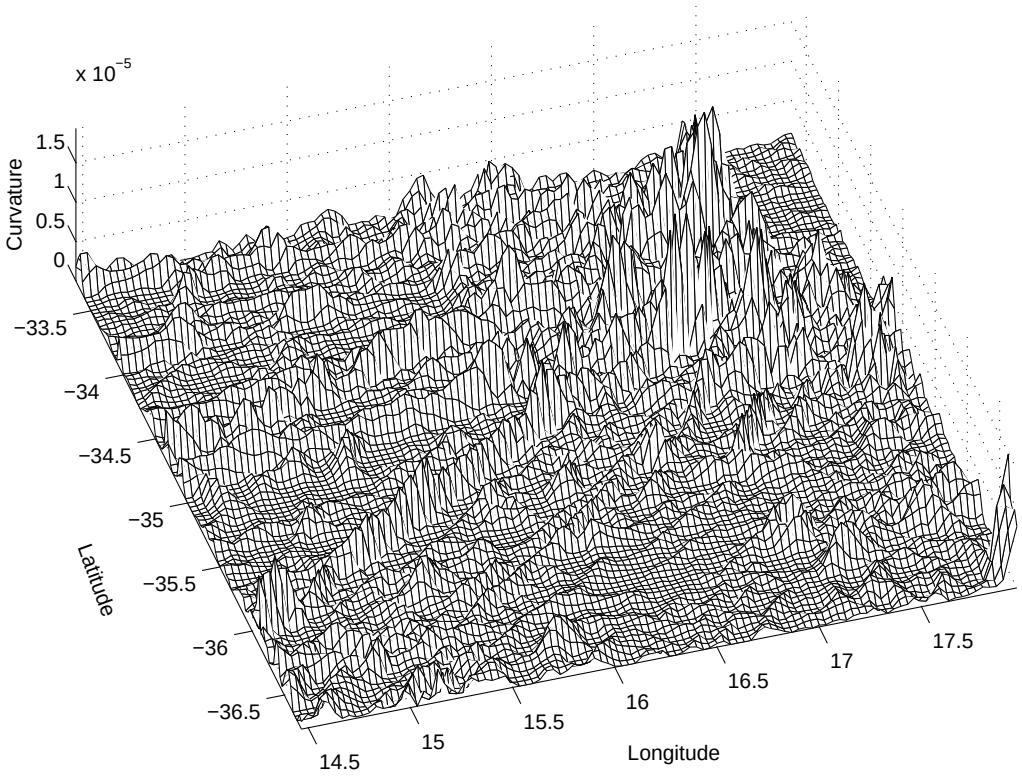

(a) Surface plot of the SMC

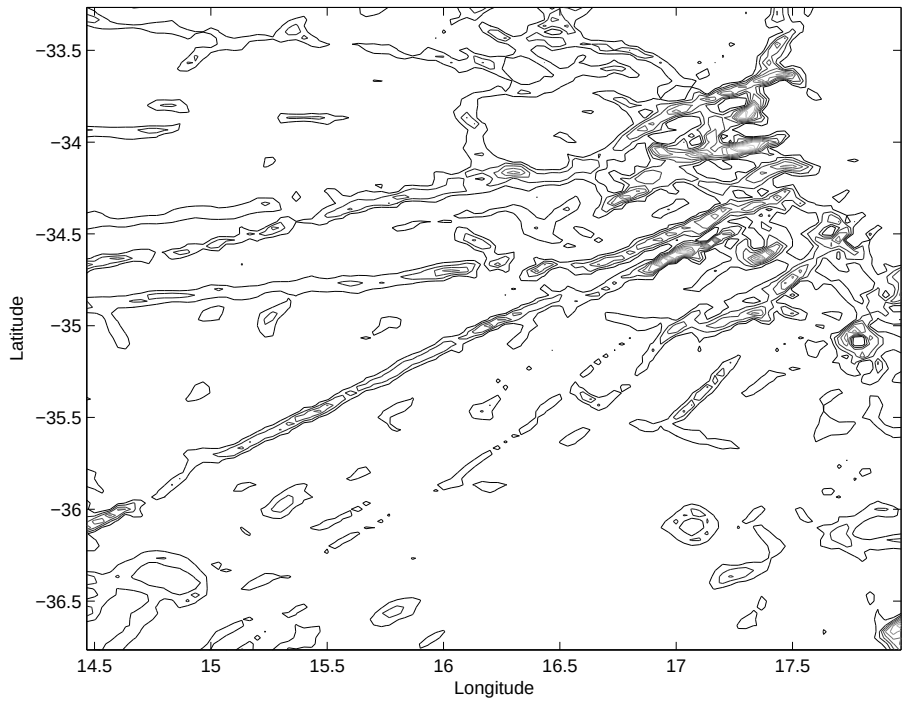

(b) Contour plot of the SMC

Figure 5.5*: The SMC for the southwest coast ETOPO two minute data set.*

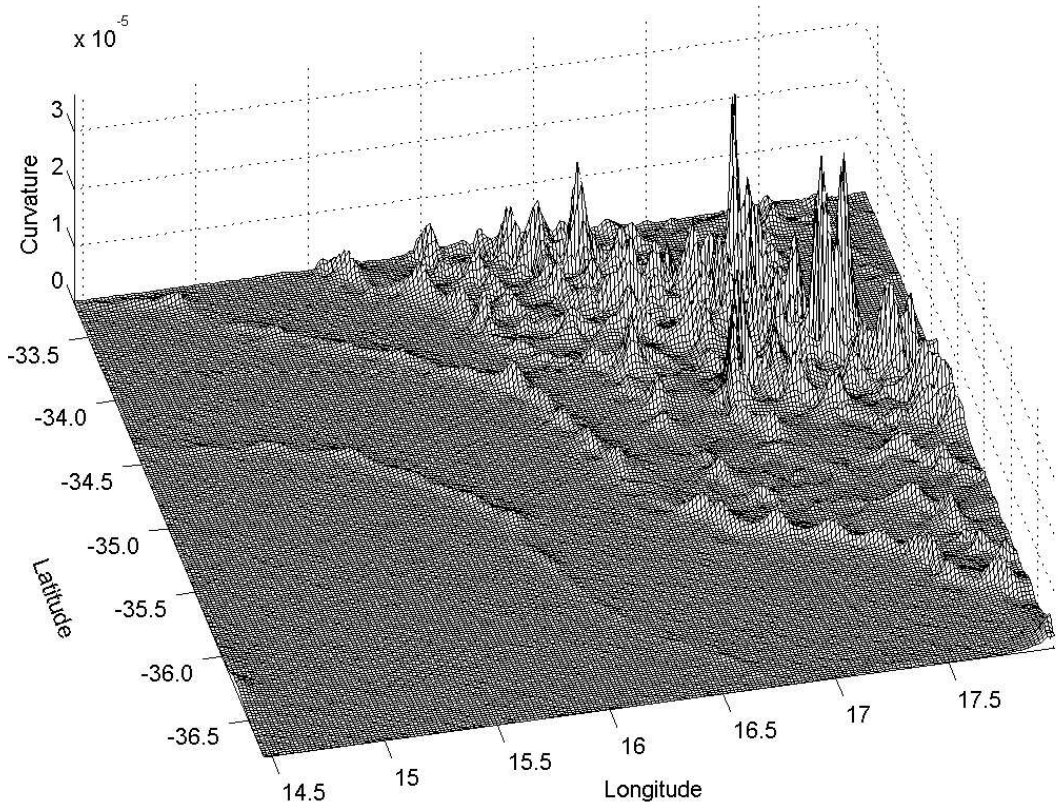

(a) Surface plot of the SMC

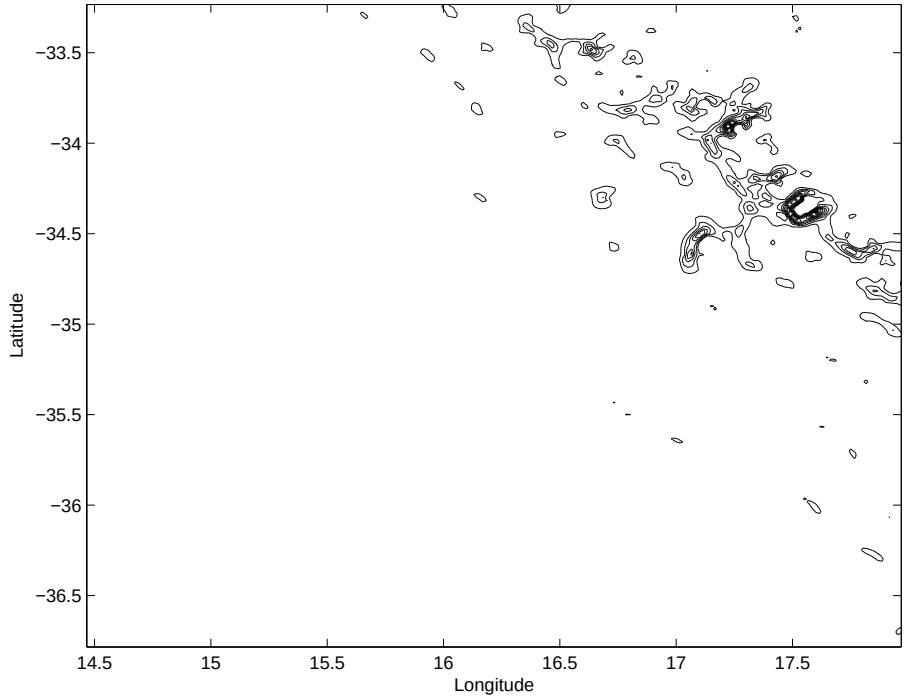

(b) Contour plot of the SMC

Figure 5.6: *The SMC for the southwest coast GEBCO one minute data set.*

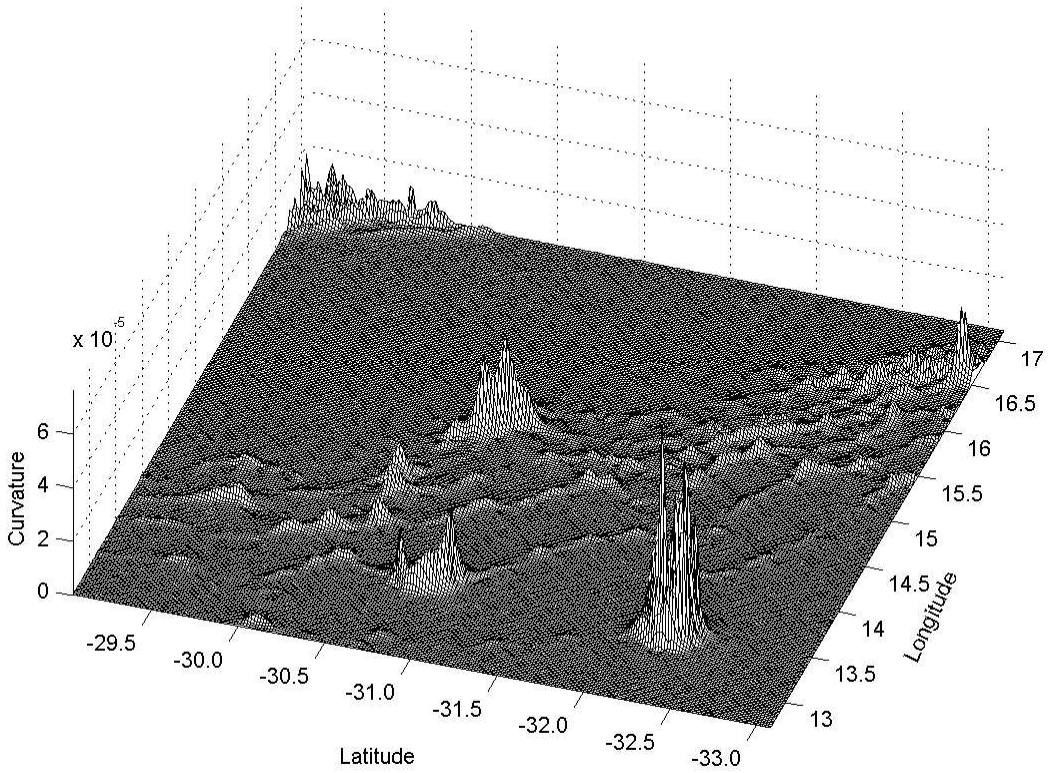

(a) Surface plot of the SMC

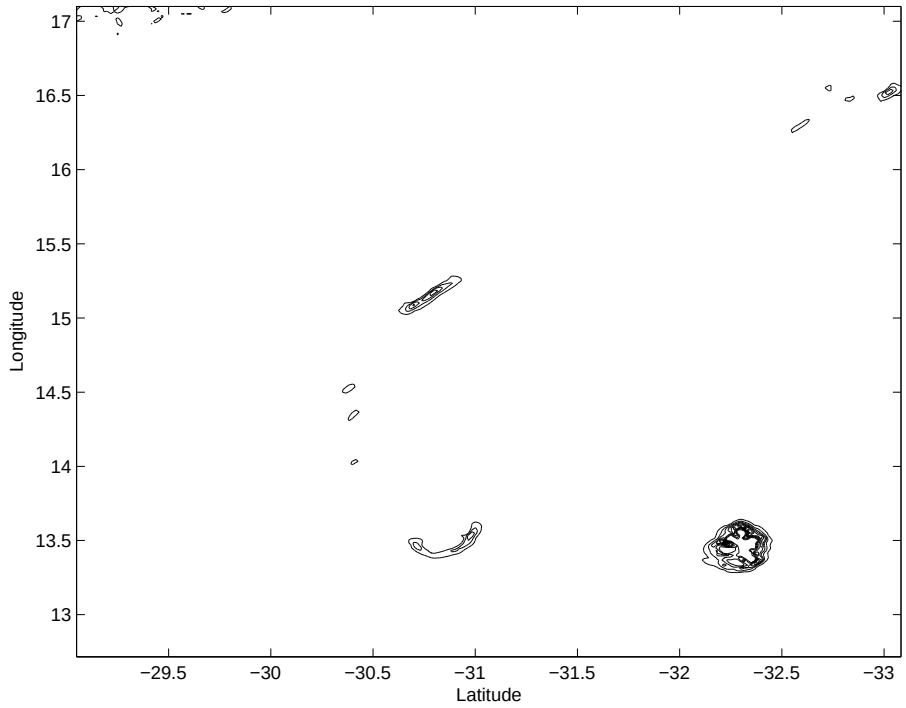

(b) Contour plot of the SMC

Figure 5.7*: The SMC for the west coast GEBCO one minute data set.*

obtained were examined and a method was conceptualised specifically for the typical characteristics found on the surfaces presented in Section 5.1. One of the requirements of the method developed was that the seaward most maximum point on the ridges would be identified as a foot line point, so that in regions where there is an area (or band) of ridge maximum, only the seaward most point would be identified as feasible. Another requirement was that the method developed should be robust with respect to noise in the data, and that a tolerance may be set so that in a case like that of the south west one minute data, where there is more than one visible traceable ridge, the ridge line to be traced could be chosen by means of a tolerance setting. These requirements pose a formidable task for conceptualisation of a semi–automated method of tracing.

The central idea behind the method, was that the search for the ridge would begin at a point (or points) specified by the user on the ocean floor ensuring that the points identified along the ridge as foot points would be the most seaward of possible points on the ridge. From this point (or points) the method would perform a search in the landward direction until a possible foot point (or points) was identified. Recalling that in the majority of graphics packages there is a function that, when invoked, fills a closed form with a user specified colour, typically referred to as a *floodfill*[1], it was thought that the concepts behind this function could be adapted to trace the ridge of maximum curvature. More specifically, a modification of this floodfill function to enable it to handle noise in the region to be filled, should allow the ridge of maximum curvature to be traced.

The resulting modified floodfill procedure developed to trace the ridge of maximum curvature is given in Algorithm 2. In Algorithm 2, the `start` input variable describes the $(row, column)$ matrix position of the starting points chosen for the algorithm. These positions indicate the matrix element's row and column numbers and are typically of the form (200,1), and do not reference the latitude and longitude coordinates of the point on the surface. For the given example of (200, 1), the starting point is found on row 200 in column 1.

The tolerance input is of the form 10^a where a is the tolerance chosen. When considering the neighbour of a point, the difference in the numerical value of the SMC at the point and its neighbour is compared with this tolerance value, and if the difference is less than or equal to the specified tolerance then the neighbour's position is added to the check list. This means that the point is skipped as a possible ridge point. The choice of tolerance therefore directly affects the resulting foot line, a tolerance that is too high will result in the possibility that the desired ridge line is "jumped" over and not considered, whereas a tolerance that is too low will result in the algorithm becoming trapped and identifying noise or other features seaward of the true ridge line as a ridge line.

Line 1 of Algorithm 2 initialises the output matrix, a matrix consisting of zeros (indicating the color black) that has the same dimensions as that of the input matrix (given by the `size` command in *Matlab*). The second line initiates the list of points to investigate by setting it equal to the starting point(s) specified in the input variable `start`. This list is used to identify which points' neighbours still require investigation so as to identify whether the fill procedure should continue. This list adopts a First–In–First–Out (FIFO) format. The while–loop spanning lines 3 to 25 ensures that the algorithm keeps investigating points and their neighbours until the list of points to investigate is empty. This list is updated within the while–loop itself. For the current investigation point under consideration (this is the first entry in the check list), the value of the corresponding entry in the output matrix is identified, on line 4, and if the value of this point is 0, indicating that it has not yet been investigated, it is marked as checked (given the value of 1 — indicating the colour white) and its neighbours are investigated. Should the point be marked as checked already, then the check point is removed from the list of points to check (line 24). This is achieved by simply moving the entire list up one position, according to the FIFO rule.

The variable used later in the algorithm to identify whether or not a point is situated on one of the extremities of the data, `edge`, is initiated to be false (given the value of zero) in line 5. Now that the

[1]In graphics packages, the user chooses the floodfill tool from a menu of graphics options and then clicks the mouse somewhere in the region that should be filled with the specified colour. The application of the standard floodfill function involves the function starting at the point in the graphic where the user clicks and then testing the colour value of each of the neighbours of that point: where the colour value of the neighbouring point is the same as that of the start point similarly changing its colour value to the specified fill colour. Generally, in a graphics package, the form to be filled is monotone in colour, with a distinct boundary of a different colour. All points spreading outward from the starting point are tested and filled until the method encounters the different colour value that identifies the edge of the form's boundary.

Algorithm 2 `Modified Floodfill Tracing`

Input: The data matrix, `In`, of the SMC for which a ridge trace is required, a $2\times n$ matrix of user specified starting points for the algorithm, `start`, the tolerance required, `tol`, and the value of the boolean variable, `trace`, identifying whether the final ridge line should be highlighted — a zero indicates that no final tracing takes place and a one that it does.

Output: A matrix with the same dimensions as the input matrix, (`Out`), containing elements of values 0, 1 or 2. Indicating the boundary encountered by the floodfill method (given the specified value deviation tolerance), and if `trace = 1`, the higlighted (traced) ridge line.

```
1: Out = zeros(size(In));
2: check = start;
3: while (size(check, 1) > 0) do
4:   if (Out(check(1, 1), check(1, 2)) == 0) then
5:     Out(check(1, 1), check(1, 2)) = 1;
6:     edge = 0;
7:     for all i = max(-1, 1-check(1, 1)) to i = min(1, size(In, 1)-check(1, 1)) do
8:       for all j = max(-1, 1-check(1, 2)) to j = min(1, size(In, 2)-check(1, 2)) do
9:         if (i ≠ 0) or (j ≠ 0) then
10:          if  In(check(1, 1)+i, check(1, 2)+j) - In(check(1, 1), check(1, 2)) ≥ -tol
             then
11:            check = [check; check(1, 1)+i, check(1, 2)+j];
12:          else
13:            if (i == 0) or (j == 0) then
14:              edge = 1;
15:            end if
16:          end if
17:        end if
18:      end for
19:    end for
20:    if (trace ≠ 0) and (edge ≠ 1) then
21:      Out(check(1, 1), check(1, 2)) = 2;
22:    end if
23:  end if
24:  check = check(2:end, :);
25: end while
```

point has been marked as being checked, its neighbours are investigated.

The analysis of a point's neighbours is performed on lines 7 through 19. The for–loop on line 7 specifies the x coordinate that describes the neighbouring point either above, below or in the same row as the check point. This specification is designed to take into account the boundaries of the data and not specify a neighbour outside of these boundaries. Where a check point does fall on a boundary, the x coordinate for a neighbour that is situated outside the boundary is given the value of zero. Similarly the for–loop on line 8 specifies the y coordinates of the neighbours to be checked. If either the x or y coordinate is zero, the neighbour corresponding to that specification is marked as an edge (the edge variable is set to 1). For neighbours residing in the data matrix (as opposed to outside it), the difference between the numerical value of the SMC at the neighbour and at the check point is then evaluated on line 10, and if this difference is less than or equal to the specified tolerance, then the neighbour's position is added to the end of the list of points to be investigated. Once all neighbouring points have been analysed, if the input variable `trace` specifies that a tracing should be made (`trace`=1), and the point has not been identified as being on the edge of the data, then the point is marked as a ridge point by assigning it the value of 2. Once this is done, the point is removed from the list of points to be investigated and the next point specified in the list is investigated.

The method of tracing is now illustrated by means of tracing a ridge on the one minute south coast SMC. The one minute south coast SMC was chosen due to the distinct ridge line formed, as this ridge line is a good visual indication of what shape the FoS should take. During the tracing of the ridge

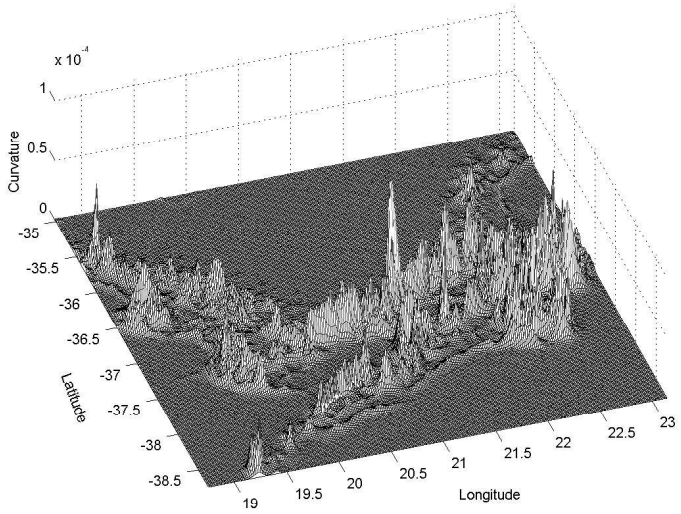

(a) The one minute south coast surface of maximum curvature

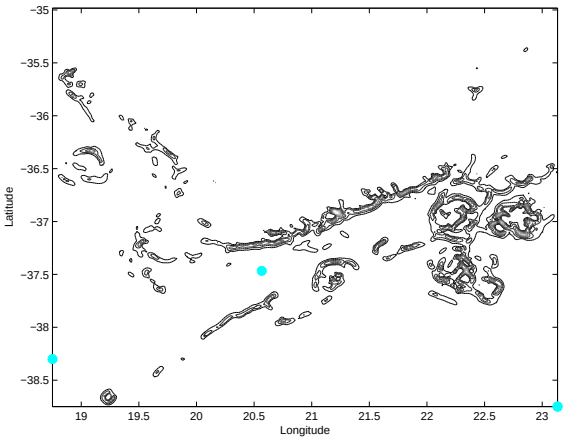

(b) Contour plot of the SMC with starting points marked in cyan

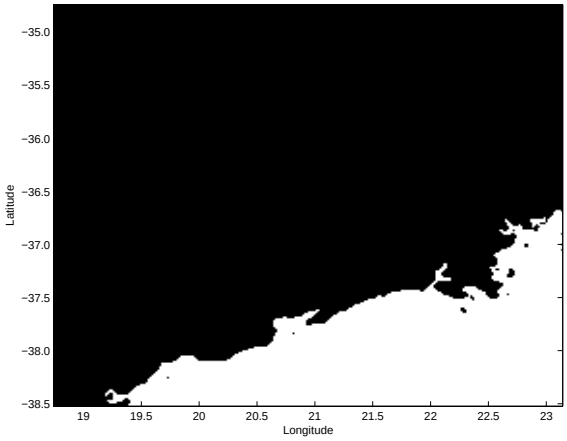

(c) Starting point 1

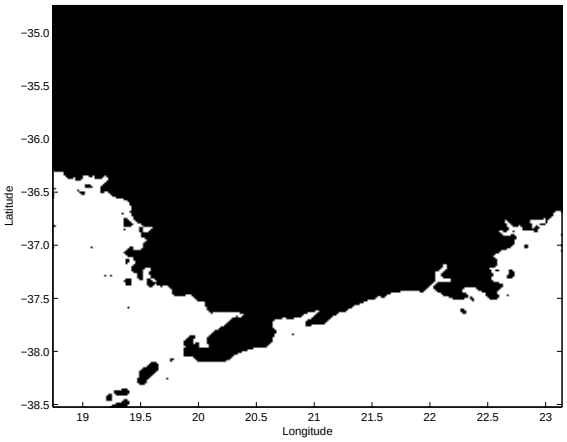

(d) Starting points 1 and 2

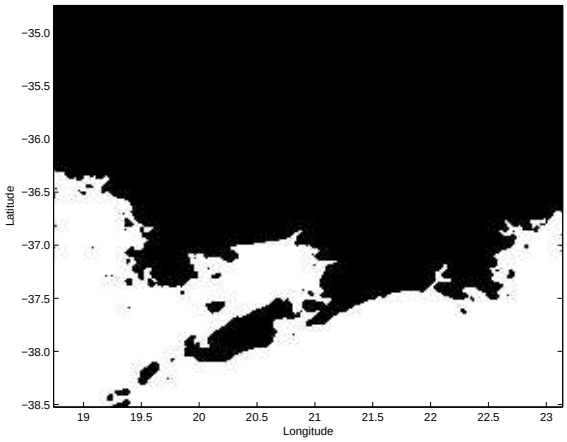

(e) Starting points 1, 2 and 3

Figure 5.8: *The initial tracing results obtained for different numbers of starting points for the one minute south coast SMC.*

line on the SMC, Algorithm 2 was called twice. The first time the algorithm was called to identify the seaward extent of the ridge on the SMC data matrix passed to the algorithm as input. For this call, the boolean variable, `trace`, was set to zero, indicating that the ridge line is not to be traced. This run of the algorithm is the initial phase of tracing and is the run where the user can test the effects of different tolerance values and starting points. For this call of the algorithm the starting points are situated seaward of the expected position of the FoS. An illustration of the output generated by calling the algorithm with these input values, and of how the number of starting points specified affects the results, for the one minute south coast SMC, is given in Figure 5.8. The algorithm calls used in tracing the GEBCO one minute south coast SMC ridge, are given below.

```
ridge = floodfill(smc, [size(smc, 1), size(smc, 2);200,1;150,110], 10^-7, 0);
ridge = floodfill(1-ridge, [1, 1], 0, 1);
```

The first starting point, (size(smc, 1), size(smc, 2)), is the point at the bottom right corner of Figure 5.8(b) with latitude–longitude pair approximately $(-39.5°S;\ 23.25°E)$, the second starting point, (200, 1), is the point at the bottom left side of Figure 5.8(b) with latitude–longitude pair approximately $(-38.6°S;\ 18.25°E)$ and the third starting point, (150, 110), is the point mid–centre in Figure 5.8 (b) with latitude–longitude pair approximately $(-37.5°S;\ 20.5°E)$. The tolerance for the tracing algorithm was 10^{-7} for the first call.

Once satisfied that the tolerance chosen and the starting points specified have yielded a result that is similar to the expected ridge line based on observation of the SMC (Figure 5.8 (a)), the results of this run were passed to the algorithm again. The ability of the user to specify tolerances and starting points, and to choose the resulting initial trace that will be used to identify the final line therefore introduces a level of subjectivity or expert bias to the tracing process.

The floodfill algorithm is extremely sensitive, and a decimal change in the tolerance specified can result in a ridge being "jumped" over by the algorithm during the initial tracing. Further, due to the extreme tolerance sensitivity, a slight change in the position of a specified starting point can yield a completely different result. This is directly related to the features around the specified point on the SMC given as input and whether these features are outside the set tolerance.

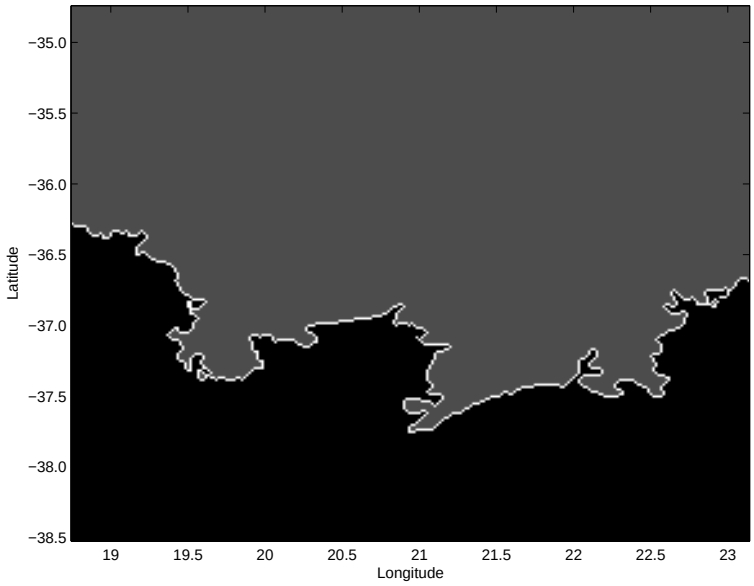

Figure 5.9*: The final result of the tracing process for the one minute south coast SMC.*

The purpose of the second call of the algorithm was to remove the seaward detail invariably included in the results of the first run and to isolate and trace the ridge line. This detail is as a result of smaller ridges and features on the SMC that fall short of the set tolerance and are therefore not filled. The second call of the algorithm uses the negative image of the result obtained in the first call, a starting

point in the black section of the result of the first call, a tolerance of zero and the `trace` variable value of 1 for input. The output from the second call of the algorithm colours the area seaward of the ridge line black, the ridge line itself white and the area landward of the ridge line gray. The results of the second call of the algorithm, using the result of the first algorithm call for the one minute south coast SMC run with three starting points, is shown in Figure 5.9. The desired ridge line is then the elements of the output matrix with a colour value of 1, and these points are easily taken to vector format with a simple **find(Out==1)** command in *Matlab*.

The results of the tracing process are described in detail in the following sections, arranged with respect to the region under consideration. The exact algorithm call commands are given for each data set and the resulting traced foot lines shown on the seafloor surface and seafloor contours for each data set. The foot lines computed for the one and two minute data for each region are then discussed and compared on the contour plot of the one minute seafloor contours for the region. For the following discussions the computed foot line for the one minute bathymetric data is always indicated by means of a cyan line, and the computed foot line for the two minute bathymetry by means of a magenta line.

5.2.1 East Coast FoS

For east coast SMC, computed using the GEBCO one minute bathymetry data, the algorithm calls made in the tracing process are given below.

```
ridge = floodfill(smc1, [size(smc1, 1), size(smc1, 2)], 10^-7, 0);
ridge = floodfill(1-ridge, [1, 1], 0, 1);
```

Similarly the algorithm calls made for the east coast SMC computed using the ETOPO two minute bathymetry data are given below.

```
ridge = floodfill(smc2, [size(smc2, 1), size(smc2, 2)], 10^-6.4, 0);
ridge = floodfill(1-ridge, [1, 1], 0, 1);
```

For both sets of data the same starting point was used. This data set only required the definition of one starting point; addition of further points did not change the results obtained. For the two minute data, the tolerance chosen was more accommodating than that used for the one minute data. This was done specifically to accommodate the noise seen on the SMC for the two minute data. However, there were areas of noise where this tolerance was not high enough and as a result the foot line for these areas is situated further seaward than expected. Increasing the tolerance in an attempt to accommodate these areas resulted in the ridge line being missed by the tracing algorithm, and as a result it was decided that a few areas of inaccuracy were more acceptable than not being able to compute a foot line at all. The computed foot lines for the east coast two and one minute data sets are given in Figures 5.10 and 5.11 respectively. The foot line computed for the one minute data seems to follow a specific contour, with some areas where it does deviate from this contour. Inspection of the foot line on the seafloor surface in Figure 5.11 reveals that, although consideration of the contour plot may give an indication as to inaccuracy of the line, the positioning of the computed line on the seafloor surface appears to be consistent with the expected position of the FoS. Inspection of the position of the computed foot line for the two minute data on the corresponding seafloor surface, however, does not seem accurate. The foot line seems to correspond to the foot of what could be perceived as the continental rise for the seafloor surface and, in some areas, is situated even further seaward than this. As was expected during consideration of the SMC for the two minute data, the foot line has been displaced seaward as a direct result of the noise introduced by the reduction in data resolution.

In order to compare the two computed foot lines, both of these lines were plotted on the contour plot for the one minute data, and are shown in Figure 5.12. Figure 5.12 reveals that the two minute computed foot line is indeed further seaward than the one minute line. The areas where the two minute footline extends a considerable distance further offshore than the one minute foot line is of particular interest. These areas are precisely where the worst of the noise on the two minute SMC were observed, indicating that (sensitivity of the tracing algorithm aside) although the computed foot line for the two minute data

offers a greater claim area, the confidence rating of the choice of line is lower than that of the one minute computed line [43].

5.2.2 South Coast FoS

For the south coast SMC, computed using the GEBCO one minute bathymetry data, the algorithm calls made in the tracing process were given during the explanation of the working of the tracing algorithm. The algorithm calls made for south coast SMC computed using the ETOPO two minute data are given below.

```
ridge = floodfill(smc2, [size(smc2, 1), size(smc2, 2);100,1;70,65], 10^-6.2, 0);
ridge = floodfill(1-ridge, [1, 1], 0, 1);
```

For the south coast data, both the one and two minute tracing required the definition of three starting points. This is as a result of the seaward most line of seamounts effectively sectioning the surface into two portions, and due to smaller ridges associated with the seamounts terminating the tracing algorithm before the search had reached the actual ridge line. The consequences of including areas of perceived seamounts in the area demarcated by the foot line are discussed in Section 5.3. The computed foot line for the GEBCO one minute data is shown in Figure 5.14. The foot line plotted on the seafloor surface for the one minute data does not look accurate. This is because the foot line sections off a portion of the seamount line and the line running over this area is visually disturbing. However, consideration of the foot line plotted on the seafloor surface contour plot offers a more acceptable result. Although there is a large area included inside the line where seamounts are evident, the positioning of the foot line appears accurate. Consideration of the computed foot line for the two minute data, given in Figure 5.13, reveals the foot line situated further offshore than would be expected. Due to the extensive noise in the two minute data, the computed foot line (although partially accurate) is not deemed accurate enough for serious consideration [43].

In order to facilitate a visual comparison of the positioning of the two computed foot lines, relative to each other, the lines were both plotted on the seafloor surface contour plot for the one minute data, given in Figure 5.15. It can be seen that while the two minute foot line is generally situated a substantial distance away from the one minute footline offshore, there is one area where the approximation offered by the two minute data would be considered more acceptable than that of the one minute data, namely in the longitude region of 21 to 21.5 degrees. This does not, however, increase the confidence rating of the computed two minute foot line, which is considered to be lower than that for computed foot line for the east coast two minute data [43].

The south coast results serve as a preliminary indication that the methods of this thesis are better suited to a non–transform margin type, and that where there is benefit in application of the methods to data from a transform margin region, this benefit does not include the computation of the foot line for the region. A more detailed discussion of how the computation of the SMC for data from a region such as this could be used to benefit a claim submission, or validation process, is offered later.

5.2.3 South West FoS

The south west coast region is a special case of where there was more than one visible and traceable ridge on the SMC for the one minute data, but also where the two minute data could not be used to determine a FoS. A green line is used in this section to indicate the second ridge line traced for the one minute data. For the GEBCO one minute bathymetric data, the algorithm calls made in the tracing process, for determination of the first of the two visible ridges on the SMC for the region are given below.

```
ridge = floodfill(smc, [200, 20;20,20;70,80;180,180], 10^-7.5, 0);
ridge = floodfill(1-ridge, [1, 200], 0, 1);
```

The line that these algorithm calls traces is the line situated further inshore (green line in Figure 5.16). For the more seaward of the lines (cyan line in Figure 5.16), the following algorithm calls were made:

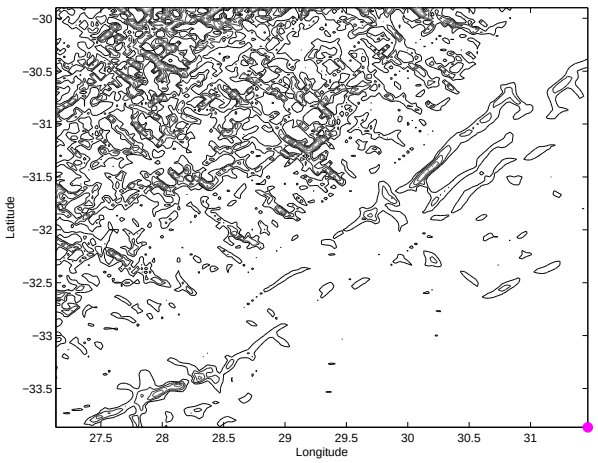

(a) Contour plot of the SMC with starting points marked

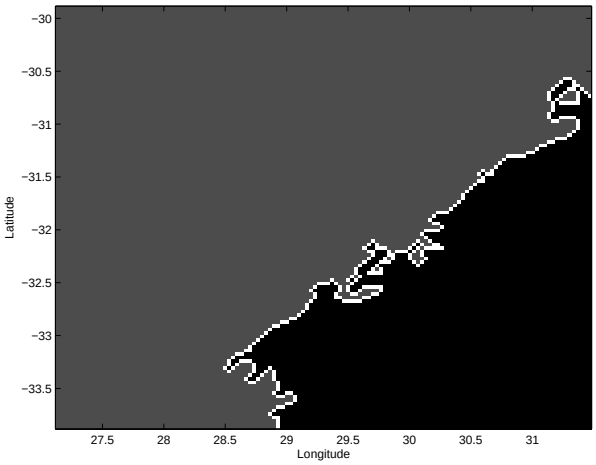

(b) Final tracing result

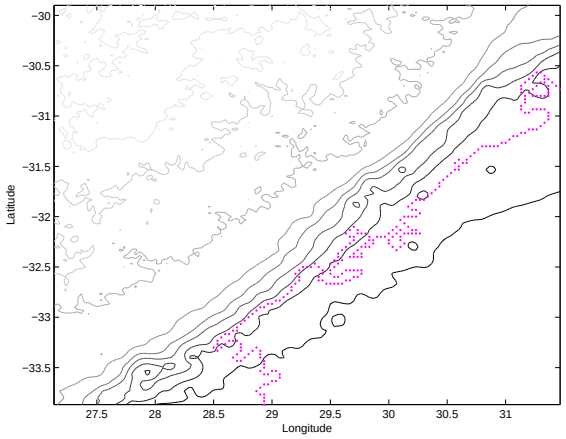

(c) The position of the foot line on the seafloor contour plot

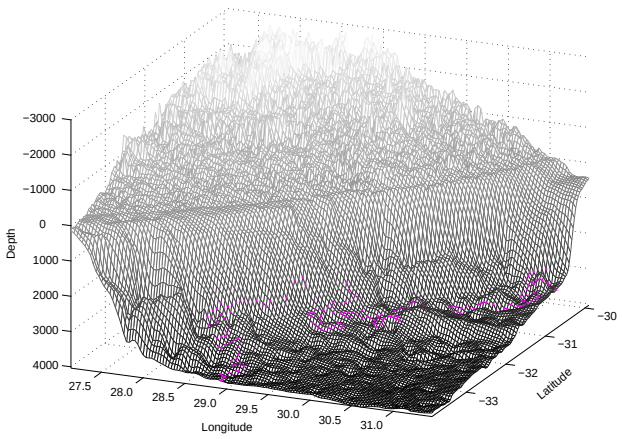

(d) The position of the foot line on the seafloor surface

Figure 5.10: *The computed foot line for the ETOPO two minute east coast data.*

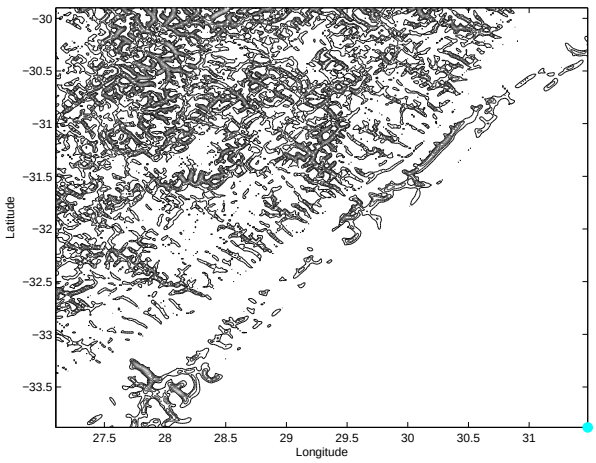

(a) Contour plot of the SMC with starting points marked

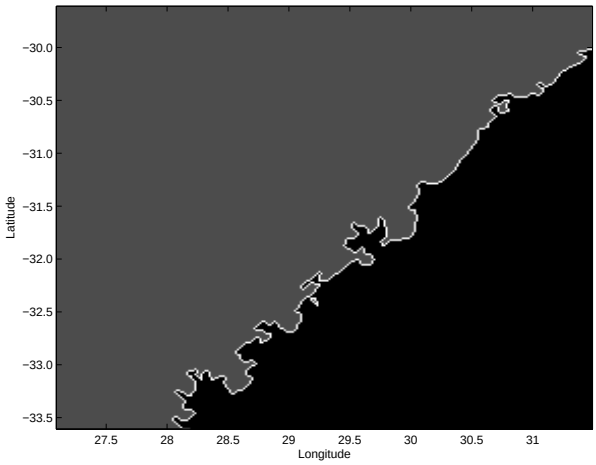

(b) Final tracing result

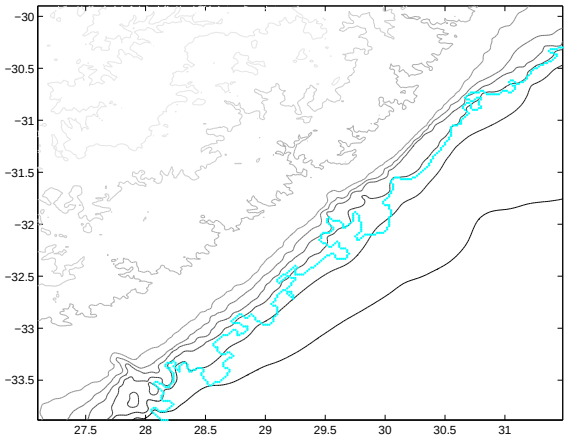

(c) The position of the foot line on the seafloor contour plot

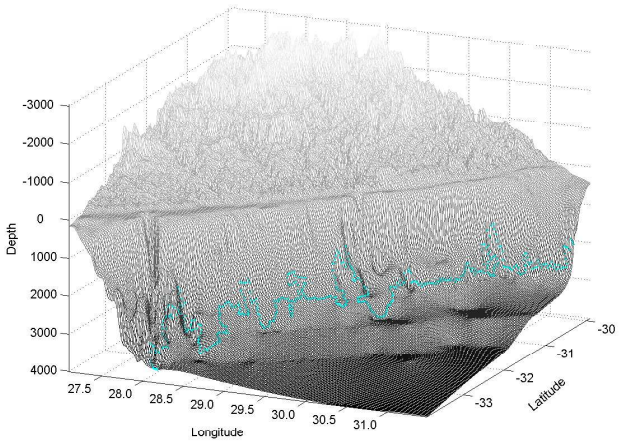

(d) The position of the foot line on the seafloor surface

Figure 5.11: *The computed foot line for the GEBCO one minute east coast data.*

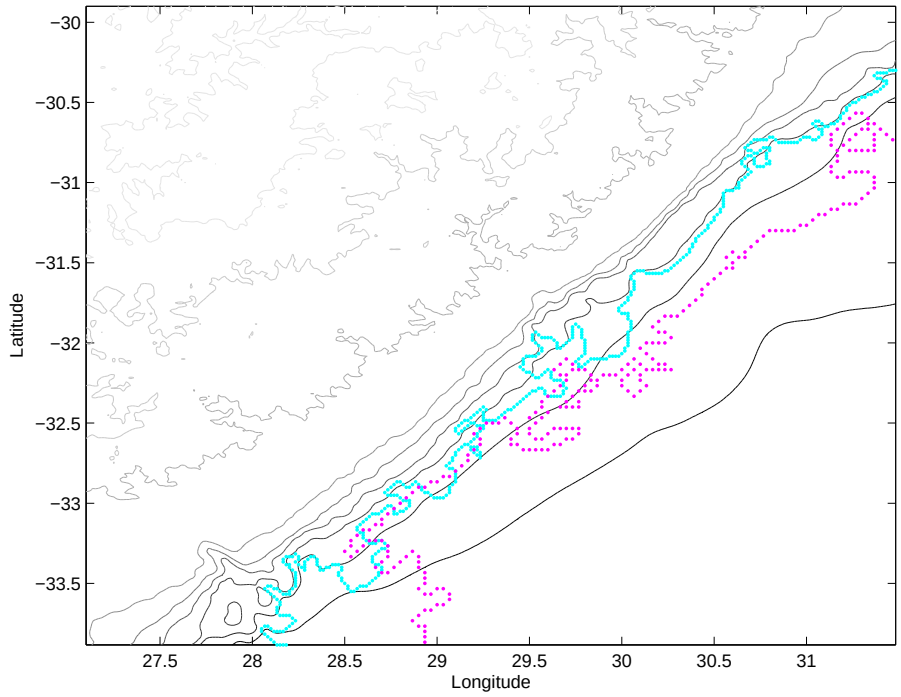

Figure 5.12: *A comparison of the computed foot lines for the one and two minute east coast data. The cyan line represents the one minute footline and the magenta line represents the two minute footline.*

```
ridge = floodfill(smc, [200, 10;120,20;200,100;80,1;90,20;], 10^-20, 0);
ridge = floodfill(1-ridge, [1, 200], 0, 1);
```

The computed foot lines for the southwest coast GEBCO one minute data set is given in Figure 5.16. Inspection of the position of the two computed lines on the seafloor surface, indicates that the cyan line most likely corresponds to the foot of the continental rise, and the green line corresponds to the FoS. It is very beneficial to be able to trace the foot of the continental rise, as the resulting line offers an upper bound on the seaward position that may be considered for the submitted FoS line. The green line could therefore be used by either the United Nations Commission on the Law of the Sea, in the validation of a submitted claim and in the bounding of acceptable positions of the FoS for the region, or by the claimant, to verify that the FoS line chosen, lies landward of the upper bound offered by the green line. Each region of data described in this thesis is a case study of a particular margin type found around South Africa. The south west coast is a region of transition from the transform–sheared margin type in the south to a sediment–rich, non–volcanic divergent–rifted margin type in the west. The south west region, therefore, is an important case study in this thesis. The region is unique in that it is the only region where two distinct and identifiable ridges were established and traced.

5.2.4 West Coast FoS

The west coast is, similar to the south west coast, an important case study in this thesis. It is the only region where a continuous ridge was not observed on the SMC. Even though there is not a definite ridge to trace, the tracing algorithm was applied to these data to illustrate how a careful choice of tolerance and starting points can force a line to be traced, even where this should not be possible. This is intended as an illustration that the tracing algorithm, besides introducing some subjectivity to the determination of the FoS, can be forced into tracing a line of little practical relevance. The algorithm calls made in the tracing process are given below.

```
ridge = floodfill(smc, [200, 10], 10^-7.2, 0);
ridge = floodfill(1-ridge, [1,264], 0, 1);
```

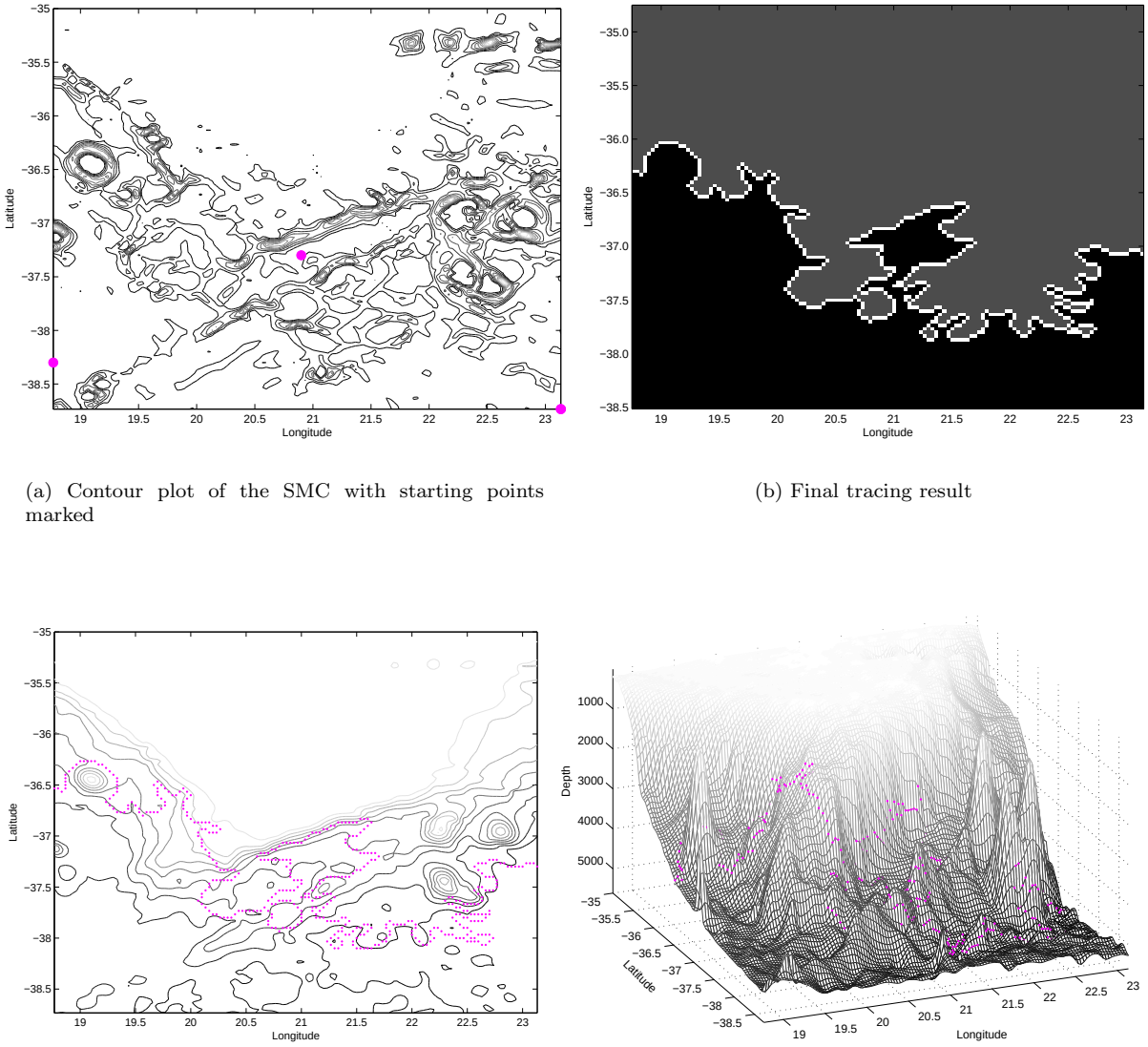

(a) Contour plot of the SMC with starting points marked

(b) Final tracing result

(c) The position of the foot line on the seafloor contour plot

(d) The position of the foot line on the seafloor surface

Figure 5.13: *The computed foot line for the ETOPO two minute south coast data.*

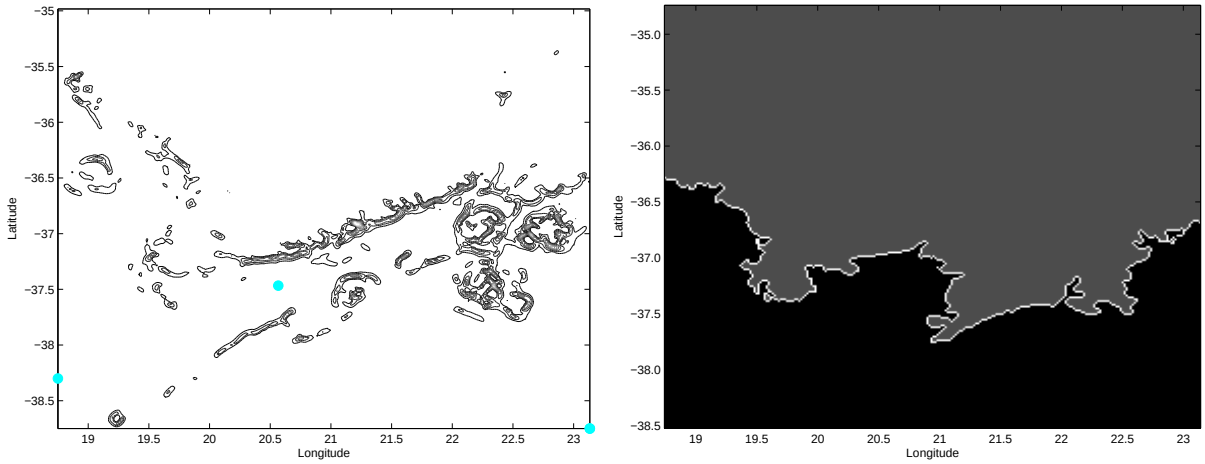

(a) Contour plot of the SMC with starting points marked

(b) Final tracing result

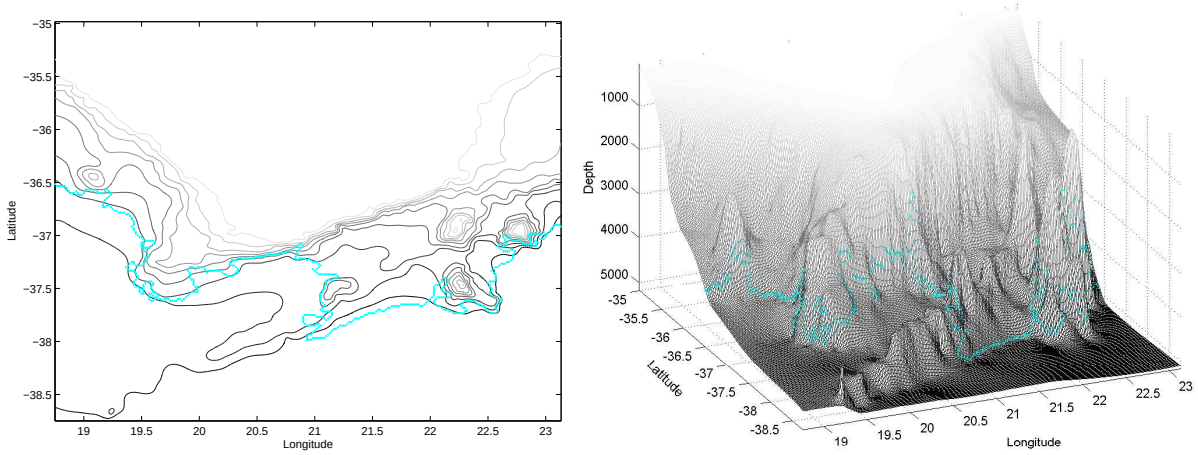

(c) The position of the foot line on the seafloor contour plot

(d) The position of the foot line on the seafloor surface

Figure 5.14: *The computed foot line for the GEBCO one minute south coast data.*

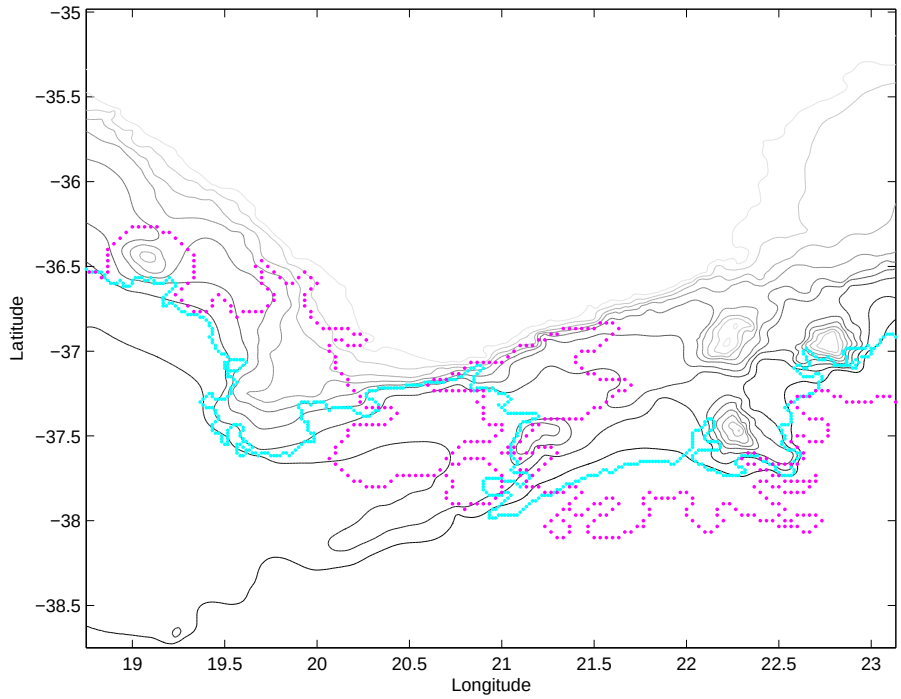

Figure 5.15*: A comparison of the computed foot lines for the one and two minute south coast data. The cyan line represents the one minute footline and the magenta line represents the two minute footline.*

Although there is only one starting point defined for this surface, it is the only point found (during a large number of failed attempts) that produced a traceable line. The computed foot line for the west coast GEBCO one minute data SMC is given in Figure 5.17. Inspection of the position of the computed foot line on the seafloor surface shows that visually the line appears grossly inaccurate [43]. It in no way represents the true nature of the seafloor it is meant to be related to. In one section the computed line almost traces the start of the continental slope as opposed to its foot. This computed foot line should not be considered for use and clearly negates the use of this methodology for such a margin type.

5.3 *Caris Lots* Example Foot Line Comparison

In the previous section, the computed foot lines for each region were discussed and shown graphically on their respective seafloor surfaces. In this section these computed foot lines are compared to the foot points determined by means of the *Caris Lots* software package, in addition to a possible optimal foot line obtained from these points. The points to be used in this section were again chosen using the Douglas Peucker filter in *Caris Lots* and are referred to as a "Peucker Pick." For the sake of completeness, all of the foot points defined for a region are shown in the comparison, not just those that form the optimal foot line. Once again, the computed foot lines for the one and two minute data (where applicable) as well as the *Caris Lots* data are plotted on the one minute seafloor surface contour plot for the region under consideration. It is to be stressed that the *Caris Lots* points used in this thesis are merely example points that would typically be chosen by an experienced *Caris Lots* operator.

It is beneficial at this stage to repeat that in determination of the FoS in *Caris Lots*, the operator has access to the same GEBCO one minute and ETOPO two minute gridded data as used in this thesis. The *Caris Lots* operator is, however, further advantaged by other supporting public domain data sets (such as density and sediment thickness) in order to make an optimal FoS selection.

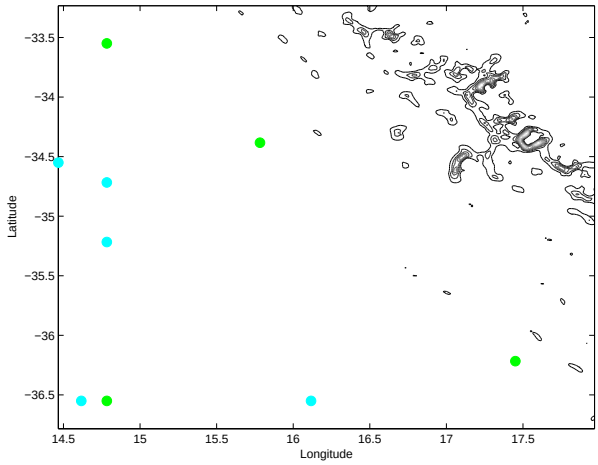

(a) Contour plot of the SMC with starting points marked

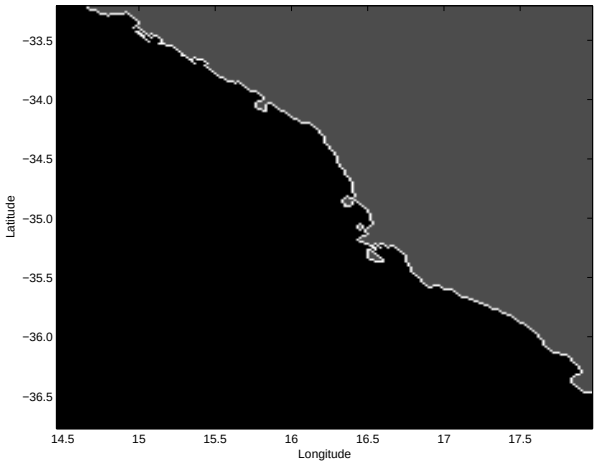

(b) Final tracing result, ridge 1

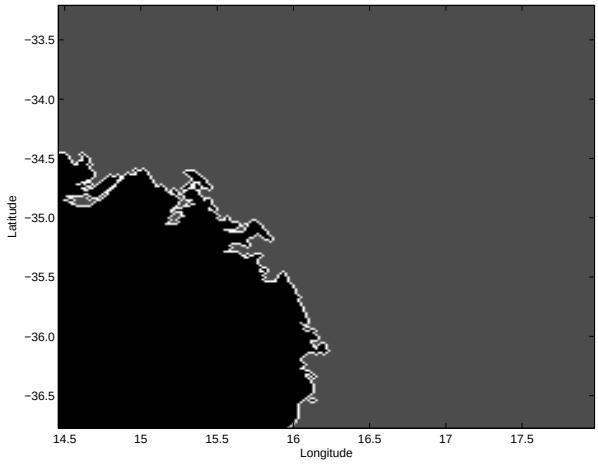

(c) Final tracing result, ridge 2

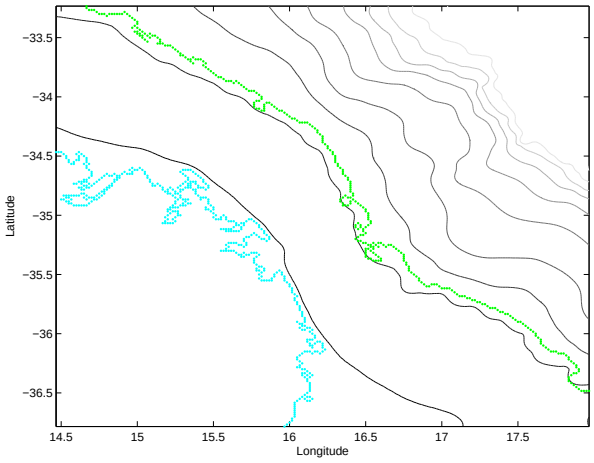

(d) The position of the foot lines on the seafloor contour plot

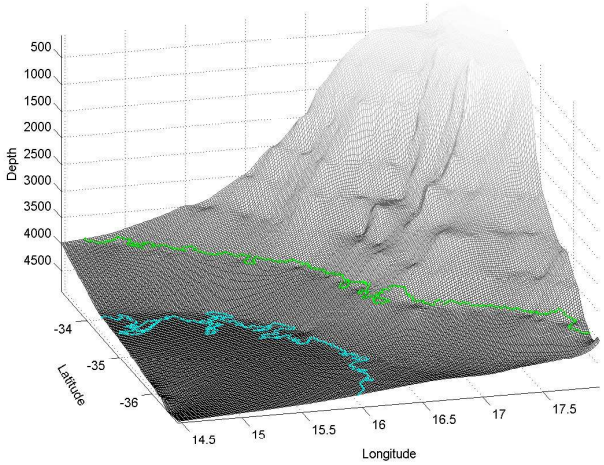

(e) The position of the foot lines on the seafloor surface

Figure 5.16*: The computed foot lines for the GEBCO one minute south west coast data. The cyan line represents a possible Foot of the Continental Rise position and the green line represents the FoS position.*

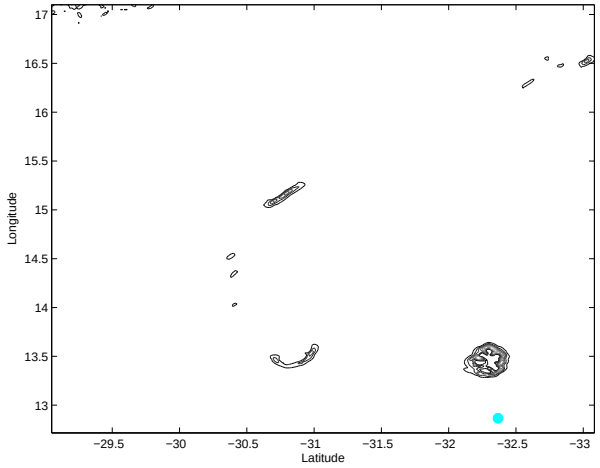

(a) Contour plot of the SMC with starting points marked

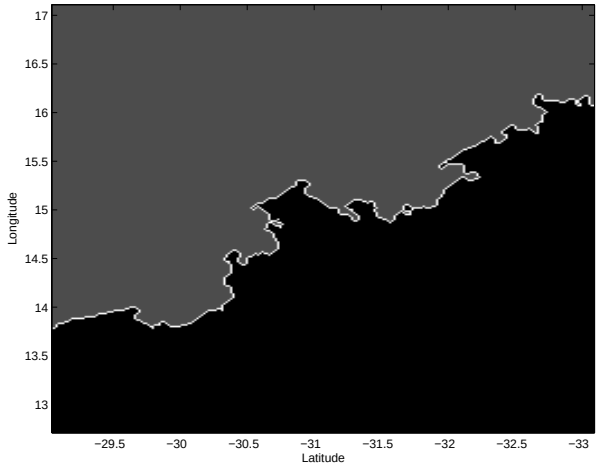

(b) Final tracing result

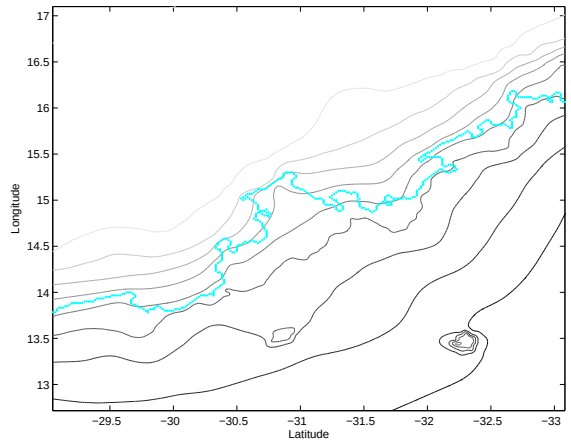

(c) The position of the foot line on the seafloor contour plot

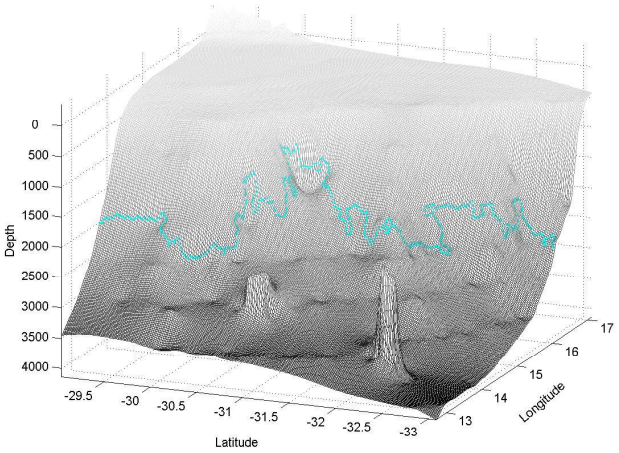

(d) The position of the foot line on the seafloor surface

Figure 5.17: *The computed foot line for the GEBCO one minute west coast data.*

5.3.1 East Coast

What is immediately evident in the comparison of the computed foot lines and the *Caris Lots* points for the east coast, shown in Figure 5.18, is that both of the computed foot lines are situated further inshore than the possible optimal *Caris Lots* line. It is also obvious that the foot lines computed in this thesis are of a much higher resolution than the *Caris Lots* line. This higher FoS line resolution boosts the confidence rating of the computed 3D lines to be higher than that of the 2D *Caris Lots* line. The scientific method behind the computation of the choice of the computed foot lines in this thesis is also better than that for the *Caris Lots* line. The computed foot line for the two minute data lies seaward of the *Caris Lots* line in some regions, and this is an immediate indication of where the noise in the data causes inaccurate results. The fact that the *Caris Lots* line is further offshore than the computed one minute line could give indication that the method employed in *Caris Lots*, for the points offered for this region, should be questioned or at least be used in a validation process.

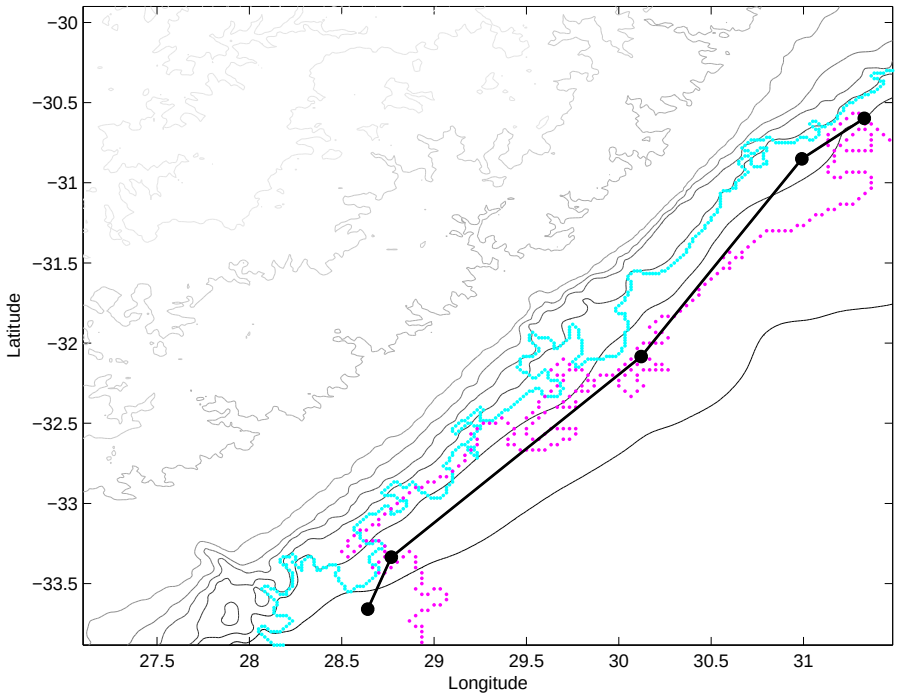

Figure 5.18: *A comparison of the computed foot lines and a possible Caris Lots line for the east coast. The cyan line represents the one minute footline, the magenta line represents the two minute footline and the black line represents a possible optimum Caris Lots line.*

5.3.2 South Coast

The conclusion in the previous section (Section 5.2) was that the method to determine the FoS established in this thesis was perhaps not entirely suited to the margin type found in this region. Where the method might not be suited for computation of an FoS for use in a claim, the value lies in the motivation that the results offer with regards to further surveying that needs to be undertaken. The computed foot points and the *Caris Lots* points are given in Figure 5.19. In this figure it may be seen that both the one and two minute computed foot lines include an area indicative of seamounts. It is, however, uncertain as to whether these peaks are in fact seamounts, or whether they form a part of the continental slope. Article 76 of the LoS specifically prohibits inclusion of seamounts in cases where inclusion of the seamount results in a region of ocean floor being incorporated in the claim area. For the south coast, the computed foot lines (within the desktop study) could motivate the necessity of a survey to identify whether or not the submarine structures observed are, in fact, seamounts. This is particularly important where seamounts are attached to the continental slope. The method further helps to isolate seamounts in an area of

complex bathymetry. The overall conclusion for this margin type is that the mathematical method offers a FoS determination which will provide a larger maritime estate claim than that of the *Caris Lots* FoS determination, but the burden of responsibility, with use of the mathematical results, is to prove that the perceived seamounts included in the claim are not seamounts. This would likely involve a geological survey.

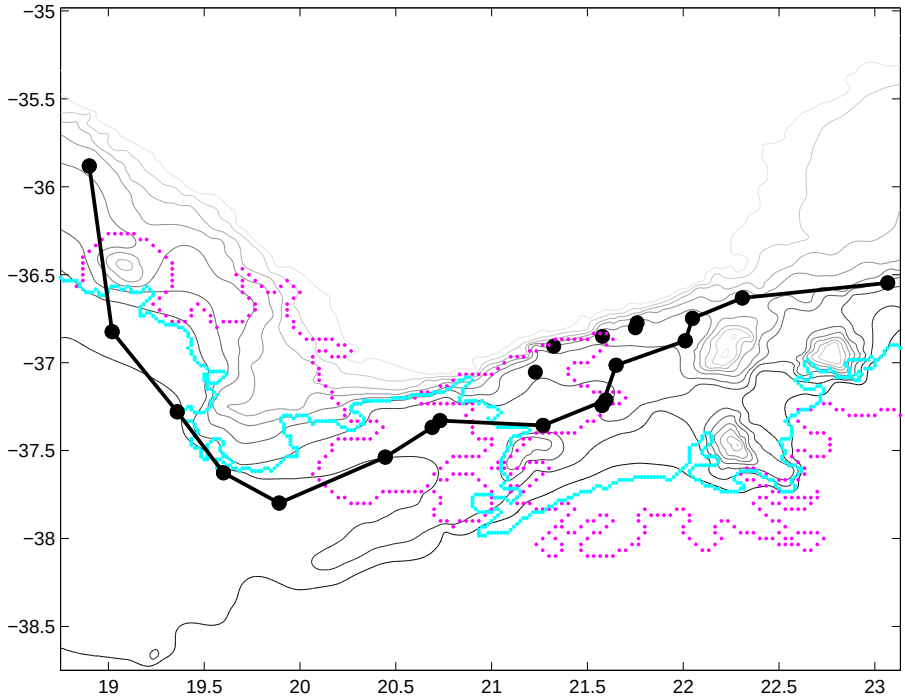

Figure 5.19*: A comparison of the computed foot lines and a possible Caris Lots line for the south coast. The cyan line represents the one minute footline, the magenta line represents the two minute footline and the black line represents a possible optimum Caris Lots line.*

5.3.3 South West Coast

As was discussed in the previous section, the computed foot line represented in cyan is thought to correspond to the foot of the continental rise. This is evidenced by the cyan line (in Figure 5.20) having the most seaward position. The second of the traced lines, represented in green and equated to the FoS, offers a more advantageous claim line than the *Caris Lots* line in one area, but otherwise is situated inshore of the *Caris Lots* line. The area of more advantageous approximation could be as a result of *Caris Lots* including gravity, magnetics and sediment thickness variables in its computation of the FoS. One or more of these variables could be responsible for attracting the *Caris Lots* line further inshore than the computed line.

5.3.4 West Coast

The position of the *Caris Lots* line in Figure 5.21 serves to justify the decision in the previous chapter that the west coast data is not suitable for use in computation of a FoS. Further, the line computed to illustrate that the tracing algorithm is fallible, is situated far from the *Caris Lots* line towards the land, further backing the statements made with regards to this matter in Section 5.2.

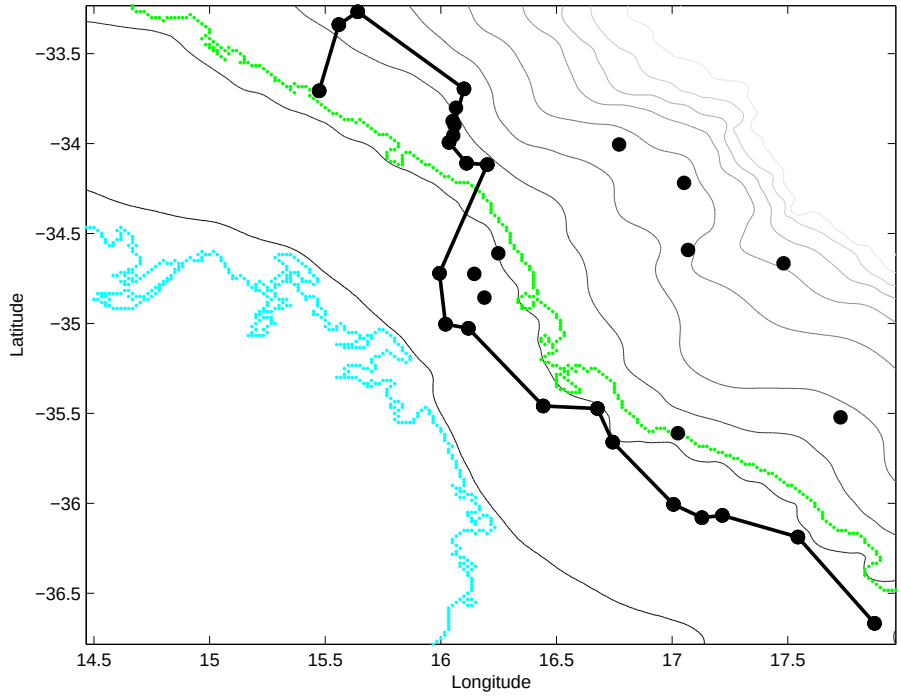

Figure 5.20: *A comparison of the computed foot lines and a possible Caris Lots line for the south west coast. The cyan line represents the FoS position, the green line represents a possible Foot of the Continental Rise position and the black line represents a possible optimum Caris Lots line. A two minute footline could not be computed for this region.*

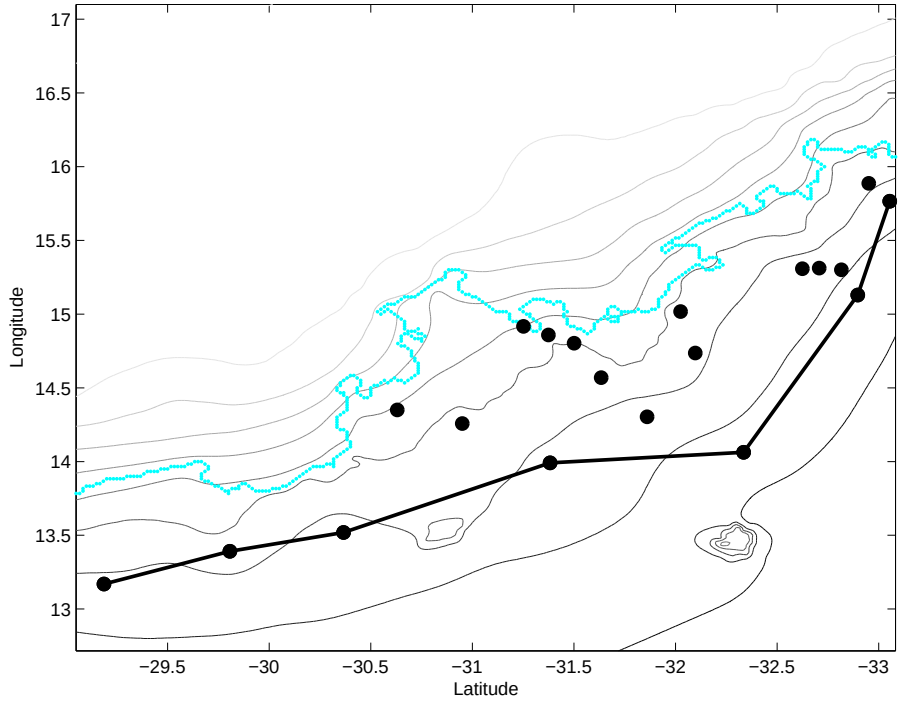

Figure 5.21: *A comparison of the computed foot lines and a possible Caris Lots line for the west coast. The cyan line represents the one minute footline and the black line represents a possible optimum Caris Lots line. The two minute footline was not determined for this region.*

5.4 Chapter Summary

In this chapter, the mathematical method described in Chapter 3 for determination of the SMC for a given seafloor surface was applied to the one and two minute data sets of the four regions identified in Chapter 4. The resulting SMCs were compared with respect to the effect of a reduction in the resolution of data. A method to trace the ridges formed on these SMCs was then introduced and discussed. The working of the method was illustrated by means of use of the one minute south coast data. The foot lines for each data set were then computed using this method and the results obtained were discussed. These computed foot lines were finally compared to *Caris Lots* determined foot lines.

Chapter 6

Conclusion

South Africa is a signatory to the LoS and, as such, has until May 2009 to submit a claim to the United Nations for extended seaward estate beyond its 200M EEZ. South Africa may stand to gain a substantial area of approximately 400 000 km^2 of seafloor. This figure may change for the positive or the negative, pending the outcome of the desktop study currently in progress. For a coastal state as a signatory to UNCLOS, the onus exists to measure and prove continental shelf extension, according to strict criteria. One important criterion is the accurate numerical determination of the FoS as defined in the regulations, which is critical in defining the offshore claim extent. The scope of this thesis, therefore, was the determination of the FoS as mathematically defined by "... the point of maximum change in the gradient at its base."

Consideration of a mathematical method to determine the FoS excludes any geological considerations that may be included in the restrictions specified by the Convention. The focus in this thesis was on the curvature (a measure of the directional gradient) of the seafloor and how this may be used in the determination of the FoS. Further, a method for tracing of the foot line so obtained was put forth so as to make tracing feasible for computation purposes (from bathymetric data) and was not specifically designed to comply with all of the restrictions pertaining to the FoS as specified by the Convention.

6.1 Thesis Summary

The main drive behind the proposition of this thesis was to ascertain whether a more objective and mathematically based method of computation of the FoS was possible and, if so, whether it would be beneficial to the claim process. Benefit, in this sense, is seen as a mathematically defendable maximization of the area proposed for claim. Taking advantage of the high resolution grids of recent bathymetric data and applying a spatial analysis method, a FoS was determined in a mathematical sense. The mathematical method to determine the FoS was divided into two sections: the determination of the SMC and the tracing of the ridge on the SMC. The method for determination of the surfaces of extremal curvature was discussed in Chapter 3 (Sections 3.1 and 3.2), and forms the realisation of Objective I of this thesis, specified in Section 1.3.

The method to determine the surface of maximum curvature, presented in this thesis, was first applied to two smooth, hypothetical sample seafloor surfaces in Sections 3.3 and 3.4, before utilization on the bathymetric data used in this thesis. The determination of the SMC for the one and two minute gridded bathymetric data was performed in Section 5.1, realising Objective II of this thesis. It was found that data resolution had a significant impact on the quality of the SMCs obtained, with the most important result being that the data resolution of the two minute gridded bathymetric data yielded a SMC that could not be used in the process to determine the FoS.

The tracing of the ridges formed on the SMCs was discussed in Section 5.2 and a tracing algorithm proposed. This algorithm satisfies Objective III of this thesis, but it is highlighted that this tracing method is a preliminary attempt at putting forth a semi–automated method to trace the ridge formed

on the SMC, and that it should be developed further before the results may be considered seriously for use in a claim process. The tracing algorithm was then applied to the one and two minute SMCs, determined in Section 5.1 — realising Objective IV of this thesis. The one and two minute computed foot lines for each region of data were then compared to ascertain the robustness of the method, thus achieving Objective V of this thesis. It was found that the method is best suited to regions with a margin type similar to that found in the east coast (a sediment–rich, non–volcanic divergent–rifted margin type) and south west coast (a region of transition from the transform–sheared margin type in the south to a sediment–rich, non–volcanic divergent–rifted margin in the west) regions. The method offers advantageous results in the south coast region (a non–volcanic transform–sheared margin type) with the drawback that these results may need to be verified geologically. The west coast region indicated that the method was poorly suited to a sediment–rich, non–volcanic divergent–rifted margin type where there was extensive continental deposition (causing a very gradual continental slope). It was further discovered that the south west coast region was a unique and special area, and that there were two possible ridge lines to trace on the one minute SMC — one corresponding to the foot of the continental rise and one to the FoS.

In Section 5.3 the one and two minute results were compared to the foot lines determined for comparison in *Caris Lots* (achieving Objective VI of this thesis). It was found that the value of the methods discussed in this thesis for computation of the FoS are not necessarily directly related to the determination of any particular claim for any particular state, but rather to the evaluation and validation of a desktop study for a claim. In some cases the results may be used to help identify optimal bathymetric survey lines and areas where further surveying should be undertaken in order to optimise the claim. Furthermore, the results obtained from application of these methods may be used by a state for comparison and validation of its claims, and in this way provide a backing for the FoS choice in the claim. It was further found that the subjectivity introduced in the tracing of the FoS introduces a bias that should be removed by means of improvement and adaptation of the method detailed in this thesis.

6.2 Recommendations

Only the method proposed by Vaníček and Ou [38], in 1994, was evaluated and implemented in this thesis. The motivation for excluding the second method, proposed by Bennett [4] in 1998, was a hypothesis made by the author regarding the data resolution used by both methods, namely that the data resolution was responsible for the perceived drawbacks in the 1994 method. This hypothesis has not been tested and it is therefore recommended that it be investigated by evaluating Bennett's method in the same amount of detail and based on the same data sets used in this thesis and comparing the results obtained to the results found here. It is further not known what tracing algorithm was used in these methods (and whether the same tracing procedure was used by both methods), and this should be investigated further.

The tracing algorithm developed for this thesis is a preliminary attempt at a semi–automated method of FoS determination. There is an introduction of some subjectivity (or expert bias) to the method, residing in the choice of starting points and tolerances and the fact that the operator decides when the result is satisfactory. It is recommended that the tracing algorithm be developed further, reducing the subjectivity introduced and improving the reliability of the results, by making the algorithm fully automated.

It is recommended that the results obtained for the different margin types around the South African coast be compared to a study of other similar margins elsewhere. These comparisons could then be used to better determine which margin types are best suited to the methods of this thesis. This comparison will also facilitate insight as to whether a standard tracing tolerance may be determined for a specific margin type.

The method to determine the surface of maximum curvature may, at this stage, only be applied to regularly spaced gridded data. It is recommended that the algorithms for implementation of the method be adapted to allow for an irregular data spacing. South Africa intends to use a Multi–Beam Bathymetry Sounder (amongst others) for the surveying in its claim process, and this sounder yields results in a grid of irregularly spaced, but extremely high resolution data. It would be beneficial to be able to apply these methods to this very high resolution, yet irregular data.

Determination of the FoS in *Caris Lots* includes other methods and data to assist in making the most advantageous approximation of the foot line possible. Some of these methods and data may also be included or added to the methods used in this thesis to similarly add advantage to the methods of this thesis. Typical data that, if included, would improve the overall scientific backing of a foot line choice, include factors such as density, sediment thickness, gravimetric measurements, magnetic measurements and other geological factors.

After the above recommended improvements and adaptations have been implemented, the revised method and its results may be used for promotion of the method as a tool — incorporated into a software package (such as *Caris Lots*), or as a stand alone tool. This tool could then be used by a state during the compilation of a claim for validation and comparison purposes; in other words to investigate the strength of the conviction behind a proposed claim area, by comparison with results obtained from a mathematical three–dimensional method.

With refinement and development of a user interface the method could be used by the United Nations Commission on the Law of the Sea to compare or assess FoS claims submitted by providing:

1 An indication of the location of the continental rise from the ridge with the most offshore extent on the SMC. This benefit would typically be found in situations similar to those found on South Africa's south west coast, where there are two distinct traceable ridges on the SMC — one corresponding to the foot of the continental rise and one corresponding to the FoS. The continental rise could be used as a maximum boundary for submitted claims, any claim area extending further offshore than this determined edge of the continental rise should be rejected.

2 A method to compare submitted claims, especially by providing a more detailed interpretation through three dimensional processing than is currently offered in two dimensions.

3 A contour plot of the SMC computed. That may be used to define the edges of offshore features (e.g. seamounts). This definition may then be used in the verification of such features and whether they are legally permitted to be included in a claim in terms of Article 76. A typical example of this is the South African south coast, where it is uncertain whether the submarine features observed are seamounts or a portion of a complex margin topology.

4 A validation of areas where mathematical methods cannot be applied practically, as described in Article 76 for determination of the point of maximum change in gradient at the base of the continental slope. This may provide for the invocation of the "evidence to the contrary" argument offered in Article 76 and provide a motivation for the use of a geologically determined FoS.

During the finalisation of work on this thesis some interesting developments occurred in both the international and South African arenas. The results of this thesis were presented to the South African Working Group on the 20th October 2004. All parties present were impressed by and interested in the work, the application of the methods and how the methods proposed could be included in the South African claim process. Members of the South African Working Group, who had recently returned from a claim–related trip to France and the United Kingdom, raised the point that the general international consensus was that the "Peucker Pick" in *Caris Lots* would not be considered as a basis for a claim as a direct result of the filter attracting the line too far offshore. Generally, it was found that the "Peucker Pick" line is located over deep ocean floor, which is unacceptable to the United Nations Commission on the Law of the Sea. This finding, although very recent, has prompted the Commission to consider issuing a formal statement with regards to the unacceptability of a claim based on this FoS choice. Indeed, the results of this thesis seem to support the general mistrust in the FoS determination via the "Peucker Pick," in the sense that the mathematically determined FoS (found via the methods described in Chapters 3 and 5) was observed to be significantly more inshore than the "Peucker Pick" FoS in most cases, when using the South African bathymetric data.

References

[1] *ABSTRACTS of the ABLOS Conference 2001, Accuracies and uncertainties in maritime boundaries and outer limits.* International Hydrographic Beureau, Monaco.

[2] Author Unknown, *World Geodetic System 1984 [WGS84]*, [Online], [Cited July 6th, 2004], Available from `http://www.wgs84.com/wgs84/wgs84.htm`

[3] Barker C, 1982, *Oil and Gas on Passive Continental Margins*, in Watkins S & Drake CC (EDS), *Studies on Continental Margin Geology*, Tulsa, Oklahoma, United States of America.

[4] Bennett JO, 1998, *Mapping the Foot of the Continental Slope with Spline-Smoothed Data Using the Second Derivative in the Gradient Direction*, U.S. Department of the Interior, Minerals Management Service, Resource Evaluation Division, OCS Report MMS 97-0018.

[5] Caris, 2003, *Caris Training Manual — Caris Lots 4.0.* CARIS, Canada. `http://www.caris.com/`

[6] Churchill RR & Lowe AV, 1988, *The Law of the Sea*, Manchester, United Kingdom.

[7] Cook PJ & Carleton CM (EDS), 2000, *Continental Shelf Limits, The scientific and legal interface*, Oxford University Press, Oxford, United Kingdom.

[8] Cronan DS, 1980, *Underwater Minerals*, Whittles Publishing, London, United Kingdom.

[9] Dally AW, 1981, *Atlantic Type margins, Geology of Passive Continental Margins: History, Structure and Sedimentologic Record (with emphasis on the Atlantic Margin)*, American Association of Petroleum Geologist Education Course Note Series, **19**, 1–48.

[10] Deetz CH & Adams OS, 1934, *Elements of Map Projections with Applications to Map and Chart Construction, Fourth Edition*, U.S. Coast and Geodetic Survey Special Publication 68, Washington DC, United States of America.

[11] Douglas DG & Peucker TK, 1973, *Algorithms for the Reduction of the Number of Points Required to Represent a Digital Line or its Caricature*, Canadian Cartographer, Vol 10, No 2, 112–122.

[12] Duncan GC, *Numerical Differentiation*, [Online], [Cited May 16th, 2004], Available from `http://chandra.bgsu.edu/ngcd/numdiff/node1.html`

[13] Eldholm O, Skogskeid J, Plank S & Gladczenko TP, 1995, *Volcanic Margin Concepts*, pp 1–16 in Band E, Talwani M & Toné (EDS), *Riften Ocean–Continent Boundaries: NATO ASI Series*, Dorderecht, Netherlands.

[14] Emery KO, 1994,*Continental Margins — Classification and Petroleum Prospects*, American Association of Petroleum Geologists Bulletin **64**, 297–315.

[15] Garnett W, 1924, *A little book on map projection*, Third Edition, George Philip and Son LTD., London, United Kingdom.

[16] Hamman D, Wainman CK & Law BD, 2001, *South Africa's outstanding Maritime Zones Claims and Boundries: Time is running out!*, A Navy for Africa Conference Paper, Institute for Maritime Technology, Simons Town, South Africa.

[17] Iliffe JC, 2000, *Datums and Map Projections for Remote Sensing, GIS and Surveying*, Whittles Publishing, London, United Kingdom.

[18] Information Brochure, *Hartebeesthoek 94, The new South African Datum*, Chief Directorate: Surveys and Mapping, Department of Land Affairs, Cape Town, South Africa.

[19] Jasc Paint Shop Pro. 2000. Version 7.02. *Jasc Software, Inc.*, [Online], [Cited October 16th, 2004], Available from `http://www.jasc.com/products/paintshoppro/`

[20] Kvenvolden KA, 1993, *Gas Hydrates as a Potential Energy Resource: A Review of their Methane Content*, pp 555–561 in Howell DG et al (EDS), USGS Professional Paper **1570**.

[21] Lass H, 1950, *Vector and Tensor Analysis*, McGraw-Hill, New York, United States of America.

[22] Lee LP, 1944, *The nomenclature and classification of map projections*, Empire Survey Review, **7**, 190–200.

[23] Mathematica. *Wolfram Research*, [Online], [Cited October 16th, 2004], Available from `http://www.wolfram.com/`

[24] Student Matlab. 2003. Release 13. *The Mathworks, Inc.*, [Online], [Cited October 16th, 2004], Available from `http://www.mathworks.com/`

[25] Microsoft Excel. 2002. *Microsoft Office XP Professional, Microsoft Corporation*, [Online], [Cited October 16th, 2004], Available from `http://www.microsoft.com/`

[26] Nord J, 1996, *Mercator's Rhumb Lines: A multivariable application of arclength*, College Math, **J27**, 384–387.

[27] Snyder JP, 1993, *Flattening the Earth: Two Thousand Years of Map Projections*, University of Chicago, Chigaco, United States of America.

[28] Snyder JP, 1983, *Map projections used by the U.S. Geological Survey*, Geological Survey Bulletin 1532, Second Edition, U.S. Department of the Interior, U.S. Government Printing Office, Washington DC, United States of America.

[29] Sobel D, 1995, *Longitude: The True Story of a Lone Genius Who Solved The Greatest Scientific Problem of his Time*, Fourth Estate, New York, United States of America.

[30] Sondergaard P & Hansen JV, *Numerical Differentiation*, [Online], [Cited May 16th, 2004], Available from `http://www.imm.dtu.dk/npch/Projekter/Shock/Main/node61.html`

[31] Stead T, 2002, *Outer Limits of the Continental Shelf, Submissions from Developing Countries: South Africa a Case Study*, Masters Thesis, University of Plymouth, Plymouth, United Kingdom.

[32] Steinhaus H, 1999, *Mathematical Snapshots, Third Edition*, pp 217–221, New York, United States of America.

[33] Summerfield MA, 1991, *Global Geomorphology: An Introduction to the Study of Landforms*, Essex, United Kingdom.

[34] Taylor, B (ED), 1995, *Backarc Basins, Tectonics and Magmatism*, McGraw Hill, New York, United States of America.

[35] Unclos, 1999, *Commission on the Limits of the Continental Shelf. Fifth Session, May 1999, Scientific and Technical Guidelines of the Commission on the Limits of the Continental Shelf*, Document No. CLCS/11.

[36] Unclos, 1999, *Commission on the Limits of the Continental Shelf. Sixth Session, September 1999, Scientific and Technical Guidelines of the Commmission on the Limits of the Continental Shelf, Annexes II - IV to the Guidelines*, Document No. CLCS/11/Add.1.

[37] United Nations, 1983, *United Nations Convention on the Law of the Sea*, New York, United States of America.

[38] VANÍČEK P & OU Z, 1996, *Automatic Tracing of the Foot of the Continental Slope*, Marine Geodesy, **19**, 181–195.

[39] VANÍČEK P & OU Z, 1996, *Automatic tracing of continental foot-line from real bathymetric data*, University of New Brunswick, Fredericton, Canada.

[40] VAN VUUREN JH, 1996, *Applied Partial Differential Equations. Lecture notes for an introductory graduate course*, University of Stellenbosch, Stellenbosch, South Africa.

[41] WAINMAN CK, 2002, *South Africa's Extended Continental Shelf Claim*, Internal Report, Institute for Maritime Technology, Simons Town, South Africa.

[42] WAINMAN CK. *Personal Communication.* [16/08/2004]. Contactable at: `ckw@imt.co.za`

[43] WAINMAN CK. *Personal Communication.* [29/09/2004]. Contactable at: `ckw@imt.co.za`

[44] WEIMER N, *The Mercator Conformal Projection*, [Online], [Cited July 6th, 2004], Available from `http://www.ualberta.ca/~norris/navigation/~Mercator.html`

[45] WENK E, 1969, *The Physical Resources of the Ocean*, Scientific American, **248**, 167–176.

[46] WYLLIE PJ, 1979, *The way the Earth works*, McGraw Hill, New York, United States of America.

[47] YOUNG P, *Physics 115/242 Numerical Differentiation*, [Online], [Cited May 20th, 2004], Available from `http://bartok.ucsc.edu/peter/115/diff/node1.html`